Analysis of genomic DNA methylation variations and roles during grape berry ripening

Junhua Kong

THÈSE PRÉSENTÉE

POUR OBTENIR LE GRADE DE

DOCTEUR DE

L'UNIVERSITÉ DE BORDEAUX

ÉCOLE DOCTORALE SCIENCES DE LA VIE ET DE LA SANTÉ

SPÉCIALITÉ BIOLOGIE VÉGÉTALE

Par Junhua KONG

Soutenue le 25 June 2019

Analysis of genomic DNA methylation variations and roles during grape berry ripening

Sous la direction de : Philippe Gallusci

Président du jury :

M. Serge Delrot	Professeur	Université de Bordeaux	

Membres du jury :

M Nicolas Bouché	Directeur de recherche	INRA centre Versailles-Grignon	Rapporteur
M Yiguo Hong	Professeur	Hangzhou Normal University	Rapporteur
Mme Rossitza Atanassova	Professeur	Université de Poitiers	Examinateur
Mme Marie Mirouze	Chargé de recherche	IRD	Examinateur
M Philippe Gallusci	Professeur	Université de Bordeaux	Directeur

Acknowledgement

I am very grateful to my supervisor Professor. Philippe Gallusci, for his gentle encouragement, insightful guidance, tireless assistance and constant support throughout my Ph.D. studies at EGFV, INRA Bordeaux. Meanwhile, I wish to give my special thanks to Emeline Teyssier for her support in work and life. Both gave me many thoughtful thoughts and creative ideas on the experiment design and research plan, and spent time to revise my manuscripts and dissertation in every detail. I would also like thanks to Linda Stammitti, Margot Berger and Amelie Colling, especially Margot for her kind help.

I wish to thank all my colleagues at EGFV for their ideas, suggestions, and assistance. My special thanks to Zhanwu Dai, who helped a lot during my work. I would like to thank Fatma Lecourieux and David Lecourieux, who offer me many useful suggestions on my work. I wish to thank Ghislaine Hilbert, Christel Renaud for their help for metabolic analysis, Enrich Zehraoui for qPCR analysis, Stephanie Cluzet for stilbene analysis, Alain Decendit, who provided the grape GT cell, Agnes Destrac-Irvine for the access to Cabernet sauvignon plants. I wish to thank Virginie Garcia, Jinliang Chen, and Ruie Liu who never hesitate to discuss with me on RNA seq analysis. I would like to thank Catherine Chabirand, Cathy Thioulouse for their perfect work.

I wish to thank our collaborators, Zhaobo Lang and Huan Huang for bisulfite sequencing and analysis; Mickael Malnoy and Lorenza Dallacosta for generating grape transgenic plant; Yiguo Hong, Tongfei Lai, Zhiming Yu for all their support and help during my studies.

I would also like to thank all the members of my thesis jury, Pr Serge Delrot, Pr Rossitza Atanassova, Dr Marie Mirouze, Dr Nicolas Bouché and Pr Yiguo Hong for their critical reading and valuable suggestions on my thesis work.

I thank Chinese Scholorship Councile (CSC) and Conseil Interprofessionnel du Vin de Bordeaux (CIVB) for providing a thesis grant and make possible for me to study and work in France.

I want to thank all my friends, Jing Wu, Zhenhui Chen, Le Guan, Lina Wang, Jiaojiao Wang, they helped a lot in my daily life.

Finally, I thank all my families and friends who always support me in my life.

Title: Analysis of genomic DNA methylation variations and roles during grape berry ripening

KEY WORDS: DNA methylation, grape berry, ripening

Summary

Grapevine is a worldwide cultivated fruit crop with high economic importance mainly because of its usage for wine production. Grape berry is also one of the main models for non-climacteric fruits to study the mechanisms controlling the ripening process. Grape berry development is characterized by two phases of rapid size increase separated by a lag phase at the time of ripening induction. Grape berries are composed of three main tissues, the skin (exocarp and cuticle), the pulp (mesocarp and endocarp) and the seeds. Skin and pulp present distinct structure and metabolite composition and contribute in a different way to wine quality, the pulp providing sugar, amino and organic acids whereas the skin is important for anthocyanins and other phenolic compounds. The molecular mechanisms involved in the control of grape berry ripening are still poorly understood. Recent results indicate that both abscisic acid (ABA) and sugar may be important signals together with various transcription factors. In addition, epigenetic mechanisms are now emerging as important regulators of fleshy fruit development, DNA methylation being critically important for tomato, sweet range and strawberry ripening.

The present thesis aims at analyzing the potential role of DNA methylation in the control of grape berry ripening. It also investigates the potential role of DNA methylation in the synthesis of anthocyanin, that are important compounds for the color of red grape berries, using *in vitro* grown fruit cells. To address these questions, grape berries cultivated *in vitro* were treated with DNA methylation inhibitor. Treatments resulted in delayed and reduced grape berry ripening, therefore sustaining the idea that DNA methylation plays critical roles at this developmental step. Grape berries harvested at various developmental stages were then dissected and each tissue was separately analyzed for transcriptomic, metabolic and DNA methylation variations. Main results indicate significant and distinct metabolic and transcriptomic variations consistent with each tissue following specific modifications during ripening. In addition, analysis of DNA methylation variations at two developmental stages in each tissue indicates both common and tissue specific changes in DNA methylation patterns during fruit ripening. A very small proportion of differentially methylated regions (DMRs) is found similarly in the pup and the skin, but most are tissue specific, also consistent with tissue specific control at this developmental phase. Of note, among the different DMRs identified in each tissue, only a few were associated with differentially expressed genes (DEG) during ripening, whereas most were not, questioning the general role of DNA methylation in the control of gene expression at this developmental transition in grape.

As anthocyanins are the most abundant polyphenolic compounds in the skin of red grape berries, we used grape cell suspensions of the Gamay Teinturier genotype, known to accumulate anthocyanins under light conditions, in order to analyze the potential role of DNA methylation in their synthesis. GT cells cultivated in light conditions and treated with the DNA methyltransferase inhibitor zebularine, accumulate higher quantities of anthocyanins than untreated cells. Note worthy, GT cells grown in the absence of light do not accumulate anthocyanins. However, zebularine was sufficient to induce anthocyanin accumulation in the absence of light. Zebularine treatments had significant additional effects on grape cells including, cell growth limitation, and modification of soluble sugars, organic acid or stilbene accumulation, together with important transcriptomic reprogramming, consistent with a general effect on cells rather than a specific effect on anthocyanin accumulation.

Taken together, the results suggested that DNA methylation may be important in the control of grape fruit ripening, although the precise mechanisms underlying methylation variations and roles in grape berries remain to be deciphered.

Title : Analyse des variations et du rôle de la méthylation de l'ADN génomique lors de la maturation des baies de raisin

MOTS-CLES : méthylation de l'ADN, baies de raisin, maturation

Résumé

La Vigne est une plante cultivée dans le monde entier ayant une grande importance économique, principalement en raison de son utilisation pour la production de vin. Le raisin est également l'un des principaux modèles d'étude pour les fruits non climatériques dans le but de mieux comprendre les mécanismes contrôlant le mûrissement des baies. Le développement du raisin est caractérisé par deux phases de croissance rapide séparées par une phase de latence se produisant au moment de l'induction de la maturation. Les baies de vigne sont composées de trois tissus principaux: la pellicul (exocarpe et cuticule), la pulpe (mésocarpe et endocarpe) et les pépin. La pellicul (ou peau) et la pulpe présentent une structure et une composition en métabolites distinctes et contribuent de manière différente à la composition du vin, la pulpe fournissant essentiellement le sucre, les acides aminés et les acides organiques alors que la peau contient beaucoup anthocyanes et d'autres composés phénoliques. Les mécanismes moléculaires impliqués dans le contrôle de la maturation des baies de raisin sont encore mal compris. Des résultats récents montrent que l'acide abscissique (ABA) et les sucres ainsi que différents facteurs de transcription jouent un rôle important dans le contrôle de cette phase de développement. Cependant, des résultats récents montrent aussi que les mécanismes épigénétiques peuvent réguler le développement des fruits charnus, la méthylation de l'ADN étant d'une importance capitale pour la maturation des tomates, des fraises et de l'orange douce.

Le mémoir de thèse présenté ici analyse le rôle potentiel de la méthylation de l'ADN dans la maturation du raisin. Il propose d'étudier également le rôle de la méthylation de l'ADN dans la synthèse des anthocyanes, composés inportants pour la coloration des pellicules de raisin rouge, en utilisant comme système modèle des baies cultivées *in vitro*. Pour étudier le rôle de la méthylation dans le contrôle de la maturation des baies, des fruits ont été cultivés *in vitro* avec ou sans traitement à l'aide d'inhibiteurs de la méthylation de l'ADN. Les traitements inhibent la maturation du raisin, suggérant que la méthylation de l'ADN intervient dans cette étape du développement chez la Vigne aussi. Les baies récoltées à divers stades de développement à partir de plantes cultivées au vignoble, ont ensuite été disséquées pour séparer la pellicule de la chair. Chaque tissu a été analysé séparément pour déterminer les variations des transcriptomes, de l'abondance de différents métabolites, et de la méthylation de l'ADN. Des variations des métabolites et du transcriptome sont observées, avec des spécificités liées au tissu analysé. En outre, l'analyse de la méthylation de l'ADN à deux stades de développement dans chacun des tissus de la baie révèle tant l'existence de variations de methylation spécifiques

à chaque tissu, tandis que les variations communes aux deux tissus, en nombre limité. Ces résultats suggèrent un contrôle de la méthylation de l'ADN spécifique à chaque tissu lors de la maturation de la baie. De façon notable, parmi les différentes régions différentiellement méthylées identifiées dans chaque tissu, seules quelques-unes sont associées à des gènes exprimés différentiellement (DEG) au cours de la maturation, ce qui pose la question du rôle général de la méthylation de l'ADN dans le contrôle de l'expression génique lors de la maturation du raisin.

Pour analyser le rôle de la méthylation de l'ADN dans le contrôle de la synthèse des anthocyanes chez le raisin, nous avons utilisé des suspensions de cellules de raisin du génotype Gamay Teinturier (GT), connues pour accumuler des anthocyanines lorsqu'elles sont cultivées à la lumière. Les cellules GT cultivées en présence de lumière traitées avec la zébularine, un inhibiteur de l'ADN méthyltransférase, accumulent des quantités plus importantes d'anthocyanes. De façon remarquable, les cellules GT cultivées en l'absence de lumière n'accumulent pas d'anthocyanes, sauf si elles sont traitées à la zébularine. Celle-ci est donc suffisante pour induire l'accumulation d'anthocyanes en l'absence de lumière. Les traitements à la zébularine ont cependant des effets supplémentaires importants sur les cellules de Vigne, notamment une limitation de la croissance cellulaire et une modification de l'accumulation de sucres solubles, d'acides organiques et de stilbènes, ainsi qu'une reprogrammation importante du transcriptome. Ces résultats suggèrent un effet général de la zebularine sur les cellules GT plutôt qu'un effet spécifique sur l'accumulation d'anthocyanes.

Dans l'ensemble, les résultats indiquent que la méthylation de l'ADN est importante pour le contrôle de la maturation du raisin, bien que les mécanismes qui sous-tendent les variations de la méthylation et leur rôles dans les différents tissus des baies restent à préciser.

Table of Content

INDEX of figures

CHAPTER I

CHAPTER II

CHAPTER III

CHAPTER IV

Index of Tables

CHAPTER I

General Introduction

Grape plant: general introduction

Part of this introduction has been used in the book chapter by JH Kong et al, 2019 “Epigenetic regulation in fleshy fruit: perspective for grape berry development and ripening” in press in “The Grape Genome. 2019 Eds: Dario Cantu & M. Andrew Walker”; https://www.springer. com/gp/product-marketing-tool/flyer/9783030186005?downloadType=PRODUCTFLYER”

1.1.1 Grape plant: economic importance

Grapevine (*Vitis vinifera L*.) is a word-wide cultivated fruit crop with a high economic value (Figure I-1, 2). Grape berries are rich in sugar, pigments, aroma and polyphenolic compounds which are beneficial to human health (Fraige et al., 2014). Grape berries can be used as fresh fruit, raisin, but most of grape-fruit production is fermented to produce wine which conveys a far greater economic value than that of grapes. In 2017, the total vineyard area in the world was 7534 thousand of hectares (kha), producing 282 million hectoliters (mhl) wine, which is the highest production recorded since 2000. The wine trade has continuously increased since 2001, to reached 30 billion euros in 2017 (OIV, 2018) .

In France, vineyards, which rank in the top third largest vineyard in the world after Spain (967 kha) and China (870 kha), cover 786 kha. According to 2018 statistics, 5.5 million tons of grape berries were produced in France, among which nearly 99% were used for wine production. This represents 46.4 million hl wine with a total value of 9.0 billion euros (OIV, 2018).

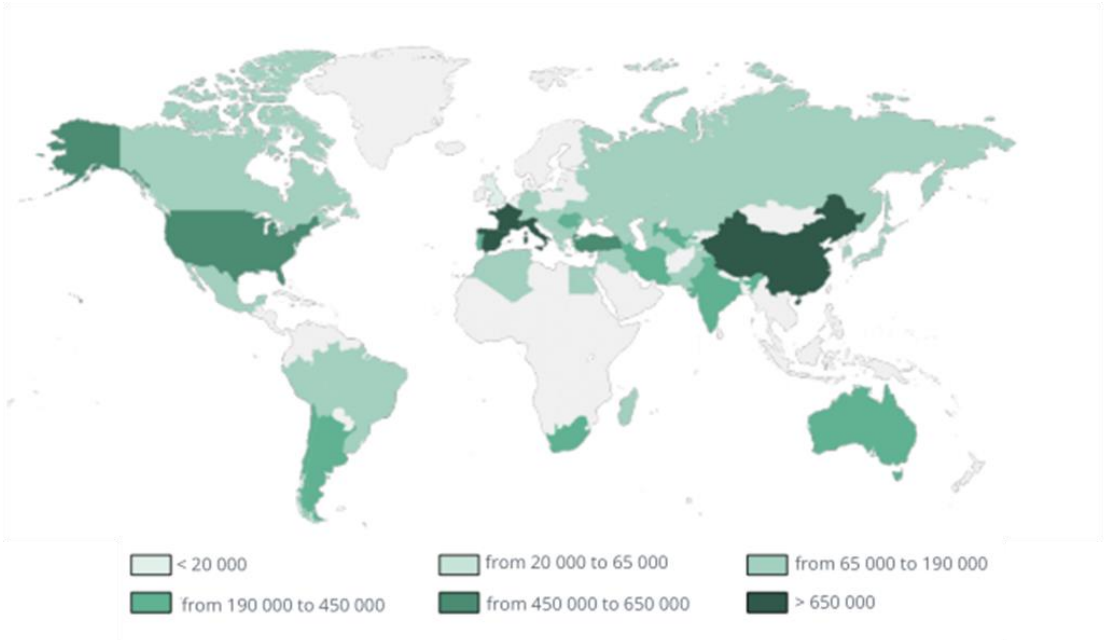

Figure I-1. Grape is widely cultivated in the world (OIV, 2018). Color indicated the total area of vineyard in each country.

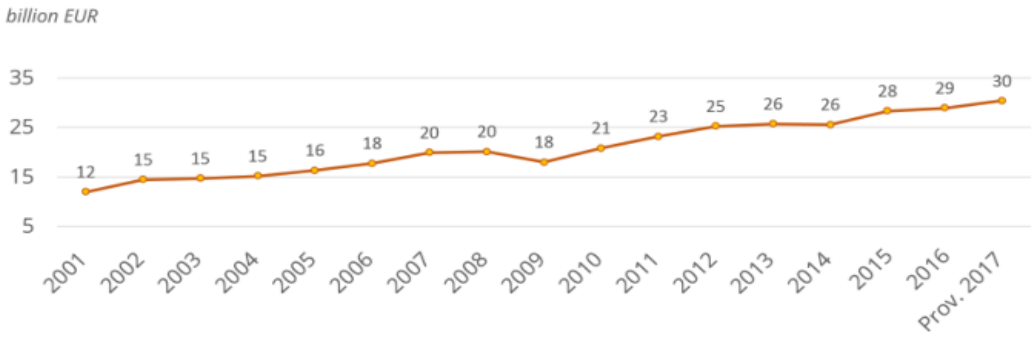

Figure I-2. Evolution of wine trade between 2001 and 2017. The total wine trade gradually increases in the past 16 years (OIV 2018).

1.1.2 Grape: a model for woody perennials fruit crops

Grape is a grafted perennial woody plant. As many perennial crops, it differs from annual crop plants on several aspects. The first one is that many perennial crops are clonally propagated, whereas annuals are multiplied through sexual reproduction (Judd et al., 1999). Indeed, clonal propagation allows keeping the genetic combination that have been selected, but does not allow new genetic combinations (Miller & Gross, 2011).

A second important point is that in many countries, grape plants are grafted (Kyriacou et al., 2017). Grafting is a well-developed horticultural technique that is widely used in vineyards. Classically, the shoot of a plant, named the scion, is grafted to the root system of a different plant, the rootstock, with the aim to improve the robustness of the graft partners. Grafting can impact several traits that are important in agriculture including scion vigor, fruit size, yield or quality. However, the effects depend on the specific properties of the rootstocks and scions that have been used as well as on their interaction (Warschefsky et al., 2016). An important aspect of Grafting usage, is the possibility this technology offers to grow plants in new environments or to adapt plants to new constraints of the environment, due to an enhanced abiotic and biotic stress resistance, as illustrated by the use of grapevine rootstocks resistant to phylloxera (*Daktulosphaira vitifoliae*) to save the French vineyard in the 19th century (Mudge et al., 2009). This insect which was introduced from North America does not infest American grape species, suggesting that they are resistant to this pest. Scions from French cultivar were grafted on native American rootstocks species which was sufficient to confer resistance to phylloxera to the scion allowing to save the French wine industry (Mudge et al., 2009). Nowadays, grafting is widely used in arboriculture and viticulture, and its usage has been extended to vegetables such as potato and tomato as it allows combining specific traits of both the rootstock and the scion to meet the current challenges of fruit and vegetable production(Kyriacou et al., 2017)(Melnyk & Meyerowitz, 2015).

A third characteristic of perennials is that they go through recurrent seasonal cycles of growth and dormancy. At the end of the growing season, grape plants cease development and enter a dormant state which aims at protecting buds against unfavorable winter conditions. There is a precise series of events during one season of grape plant development: (1) bud break occurs in spring, and is followed by (2) leaf,

and (3) cluster formation and blooming in late spring, early summer. (4) Fruit set, development and ripening take place in summer, (5) leaf fall in autumn and (6) bud dormancy in winter. The time frame from bud burst to leaf fall requires about 7 months although it may widely vary depending on environment and management. The whole life cycle of grape plant was precisely divided into 47 obvious distinct growth stages that are currently used as a guideline for grape plant management (Coombe et al., 1995). There are thousands of grape cultivars in use in the worldwide today. Yet, only 12 grape varieties (representing only 1% of the cultivated varieties available) make up nearly 80% of the vineyards of certain countries, and in some cases up to 75% of vineyard surfaces are devoted to a single grape variety, Cabernet-Sauvignon (Bowers et al., 1997).

Indeed, there is a very large diversity of grape varieties that present distinct features in terms of phenology, truss shape, fruits characteristics or vigor (Robinson et al., 2013 for a review). In the present work we have essentially used two of the grape varieties, Cabernet sauvignon (Bowers and Meredith 1997; Robinson et al., 1994), and Gamay teinturier (Santiago et al., 2008). Among the different red grape cultivars, Cabernet Sauvignon is described as “the world's most renowned grape variety for the production of fine red wine” (Robinson et al., 1994). Genetic evidence demonstrated that Cabernet Sauvignon is the progeny of two other Bordeaux cultivars, “Cabernet franc” and “Sauvignon blanc”. Special flavors, tannins and tough, thick skins and the amazing ability to adapt to a diverse array of soils and climates make Cabernet Sauvignon a very adaptable genotype. Cabernet Sauvignon has become popular that it has its own holiday, the “International Cabernet Sauvignon Day” on August the 30th. It is the most planted wine cultivars in Bordeaux, and in many other places all around the world.

As far as red grape varieties are considered, they consistently accumulate anthocyanins in the skin of the berries (Fournier-Level et al., 2009). There are however exceptions to this situation among which the Teinturier grape cultivars (also called dyers) which accumulate anthocyanins not only in the skin but also in the pulp of the berries (Figure I-3A, Jeong et al., 2006). In addition, some Teinturier cultivars accumulate anthocyanins in other organs, such as pedicels, rachis, leaves and stem epidermis (Jeong et al., 2006; Wu et al., 2012).The content of anthocyanin in berries of Teinturier cultivars is much higher than in non-teinturier cultivars (Ageorges et al., 2006). Noteworthy, cell suspensions derived from Gamay Teinturier berries are widely used to analyze the control of anthocyanin biosynthesis in various conditions including the responses to abiotic and biotic stress (Ananga et al., 2013). Light is the key factor control anthocyanin synthesis (Koyama and Goto-Yamamoto 2008; Matus et al., 2009). In the cell suspension of Gamay Teinturier, light is necessary for anthocyanin accumulation, as no anthocyanin accumulate without light (Figure I-3B).

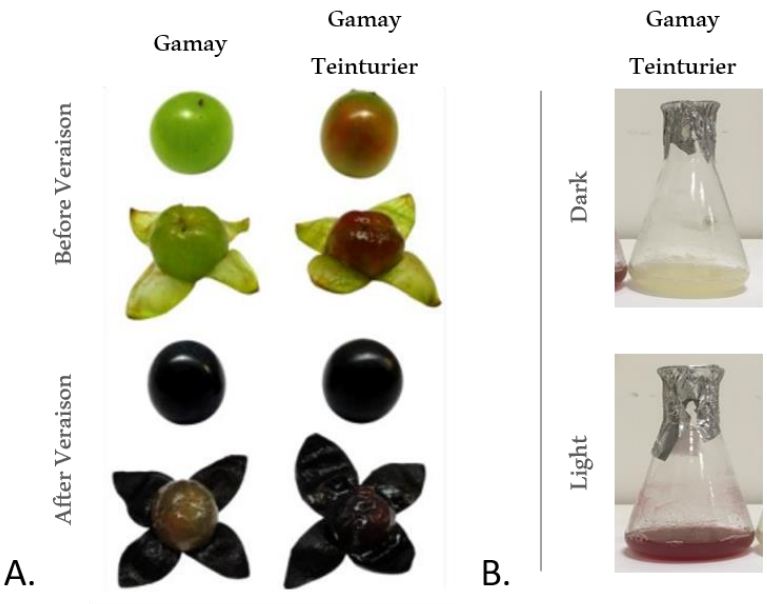

Figure I-3. Anthocianin synthesis in the Berry and cell suspension of Gamay Teinturier. (A) In Gamay, anthocyanins accumulate only in the skin after veraison. By contrast, anthocyanin synthesis occurs in the pulp of Gamay Teinturier even before veraison, while synthesis in the skin occurs only after veraison (Guan et al., 2014). (B) Light is necessary for anthocyanin accumulation in cell suspension cultures of Gamay Teinturier.

In addition to extensive knowledge available on the physiology of grape plants, genotype collections worldwide, the recent description of a high-quality draft sequence of the grapevine genome from the Pinot Noir clone ENTAV 115 (Canaguier et al., 2017)(Jaillon et al., 2007), and recently from the Riparia Gloire de Montpellier and cabernet Sauvignon provides new tools to investigate the molecular mechanisms, including epigenetic regulations, underlying developmental processes as well as the adaptation of grape to its environment.

Indeed additional tools are now necessary to be able to fully developed functional genomic studies on grape, although several laboratories have described transformation/ regeneration protocols, as well VIGS tools to analyze the functions of genes in this plant (Kurth et al., 2012). In addition, the recent description of the microvine, should also make easier some functional genomic approaches in this plant species (Chaïb et al., 2010).

Fleshy fruit development: specificities of grape berries

1.2.1 Fleshy fruit development

Fruit is an organ specific to angiosperms designed for seed protection and dispersal that has long been considered essential in the human diet because it contains fibers, various vitamins, carbohydrates and antioxidants that are essential to humans (Seymour et al., 2013; Klee and Giovannoni, 2011). Most fruits develop from ovaries although accessories tissues, for example the receptacle in strawberry may be used as well (Seymour et al., 2013). The development of fleshy fruits, which have been suggested to all derive from a dry ancestor, is generally initiated by fertilization and is characterized by two main steps that precede fruit ripening: (1) a cell division phase which is initiated shortly after pollination and followed by (2) a cell extension phase that is responsible for the increase in fruit size (Gillaspy et al., 1993). In contrast to dry fruits that will get lignified, fleshy fruits enter a complex ripening process characterized by extensive metabolic modifications, such as soluble sugar accumulation, cell wall degradation, and synthesis of a wide range of secondary compounds of high nutritional value such as carotenoids or anthocyanins, and several vitamins. In most cases, fruit ripening results in significant changes in fruit appearance, including fruit color modifications and fruit softening (Seymour et al., 2013; Lee et al., 2012). However, fleshy fruits are very diverse and many present specific features as in case of grape berries (Seymour et al., 2013).

1.2.2 Specificity of grape berry development

Based on the distinct characterizations of structures and metabolite compositions, grape berry is divided into three types of tissue: skin (cuticle and exocarp), pulp (mesocarp and endocarp) and seed covered with endocarp comprising a thin layer of inner epidermis cells (Figure I-4), accounting for about 15%, 80%, and 5% of total berry fresh weight, respectively (Roby and Matthews., 2004). Primary metabolites including sugar, organic acids and amino acids predominantly accumulate in pulp, at to a lower level in skin (Fontes et al., 2011). Phenolic compounds, which are the most important secondary metabolism mainly accumulate in the skin and seed of berry and are also found in the stem and leaf. Tannin and anthocyanin are the most important compounds in the grape and wine that contribute to the color, astringency, bitterness of berry and wine (Revilla et al., 2000). As mentioned above, tannin biosynthesis in the skin and seeds, and anthocyanin accumulation in the skin, are also found in the pulp of Teinturier grape (Montealegre et al., 2005, 2006; Wu et al., 2012). In addition, tannins can combine with anthocyanin to form polymers that improve the stabilization of anthocyanin (Waterhouse et al., 2002). Major volatile flavor components are localized in the skin (Lund et al., 2006).

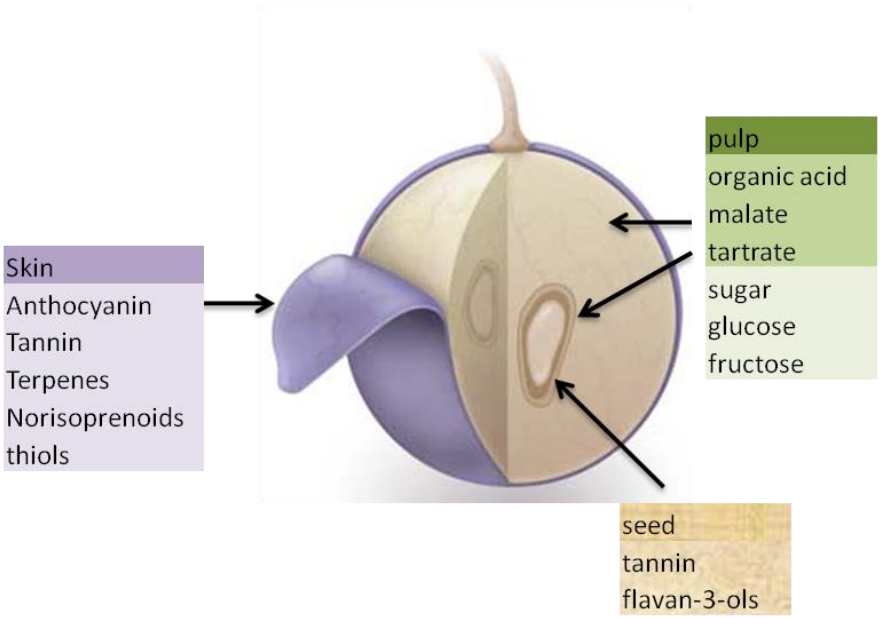

Figure I-4. Berry structure and certain metabolite locations, adapted from Lund et al (2006). Grape berry contain skin (cuticle and exocarp), pulp (mesocarp and endocarp) and seed. Primary metabolites, organic acid and soluble sugar accumulate in the pulp, whereas secondary metabolites, anthocyanin, tannin, volatile flavor components accumulate in the skin. Tannin and flavan-3-ol also located in seed.

Among fleshy fruits, grape berry presents specific developmental features. In contrast to most fruits that present a simple sigmoid growth curve, grape berry growth follows a double sigmoid (Figure I-5) as fruit size will increase both before and after the induction of ripening (reviewed in Serrano et al., 2017; C. Conde et al., 2007). The first increase in berry size starts shortly after fruit set, and is mainly due to cell division and subsequent cell expansion processes. It is characterized by organic acid accumulation in vacuoles, and the synthesis of tannins and of hydroxycinnamates, which are precursors of phenolic compounds. Two main organic acids, malic and tartartic acid account for 90% of total acidity, but trace amounts of citric, succinic, lactic and acetic acids are also found (Kliewer et al., 1966; Conde et al., 2007, Dai et al., 2011). Tartaric acid accumulates to high levels in the young berry and gradually decline during berry development and ripening. By contrast, the concentration of malic acid which is relative low in young berry, reaches its maximal level at the beginning of ripening (Sweetman et al., 2009). At the end of first growth phase, berry remains green, hard and acidic. The berry size stops to increase and seeds reach maturity (Ristic et al., 2005) during the so called “lag phase” that precedes the “véraison stage”, which is characterized by berry softening, abscisic acid (ABA) synthesis and initiation of sugar, and anthocyanin accumulation in red cultivars (Castellarin et al., 2016). Following, grape berry size increases again due to additional cell expansion events in the mesocarp.

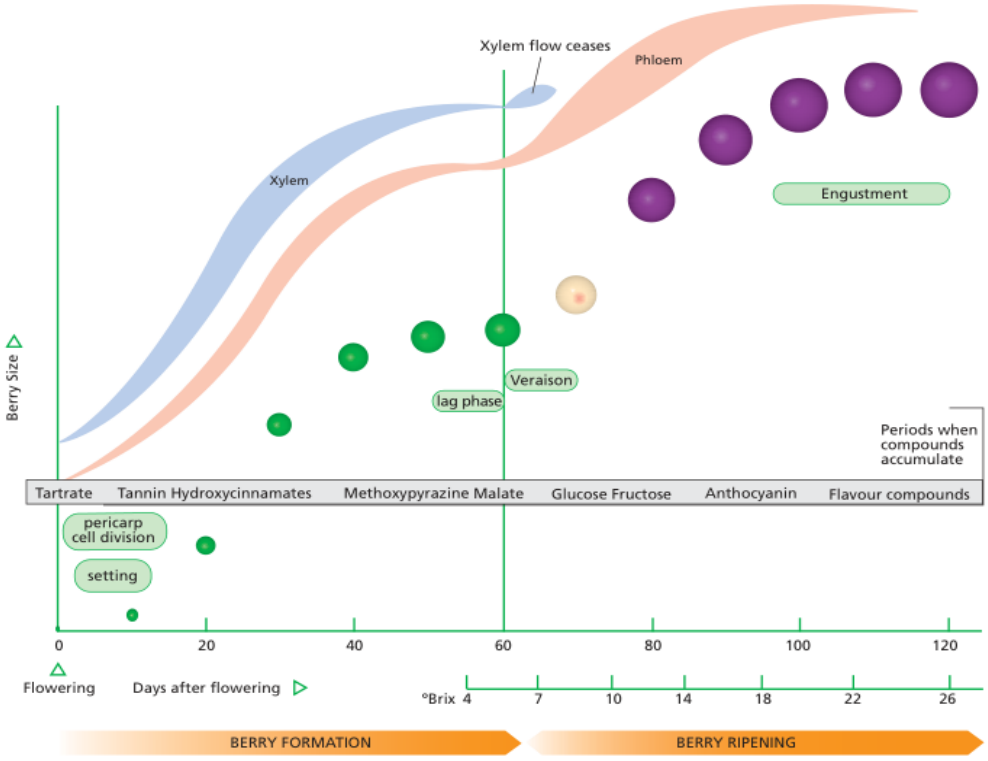

Figure I-5. A typical double-sigmoid pattern displays the development and ripening of grape berry (Kennedy et al., 2002). The size and color of berry, and main metabolic events are shown in the diagram. Grape berry display a double sigmoid growth curve. Berry size rapid increase as a result from cell division in the first three weeks after fruit set. Organic acid, tannin, hydroxycinnamates and methoxypyrazine are synthesized during this phase. Berry development cease in the short veraison stage. Softening and coloring mark the onset of ripening. The size and weight of berry increase during ripening, concomitantly to sugar accumulation.

This second growth phase, which occurs during ripening, is characterized by important metabolic changes that include the accumulation of glucose and fructose along with a decrease in organic acid levels, berry softening and the synthesis of precursors of various aromatic compounds including, terpenes, isoprenoids, esters, and thiols. At harvest, berries are edible and attractive to seed dispersal.

Fleshy fruits have been classified into two groups: climacteric and non-climacteric, based on the physiological mechanisms that control the induction of ripening (Figure I-6). Climacteric fruits for which tomato stands as a model (Giovannoni et al., 2017) is characterized by an intense respiratory burst associated with ethylene synthesis that precedes fruit ripening induction.

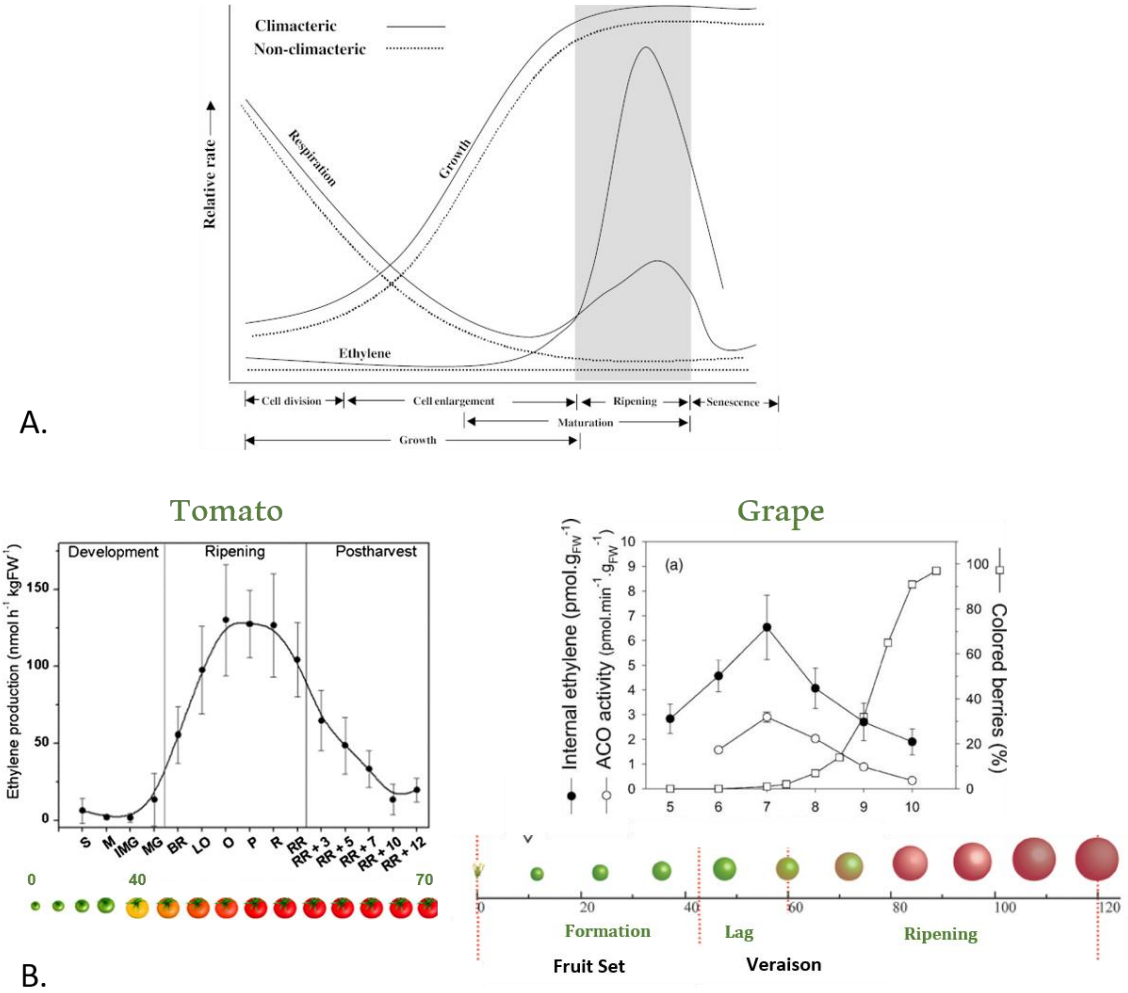

Figure I-6. Difference between climacteric and non-climacteric fruits. (A) General patterns of growth, respiration and ethylene during development, maturation and senescence of climacteric and non-climacteric fruits (Paul et al., 2012). (B) The main differences between tomato and grape berry are observed at the onset of fruit ripening. Tomato fruits are climacteric and present a sharp increase in ethylene synthesis at the onset of ripening associated with a burst of respiration. In contrast, grapefruits are non-climacteric and present a limited increase in ethylene content just prior to ripening. Chervin et al (2004,2008) reported that blocking ethylene accumulation inhibits berry growth and coloring while exposure to ethylene increases berry size by altering the expression of genes related to cell wall modification.

This contrasts with non-climacteric fruits such as grape and strawberry, for which no specific physiological parameter that marks the initiation of ripening has been identified (reviewed in Bapat et al., 2010), even if hormones, including ethylene and ABA are now known to have important roles in the ripening of this type of fruits (Fortes et al., 2015). More specifically the content in ABA increases at the onset of ripening in grape (Gambetta et al., 2010)(Castellarin et al., 2011). Exogenous ABA treatment induces early ripening together with coloring and sugar accumulation (Pilati et al., 2017). In addition, different concentration and composition of sugars have distinct effects on berry ripening (Gambetta et al., 2010,Dai et al., 2013), suggesting that sugar is likely a signal that triggers ripening.

Genetic control of ripening has also been demonstrated for climacteric fruits, mainly in the tomato model, and several mutations affecting essential regulators of ripening have been described in this plant (Gapper et al., 2014). Indeed the recent discovery that epigenetic regulators are major players in the control of fruit development, ripening and senescence has deeply changed the proposed models describing the regulation of ripening, and raises the question of the general function of such mechanisms in all types of fruits. So far, most studies have been performed on tomato (Bucher et al., 2018 ; Gallusci et al., 2016), but evidence is now accumulating that such regulators may be important in other types of fruits.

In the following parts of the introduction, I will summarize major aspects of epigenetic mechanisms before discussing the relevance of epigenetic processes in the control of fruit ripening.

Relevance of epigenetic mechanisms in plant

In Eukaryotes DNA is tightly associated with histones to form the chromatin, a highly dynamic structure that plays critical roles in genome functioning. Chromatin is made of elementary units called nucleosomes that are composed of octamers of the core histones (H2A, H2B, H3 and H4) around which 147bp of DNA are rolled up (Figure I-7). Nucleosomes are separated by a 50 bp long linker DNA that interacts with Histone H1. Traditionally two distinct chromatin states have been described: the highly condensed heterochromatin which is considered as inactive, whereas euchromatin corresponds to a less condensed and transcriptionally active chromatin state. Indeed dynamic changes on chromatin play critical roles in gene regulation and have therefore been the subject of intensive studies over the last decades both in animals and plants (Exner and Hennig, 2008; Zheng and Liu, 2019).

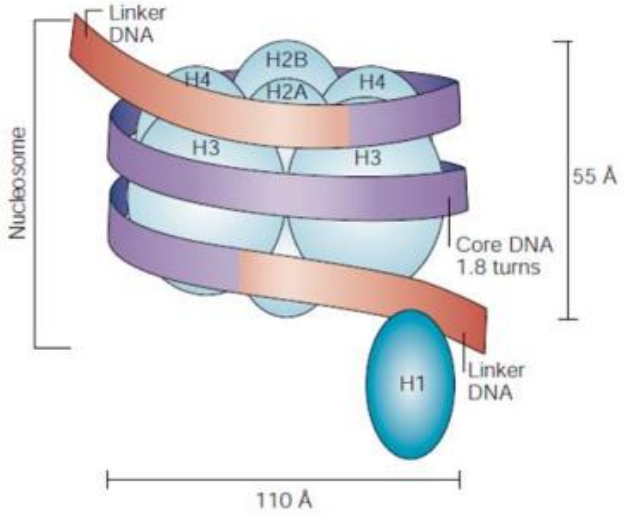

Figure I-7.The structure of nucleosome (Georgopoulos et al., 2002). Å: angstroms.

Although initially defined as “the branch of biology which studies the causal interactions between genes and their products which bring the phenotype into being” (Waddington, 1942) epigenetic now refers to “the study of changes in gene function that are mitotically and/or meiotically heritable and that do not entail change in DNA sequence (C. -t. Wu & Morris, 2001). Epigenetic regulations are mediated by the so called “epigenetic marks” that include the methylation of the cytosines on the 5th carbon (5mC) as well as several histone post-translational modifications (HPTMs), but also involve small RNAs and histone variants (Maeji and Nishimura, 2018)(Rothbart & Strahl, 2014)(Law & Jacobsen, 2010b). All types of marks contribute to defining specific chromatin states thereby gene expression patterns that can be maintained after cell division during organ and tissue development (Birnbaum, 2017)(Eichten, 2014)(Pikaard, 2014).

Epigenetic modifications are now emerging as crucial players in all aspects of plant development. Currently it is known that epigenetic is involved in controlling plant developmental transitions (Trindade, Schubert, & Gaudin, 2017) and is important for plant reproduction (G. Wang & Köhler, 2017), and root (Kawakatsu et al., 2016), seed (Kawakatsu, Nery, Castanon, & Ecker, 2017) and fruit development (Gallusci et al., 2016)(Giovannoni et al., 2017), but also participates to the response of plants to environmental stresses (Chinnusamy & Zhu, 2009)(Crisp et al., 2016, and references therein).

1.3.1 Histone post-translational modifications

The mechanisms responsible for histone post translational modifications (HPTMs) are globally conserved between plants and animals (Fuchs et al., 2006; Feng and Jacobsen, 2011). The following part presents these conserved mechanisms using examples taken from plant models (except when data were obtained from animal models only), and presents a few differences discriminating plants from animals.

a. Numerous histone post translational modifications and histone variants contribute to the epigenetic information

All histones are subjected to a wide variety of post translational modifications that include methylation, acetylation, phosphorylation, ubiquitination, and citrullination (Figure I-8) (reviewed in (Jenuwein & Allis, 2001)(Berger, 2007)(Bannister & Kouzarides, 2011)(Feng & Jacobsen, 2011)). These modifications affect various amino acids at different positions but the nucleosomal histones are mostly modified at their NH2-terminus which protrudes out of the nucleosome (Figure I-8). In addition histone H2A, histone H3 and histone H1 are encoded by small gene families, allowing the production of different isoforms usually referred to as histone variants that bear specific roles and may be subjected to differential PTMs (reviewed in (Talbert & Henikoff, 2017)(D. Jiang & Berger, 2017)). Importantly, most histone marks are found both in plants and animals, but the same histone mark can have different distribution and physiological function in different organisms. A striking example is H3K9me3 which is mostly associated with heterochromatin in organisms ranging from the fission yeast to humans (Becker, Nicetto, & Zaret, 2016), whereas it is typically found in euchromatin in Arabidopsis (Roudier et al., 2011).

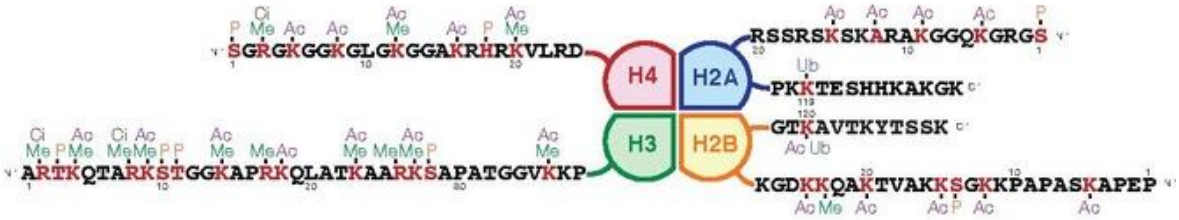

Figure I-8. Schematic representation of histone modifications (Rodriguez-Paredes et al., 2011). H2A, H2B, H3 and H4 represent four-nucleosome histones. Me, methylation;Ac, acetylation, Ci, citrullination ;Ub,ubiquitination; P, phosphorylation.

Histone modifications and histone variants control several processes linked to genome function, such as DNA replication, DNA repair, DNA recombination and transcriptional activation/inactivation (Vergara & Gutierrez, 2017). But most studies have focused on their function in gene expression, which relies on two main mechanisms (Reviews: (Berger et al., 2007)(Bannister & Kouzarides, 2011)(Engelhorn, Blanvillain, & Carles, 2014)). First some HPTMs, like histone acetylation, neutralize the positive charge of histones, and weaken the interaction between histones and the negatively charged DNA molecule therefore leading to an increased DNA accessibility to the transcriptional machinery. Recent data based on a multiscale computational study have shown that histone lysine acetylation also unfolds chromatin by decreasing tail availability for inter-nucleosome interactions, which are important for the chromatin fiber compaction (Collepardo-Guevara et al., 2015). In addition HPTMs are recognized by a diverse set of effector proteins, also called histone readers, which participate to the control of gene expression, as for example chromatin remodeling proteins or transcriptional regulators. Hence a large array of protein domains has been characterized, which recognize and bind to specific histone modifications. Some of the HPTM readers are directly responsible for a specific functional outcome such as the DNA methyltransferase CMT3 which recognizes H3K9me2 (A. Lindroth et al., 2004)(Du et al., 2012) and is responsible for CHG methylation (A. M. Lindroth et al., 2001)(see part 1.3.2 DNA methylation). Alternatively, HPTM readers can act through their interaction with effector proteins. For example, the Arabidopsis Morf Related Gene (MRG) group proteins, MRG1 and MRG2 recognize the H3K4me3/H3K36me3 marks on the FLOWERING LOCUS T (*FT*) promoter and this interaction favors the activation of *FT* gene transcription through a physical interaction between MRG1 / MRG2 and the transcription factor CONSTANS (Bu et al., 2014). Because they rely on a number of different protein partners, such mechanisms, can be precisely controlled. Finally recent data suggest that HPTMs play a role in the 3D organization of genomic DNA, contributing to the formation of specific nuclear territories, characterized by precise expression output (Liu et al., 2016)(Veluchamy et al., 2016)(Rodriguez-Granados et al., 2016).

b. The genome wide distribution of HPTMS shape the epigenetic landscape

The recent development of genome wide analysis of epigenetic mark distribution has shown that histone PTMs together with DNA methylation (see below; 5 methylcytosine, 5mC) can form specific

combinations that define genome territories with either active or repressive chromatin states in multiple organisms from plants including rice (X. Li et al., 2008), Arabidopsis (Roudier et al., 2011)(C. Luo et al., 2013)(Sequeira-Mendes et al., 2014)(C. Wang et al., 2015), and barley (K. Baker et al., 2015), to metazoa (as reviewed in (M. Baker, 2011)). These studies allowed the identification of a finite number of chromatin states along chromosomes, characterized by distinct sets of epigenetic marks. Interestingly, genomic elements are often distinguished by specific chromatin states. For example in Arabidopsis, silent heterochromatin is associated with H3.1, H3K9me2, H3K27me1 and 5mC, whereas many actively transcribed gene show around the transcription starting site a combination of H2Bub, H3K36me3, H3K4me3. Alternatively repressed genes present in euchromatic regions are associated with H3K27me3 within a nucleosome context enriched in H3.1 (Roudier et al., 2011)(Sequeira-Mendes et al., 2014). Figure I-9 gives an overview of the nine Arabidopsis chromatin states as well as their associated genomic features, as defined in (Sequeira-Mendes et al., 2014).

Interestingly some genes are associated with both active and repressive marks, as illustrated by the state 2 defined by (Sequeira-Mendes et al., 2014), where H3K4me2 and H3K27me2 coexist. Such bivalent chromatin states have been described at genes coding for important developmental regulators such as AGAMOUS (Saleh et al., 2007) or floral integrators (S. Qian et al., 2018) and could be necessary for fine tuning gene expression.

c. HPTMs dynamic is controlled by specific enzymes

Active and repressive histone marks are established and removed by specific enzymes referred to respectively as HPTM writers and erasers. The level of each HPTM is therefore determined in a dynamic fashion, by the relative abundance / activity of its specific writer(s) and eraser(s). Although HPTMs are reversible marks, their stability is variable. For example histone acetylation is a very dynamic epigenetic mark. The estimation of H3 and H4 acetylation turnover rates in human cells revealed very short half-lives (Zheng et al., 2013), with 12 histone sites displaying half-life below one hour (Weinert et al., 2018). As a consequence, modification of histone acetylation status could be essential when rapid changes in gene expression are required, for example in response to environmental stimuli (Barth & Imhof, 2010). On the contrary, H3K27me3 was initially considered as a very stable epigenetic mark that was conserved through cell division perpetuating the stable repressive state of the chromatin at specific loci. Consequently H3K27me3 is considered has a major determinant of cell identity, although it is now clearly established that this mark can be actively removed by the Jumonji-type of histone demethylases (reviewed in (Chunyan Liu et al., 2010)(X. Chen, Hu, & Zhou, 2011)(Xiao, Lee, & Wagner, 2016).

Many genes coding for HPTM writers and erasers have been identified and functionally characterized in the model plant *Arabidopsis*. Most studies have focused on histone methylation and acetylation, so that other HPTMS such as histone phosphorylation or sumoylation have been comparatively overlooked. Over the past decade, functional analyses of writers and erasers have also been conducted in a few other model and crop species, like tomato (How Kit et al., 2010)(Boureau et al., 2016) rice (S. Li et al., 2014)(M. Zheng et al., 2015)(K. Liu, Yu, Dong, & Shen, 2017)(P. Jiang, Wang, Jiang, et al., 2018; P. Jiang, Wang,

Zheng, et al., 2018), *Brassica napus* (L. Jiang et al., 2018), poplar (Fan et al., 2018), wheat (J. Liu et al., 2018) or maize (Rossi et al., 2007)(Forestan et al., 2018). These studies are mainly based on the characterization of genes presenting homologies with the genes originally identified in *Arabidopsis*. As shown in Figure I-9, each histone mark is set up by a specific set of enzymes, which are frequently specialized in the addition of a precise number of modifications. For example whereas ARABIDOPSIS TRITHORAX-RELATED PROTEIN 5 (ATRX5) and ATRX6 proteins of the trithorax group are responsible for the addition of one methyl group at histone 3 lysine 27 (H3K27me1) (Jacob et al., 2009), Enhancer of Zeste proteins from the Polycomb group family are part of the Polycomb repressive Complex 2 (PRC2) and are in charge of the addition of 2 and 3 methyl groups at the same residue (H3K27me3) (reviewed in (Chunyan Liu et al., 2010) (Figure I-9).

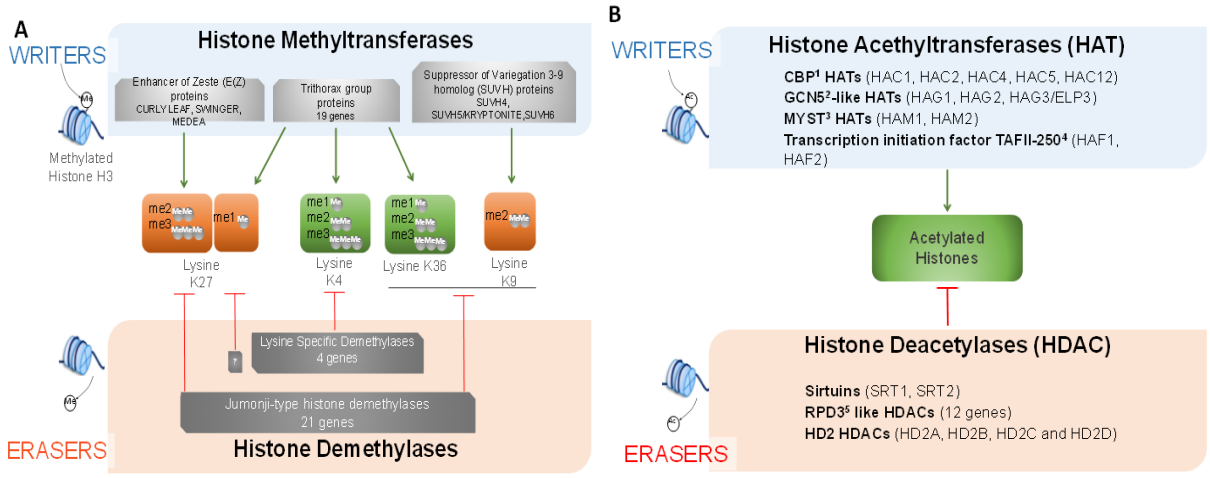

Figure I-9. Specific enzymes involved in Histone Methylation (A) and Acetylation (B).

A. Proteins responsible for histone H3 methylation / demethylation. Depending on the modified lysine residue (lysine K4, K9, K27, or K36), different protein families are involved. Moreover different proteins may be required depending on the number of methyl residues added / eliminated, as reviewed in Avramova et al (2009); Liu et al (2010); Berr et al (2011); Chen et al (2011); and Xiao et al (2016). B. Proteins responsible for histone acetylation and deacetylation, as reviewed in Hollender and Liu J (2007), Berr et al (2011) and Ma et al (2013).

For each type of regulators, the number of genes found in the Arabidopsis genome is specified. In a few cases, the name of these genes is indicated. Of note, for gene families which includes a large number of genes, such as the trithorax group proteins, only a few genes have been functionally characterized. The transcriptional state (active or inactive) mainly associated with each HPTM is indicated using the following color code: active in green / inactive in red.

In addition, most writers and erasers function as multiprotein complexes. As mentioned above, the enhancer of zeste (E(z)) proteins which are the enzymes catalyzing H3K27 trimethylation, function as a part of the PRC2, which contains three additional core proteins, a protein of the suppressor of zeste 12 (Su(z)12) family, a protein of the extra sex comb (ESC) family and a Multicopy Suppressor of IRA 1 (MSI) protein. Whereas only E(z) protein harbors the methyltransferase catalytic domain (the so called SET domain), the four PRC2 core proteins are necessary for PRC2 to function *in vivo* (reviewed in (Schubert, Clarenz, & Goodrich, 2005)). Many HDACS have also been shown to associate with other proteins to form multi subunit complexes, suggesting that they function cooperatively with other epigenetic regulators

and in association with transcription factors (For recent results see (Yu et al., 2017)(Hung et al., 2018)(Y. J. Kim et al., 2016)).

Another important common trait to the writers and erasers is that they are encoded by multigene families leading to the production of multiple isoforms that controls each histone PTM. For example in Arabidopsis E(z) proteins are encoded by 3 genes, respectively CURLY LEAF (CLF), SWINGER (SWN) and MEDEA (MEA). Hence a variety of PRC2 complexes are produced, which act at distinct and overlapping developmental transition during *Arabidopsis* life cycle (Chanvivattana et al., 2004)(Kinoshita, Harada, Goldberg, & Fischer, 2001) reviewed in (Derkacheva & Hennig, 2014)(Mozgova & Hennig, 2015).

d. A diversity of mechanisms are involved in the targeting of histone writers / erasers

The molecular mechanisms responsible for the recruitment of the epigenetic writers and erasers to their specific target loci have been a long-standing question. Recent data suggest that different mechanisms may be involved (Deng et al., 2018). Although this does not appear as a general feature, some enzymes responsible for histone mark editing contain DNA binding domains, which participate in their recruitment at specific DNA consensus sequences. As an example RELATIVE OF EARLY FLOWERING (REF6), also known as Jumonji domain-containing protein 12 (JMJ12), which specifically demethylates H3K27me3 (Lu et al., 2011), recognizes a CTCTGYTY motif through its four Cys2His2 zinc fingers (Xia Cui et al., 2016)(C. Li et al., 2016). A second and more general mechanism involves transcription factors and corepressors, which can recruit epigenetic regulators through direct protein-protein interactions, or because they are partners in the same multi subunit complexes (reviewed in (Vachon, Engelhorn, & Carles, 2018)). This has been demonstrated for a number of different epigenetic regulators including PcG proteins (Yuan et al., 2016)(Xiao et al., 2017)(Zhou et al., 2018)(Roy et al., 2018)(Questa et al., 2016), Jumonji domain-containing histone demethylases (Hou et al., 2014)(Ning et al., 2015)(S. Zhang et al., 2015)(S. Cheng et al., 2018), or HDACs (N. Tang et al., 2016)(Y. Tang et al., 2017)(X. Cheng et al., 2018). Opposite, transcription factor binding at specific gene regulatory regions can induce the displacement of writers / erasers from their target loci, as demonstrates at least in two plant studies (Sun et al., 2014)(X. Luo et al., 2018). Non coding RNAs are also involved in the targeting of HPTM regulators. Indeed two long non coding RNAs play a role in the repression of Flowering Locus C (FLC) expression by PcG proteins (Heo & Sung, 2011)(D. H. Kim, Xi, & Sung, 2017a)(D. H. Kim & Sung, 2017b), participating in their recruitment through an uncharacterized mechanisms (D. H. Kim et al., 2017). Also an intronic non coding RNA was shown to be necessary for CLF dependent repression of AGAMOUS (Wu et al., 2018). Whether this mechanisms is more general remains to be demonstrated. Finally a few epigenetic regulators are recruited through their interaction with other epigenetic marks, or of histone variants, thereby generating specific epigenetic mark combinations. For example, according to the canonical model, PRC1 complexes are recruited to PcG target genes through the recognition of H3K27me3, leading to the addition of the H2Ub marks at the same loci, and to the stable repression of the corresponding genes (reviewed in (Del Prete et al., 2015)).

Altogether these mechanisms ensure that writers and erasers are recruited only at specific loci at specific times. In addition, HPTM editing can be controlled through the regulation of the production of the writers / erasers, and of their enzymatic activity.

e. Regulation of HPTM remodeling

A few epigenetic regulators are expressed at specific developmental stages or in response to precise environmental changes. For example, the E(Z), MEDEA, coding for an H3K27me3 methyltransferase, is specifically expressed in the female gametophyte, in the endosperm or in response to an infection by a pathogen (Chaudhury et al., 1997)(Spillane et al., 2000)(Yadegari et al., 2000)(Roy et al., 2018). Another example is the histone demethylase JMJ30, whose expression oscillates with a circadian rhythm and plays a role in the regulation of the period length (Jones et al., 2010)(Lu et al., 2011). Hence, as a first regulation level, cells can control the timing of epigenetic changes by a tight regulation of the synthesis of the epigenetic writers / erasers, at least in some specific cases. In addition epigenetic regulators can be post-translationally regulated through direct interactions with protein interactors For example the activity of the histone deacetylase HDA6 has been shown to be regulated by phosphorylation (Yu et al., 2017), the activity of histone methyltransferase ATX1 by O-GlcNacylation (Xing et al., 2018), and the activity of the histone methyltransferase CLF by an F-box protein responsible for protein ubiquitination (Woong et al., 2011). Moreover, as described above (part 1.3.1c), histone modifiers can also be controlled by transcription factors through a regulation of their recruitment and/or eviction to/from their target sites. On top of that, an increasing number of data suggest that HPTM are under metabolic control (for a review see: (Shen et al., 2016). Indeed, several epigenetic regulators use metabolites as substrate or cofactor, as for example histone acetyltransferases, which necessitate acetyl-coA, or histone methyltransferases, which depend on S-adenosyl-methionine availability.

As described in the above paragraph, our knowledge about the mechanisms underlying gene expression regulation through HPTM is rapidly growing, revealing a tight crosstalk between histone modifiers, chromatin remodeling complexes, and the transcription machinery (Ojolo et al., 2018). In addition multiple histone-related epigenetic regulators may be required in a highly coordinated manner for the proper control of gene expression, as it has been demonstrated for FLOWERING LOCUS C (FLC) coding for a central floral repressor in Arabidopsis (Berry & Dean, 2015)(Hepworth & Dean, 2015)(Fletcher, 2017) (Whittaker & Dean, 2017). In addition, HPTMs don't act alone, but in combination with DNA methylation, and several data suggest a functional coupling between histone and DNA methylation, including the aforementioned interaction between H3K9me2 and the DNA methyltransferase CMT3 (for reviews: (Du et al., 2015)(Torres & Fujimori, 2015)).

1.3.2 DNA methylation

DNA methylation is an important and a highly conserved epigenetic mark that has been studied in many details in fungi, animals and plants and plays fundamental roles in genome functioning and protection. It refers to the transfer of a methyl group to the fifth position of the cytosine ring of nuclear DNA to form 5 methylcytosine (5mC). In contrast to mammalian where DNA methylation mainly occurs at CG sites, in plants genomic DNA can be methylated in all cytosine sequence context, including the symmetrical CG, CHG sequence context and the non-symmetrical CHH motif (which H represents A, T or C)(Law & Jacobsen, 2010b)(He, Chen, & Zhu, 2011). Each sequence context requires different mechanisms for establishment and maintenance of DNA methylation.

a. Mechanisms of DNA methylation in plants

The mechanisms that control both initiation and maintenance of DNA methylation have received much attention in the model plant *Arabidopsis thaliana* (Matzke et al., 2015, 2014)(Law & Jacobsen, 2010b) although several studies have also been performed in crop plants including corn, rice or tomato (Corem et al., 2018)(Fu et al., 2018)(Hu et al., 2014)(Eichten et al., 2013)(Xin Li et al., 2012)(Chodavarapu et al., 2012). DNA replication which is a semiconservative process leads to the formation of hemi-methylated DNA molecules. During replication, only non-methylated cytosines are incorporated in the newly synthesized DNA strand. Cells have therefore developed specific mechanisms to fully re-establish DNA methylation patterns. In mammalian this is insured by the enzyme Dnmt1 that recognizes hemi-methylated DNA template (Law & Jacobsen, 2010a). In plants, different mechanisms that are specific to each of the sequence context for DNA methylation have been identified that fulfill these tasks (Figure I-10). The DNA Methyltransferase 1 (MET1), which is orthologous to the mammalian Dnmt1, is required for the maintenance of methylation at CG sites (Vongs et al., 1993). MET1, as Dnmt1 in mammals (Sharif et al., 2007)(Achour et al., 2007), is recruited to hemi-methylated DNA by VIM1 and 2 (Variant in Methylation 1 and 2). Both proteins contain an SRA (SET- and RING-associated) domain that mediates their binding to hemi-methylated DNA (Woo, Dittmer, & Richards, 2008)(J. Kim et al. 2014a). The CHG methylation is maintained by plant specific DNA methyltransferases, namely the Chromomethylases (CMTs), that include CMT3 in *Arabidopsis* (Bartee et al., 2001)(Jackson et al., 2002)(Bewick et al., 2017) and its maize homologue ZMET2 (Papa et al., 2007)(Du et al., 2012). CMTs contain a BAH domain (bromo-adjacent homology) and a chromodomain (Chromatin Organization Modifier) that are necessary for their binding to histone H3 when dimethylated on lysine H9 (H3K9me2). Genome wide analysis of CMT3 distribution has demonstrated that it co-localizes with H3K9me2, an interaction that seems necessary to CMT3 activity *in vivo* (Bernatavichute et al., 2008)(Du et al., 2012). So far, the current model proposes that CMT3 and ZMET2 are recruited to their targets following binding to H3K9me2, which is set up by Suppressor of Variegation Homolog 4 (SUVH4)/ KRYPTONITE (KYP), SUVH5 and SUVH6 (Jackson et al., 2002)(Du et al., 2014)(Gouil & Baulcombe, 2016). Consistent with this view, mutations impairing SUVH4/ KRYP present a dramatic reduction in both H3K9me2 and CHG methylation levels (Jackson et al, 2002)(Malagnac et al., 2002). As SUVH4/KRYP contains an SRA domain that allows its recruitment to methylated DNA, it is thought that CMTs and KRYP are working in a regulatory loop to maintain CHG

methylation (Du et al., 2014). Finally, CHG methylation and H3K9me2 interactions are further highlighted by the study of the i*bm1* mutant (Increase in bonsai methylation) that shows an increased level of both H3K9me and CHG methylation at active genes. The *IBM1* gene encodes a Jumanji type of histone demethylase necessary to eliminate H3K9me2 at genes thereby preventing CHG methylation and insuring an active chromatin state (Saze et al., 2008)(Inagaki et al., 2010). Recently in Arabidopsis, an additional CMT proteins, CMT2, was shown to maintain CHH and CHG methylation in large heterochromatin pericentromeric regions enriched in large transposons (TEs, (Zemach et al., 2013)), most likely via its interaction with the H3K9me2 histone PTMs (Stroud et al., 2014).

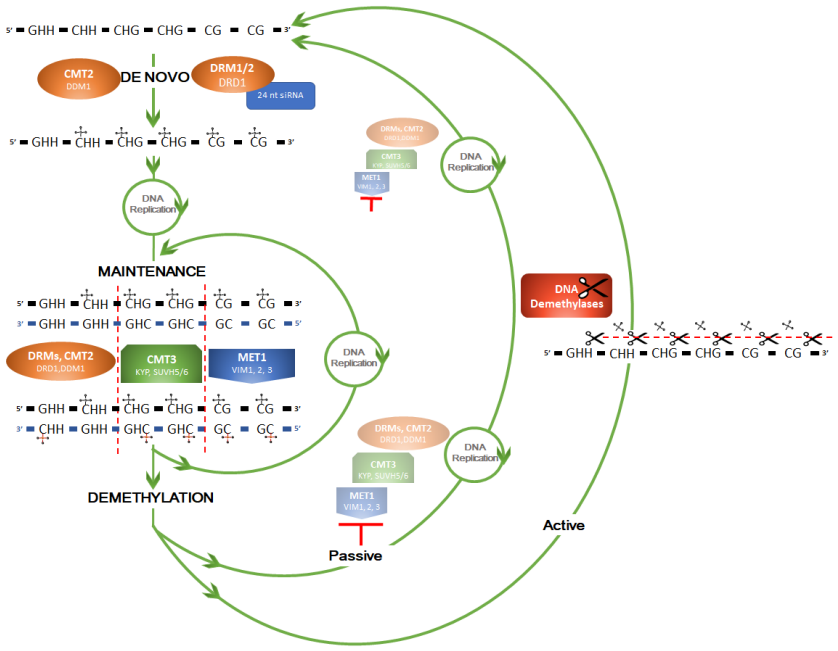

Figure I-10. Enzymes involved in regulating DNA methylation in plants.

DNA Methyltransferases and demethylases are involved in 5mC de novo methylation, maintenance methylation, and demethylation in higher plants. Names of enzymes are those identified in the Arabidopsis model. De novo DNA methylation is set up by the RNA directed DNA Methylation (RdDM) pathway involving the DRM1/2 methyltransferases, DRD1 and 24nt long small RNAs, and by the chromomethylase CMT2 with DDM1 in the CHH sequence context at heterochromatic regions (Zemach et al., 2013). After replication, newly produced DNA is hemi-methylated at CG and CHG symmetrical sites, but at the non-symmetrical CHH sites only one of the two newly synthesized DNA molecules is not methylated. Maintenance methylation in the CG context depends on MET1 and VIM1, 2 and 3, and maintenance in the CHG context is catalyzed by CMT3. CHH methylation maintenance depends both on the RdDM pathway and on CMT2 activity. Both CMTs are dependent on histone methylation mediated by KYP and SUVH5 and 6. DNA demethylation can occur passively in a replication dependent way, when the methylation machinery is not or poorly active. 5mC cytosine can be actively removed by DNA glycosylase-lyase, also called DNA demethylase, independently from DNA replication (Gong et al., 2002, Gehring et al., 2006, Ortega-Galisteo et al., 2008). Newly synthesized DNA strands are colored in deep blue. Shaded figures represent enzymes showing reduced activity. Enzymes names are from the Arabidopsis model. DRM1/2, CMT2/3 (CHROMOMETHYLASE2/3), MET1 (cytosine-DNA-methyltransferase 1), VIM1–3 (VARIANT IN METHYLATION1–3), KYP/SUVH4 [KYP/Su-(var)3–9homolog4],SUVH5/6 [Su-(var)3–9homolog5/6], DRD1 (DEFECTIVE IN RNA-DIRECTED DNA METHYLATION), DDM1 (DECREASE IN DNA METHYLATION), and 24nt siRNA (24 nucleotide small interfering RNAs).

Maintenance methylation at CHH sites as well as initiation of DNA methylation at non methylated sites irrespective to the sequence context, are both catalyzed by a third class of DNA methyltransferases, the Domain Rearranged Methyltransferases (DRMs; for a review see (Law & Jacobsen, 2010b)). These enzymes are directed to their target loci by 24 nt small interfering RNA (siRNA) in a process named the RNA directed DNA methylation process (RdDM; (Matzke et al., 2015)). The synthesis of these small RNAs have been studied in great details in the model plant Arabidopsis over the last decades and will not be discussed here as several recent reviews are available (Wendte & Pikaard, 2017)(Matzke et al., 2015) (Matzke & Mosher, 2014).

b. DNA demethylation

Although DNA methylation is a very stable epigenetic mark, reprogramming of DNA methylation patterns has been observed in various plant tissues and at specific developmental stages (Y. Li, Kumar, & Qian, 2018). DNA methylation can be either actively removed or passively lost (Figure I-10, (Law & Jacobsen, 2010b)). Passive demethylation occurs after DNA replication when non-methylated cytosines incorporated in the newly synthesized DNA strand cannot be methylated because the DNA methylation machinery is not operating. This results in a rapid dilution of methylation, in a non-specific way though, as was observed in *met1* and other mutants affected in methylation control that presented a general decrease in DNA methylation levels (Stroud et al., 2013)(Cokus et al., 2008). In contrast active demethylation, a process that has been observed during endosperm development and imprinting (Bauer & Fischer, 2011)(Schoft et al., 2011)(Hsieh et al., 2009)(Choi et al., 2002), gametophyte and gamete development (Park et al., 2016), tomato fruit ripening (R. Liu et al., 2015) and in *Medicago* for the establishment of a successful symbiosis with Bradyrhizobium (Satgé et al., 2016) can eliminate methylated cytosines at specific loci. Plant active DNA demethylation is catalyzed by bifunctional enzymes, the DNA Glycosylase Lyases (DNA GL) initially identified in Arabidopsis. The Arabidopsis genome contains four genes encoding DNA GLs namely, REPRESSOR OF SILENCING 1 (ROS1), DEMETER (DME), and two DEMETER-LIKE (DML) proteins, DML2 and DML3 (Choi et al., 2002)(Gong et al., 2002)(Penterman et al., 2007)(Ortega-Galisteo et al., 2008). ROS1 and DME display *in vitro* nicking activity on methylated DNA consistent with their DNA GL activity results in the removal and replacement of methylated cytosines via a pathway related to base excision repair (BER, (Agius et al., 2006)). Following methylated cytosine removal, this process requires the cleavage of the DNA backbone at the site of cytosine removal mediated by the AP lyase activity of ROS1, and subsequent reparation by an unknown mechanism which likely involves a putative polynucleotide kinase, a DNA polymerase and a DNA ligase (reviewed in (Y. Li et al., 2018)).

Studies in *Arabidopsis* have suggested that multiple factors may lead the DNA demethylases to their targets (reviewed in (Y. Li et al., 2018)). These include ROS3 (X. Zheng et al., 2008), R0S4 a histone acetyltransferase, also known as IDM1 (Increase in DNA methylation 1, (W. Qian et al., 2012)), the methyl CpG binding protein 7 (MBD7, (Lang et al., 2015)), the Harbinger transposon derived protein 1 and 2 (HDP1 and 2, (Duan et al., 2017) and other partners (reviewed in Li et al., 2018) that cooperate to address ROS1 to its target loci. In addition, expression of *DML* genes seems to be tightly controlled in

plants. Indeed, *ROS1, DML2* and *DML3* gene expression is rather ubiquitous in Arabidopsis (Ortega-Galisteo et al., 2008)(Penterman et al., 2007) as is the expression of the tomato *ROS1* orthologous genes, *SlDML1* and *SlDML2* (R. Liu et al., 2015). However, some of the DMLs display specific expression patterns and have been recruited for specific developmental functions. This is the case for *DEMETER (DME)* gene in *Arabidopsis* and related species which is specifically expressed in the central cell of the megagamétophyte, restricting DME activity to this cell type. Another example is the *SlDML2* gene that in addition of its general expression in young plant tissues together with *SlDML1*, is the only tomato *DML* gene strongly overexpressed at the onset of fruit ripening, which is correlated with its role in the induction of fruit ripening (R. Liu et al., 2015). Recent evidence also indicates that DNA methylation levels may also participate to controlling *DML* gene expression. This was suggested following the observation that in *Arabidopsis met1* or *rddm* mutants characterized by an hypomethylated genome, the expression of the *ROS1* gene is repressed (Mathieu et al., 2007). More recently, the *ROS1* promoter was shown to contain a 39 bp DNA methylation monitoring sequence (MEMS), that acts like a methylstat able to sense DNA methylation level and control *ROS1* expression thereby maintaining a dynamic balance between DNA methylation and active DNA demethylation (Lei et al., 2015)(Williams et al., 2015).

c. DNA methylation distribution in plants

The development of genome wide strategies to analyze DNA methylation such as Methyl DNA Immunoprecipitation (MeDIP)- seq or Whole Genome Bisulfite Sequencing (WGBS, (Yong et al., 2016)(K. Do Kim et al., 2014)(Beck & Rakyan, 2008)) has allowed determining the distribution of DNA methylation in several eucaryotes. Among these methods WGBS is considered as the golden standard method as it allows unraveling the position at one base resolution and therefore provides the most accurate view of the distribution of 5mC in eukaryotes genomes (Yong et al., 2016). As far as plants are concerned, the description of the genome wide distribution of methylated cytosines was initially reported in Arabidopsis (Cokus et al., 2008)(Zilberman et al., 2007)(Zhang et al., 2006) but an increasing number of plant methylomes has now been investigated (Niederhuth et al., 2016) including several crops such as rice (Xin Li et al., 2012b), maize (Eichten et al., 2013), or tomato (Zhong et al., 2013). Results indicate that DNA methylation levels varies significantly between species irrespective to the sequence contexts although in most cases similar rules seem to apply (Niederhuth et al, 2016)(Figure I-11). Hence, CG methylation is the highest in all species tested and can vary up to three fold between species, the lowest mCG content being found in Arabidopsis (30%) and the highest in *Beta vulgaris* (90%). In the plant species analyzed, mCHG and mCHH contents were found at lower levels than CG methylation and ranged between 9.3 and 81.2%, and between 1.4 and 18.8 %, respectively. The range of methylation variations in these two contexts is therefore much higher than the one observed for the CG context. When considering the distribution of mC within genomes, various studies have shown that the centromeric and pericentromeric regions of chromosomes, that are enriched in transposable elements (TEs) and tandem repeats are the most heavily methylated (Cokus et al., 2008)(Lister et al., 2008)(Seymour et al., 2014) although some variations between plant species were observed (Niederhuth et al., 2016). High methylation levels at transposons (TE) is consistent with 5mC being of primary importance in the control of their activity and is thought to inhibit their transcription (Cui et al., 2014).

The distribution of DNA methylation differs in genes as compared to TEs and present common features between plant species. First, early work on *Arabidopsis* has shown that only 5% of the genes were methylated within their promoter region (Cokus et al., 2008). However such studies were performed using mixture of tissues making difficult to determine the precise number of genes with methylated promoters and relation with gene expression. Since that time, other works have analyzed organ specific DNA methylation patterns in relation with gene expression profiles demonstrating an inverse correlation between DNA methylation in promoters and gene expression. For example analysis of DNA methylation during soybean seed development and maturation has allowed identifying 40, 66 and 2136 genes with changes in DNA methylation levels in the CG, CHG and CHH contexts, respectively. Most of the genes with differentially methylated regions in the CHH context showed a negative correlation between methylation and expression levels (An et al., 2017). Similarly in tomato fruits, low methylation levels at promoters of a subset of ripening induced genes has been correlated with gene expression (Lang et al., 2017)(R. Liu et al., 2015)(Zhong et al., 2013). Thus, promoter methylation is likely associated with the repression of gene expression although recent evidence suggests that the converse is also possible (Lang et al., 2017, Cheng et al., 2018, Huang et al., 2019).

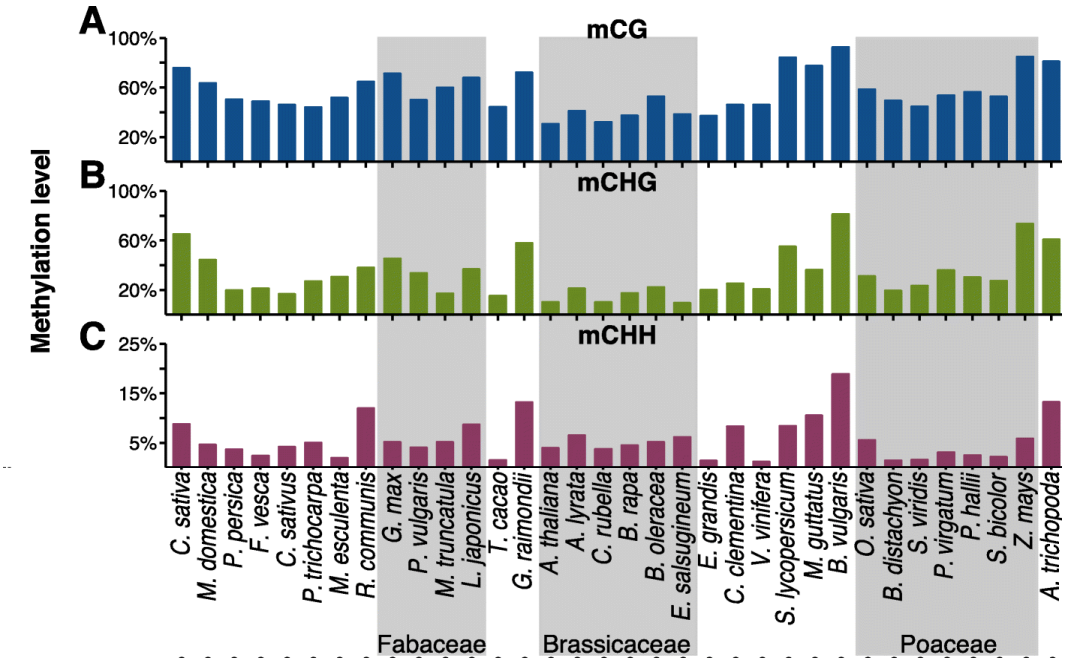

Figure I-11. Genome-wide methylation levels for different cytosine contexts (CG, CHG, and CHH). In plants, DNA methylation occurs in three cytosine contexts CG, CHG, and CHH. The distribution of methylation vary in 34 plant species (adapted from Niederhuth et al., 2015)

Noteworthy the body of genes can also be methylated, only in the CG context though. This is consistent with CHG and CHH methylation being antagonist to transcription elongation whereas CG methylation is not (Coleman-Derr et al., 2012)(Takuno et al., 2012)(Feng et al., 2010)(Zemach et al., 2010)(Zilberman et al., 2007)). For now, the function of gene Body methylation (GbM) is not understood, although more than 30% of genes are concerned in *Arabidopsis* that correspond to gene expressed in a rather constitutive and moderate way (Zhang et al., 2006)(Zilberman et al., 2007). However, some plants exist where CMT3 and GbM methylation have been lost, suggesting they are either not required for plant

viability, or can be compensated by other mechanisms (Bewick et al., 2017). However, such situations are rare which would suggest that GbM has some important functionality still to be discovered. Noteworthy GbM seems to depend on latitude in Arabidopsis which may suggest an adaptive function to the environment (Dubin et al., 2015).

These results indicate that the function of DNA methylation in plants is complex and depends both on the sequence context and localization, an idea further sustained by the analysis of DNMT mutants (Stroud et al., 2013).

Epigenetic regulations in fleshy fruits

Genetic control of ripening has been demonstrated for climacteric fruits, mainly in the tomato model, and several mutations affecting essential regulators of ripening have been described in this plant (Gapper et al., 2014). Indeed the recent discovery that epigenetic regulators are major players in the control of fruit development, ripening and senescence has deeply changed the proposed models describing the regulation of fruit development, and raises the question of the general function of such mechanisms in all types of fruits. So far, most studies have been performed on tomato (Bucher et al., 2018; Gallusci et al., 2016), but evidence are now accumulating that such regulators may be important in other types of fruits (Huang et al.,2019; Cheng et al.,2018).

1.4.1 Evidence that HPTMs are essential to fleshy fruit development

As mentioned above, HPTMs are critical to many plant development processes, and recent evidence indicate that these epigenetic marks are essential during fruit development and ripening (reviewed in (Bucher et al., 2018)(Gallusci et al., 2016)).

Genes encoding histone deacetylases (HDACs), histone acetyltransferase (HATs), histone methyl transferases (HMT) or histone demethylases (HDMTs) have been identified in several fleshy fruit species among which apple (Janssen et al., 2008), banana (Fu et al., 2018), kiwifruit (Peng et al, 2017), sweet orange (Xu et al., 2015), strawberry (Gu et al., 2016), and tomato (Cigliano et al., 2013)(Zhao et al., 2015). Studies have shown that some of the genes encoding histones modifiers are preferentially expressed in fruits, with stage specific expression patterns that depend both on fruit species and HPTM modifiers. In grapevine, genome wide analysis have revealed 7 and 13 genes coding for putative HATs and HDAC respectively, 33 genes encoding proteins containing a SET Domain, and genes encoding protagonists of PRC2s, that for some of them present expression patterns consistent with a possible involvement in grape berry development and ripening (Aquea et al., 2010, 2011)(Almada et al., 2011). Taken together, these results suggested that the corresponding proteins were recruited for the control of fruit development, ripening and abscission in fleshy fruit species. However evidence of their role in fruit

development was provided essentially by loss or gain of function studies in tomato (recent reviews (Bucher et al, 2018; Giovannonni et al, 2017; Gallusci et al, 2016)).

Early studies have focused on the tomato high pigment mutants (*hp1, hp2*) which present increased carotenoid content. The corresponding tomato genes encode 2 subunits of an ubiquitin ligase complex, namely DDB1 and DET1 respectively (Tang et al., 2016b). In human, this complex is known to target histone proteins for ubiquitination in response to DNA damages (Hu et al., 2004)(Wang et al., 2006). In tomato, by impeding light signal transduction through preventing the ubiquitination of H2B histones (Benvenuto et al, 2002)(Lieberman et al., 2004), these mutations may affect the transcriptional repression of genes involved in the production of carotenoids and other compound, therefore generating the enhanced pigmented fruit phenotype. In addition, silencing studies were conducted in tomato on different components of the histone modifier complex PRC2 (Polycomb repressive complex 2). Silencing studies were conducted to repress genes encoding the Enhancer of Zeste EZ1 and EZ2 proteins (How-Kit et al. 2010)(Boureau et al., 2016) and the FIE protein (Fertilisation Independent Endosperm Development (Liu et al., 2012b), and revealed essentially roles during flower formation and early fruit development (reviewed in Bucher et al, 2018; Gallusci et al, 2016). In a more recent work, impairment of MSI1 (Multi Suppressor of Ira 1) a putative component of the tomato PRC2s, was shown to affect fruit ripening (Liu et al., 2016b). However MSI1 is also a member of the FAS complex involved in chromatin assembly. As none of the other PRC2 components do affect fruit ripening when repressed, it is more likely that the effect on ripening is due to the FAS complex than to PRC2 activity. Indeed FAS activity might be of primary importance in tomato fruits due the high endoreduplication level achieved (Teyssier et al., 2008). Finally, other studies have shown that the control of histone acetylation is also important to fine tune the ripening induction. For example plants with reduced activity of various HDACs, present delayed carotenoid accumulation and ripening ((Guo et al., 2017a)(2017b)) or an opposite effect on both processes (Guo et al., 2018).

Evidence of the role of HPTMs in fruits was further provided in the frame of the fruit ENCODE project that aimed at analyzing the evolution of fleshy fruit ripening control in angiosperm. Combined genetic and epigenetic approaches was implemented on 13 different fruit species including (i) climacteric fruit species (tomato, apple, pear, banana, melon, papaya, an peach), (ii) non-climacteric fruit species (grape, strawberry, cucumber and water-melon) and (iii) dry fruit species (Arabidopsis and Rice) (Lü et al., 2018). The project allowed generating multidimensional dataset based on transcriptomic, DNA methylation and histone PTMs with a focus on H3K27me3 and H3K4me3 profiles to decipher genetic and epigenetic events controlling fruit ripening (Lü et al., 2018). In this context, researchers focused on key molecular players involved in ethylene-dependent ripening circuits in climacteric fruit and their orthologues in non-climacteric and dry fruits. Although global and locus specific DNA methylation changes were observed in all fruit species during ripening induction, DNA demethylation was suggested to be only required for tomato ripening. However these conclusions were based on correlative studies without any functional foundation, and are not consistent with the recent demonstration that in addition to tomato fruit ripening (see below, (R. Liu et al., 2015)(Lang et al., 2017)), strawberry and sweet orange fruit ripening is also under DNA methylation control although different mechanisms are operating (Cheng et al., 2018) (Huang et al., 2019). In contrast, Lü et al (2017) suggested that, instead of DNA methylation, the

repressive mark H3K27me3 may play a conserved – and maybe central – role in regulating fruit ripening, although its precise function and importance may vary between fruit species. Indeed, for a few ripening related genes, a correlation was found between their induction during ripening and the removal of H3K27m3 in several fruit species, therefore suggesting an ancestral inherited role for this mark in angiosperm fruit ripening (Lü et al., 2017). Interestingly, a recent study indicates that H3K27me3 may be involved in the control of Methoxypyrazines (MPs) in grape fruits, a compound known to contribute to the herbaceous characters in wine (Battilana et al., 2017). MPs biosynthesis depends on the expression of the *VvOMT3* gene which encodes a protein controlling the final and key step of this biosynthetic pathway in grape. However, MP accumulation is variety dependent. For example berries from Cabernet Sauvignon accumulate MPs, but those of Pinot Meunier dwarf do not. Recent study have shown the mark H3K27me3 is abundant at the *VvOMT3* locus in Pinot Meunier dwarf but not in Cabernet Sauvignon berries (Battilana et al., 2017), suggesting that H3K27me3 inhibits VvOMT3 gene expression resulting in the inhibition of MP biosynthesis. Although these results are consistent with an important role of H3K27me3 in fruit ripening control this mark does not seem to be critical for ripening in all fleshy fruit species (How-Kit et al. 2010)(Boureau et al., 2016)(Liu et al., 2012b). The characterization of PRC2 mutants or of mutants affected in the removal of the H3K27me3 mark will now be necessary to better assess the importance of this epigenetic mark in modulating the epigenetic landscape and its consequences on gene expression and fruit phenotypes

1.4.2 Genome wide DNA methylation reprogramming is critical to fruit ripening

a. DNA methylation role in fruit development and shape

At the present time, very few studies have investigated the possible role of epigenetic mechanisms in the control of the organogenesis and early development of fruits. However there are a few examples showing that DNA methylation is likely part of the regulatory networks that control fruit shape and size. One recent examples is provided by the analysis of the mantled phenotype in Oil palm *(Elaeis guineensis*) that was identified in plants generated by somatic embryogenesis (Rival et al., 1998). Oil palm plants with the mantled phenotype are characterized by the development of flowers with carpeloid structures in place of male organs leading to various phenotypes ranging from normal looking fruits to very small fruits (Dussert et al., 2000). This phenotype was recently shown to be due to the hypo-methylation of Karma-like Line retrotransposon located within an intron of the *DEFICIENS* (*DEF*) gene. Normal fruits develop when the Karma retrotransposon is methylated, whereas its hypo-methylation leads to the mantled phenotype due to the inhibition of *DEF* splicing (Ong-Abdullah et al., 2015) For tomato, impairing DNA demethylases inhibits ripening (see below, part 1.4.2b), but in addition some lines also presented abnormal flower and fruit shape. More particularly fruits presented an important increase in locule number that resulted from an increased number of carpels formed during flower development (R. Liu et al., 2015). It is however still unclear whether this effect is a direct or indirect consequence of a deficient demethylation process.

A final example comes from the analysis of apple fruit development. Double haploid apple varieties have been generated that developed fruits with contrasted sizes that were correlated to cell number in the fruits (Daccord et al., 2017). Interestingly both varieties had very similar genomes that only differed by a limited number of single nucleotide polymorphisms (SNPs). In contrast 294 differentially methylated regions (DMRs) were identified close to genes that have been suggested to be involved in fruit growth and development. Indeed a causal relationship between some of these DMRs and difference in fruit size is still missing, but at least two of these DMRs are located in the vicinity of candidate genes that were shown to participate in fruit size control in other plant species (Daccord et al., 2017).

b. Evidence that DNA methylation is critical to fruit ripening

DNA methylation changes were first documented in tomato decades ago by Hadfield (Hadfield et al., 1993) that showed that genes induced at the onset of fruit ripening had changes in their methylation state. Since that time, the description of the *Colorless Non Ripening* (*Cnr*) epimutation provided compelling evidence that DNA methylation control is essential to fruit ripening(Figure I-12) (Manning et al., 2006). Fruits of the *Cnr* epimutant are characterized by a severe reduction in ethylene production, an inhibition of fruit softening, and a lack of carotenoid synthesis and accumulation (Thompson et al., 1999) (Eriksson et al., 2004). The *Cnr* epimutant phenotype is very stable, and reverting sectors were only observed on 3 individual fruits on independent plants from more than 3000 plants. This allowed the positional cloning of the *CNR* locus that was shown to contain only one gene differentially regulated between *Cnr* and WT fruits, yet without any sequence differences between both genetic backgrounds (Manning et al., 2006). This gene which encodes a SQUAMOSA Promoter Binding protein-like (SBP-box/SPL) transcription factor, presented a 286 bp long hypermethylated region located 2.3kb upstream of the TSS. Hyper-methylation was only found in the *Cnr* background, and resulted in *CNR* gene repression and blocking of fruit ripening (Manning et al., 2006). Additional evidence that methylation upstream of the promoter was responsible for the repression of the *CNR* gene, was provided using Virus Induced Gene Silencing (VIGS) to repress the expression of the tomato *CMT3* gene in the *Cnr* background that allowed reversing the *Cnr* phenotype to WT, whereas the same approach using M*ET1* or the *DRM* genes had much weaker effects (W. Chen et al., 2015). This approach was sufficient to reduce methylation at the CHG sites located in the hyper-methylated 286-bp region of the *LeSPL-CNR* promoter, and increase the expression of LeSPL-CNR indicating that the methylation of LeSPL-CNR gene in the Cnr background requires the a functional maintenance methylation machinery. Hence maintenance of methylation at the *Cnr* locus is necessary for the somatic stability of the epimutation (W. Chen et al., 2015). Since the description of *Cnr*, other studies have led to the identification of epialleles in tomato. They include the demonstration that variations in Vitamin E content of tomato fruits are determined in part by the methylation level of the promoter region of *VTE3,* a gene which encodes a 2-methyl-6-Phytylquinol methyltransferase, responsible for an essential step in tocopherol biosynthesis (Quadrana et al., 2014). Methylation variations were observed between tomato accession that were correlated with changes in VTE3 gene expression and fruit Vitamin E content. Additional epialleles were also identified in the progeny of crossings between M82, a commercial tomato accession, and *Solanum penellii*, a wild tomato relative (Gouil et al., 2018). However, the stability of the newly generated epialleles was not

established in this later case. Epialleles that determine the color of the skin were also found in apple and pear (El-Sharkawy et al., 2015)(Wang et al., 2013)(Telias et al., 2011). In both cases, hyper-methylation of the promoter region of *MYB10* gene was associated with repression of the gene and of anthocyanin biosynthesis in the skin. Interestingly, somatic embryogenesis was also shown to generate epialleles in oil palm with important impact on agronomical traits of the plants (Ong-Abdullah et al., 2015).

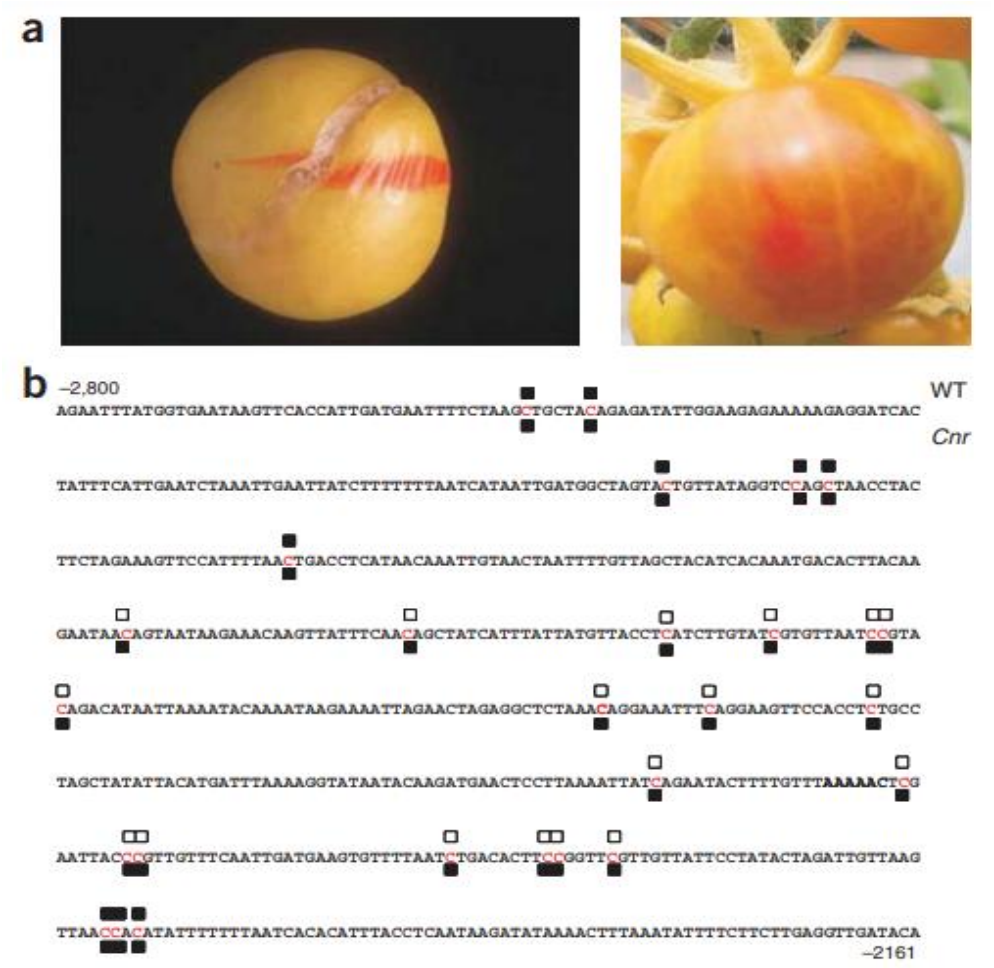

Figure I-12. A naturally occurring epigenetic mutation Cnr. (A) Revertant sectors occasionally seen on mature Cnr fruits. (B) Location of methylated cytosines in DNA from wild-type (boxes above sequence) and Cnr (boxes below sequence) fruit in a 286-bp contiguous region upstream of the predicted ATG start codon of ORF 7, the SQUAMOSA promoter binding protein–like gene, as determined by bisulfite sequencing. Unmarked cytosines were unmethylated in both wild-type and Cnr. The cytosines in this region that are fully methylated in all individuals carrying the Cnr phenotype are shown as filled boxes; these cytosines are largely unmethylated in wild-type fruits (open boxes). Other methylated cytosine residues outside the 286-bp contiguous region showed no association with the fruit phenotypeDNA methylation reprogramming in fleshy fruits (Manning et al.,2006).

Analysis of the global DNA methylation level at different stages of tomato fruit development indicated that the total content in 5meC decreased in the pericarp of tomato fruits from 29.9% at the breaker stage to 20.1% at the red ripe stage (Teyssier et al., 2008). This decrease in DNA methylation level was confirmed by whole-genome bisulfite sequencing (WGBS) of the tomato fruit genomic DNA at four developmental stages, namely immature green, breaker, turning and fully ripe fruits of WT plants and also at two stages in the *Cnr* and *ripening inhibitor* (*rin*) mutant genetic background, both impaired in the ripening process (Zhong et al., 2013). Results indicated that in addition to a decrease in methylation level at CG sites observed in TEs rich regions, DNA methylation was also reduced at promoter of genes that are induced during fruit ripening, including genes encoding proteins with important role in this process, such as the *CNR*, the *RIN* or the *NOR* genes (reviewed in (Bucher et al., 2018)(Giovannoni et al., 2017) (Gallusci et al., 2016)).

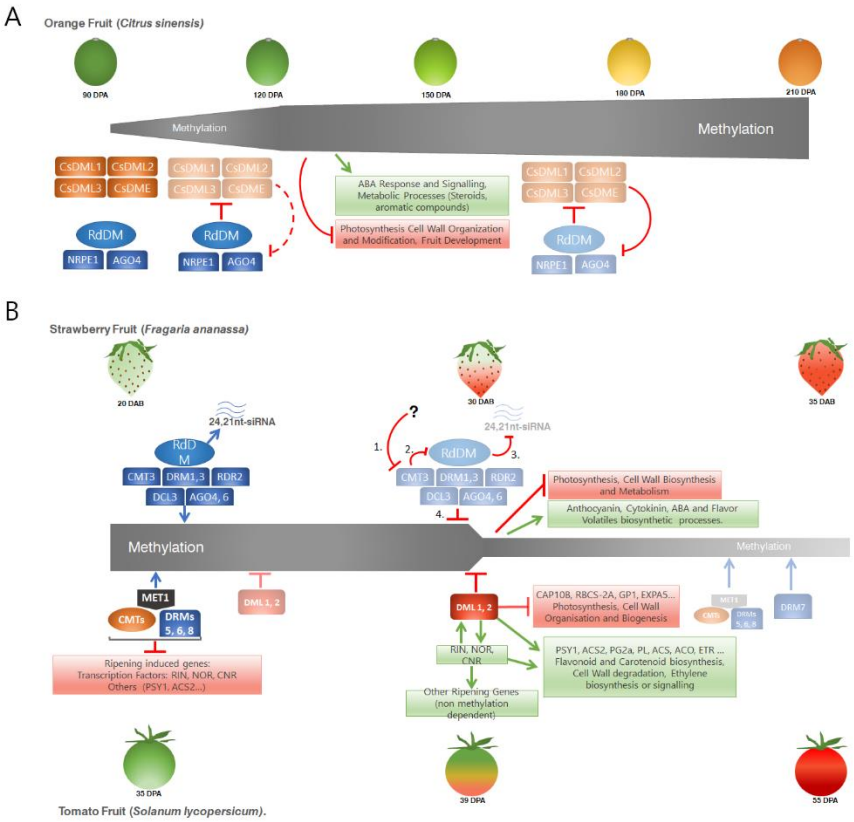

Figure I-13. Diversity mechanisms of DNA methylation in controlling flesh fruit ripening.

(A) Function of DNA methylation in sweet orange fruits: *Genomic DNA methylation increases from 13% of total cytosine in 90 dpa old sweet orange fruits to 14.5% in 210 DPA old fruits. Increase I DNA methylation is correlated with the gradual decrease in the expression of DNA demethylase (DML) genes and of genes involved in the RNA directed DNA Methylation pathway (NRPE1, AGO4). Ripening associated hyper-methylated regions were associated with hundreds of genes normally expressed at early stages of fruit development, as those involved in photosynthesis, but also with the induction of several genes involved in orange fruit ripening. Results suggest that DNA methylation is critical to ripening of sweet orange fruits, as confirmed by the ripening inhibitory effect of Aza-Cytidine an inhibitor of genomic DNA methylation. Up and down regulated Processes shown on the figure are respectively associated with DEGs correlated to hyper-DMR (gain of methylation during ripening; Huang et al, 2018).*

***(B) Function of DNA demethylation in strawberry fruits and in tomato fruits**: Genomic DNA methylation in young strawberry immature fruits is 7.5% and decreases during fruit ripening. Loss of methylation occurs at genes involved in the ripening process (anthocyanin accumulation, secondary compounds synthesis,..), suggesting that demethylation is necessary for ripening induction. Consistent with this view, fruit treatment with Aza-cytidine results in early ripening. Reduction of methylation was correlated with the reduction of the expression of genes involved in the RdDM pathway, and with reduced accumulation of short interfering RNAs of 24 nt. In contrast DNA demethylases encoding genes are not induced.*

Genomic DNA methylation decreases from 30% of total cytosine in young immature fruits to 20% in red ripe fruits (Teyssier et al, 2008). Decrease in DNA methylation correlates with up-regulation of SlDML2 one of the tomato DNA demethylases. Genes encoding RIN, NOR, CNR transcription factors that control fruit ripening and other genes encoding enzymes necessary to ripening (Phytoene Synthase 1, Polygalacturonase, etc..) have hyper-methylated promoters and are repressed in immature green tomato fruits (Liu et al, 2015, Lang et al, 2017). Some of the genes involved in photosynthesis are expressed in young fruits even though their promoter is methylated at this stage (Lang et al, 2017). Reduction of DNA methylation that occurs at the onset of fruit ripening, necessitates the expression of the SlDML2 gene (Liu et al, 2015), and correlates with the reduced expression of genes involved maintenance DNA methylation (Teyssier et al, 2008). Demethylation occurs in the promoter region of many of the genes encoding the CNR, RIN and NOR transcription factors, as well as of genes involved in carotenoid (Phytoene Synthase 1), ethylene synthesis (Acc Synthase 2) and cell wall metabolism (Polygalacturonase, etc..), among others and is associated with their expression and fruit ripening (Liu et al, 2015; Lang et al, 2017). For some genes (CAP10, RBCS, ..) demethylation was correlated with gene repression (Lang et al, 2017).

SlMET1 (cytosine-DNA-methyltransferase1), CMT(CHROMOMETHYLASE), DRM(DOMAIN, REARANGED METHYLTRASFERASE), DML (DEMETER LIKE DMETHYLASE), PSY1 (PHYTOENE SYNTHASE 1), ACS2 (ACC SYNTHASE 2), RIN (RIPENING INHIBITOR), NOR (NON RIPENING), CNR (COLOURLESS NON RIPENING).

Genes in boxes with intense colors (orange, blue or grey) are strongly expressed. Those in boxes with pale colors are weakly expressed. Green arrows indicate activation, and red bars repression. Repressed processes and genes are indicated I red, and those activated in green.

Noteworthy, CHH methylation is high in tomato (11% in ripe fruits, 13% in non-ripe fruits and 8.3%; leaves (Zhong et al., 2013) as compared to previously described CHH methylation levels in *Arabidopsis* (1.5%, (Cokus et al., 2008)) and in other plants (Niederhuth et al., 2016), and was found higher in fruits. Higher CHH methylation levels in fruits was correlated with enhanced expression of selected DRMs at specific phases of fruit development (Teyssier et al., 2008) and to 24nt siRNA accumulation (Zhong et al., 2013). With the aim to investigate the mechanisms underlying the loss of genomic DNA methylation occurring at the onset of fruit ripening, Liu et al (R. Liu et al., 2015)have identified 4 tomato genes encoding putative DNA demethylase. One of them, *SlDML2* was strongly upregulated at the onset of ripening, simultaneously to the decrease in DNA methylation. Inhibition of *SlDML2* gene expression using RNAi and VIGS strategies (R. Liu et al., 2015) or by Crisper Cas9 mediated mutagenesis (Lang et al., 2017) indicated that SlDML2 is an absolute requirement for tomato fruit ripening to occur. Ripening inhibition was associated with the repression of genes encoding the RIN, NOR and CNR transcription factor that play major role in the induction of tomato fruit ripening (R. Liu et al., 2015)(Lang et al., 2017), Figure I-13B). Of note, the promoter region of these transcription factors is normally demethylated during fruit ripening, whereas, loss of DML2 function was associated with the absence of demethylation and gene repression. A similar situation was observed at 600 ripening induced genes that failed to be expressed and remained hypermethylated in their promoter region. Interestingly, 598 other hypermethylated genes normally repressed during the ripening of wild type tomato fruit, maintained their expression level in the mutant background ((Lang et al., 2017),Figure I-13B), suggesting that DNA methylation is also associated with gene expression in tomato fruits.

It was recently suggested, in the Frame of a Fruit Encode project that DNA demethylation might not be a general process controlling fleshy fruit ripening and dry fruit maturation, in contrast to H3K27me3 (Lü et al., 2018). However, recent works indicate that DNA methylation control is likely important in other fruits as well. The recent description of the strawberry fruit methylome indicated that fruit genomic DNA becomes massively demethylated during the ripening process ((Cheng et al., 2018), Figure I-13B), as observed in tomato (Teyssier et al, 2008; Zhong et al, 2013). Demethylated regions were enriched at ripening related genes induced during ripening suggesting a direct link with the expression of ripening induced genes, consistent with the demonstration that the treatment of strawberry fruits with a demethylating agent accelerates fruit ripening (Cheng et al., 2018). Interestingly, in strawberry, no demethylase encoding gene could be identified that was involved in the loss of methylation. Decrease in methylation was rather associated with repression of the RdDM pathway that could in turn lead to demethylation at specific loci (Cheng et al., 2018). In a more recent study, Huang et al (Huang et al., 2019)(Figure I-13A) have analyzed the changes in genomic DNA methylation in the skin of orange fruits and demonstrated a general increase in DNA methylation along with fruit development and ripening. Inhibition of methylation by means of azacytidine a demethylating agent resulted in delayed ripening indicating that increase in DNA methylation is necessary for orange fruit ripening to occur ((Huang et al., 2019),Figure I-13A). Taken together these results highlight the general importance of DNA methylation control in fleshy fruits, even though it becomes clear that a diversity of mechanisms are operating depending on the plant species under study.

1.4.3 Interaction between hormones and epigenetic regulations in fleshy fruit development and ripening

Other important regulatory pathways, including hormones and transcription factors, are operating to control fruit ripening and their complex interactions with chromatin based regulations needs to be investigated. Indeed, several recent work have illustrated that hormones signaling may involve an epigenetic component (Yamamuro et al., 2016), but very few studies have addressed this question in fruits so far (Zuo et al., 2018)(Lü et al., 2018).

As far as fruit development is concerned, fruit set is known to be under hormonal control, and a diversity of hormones plays a critical role in this process. They include auxins, gibberellic acids or cytokinins that can promote parthenocarpic fruit development when applied alone, although their combined action appears much more efficient both in dry and fleshy fruits (for recent reviews, (Joldersma et al., 2018) (Kumar et al., 2014)). The involvement of epigenetic regulation during this developmental phase is still poorly studied. At present, evidence is mounting that PRC2 complexes might be involved is this process as illustrated by elongation of fruit in the absence of fertilization in *Arabidopsis* PRC2 mutants (Goodrich et al., 1997) and on parthenocarpic fruit development in tomato (Liu et al., 2012a). However, it is not clear whether PRC2s control fruit elongation directly or through auxin signaling. Consistent with the later, it has been shown that genes involved in auxin biosynthesis or signaling, are enriched in the H3K27me3 repressive mark, which is set up by PRC2s (Lafos et al., 2011). In addition, *met1* mutants show an elongation of fruits without pollination, suggesting that DNA methylation maintenance is necessary to

prevent fruit development in the absence of fertilization (FitzGerald et al., 2008). In this case, interaction with hormonal regulations has not been investigated, even though interplay between PRC2 and DNA methylation has been suggested in the mega-gametophyte of *Arabidopsis* developing flowers (Schmidt et al., 2013). Hence auxins, DNA methylation and histone marks could control the induction of seed and fruit development in a coordinate manner.

When considering fruit ripening control, the role of hormones vary between fruit types, ethylene being the major player in climacteric fruits, whereas ABA appears to have a more prominent role in non-climacteric fruits (McAtee et al., 2013) including grape (Fortes et al., 2015). Yet, the relationship between hormonal and epigenetic regulations in fruit ripening control is still poorly investigated. As far as histone PTMs are concerned, a recent study performed in banana has shown that the *ETHYLENE RESPONSE FACTOR11 (MaERF11),* a negative regulator of banana fruit ripening, may recruit the MaHDA1 HDAC at the promoters of the *MaEXP2, MaEXP7* and *MaEXP8*, and *MaACO1* genes in immature green fruits (Han et al., 2016). This would result in deacetylation and repression of these genes, before ripening induction, an effect that would be relieved by the massive synthesis of ethylene occurring at the onset of ripening (Han et al., 2016). HDACs were also suggested to interact with ethylene to regulate gene expression involved in longan fruit senescence (Kuang et al., 2012). There is however stronger evidence that ethylene and DNA methylation interact to control fruit ripening, at least in the tomato (R. Liu et al., 2015), and genes involved in ethylene biosynthesis are missregulated in *Sldml2* tomato mutants (Lang et al., 2017). Inversely, tomato plants affected in ethylene signal transduction were shown to have deeply modified fruit methylation patterns, consistent with a loop regulation between DNA methylation/demethylation and ethylene biosynthesis in tomato fruits (Zuo et al., 2018).

As far as non-climacteric fruits are concerned, ABA is thought to play a much more prominent role in the control of fruit ripening (McAtee et al., 2013). A recent work has shown that in strawberry, some of the ABA biosynthetic genes are indeed hypomethylated in their promoter region and present an enhanced expression during ripening (Cheng et al., 2018). However, there is no evidence of a causal interaction between ABA synthesis or transduction signal and variations in DNA methylation at these genes. Additional work is now necessary to determine the functional links between both processes.

Objectives of the PhD project

A general question that derives from the study of DNA methylation function in tomato, sweet orange, and strawberry (Liu et al., 2015; Lang et al., 2017; Cheng et al., 2018; Huang et al.,2019, see introduction part 1.4.2b, page 42) is to which extend DNA methylation is a general mechanisms that control fleshy fruit ripening in general. As far as grape is concerned, there was no evidence at the time of the initiation of my thesis project of a possible role of DNA methylation in grape berries.

Therefore, the general objectives of my thesis project were to study, which extend DNA methylation is involved in the control of grape berry ripening, and more specifically to determine what ripening specific processes might be under methylation control. Indeed an important question is whether epigenetic mechanisms similar to those describe in tomato, or in other fleshy fruit species other are also operating in grape berries. An additional objective was to determine whether the accumulation of anthocyanins, a secondary compound of high importance in grape berries, is controlled by DNA methylation.

To address these questions, my thesis project has been separated in two complementary parts:

1.5.1 Analysis of the role of DNA methylation in grape berry ripening:

To address the question of the role of DNA methylation in grape berry, we have developed two complementary approaches.

- First, we have investigated the variations of DNA methylation levels, gene expression and metabolic content between two different berry tissues, the pulp and the skin, at two different developmental stages, before and after the induction of ripening. This aims at correlating changes in gene expression and in metabolic abundance with variation of DNA methylation at genes. In addition, we wish to compare the general distribution of DNA methylation over the genome between specific tissues of the berry and determine eventual tissues specific DNA methylation signature related to the ripening process (chapterII: 2.3.2; 2.3.3; 2.3.4)

- To determine the potential role of DNA methylation, a second approach is aimed at interfering with DNA methylation during berry development and ripening. To this aim DNA methyltransferase inhibitors were used to treat *in vitro* cultured grape berries (chapterII: 2.3.1). In addition, I have initiated , in collaboration with the group Of M Malnoy (Department of Biology and Genomic of Fruit Plants, Foundation Edmund Mach, Italy) to generate grape with reduced expression of MET1, (involved in CG methylation maintenance), and of DMLs (involved in active DNA demethylation) using an RNAi approach.

1.5.2 The use of in vitro grape cell culture as a model system to evaluate the potential role of DA methylation on anthocyanin synthesis in grape cells

As mentioned in the introduction (see part 1.2.2, page20) accumulation of anthocyanin is the skin of berries is one of key biological processes related to berry ripening and quality in red grape cultivars. We have taken advantage of grape cell suspension vs. Gamy Teinturier, a grape cultivar that accumulate anthocyanin when cultured in light (Cormier et al.,1996), to investigate the possible consequences of DNA methylation inhibition on anthocyanin accumulation. To this end GT cells were cultivated in the presence or absence of light and treated with zebularine, a potent DNA methyltransferases inhibitor.

A summary of the strategies developed is shown in Figure I-14.

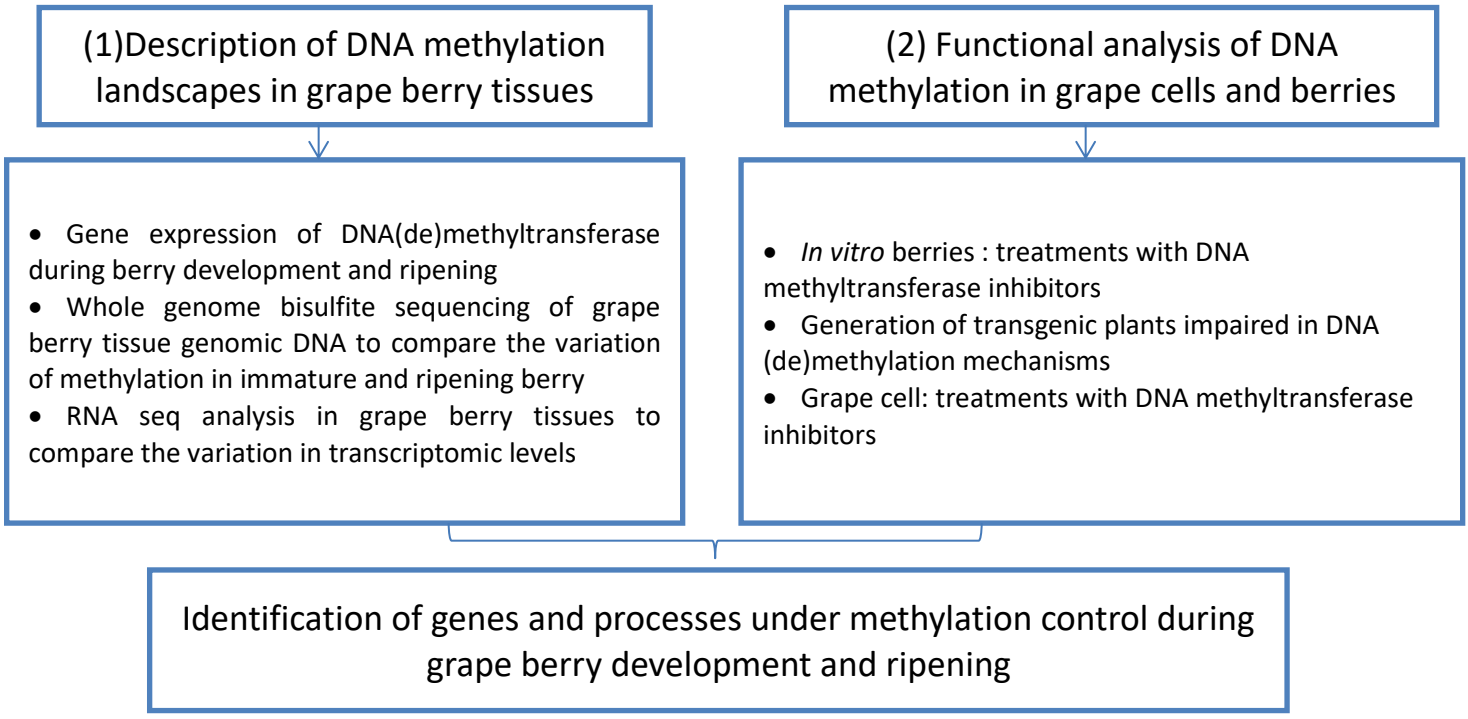

Figure I-14.Overviews of the strategies developed to study the function of DNA methylation in grape berries. Complementary approaches were developed with the aim (1) to unravel the variations of DNA methylation in grape berry tissues and correlation with changes in gene expression and metabolic content during ripening; (2) in terfere with DNA methylation processes in grape berries and in grape cells to determine the functional importance of DNA methylation.

CHAPTER II

Analysis of genomic DNA methylation variations and roles during grape berry ripening

Abstract

DNA methylation is a conserved epigenetic modification that is involved in the control of gene expression and transposon mobility. Studies in *Arabidopsis* and other plants have demonstrated that variation in DNA methylation level and distribution contributes to control a diversity of plant developmental processes and stress responses. Recent reports revealed that DNA (de)methylation is a key regulator of fleshy fruit ripening, in tomato, sweet orange and strawberry. But the function of DNA methylation in grape berry ripening has not been investigated. To address this question we have analyzed the methylome, transcriptome and metabolite composition of grape berry tissues: pulp and skin separately. We observed both tissue specific and coordinated changes in metabolite composition and transcription patterns during fruit development and ripening. However, in contrast to all the fruit species analyzed so far that showed extensive DNA methylation modifications, changes in methylation level and distribution detected in grape berry tissues during ripening were much more limited. However results indicate a moderate increase in DNA methylation level as illustrated by a higher number of hyper- than hypo-methylated DMRs in ripe berries compared to immature berry. Correlation analysis between change in methylation level in promoters of genes and gene expression did not reveal significant relationship between both. However, application of DNA methylation inhibitors to young berries impaired ripening, suggesting that DNA methylation is indeed involved in the control of berry ripening. In summary, DNA methylation is likely involved in the control of grape berry ripening but it has limited effect on gene expression at the stages analyzed in this work.

Introduction

Grape is a worldwide cultivated fruit crop with high economic importance. Grape berry, which is a non-climacteric fruit, develops following a double sigmoidal growth pattern with two phases of rapid growth separated by a lag phase at the Véraison stage. Grape berries at these different developmental phases present clearly distinct features of size, color, texture and metabolic composition (Coombe et al.,1995) (Waters et al., 2005). The first growth phase is characterized by a rapid increase in berry size and weight resulting from intense cell divisions during the first 2 weeks after fertilization and continuous cell expansion in the following 60 days. Two main organic acid, tartrate and malate are synthesized and accumulated their maximum level during this phase I, as well as the precursors of phenolic volatiles, such as tannins, amino acid and hydroxyl cinnanic acid (Deluc et al., 2007)(Conde et al., 2007)(Kennedy et al., 2002)(Kennedy et al., 2000). The lag phase is characterized by the initiation of soluble sugar accumulation concomitantly to the reduction in organic acid content. During this lag phase, berry turns white-green with a reduction of tits photosynthesic capacity and seed reach maturity (Deluc et al., 2007) (Palliotti et al., 2009). Véraison marks the beginning of ripening, which is characterized by berry softening and color acquisition in red cultivars. Following, berries enter the second rapid growth phase, during which their size and weight double. This phase is also characterized by complex and diverse metabolic changes, including soluble sugar accumulation, water influx, anthocyanin accumulation in red berries, and the synthesis of a diversity of flavor compounds and volatile aromas that contribute to berry quality (Robinson et al., 1992). All these changes make berry edible and attractive to seed dispersal (Conde et al., 2007). Of course, pulp and skin are two distinct tissues characterized by important differences in metabolic composition and following distinct developmental processes (Lijavetzky et al., 2012)(Grimplet et al., 2007).

Fleshy fruits have been separated in two groups based on the mechanisms that control ripening. Climacteric fruits such as tomato are characterized by an intense respiratory burst concomitantly to a sudden increase in ethylene synthesis occurring prior to fruit ripening induction. In contrast, non-climacteric fruits among which grape and strawberry do not have specific physiological event associated with ripening induction (reviewed in (Bapat et al., 2010)). Indeed in the case of grape, both ethylene and ABA have been shown to be involved in the control of ripening (Fortes et al., 2015). In addition, evidence that genetic control plays a major role in ripening induction of climacteric fruit has been accumulating over the last decades, mainly using the tomato model, and several mutants impaired in the ripening process have been isolated in this plant (Gapper et al., 2014). More recently, epigenetic mechanisms have been demonstrated to contribute to control fruit development and ripening, suggesting that this new layer of regulation may bridge the mechanisms controlling ripening in both climacteric and non-climacteric fruits. Although initial studies are limited to tomato, (Bucher et al., 2018)(Gallusci et al., 2016), recent evidence indicates that epigenetic regulations, essentially DNA methylation, but also histone marks are important in other types of fruits (Bucher et al., 2018), such as sweet orange (Huang et al., 2019) and strawberry (Cheng et al., 2018).

DNA methylation refers to the transfer of a methyl group onto the C5 position of the cytosine to form 5-methylcytosine (5mC). Details of mechanisms involved in DNA methylation regulations have been developed in the general introduction (part1.3.2a, page 32). Briefly, in plants, DNA methylation exists in all sequence contexts, CG, CHG, and CHH (where H = A, C, or T). Three main types of DNA methyltransferases control DNA methylation homeostasis in plants: methylation at new sites in all sequence context, also referred to as *de novo* methylation is set up by Domain Rearranged Methyltransferases (DRMs), that are guided by small RNA in a process called RNA directed DNA methylation (Zhong et al., 2014). DRMs are also necessary to maintain methylation in the CHH context in gene rich regions (Zemach et al., 2013), whereas another enzyme the Chromomethylase 2 (CMT2) is responsible for CHH methylation maintenance in heterochromatic regions (Stroud et al., 2014). Once methylation established, the Methyltransferase 1 (MET1) is necessary for DNA methylation maintenance in the CG context (Kankel et al., 2003) and the chromomethylase3 (CMT3) in the CHG context (Lindroth et al., 2001)(Cao et al., 2002). Also considered as very stable epigenetic mark, DNA methylation can passively lost or actively removed (Law & Jacobsen, 2010). Limited methylation maintenance activity or reduced availability of methyl donor during DNA replication can result in passive demethylation(Cokus et al., 2008) (Law & Jacobsen, 2010). Whereas active demethylation is controlled by plant specific enzymes, called the DNA glycosylase Lyase or DNA demethylases (Agius et al., 2006)(Gong et al., 2002)(Choi et al., 2002).

A detailed description of the role of DNA methylation in fruits is provided in the general introduction (see part1.4.2b page40). Initial evidence that DNA methylation is provided by the description of Cnr epimutation that resulted in ripening inhibition (Manning et al., 2006). More recently, the demonstration that global DNA methylation dropped from 30% to 20% during tomato fruit ripening suggested that DNA demethylation could be critical to fruit ripening (Teyssier et al., 2008). Consistent with this view, the use of 5-azacyditine, a potent DNA methyltransferase inhibitor to treat immature fruits resulted in premature ripening induction (Zhong et al., 2013). It is now clearly established that active DNA demethylation mediated by the *SlDML2* gene plays a critical role in ripening induction (Liu et al., 2015)(Lang et al., 2017). This gene, which is dramatically up regulated at the onset of fruit ripening, encodes a DNA Glycosylase Lyase necessary for the demethylation of essential transcription factors controlling fruit ripening as well as of hundreds of genes that participate to the various processes involved fruit ripening such as carotenoid accumulation, ethylene synthesis and many others (Liu et al., 2015)(Lang et al., 2017). Evidence of the role of DNA methylation was also provided by the analysis of sweet orange (Huang et al., 2019) and strawberry (Cheng et al., 2018) fruit development, although different mechanisms might be operating. Of course in the strawberry fruits genomic DNA is extensively demethylated during the ripening process, a situation similar to the one previously described in tomato (Cheng et al., 2018)(Teyssier et al., 2008)(Zhong et al., 2013). Several hundreds of genes that are induced during ripening are demethylated, suggesting a direct link between their expression and their methylation status. This is also consistent with the demonstration 5-Azacytidine treatment of strawberry fruits accelerates fruit ripening (Cheng et al., 2018). Demethylation is not mediated by DNA demethylase in strawberry, but is rather correlated with repression of the RdDM pathway (Cheng et al., 2018). In sweet orange fruits, a global increase of genomic DNA methylation level was observed associated with the repression of ripening-repressed genes and activation of ripening-induced genes. The use of 5-

Azacytidine, resulted in inhibition of ripening in orange fruit skin indicating that DNA methylation is required for ripening induction in sweet orange fruits (Huang et al., 2019). In addition, DNA methylation variation is involved in carotenoid degradation in citrus and anthocyanin accumulation in apple, suggesting DNA methylation regulated ripening related processes in these fruits as well (Xu et al., 2017)(El-Sharkawy et al., 2015). Taken together, DNA methylation appears as an essential regulatory process for ripening in several fruits involving distinct mechanisms though.

At present, the role of DNA methylation during grape fruit ripening is not known. In order to address this question, DNA methylation profile have been determined before and after Véraison separately in the skin and pulp of Cabernet Sauvignon grape berries and correlated with gene expression patterns and metabolic modifications. Results indicate that DNA methylation modification although present are much more limited in grape than in tomato. In addition distinct methylation changes were observed in the pulp and the skin consistent with different role of DNA methylation in these two tissues. Noteworthy treatment of grape berries with zebularine and RG108, DNA methylation inhibitor resulted in a limitation of berry ripening, suggesting that methylation and not demethylation is necessary for grape berry ripening.

Material and Methods

2.2.1 Identification of grape DNA methyltransferases and Demethylases

Eight DNA methyltransferases (MTases) and 4 DNA demethylases (DMLs) were identified both in Arabidopsis and tomato (Teyssier et al., 2008). These protein sequences were downloaded from the Arabidopsis Information Resource (TAIR, http://www.arabidopsis.org/) and the tomato genome database (http://solcyc.solgenomics.net). Blast was performed with these protein sequences in three different databases (phytozome, https://phytozome.jgi.doe.gov/pz/portal.html, CRIBI, http://genomes.cribi.unipd.it/grape/ and NCBI, https://blast.ncbi.nlm.nih.gov/Blast.cgi) to identify putative DNA methyltransferases and DNA demethylases in grape.

Identification of conserved domains in the putative grape MTases and DMLs were performed using SMART search. The motif prediction was done with MEME (Multiple Em for Motif Elicitation, http://meme.nbcr.net/meme/) and NCBI (https://www.ncbi.nlm.nih.gov/Structure/cdd/wrpsb.cgi). Phylogenetic trees were generated using the Maximum Likelihood method in MEGA v.6 based on the JTT with Freqs (+F) model. The numbers at the branching points indicate the percentage of times that each branch topology was found during bootstrap analysis (n=1000).

2.2.2 Plant Material

All experiments were carried out using the red wine grape *Vitis vinifera L*.cv. Cabernet Sauvignon. Grape berries were collected from the VitAdapt experimental block (Destrac-irvine & Leeuwen, 2016) in the Institut National de Recherche Agronomique (INRA) research station located at Villenave d'Ornon, at 44°47'23.83 N'', 0°34'39.3'' W, France. Grape vines were planted in 2009. Grape berries were harvested at 15 successive developmental stages from the 1st week after flowering to the 7th week after véraison during May to October in 2016 and in 2018. As the development of grape berry is not synchronized in one cluster, berries were labeled at two different times: flowering and veraison phase. Flowering was recorded as the time when 100% of flowers in a cluster were capped off. Individual berries were labeled at the ripening phase when berry started to turn red. In total 1509 berries were labelled at the veraison stage. Labelling and harvest of berries were performed at the same hour everyday (9-10 am). Before veraison, berries were collected according on the flowering time and the size of berry. From veraison, berries were harvested based on the date of veraison. During the sampling process, various parameters related to grape berry development and ripening were recorded including the size, diameter and weight of berry. Brries were counted and total weight was measured to determine the mean berry weight. Total soluble solids (degrees Brix; °Bx) and pH measurement were taken from veraison to the 7th week after veraison. Randomly selected 7 berries at each stage, squeezed out to obtain 3 drops of juice from each berry which was analyzed with a hand refractometer to measure the Brix. Then the extracted juice was used to measure pH using a pH meter (hanna instrument). Berry samples were frozen in liquid nitrogen immediately and further dissected to separate skin from fresh and remove seeds (except the first two stages as those berries were too small), skin and pulp were immediately frozen in liquid nitrogen. The frozen samples were ground into powder in liquid nitrogen using a ball grinder MM200 (Retsch, Haan, Germany), and then stored at -80 °C until analysis.

2.2.3 In vitro Culture of grape berries

Fruit cutting of *Vitis vinfera* L.cv Cabernet Sauvignon (Ollat and Gaudillère, 1998) were grown greenhouse condition in 2016 and 2018. Fruiting cuttings develop a signal cluster berry that was labeled at flowering. Berries were harvested in April and Mai at 2 and 7 weeks after flowering and surface sterilized as described in (Dai et al., 2014)(Dai et al., 2015) with few minor modifications. Briefly, berries were harvested with their pedicel washed with running water for 15 minutes, sterilized by immersion in 70% ethanol and 2% NaClO, and washed 4 times with sterile water. Berries were then dipped in a 20 mM EDTA solution to prevent plugging of sieve tubes by callose synthase, a strictly calcium-dependent enzyme, and re-cut at the pedicel in EDTA. Berries were the cultivated in 6 well plates (353046, Dutscher) into a culture chamber with constant temperature of 26 ± 0.5 °C, a light period of 16h/8h day/night, and light of ~50 µmol m–2 s–1. Contamination was checked and recorded every day.

To analyze the role of DNA methylation during berry ripening, surface sterilized grape berries were cultivated in MS medium or in MS medium supplemented with DMSO, or with DNA methyltransferase

inhibitors, zebularine and RG108, that are both solubilized in DMSO. In order to allow berries to ripen properly, the MS medium was supplemented with 60g/L glucose(S0809,Duchefa), 0.25g/LN-Z-AmineA (C7290,SIGMA), and vitamins (100mg/L myo-inositol, 1.0 mg/L nicotinic acid, 1.0 mg/L pantothenic acid, 0.01 mg/L biotin, 1.0 mg/L pyridoxine HCl, and 1.0 mg/L thiamine HCl. The pH was adjusted to 5.8 with 0.5 M KOH. Before autoclaving (120 °C, 20min), 9 g/L agar (HP 696, Kalys) was added. After autoclaving, 5 mL of medium was distributed in 6-well plates (353046, Dutscher).

2.2.4 Nucleic Acid extraction

Total RNA was isolated as described in (Reid et al., 2006). Amounts of extracted RNA were determined using a Nanodrop 2000 spectrophotometer (Thermo Scientific), RNA quality was evaluated on 1.2% agarose gels. Total RNA was treated with DNase I (Turbo DNA-freeTM kit, Ambion,Austin, TX, USA) according to manufacturers instructions. To control possible genomic DNA contamination, PCR was performed using primers of VvEF1. The first stand cDNA was synthesized from 1 µg purified RNA with Superscript III enzyme (Invitrogen Life Technologies, Carlsbad, CA, USA) according to the manufacturer's instructions. The cDNA obtained was diluted ten fold with ultrapure water. To check the reverse transcription, PCR was performed using primers of VvEF1.

Genomic DNA was isolated in two ways, Qiagen DNeasy plant mini kit 250 (Cat: 69106) and cetyl-trimethyl-ammonium bromide (CTAB) protocol. DNA extraction with Qiagen kit according to the manufacturer's instructions for whole genome bisulfite sequence after washing with salt: chloroform to clean up the gDNA (PacBio SampleNet – Shared Protocol). Isolation DNA with modified CTAB protocol to validate the bisulfite sequence data. The CTAB extraction buffer contain 0.5 M Tris–HCl pH 8, 1.4 M NaCl, 20 mM EDTA, 3% CTAB and 2% Polyvinylpolypyrrolidone(PVPP). 1% β-mercaptoethanol was added to the extraction buffer prior before mixing sample powder. Then samples were incubated at 65 °C for 90 minutes, centrifuged at 6500 rpm, 4 °C for 15 min.The supernatant was collected and washed twice with 1 volume of chloroform/isoamyl alcohol (24:1). The final aqueous layer was added with 0.6 volume cold isopropanol and NaAc 3M pH 5.2 to precipitate genomic DNA. Total DNA was quantified using a 2000 nanodrop, and the quality was evaluated on 0.8% agarose gels.

2.2.5 Gene expression analysis by Real-time-PCR

Absolute quantification Real time-PCR was performed as described (Whelan et al., 2003) to analyse the expression of DNA methyltransferase/demethylase encoding genes along with transcription factor VvMYBA1. PCR primers were designed with software Primer 6.0. The target fragment was cloned into pGEM-T vector (Promega). The plasmid was validated by sequencing. Dilute the plasmid in a serial dilution to construct the standard curves according to (applied Biosystems: Creating Standard Curves with Genomic DNA or Plasmid DNA Templates for Use in Quantitative PCR). VvEF1 and VvGAPDH were used as reference genes. QPCR expression analysis was carried out using the CFX96 Real-Time PCR Detection system (Bio-Rad, Hercules, CA, USA). Reaction mixes (10 µL) included 5 µL of iQTM SYBR Green

Supermix (Bio-Rad), 2 µL of diluted cDNA, and 0.5 µL of each primer (10 mM). Specific annealing of the oligonucleotides was verified by dissociation kinetics at the end of each PCR run. The efficiency of each primer pair was quantified using a plasmid serial dilution. All samples were assayed in technical duplicates. Expression data were analyzed according to (Bio-Rad: real time PCR application guides). An ANOVA two ways was performed and difference in gene expression levels between samples were assessed using a student t test (n=3; *: $p<0.05$; **: $p<0.01$; ***$p<0.001$). All primer sequences are listed in supplementary table16.

2.2.6 RNA-Seq analysis

The paired-end reads were cleaned and trimmed with Trimmomatic (Bolger et al., 2014) version 0.38 (with the options PE, LEADING:3, TRAILING:3, SLIDINGWINDOW:4:15 and MINLEN:36). Hisat2 (version 2.2.0)(Kim, Langmead, & Salzberg, 2016) with default parameters was used to align filtered reads to the 12X.2 version of the grapevine reference genome sequence from the French-Italian Public Consortium (PN40024) with the associated structural annotation (VCost.v3) provided by URGI(https://urgi.versailles.

inra.fr/Species/Vitis/Data-Sequences/Genome-sequences).The count matrices were created by importing directly BAM alignments in DESEQ2 (Michael et al., 2014)(R version 3.5.1, DESEQ2 version 1.22.2) as well as the gene models described in the previously used gff file. Reads *per* gene were counted with the summarize Overlaps function with "Union" mode and transformed with the rlog function. Sample-to-sample distances were visualized with PCA plots. Differential gene expression analysis was carried out with the DESeq pipeline with a design formula including tissue, stage and the interaction term tissue: stage. All the contrasts of interest were extracted from the results and only items with an adjusted p-value > 0.05 and a log fold change threshold of 1 were selected for downstream analysis.

2.2.7 Whole genome bisulfite sequencing analysis

The samples were sequenced at the Genomics Core Facility of the Shanghai Centre for Plant Stress Biology, Chinese Academy of Sciences using Illumina HiSeq2500. Library was constructed using Illumina's standard DNA methylation analysis protocol and the NEB Ultra II DNA Library Prep Kit. Low-quality sequences ($q < 20$) and adapters were trimmed using Trimmomatic (Bolger et al., 2014), and clean reads were mapped to the reference genome (https://urgi.versailles.inra.fr/Species/Vitis.12X.v2) using Bisulfite Sequence Mapping Program (BSMAP)(Xi & Li, 2009) (with 0.08 mismatch rate).

Identification of differentially methylated region (DMR) was conducted using methylkit. The tiling function tiled the genome with windows 500 bp length and 500 bp step-size and summarized the methylation information on each tile. Differentially methylated regions were defined with difference= 0.01 and qvalue = 0.01. Only cytosines with depth of at least four in all libraries were considered (Akalin et al., 2012)(Cooperation with Huan Huang, Shanghai, Chinese Academy of Science)

Results

2.3.1 DNA Methyltransferase inhibitors delay grape berry ripening

To analyze the potential role of DNA methylation in the control grape berry ripening, an *in vitro* ripening system previously developed for grape berries has been used (Dai et al., 2014). Berries harvested from fruiting cuttings at 2 weeks after flowering were sterilized and cultured *in vitro* in the presence of DNA methyltransferase inhibitors at different concentration (50 µM or 100 µM of zebularin or RG108) or in control conditions without (Water or 100 µM DMSO), using 48 berries for each condition.

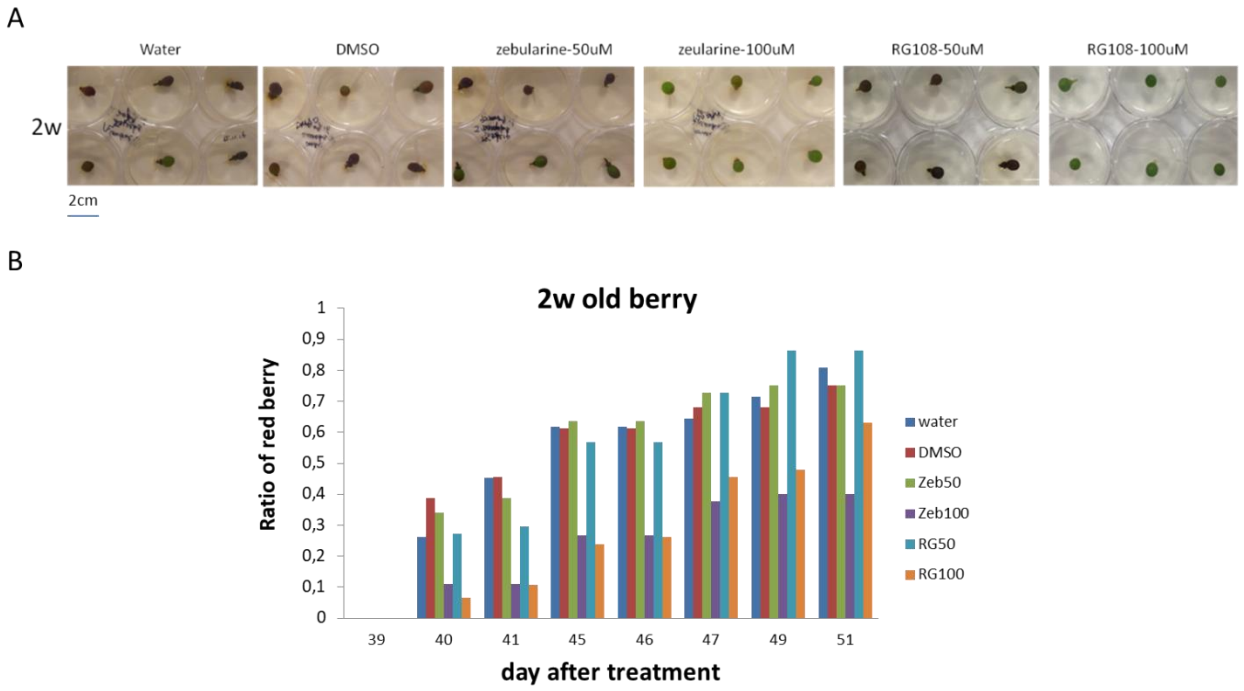

Figure II-1. DNA methylation inhibitors repress ripening 2 weeks berry. (A) The phenotype of 2 weeks berry treated with zebularine and RG108. Fruiting cutting berries were harvested at 2 weeks after flowering and cultured in vitro with zebularine, RG108 or DMSO. (B) Ratio of red berry after zebularine and RG108 treatment, first red berries were detected at 40 days after 51st day after in vitro culture.

Zebularine and RG108 were chosen for this study, because compared to other inhibitors, they present a lower toxicity and are more stable (Lyko & Brown, 2005). It is a useful way to study the function of DNA methylation by interfering with DNA methyltransferase inhibitors. Indeed there are two main types of DNA methyltransferase inhibitors: 1) analogs of cytidine, including 5-azacytidine (Santi et al., 1984) and zebularine (Zhou et al., 2002) are incorporated into DNA during replication and then are recognized by

DNA methyltransferase enzymes that form a stable reaction intermediate via the sulfhydryl side chain of the catalytic cysteine residue. Thus, DNA methyltransferase enzymes are trapped and concomitantly genomic DNA is demethylated as a result of continued DNA replication. 2) Non-analogs of cytosine, that block the catalytic pocket of free DNA methyltransferase directly without the formation of covalent reaction intermediates, such as (–)-epigallocatechin-3-gallate (EGCG) (Fang et al., 2003) and RG108 (Brueckner et al., 2005).

Contamination rate were 12.5%, 8.3%, 8.3%, 6.25%, 8.3% and 4.2%, in MS supplemented with water, DMSO, 50 µM zeb, 100 µM zeb, 50 µM RG108 and 100 µM RG108, respectively. As shown in Figure 1, red berries were first observed after 39 days of culture *in vitro* (Figure II-1A and 1B), which corresponds to approximately 8 weeks after flowering. This is similar to what is normally observed for berries developing on the plant. Noteworthy, no significant difference were observed between water and DMSO treated berries and those cultivated in the presence of 50 µM zeb or 50 µM RG108. In all cases, between 75% and 86% of berries became red between 39 and 45 days of in vitro culture (Figure II-1B). In contrast when incubated in the presence of 100µM of zebularine or RG108, a significant delay and/or inhibition of color change was observed as 60% and 37% of 100µM zeb and 100 µM RG108 treated berries failed to turn red, the strongest effect being observed with zebularine. In this case, no more color changes were observed after day 47 whereas berries incubated in the presence of RG108 went on turning red up to 51 days of *in vitro* culture. Taken together these results indicate that DNA methylation inhibitors limit ripening induction of grape berries in vitro.

A similar experiment was performed using 7 weeks old berries. Preliminary test in 2016 showed that the addition of 100 µM of RG108 to the MS medium blocked the ripening of 9 berries out of the 12 that were in culture, whereas, no effect were observed when zebularine was used at the same concentration. The difference of behavior between both DNA methylation inhibitors could be due to the fact that zebularine effect requires DNA replication which mainly occurs at early stages of fruit development (Zhou et al., 2002) whereas RG108 induced demethylation is independent of cell division (Brueckner et al., 2005).

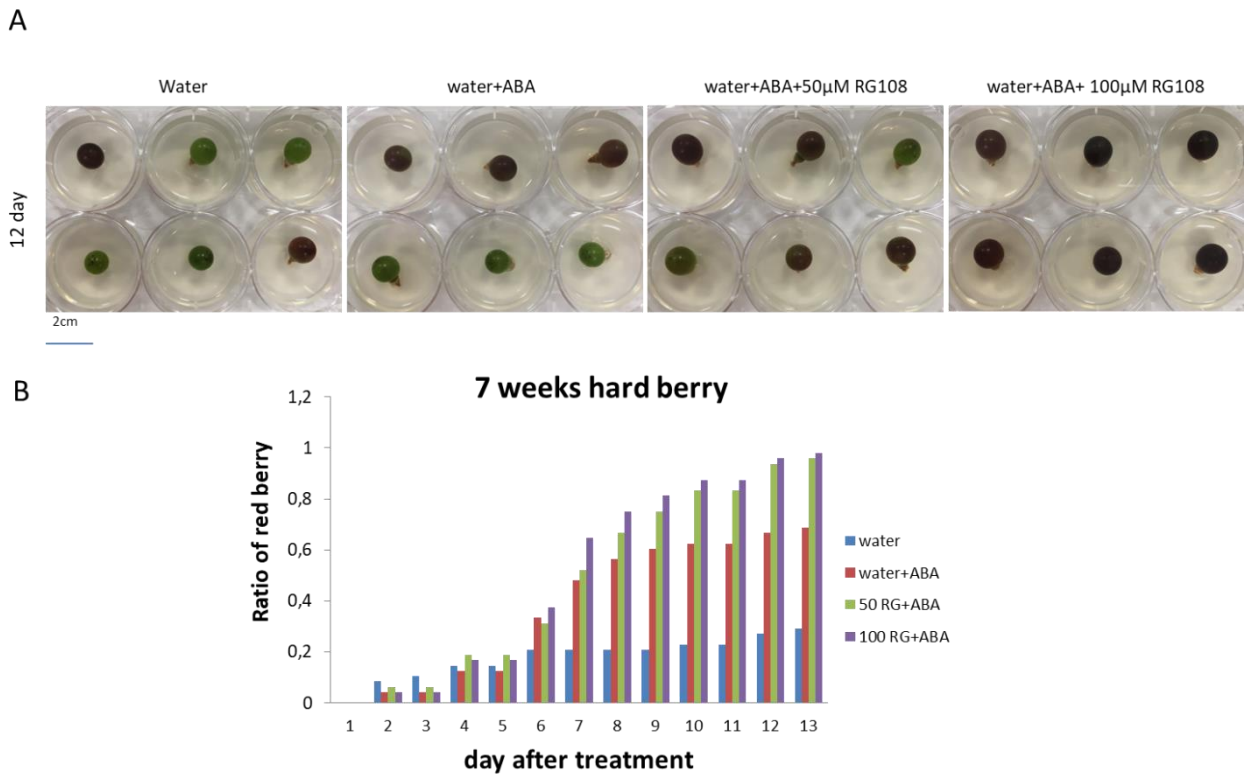

Figure II-2. DNA methylation inhibitors, RG108 supplemented with ABA induced 7 weeks green hard berry ripening. (A) ABA and RG108 induce 7weeks green hard berry ripening: grape berry harvested at 7 weeks after flower treated with ABA and RG108. In control conditions, 29% berries turned red 13day after in vitro culture initiation. In ABA conditions 69% berries turned red afer 13 days, whereas in the presence of ABA and RG108 97% berry turned red. (B). the ratio of red berry after zebularine and RG108 treatment, first red berry was detected 2 days after in vitro culture. Count and record the number of red berry every day until the 13th day, which most all berry treated with RG108 and zebulairin supplied with ABA in the medium.

A second experiment was performed in 2018 using 7 week old berries. At harvest two groups 7 week old berry were identified: hard and green-soft berries. To investigate the putative function of DNA methylation in berries of each group were harvested and treated with DNA methylation inhibitors separately. To avoid fruit damaging, difference of fruit softening was evaluated by hand and berries were cultured in the presence of zeb or RG108 as indicated in the methods, supplemented with Abscisic acid (ABA) or not. ABA was included in the medium as it has been previously reported to be a key regulator in grape berry ripening, that allow accelerating berry ripening induction (Pilati et al., 2017) and because berry softening was described to be the earliest event in the ripening process, subsequently followed by ABA accumulation (Castellarin et al., 2016). Twenty four soft or hard berries were analyzed in each condition. When considering hard berries incubated in water, 29% of the berries turned red, whereas this ratio increase to 69% in the presence of 150µM ABA consistent with previous reports indicating that ABA stimulates ripening (Pilati et al., 2017). Noteworthy 95% and 97% of the berries treated with 50µM RG or100µM RG in addition to 150µM ABA were red after the 13th day of in vitro culture. In all conditions, berries started to turn red after two days in culture (Figure II-2). When soft berries were cultivated with water, DMSO, 96% and 100% were colored after 11 days in culture, which contrast with the low rate of

color change observed with hard berries in the same conditions. The use of 100µM zeb as a control confirmed that this molecule has no effect in fruits at this stage, most likely because cell division is no more frequent. All treated berries turned red. In contrast, the ripening of 100µM RG treated berries was slightly repressed as only 83% of berries changed color during the same period of time. This result suggests that RG108 has little or no effect on ripening at this developmental stage. Addition of 150µM ABA in the medium resulted in approximately 95% of the berries turned red (Figure II-3).

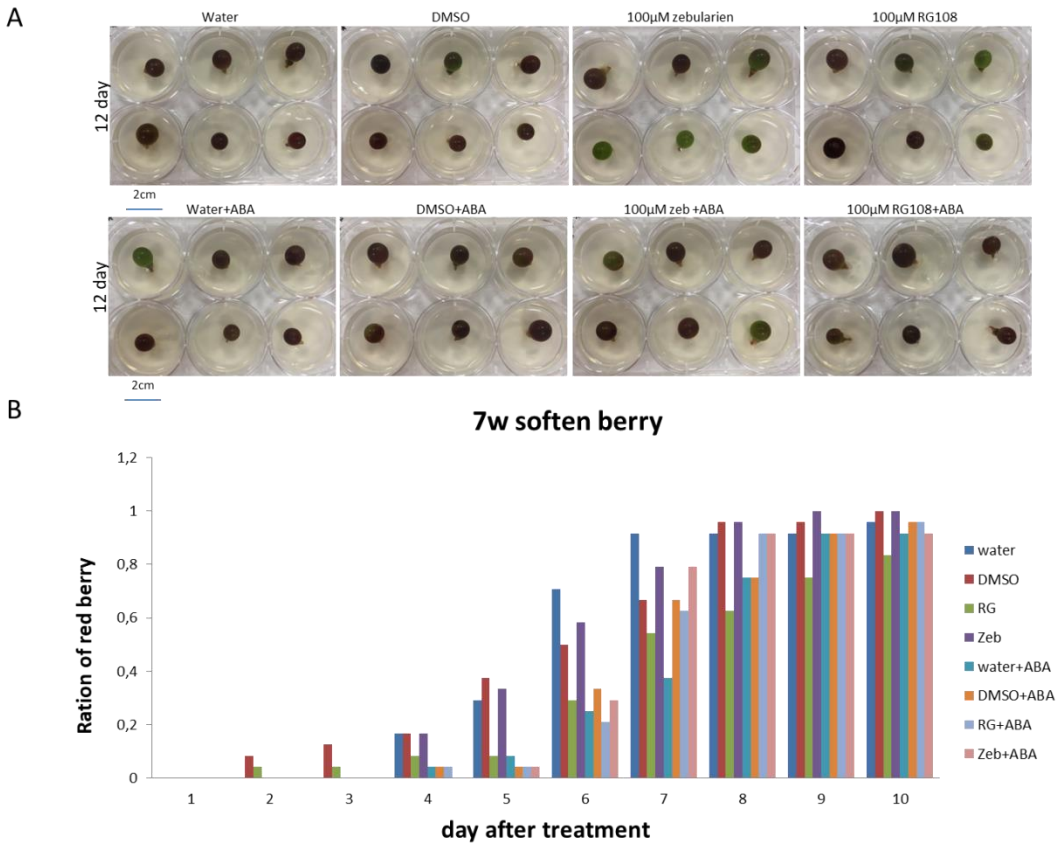

Figure II-3. DNA methylation inhibitors, RG108 and zebularine supplement with ABA or not induced 7 weeks green soften berry ripening. (A) The effect of DNA methyltransferase inhibitors with ABA or not on 7 weeks green-soften berry. (B) The ratio of red berry after zebularine and RG108 treatment, first red berry was detected at the third day after in vitro culture

All together these results suggest that DNA methyltransferase inhibitors inhibis ripening induction of young berries (2 week and 7 week green hard berries), but has little or no inhibitory effect on berries that have already started to soften (7 week green soft berries). Surprisingly, hard berries for which ripening is not yet initiated do not efficiently ripen *in vitro*. Ripening is then stimulated by the addition of ABA an effect which is enhanced in the presence of DNA methylation inhibitors. As a conclusion, DNA methyltransferase inhibitors affect grape berry ripening suggesting that DNA methylation may contribute

to regulate grape berry ripening. Molecular analysis of in vitro green berries will now be necessary to evaluate the effect of DNA methylation inhibitors on metabolite accumulation and gene expression, in relation with DNA methylation.

2.3.2 Characterization of grape berry development and ripening

In order to analyze the variations of DNA methylation in relation with gene expression variations and metabolic changes, a precise study of the development of grape berries was performed analyzing separately the skin and the pulp of berries.

a. Berry Development and Ripening

In vitro culture of grape berries suggested that DNA methylation may be one of important factor that controls grape berry ripening. To study the variation of DNA methylation during berry development and ripening, we harvested grape berries of Cabernet Sauvignon at 15 developmental stages (Figure II-4A). Veraison is the shift phase from green growth to ripening phase. Compared to other fruits species, grape berry take more time from flowering to full maturity. In the first phase, 7 weeks were needed for berry to reach the opportune size for ripening. After a short lag phase called veraison, complex metabolism starts over and the berries finally get ripen in another 7 weeks. In the green growth phase, the size of berry increase tightly associates with a quick increase of berry weight (Figure II-4C and 4D). Small berry turn red earlier, which leads to harvest many small berries at veraison. This result in a transient decrease in size and weight at veraison (Figure II-4C and 4D). At the end of veraison, sugar and anthocyanin accumulation marked the initiation of ripening. During the ripening phase, the weight of berries increase again to maximal value as a result of water and secondary metabolites accumulation that coincide with a sharp increase of Brix in parallel with berry pH. Unlike berry weight, berry size slightly increase during this period (Figure II-4C). The variation of Brix and pH suggested that soluble sugar accumulate significantly and coincide with acidity decrease during ripening (Figure II-4E and 4F).The Brix of berry reached 23.9 at 7^{th} week after veraison which was considered as maturity. In addition, significant color change was observed in the first week after veraison, the whole berry reach full red in one week (Figure II-4B). It suggested that rapid anthocyanin biosynthesis during this period. Given all measurements and records during harvest, Cabernet Sauvignon exhibit the classical double sigmoidal curve growth (Coombe et al., 1992). The relative long growth cycle indicated a more complex regulation network with diverse metabolite variations during grape berry development and ripening.

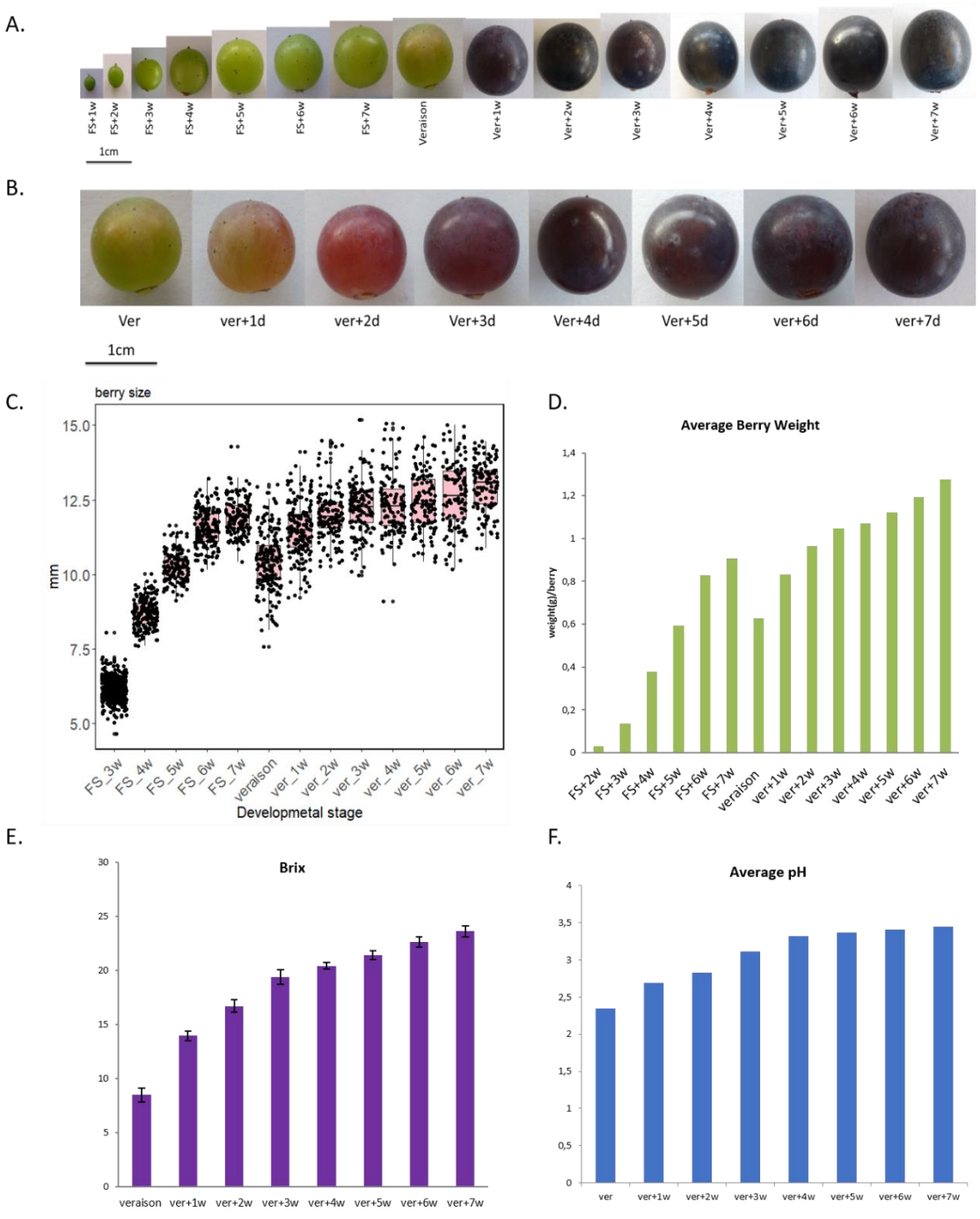

Figure II-4. Progression of grape berry development and ripening. (A) 15 consecutive developmental stages of grape berry. (B) Rapidly color change of skin in the first week after veraison. C to F images show the increase of berries size (C), weight (D), Brix (E) and Ph (F) during berry development and ripening.

b. *Tissue Specific Metabolite changes during berry development and Ripening*

Berries are complex organs made of several different tissues, including the flesh and the skin (Fig.4A), that present specific metabolic features (Castellarin et al., 2015, Fasoli et al., 2018). In order to control for metabolic differences and evolution between tissues, the flesh was separated from skin and used to analyze organic acids, soluble sugar and anthocyanin at the 15 successive developmental stages of Cabernet Sauvignon.

Organic Acid accumulation

The ratio of organic acid and sugar at maturity is an important factor to determine the quality of berry and wine. It has also been described that tartaric and malic acids are the two main organic acids accumulating in grape berry, the content of tartaric and malic acid accounting for 90% of total acids in grapevine berries (Kliewer et al., 1967, Lamikanra et al., 1995, Conde et al., 2007). In skin and pulp of 3 weeks old berries, tartaric acid abundance is 13.9 ± 2.7 mg/g FW and 13.8 ± 0.3 mg/g FW, respectively, without significantly difference between tissues. Then, the content of tartaric acid gradually decreases in both tissues with similar kinetics throughout grape berry development to reach 6.5 ± 0.51 mg/g FW at 7 weeks after "Véraison". However, the concentration of tartaric acid was always slightly higher in the skin than in the pulp at the exact same stage (Figure II-5B). In contrast to tartaric acid, malic acid accumulates during berry development with clearly distinct accumulation kinetics in pulp and skin. In pulp, the concentration of malic acid increased from the 3rd week after flowering to reach its maximum level (19.2 ± 0.20 mg/g FW), just before the "Véraison" stage. It then decreases during ripening to reach its lowest value 3.6 ± 0.18 mg/g FW at weeks after véraison, without further variations during ripening.

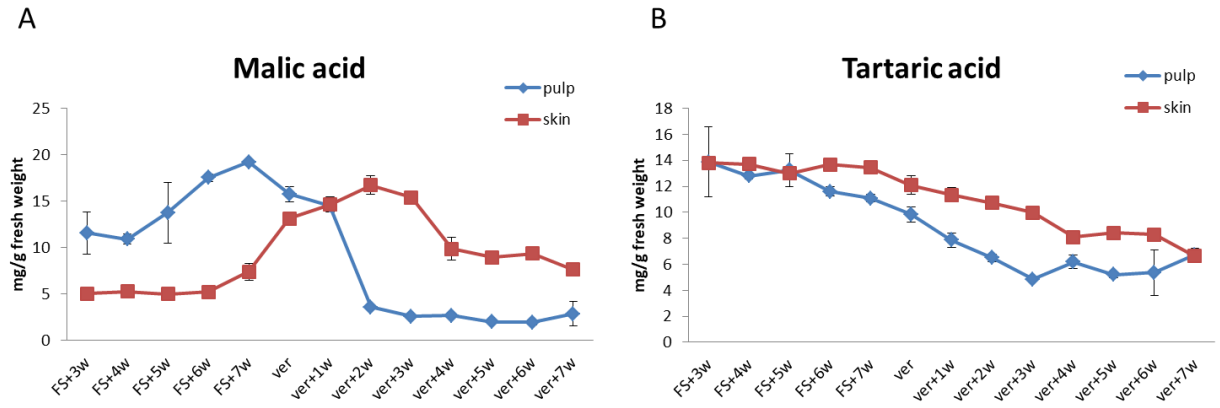

Figure II-5. Malic (A) and tartaric (B) acid content in skin and pulp during grape berry (C.Sauvignon) development. Malic and tartaric acid were determined as explained in the methods using 3 independent biological replicates (n= 3). Each replicate correspond to 40-140 (depend on the berry stages) fruits that were pooled together. Values are the mean ± SE of three biological replicates. FS, fruit set; ver, veraison.

The content of malic acid in the skin remained low at 5.2 ± 0.71 mg/g FW until 6 weeks after flowering. It then rapidly increased to 16.7 ± 0.99 mg/ g FW at the 2 weeks after Véraison and declined to 7.6 ± 0.72 mg/ g FW at the 7 weeks after véraison (Figure II-5A). The concentration of malic acid remained higher in the skin as compared to pulp. Taken together, the accumulation of tartaric and malic acid was different in developing grape: the highest concentration of tartaric acid was detected in young berries, whereas the maximal concentration of malic acid was observed close to véraison, as previously described (Lamikanra et al., 1995, Sweetman et al., 2009). These data indicate tissue specific patterns of malic acid accumulation in grape berries, whereas tartaric acid accumulation profiles were similar in pulp and skin.

Soluble sugar accumulation

Glucose and fructose are the two main sugars accumulating in grape berries essentially during ripening, whereas sucrose remains at a very low level (Liu et al., 2006). In pulp, fructose and glucose were first detected the 7th weeks after flowering, and continuously increased to its maximum concentration, 112.5 ± 3.5 mg/g and 106.5 ± 2.7 mg/g FW respectively at the 5th week after Véraison (Figure II-6A and 6B).

Accumulation of fructose and glucose was delayed in the skin, and both soluble sugars were first detected the 2nd week after veraison. Both glucose and fructose concentrations increased to a maximum level, 68.5 ± 1.76 mg/g FW and 75 ± 3.5 mg/g FW, respectively, the 5th weeks after veraison (Figure II-6A and 6B). The maximum concentration remained however lower in the skin as compared to the pulp at all developmental stages.

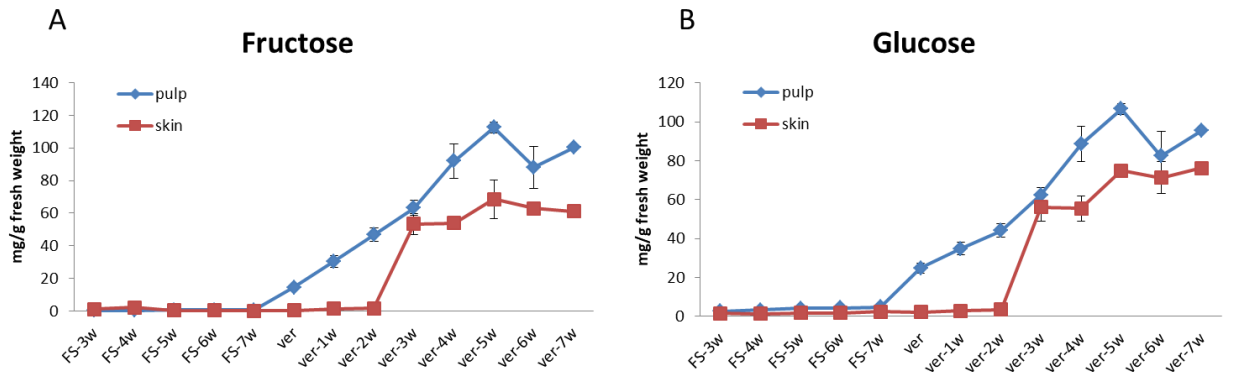

Figure II-6. Accumulation of fructose (A) and glucose (B) content in skin and pulp during grape berry (C.Sauvignon) development. Fructose and glucose were determined as explained in the methods using 3 independent biological replicates (n= 3). Each replicate correspond to 40-140 (depend on the berry stages) fruits that were pooled together. Values are the mean ± SE of three biological replicates. FS, fruit set; ver, veraison.

	glucose /fructose ratio	
	pulp	skin
ver	1,706	nd
ver-1w	0,841	nd
ver-2w	0,957	nd
ver-3w	0,988	1,051
ver-4w	0,961	1,029
ver-5w	0,947	1,092
ver-6w	0,938	1,134
ver-7w	0,953	1,247

Table II-1. Ratio of glucose / fructose in pulp and skin during ripening.

The ratio of glucose / fructose is near 1 (Table II-1) which is close to previously reported results 1 (Kliewer, 1967)(Dai et al., 2011). Results indicated both glucose and fructose accumulate more rapidly and at higher levels in the pulp than in the skin, suggesting that glucose and fructose accumulation during ripening is regulated in a tissue specific manner in Cabernet Sauvignon berries as previously reported (Castellarin et al., 2015).

Anthocyanin composition and concentration

Anthocyanins are a class of flavonoid compounds responsible for the color of flowers or fruits. They play an essential role to attract pollinators for sexual reproduction and seed dispersers (Hoballah et al., 2007). Unlike *Teinturier* cultivars that synthesize anthocyanin both in skin and pulp, Cabernet Sauvignon, as many other grapevine cultivars, specifically accumulates anthocyanin in the skin of berries (Jeong et al., 2006).

Consistently, we could not detect anthocyanins in the pulp at any of the developmental stages analyzed. In contrast, 22 anthocyanin and derivatives were identified in the skin since veraison shown in Fig7A. A sharp increase of total anthocyanins content was observed from the véraiosn stage onward in the skin to quickly reach a maximal concentration of 9.7 ± 0.94 mg/g FW at the third week after véraison and remained at a relatively stable level at later ripening stages (Figure II-7B).

In grape, anthocyanins which are responsible for red/blue color of the berries mainly correspond to five main compounds: malvidin, petunidin, delphinidin, cyanidin and peonidin and their derivatives, which differ in their patterns of hydroxylation and methylation (Mattivi et al., 2006). The exact blue/red hue of the grape berries, and wine color stability is determined by the relative proportion of these different molecules: the higher level of hydroxyl groups, the bluer the color, but the more unstable are the anthocyanins (Woodward et al., 2009). We further controlled the anthocyanin composition of Cabernet Sauvignon (CS) berries in our field conditions (Figure II-7C). In CS, under our conditions the proportion of dihydroxylated compounds, cyanidin- and peonidin-derivatives, which represent 35 % at véraison stage, progressively decrease to 10% at the 7 week after veraison, whereas tri-hydroxylated compounds

(delphinidin-, petunidin- and malvidin-derivatives) represent 90 % at the 7th weeks after véraison. Malvidin was the most abundant compound, accounting for 67% of total anthocyanin content which was consistent with previous reports that, Malvidine 3-glucoside was the predominate composition in most grape cultivars (Mattivi et al., 2006). These data suggested anthocyanin specifically synthesis in the skin of CS, and during ripening the relative content of dihydroxylated anthocyanin decline to 10%, meanwhile the precent of trihydroxylated anthocyanin increase to 90% of total content even though the total content did not obviously change. It indicated the bluer and more unstable trihydroxylated anthocyanin predominately accumulated in ripening skin.

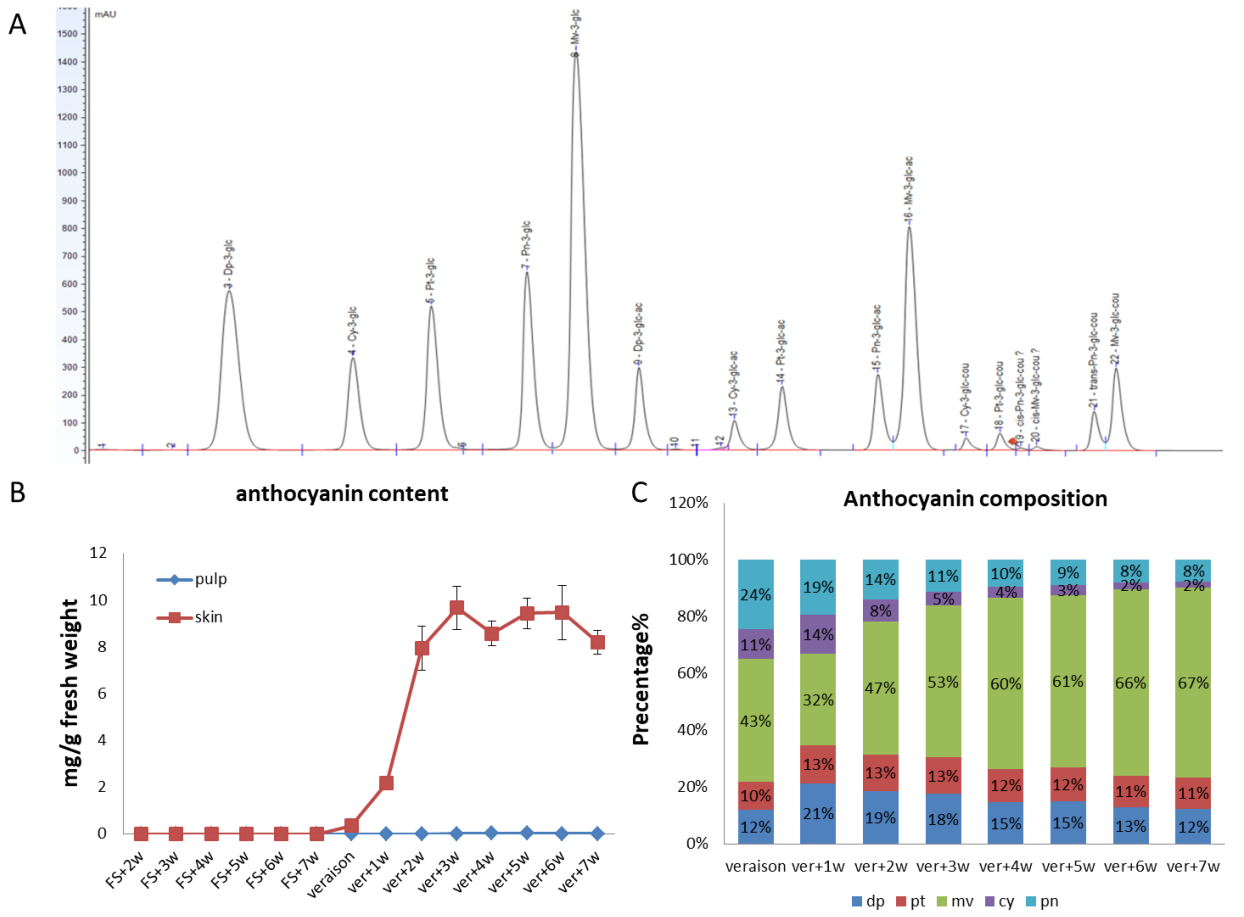

Figure II-7. Accumulation and composition of anthocyanin in skin and pulp of Cabernet Sauvignon. (A) HPLC Chromatography of anthocyanins in the peel of CS at 3 week after veraison. 22 compositions were detected in CS skin at the 3rd week after veraison. Peaks correspond to the compositions of anthocyanins. (B) Content of anthocyanin in pulp and skin in developing berry of CS: 3 replications for each stage. Each replicate corresponds to 40-140 (depend on the berry stages) fruits that were pooled together. Values are the mean ± SE of three biological replicates. FS, fruit set; ver, veraison. (C) The variation of anthocyanin compositions in the skin during berry ripening. Presentage represent the ratio of 5 compositions in total content. dp, Delphinidin and-derivatives; pt, Petunidin and-derivatives; mv, Malvidin and-derivatives; cy, Cyanidin and-derivatives; pn, Peonidin and-derivatives.

2.3.3 Transcriptomic analysis of grape berry during development and ripening

a. Summary of RNA seq data

To compare the transcript variation during berry development and ripening, RNA seq analyses of grape berry skin and pulp were performed as described in (Lijavetzky et al., 2012), at 4 developmental stages: 6 weeks after flowering (FS+6w), 1 week, 3 weeks and 7 weeks after véraison (Ver+1w, Ver+3w and Ver+7w, see Figure II-4, page 61).

A total of 12 (skin) and 11 (pulp, only 2 replicates at veraison+1w) samples were analyzed by RNA seq which generated between 10 to 38 million reads per sample (see materials and methods). After filtering 9 to 36 million reads were obtained of which 91.55% and 96.2 % could be mapped to the grape reference genome (https://urgi.Versailles.inra.fr/Species/Vitis.12X.v2, ((Canaguier et al., 2017), Table II-2). Although variations in the final number of counts were observed between samples, the current results are sufficient to determine the main differences between samples but are unlikely to allow identifying differences in weakly expressed genes (Conesa et al., 2016).

Sample_Name	Input Read Pairs	Both Surviving	Both Surviving %	Dropped	Dropped %
F6P-1	27199900	25109012	92,31	28948	0,11
F6P-2	27680594	26245715	94,82	25002	0,09
F6P-3	31694334	29582522	93,34	26289	0,08
F6S-1	38286282	36579106	95,54	27440	0,07
F6S-2	30705620	29008308	94,47	22470	0,07
F6S-3	35133015	32942164	93,76	28529	0,08
V1P-1	13160796	12451057	94,61	8828	0,07
V1P-2	14880669	14104490	94,78	10982	0,07
V1S-1	13840190	13228868	95,58	8751	0,06
V1S-2	12448831	11830601	95,03	14587	0,12
V1S-3	11348839	10750160	94,72	7575	0,07
V3P-1	26994221	24712784	91,55	50743	0,19
V3P-2	30881199	29304907	94,9	19874	0,06
V3P-3	29771220	28283615	95	19571	0,07
V3S-1	33551597	31467304	93,76	32098	0,1
V3S-2	28858706	27221116	94,33	22380	0,08
V3S-3	32207817	30333670	94,18	28555	0,09
V7P-1	11271738	10717283	95,08	12335	0,11
V7P-2	11642547	11102405	95,36	6729	0,06
V7P-3	12444891	11913576	95,73	7303	0,06
V7S-1	12308392	11563504	93,95	8253	0,07
V7S-2	16024020	15414399	96,2	7756	0,05
V7S-3	10178674	9721316	95,51	5372	0,05

Table II-2. Summary of RNA-seq reads mapped to the reference genome.

b. *Differential gene expression between pulp and skin of grape berry*

To identify genes that are differentially expressed between tissues (skin and pulp) at each developmental stage and in each of the two tissues, between developmental stages, all mRNA populations were analyzed using DESeq2. A total of 28846 and 29034 genes were expressed in at least one sample of pulp and skin, respectively, which represented approximately 68.0% (pulp) and 68.5% (skin) of all identified genes in the grape genome (https://urgi.Versailles.inra.fr/Species/Vitis.12X.v2). The size of the different libraries is shown in Table II-2. There was little variation in the total number of genes represented at each stage, similar to other fruit transcriptomic studies (Fasoli et al., 2018). Genes with low expression levels in all samples (RPKM<1 in all samples) were filtered out leaving 19543 genes in pulp and 19936 expressed genes in skin, accounting for 46.1% and 47% of all grape genes in pulp and skin, respectively. Normalized read counts from independent biological replicates within one line was highly correlated at each stage (R2>0.98, supplementary Figure II-31A, page 120), whereas the correlation between skin and pulp at each stage was much lower (for example, R2= 0.795, at stage F6W, supplementary Figure II-31B, page 120). This indicates clear differences between tissues at each stage analyzed. To evaluate changes in gene expression during berry developmental stages and tissues, a principal component analysis (PCA) was performed using RNA seq data after filtering RPKM<1. The first PC which explains 40.91% of the variability separates samples according to developmental stages. The second PC which explains 19.16% of the variability separates skin and pulp samples at all stages (Figure II-8). Consistent with correlation analysis, the 3 biological replicates of each tissue and stage grouped together indicating that samples could be used for further analysis.

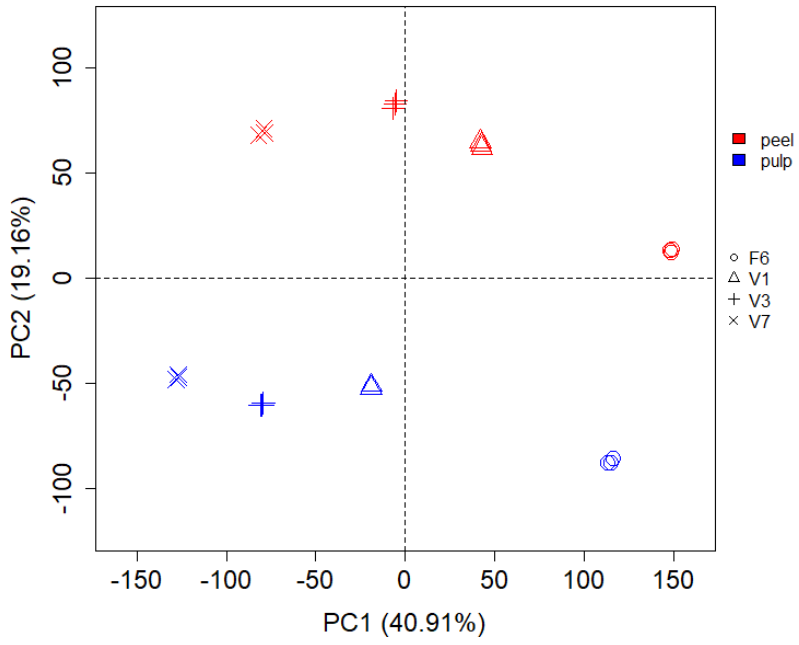

Figure II-8. Principal component analysis of RNA seq data. Color indicates the tissue: red, skin; blue, pulp. Shape indicated the stages: ○, F6; △, V1; +, V3; X, V7. PC1 and PC2 explain 60.01% of the variability. PC1 represents the variation according to developmental stages. PC2 separates sample according to tissues, skin and pulp.

c. *Differential gene expression between developmental stages*

To determine transcript variations between developmental stages, pairwise comparison was performed to identify differentially expressed genes (DEGs) during berry development and ripening in each tissue and between tissues. DEGs in at least one pairwise comparison were selected with a threshold of |log2 fold change|> 1, and an adjust p value below 0.05 (p adj <0.05). A total of 8788 and 9023 DEGs were identified in skin and pulp, respectively, corresponding to 20.7% and 21.3 % of all grape genes (https://urgi.Versailles.inra.fr/Species/Vitis.12X.v2). This indicates that the ripening of both grape berry tissues requires important transcriptional reprogramming. The numbers of up- and down-regulated genes identified after a stage by stage comparison are shown in Figure II-9A. Noteworthy, both in skin and pulp a higher number of genes are down-regulated than up-regulated during berry development and ripening. This is consistent with previous reports that have analyzed changes in RNA population in grape berries (Massonnet et al., 2017)(Fasoli et al., 2012) .

When analyzing the distribution of DEGs at each stage in skin and pulp, a similar pattern was observed between these two tissues. In pulp, adjacent stage comparison revealed 4326, 1417 and 1295 DEGs in V1/F6, V3/V1 and V7/V3 comparison, respectively. Similarly in skin, 4194, 1327 and 1731 DEGs were identified when comparing V1/F6, V3/V1 and V7/V3, respectively. This indicates that although the most important changes in mRNA populations occur at the onset of ripening, mRNA populations are still dynamic during the ripening process. Indeed mRNA populations were more different when comparing more distant samples in terms of developmental stage and physiological states. For example the highest number of DEGs is found between F6/V7 in both pulp and skin, and the lowest between V1/V3 and V3/V7.

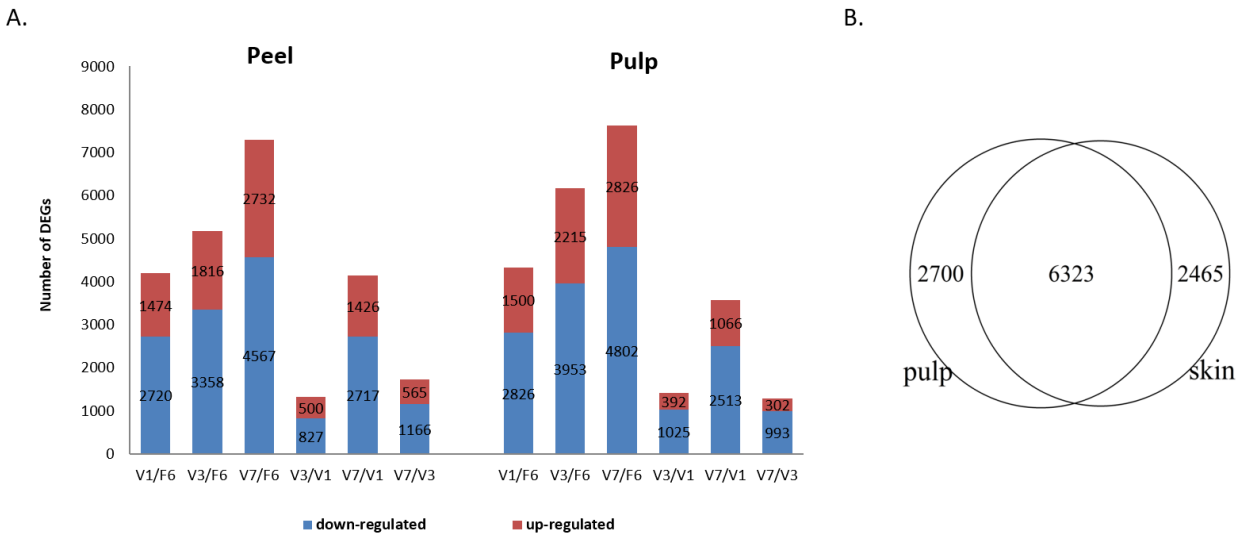

Figure II-9. Distribution of DEGs during fruit tissue development and ripening. (A). Number of DEGs in each pairwise comparison. (B) Venn diagram displaying the number of tissue specific and common DEGs between the pulp and the skin of berries. 2700 and 2465 tissue specific DEGs were found in the pulp and skin, respectively. 6323 DEGs are common to the pulp and the skin.

Taken together, these results indicate that major changes in mRNA populations occur in grape berries at the véraison stage, in both of the tissues analyzed.

To determine whether the same DEGs are involved in the transcriptional reprogramming observed in pulp and skin, DEGs common to both tissues were determined. As shown in Figure II-9B, 6323 common DEGs (approximately 70% of total DEGs) were found in both berry tissues, whereas 2700 and 2465 DEGs (approximately 30% of total DEGs) were specific to pulp and skin, respectively.

d. Validation of RNA seq data

In order to control for gene expression profile determined from RNAseq results, genes involved in DNA methylation regulation were identified and analyzed using RT-QPCR

Identification of grape DNA methyltransferases and demethylases.

Protein Blast was performed as described in the methods using protein sequences from DNA methyltransferases and DMLs identified in *Arabidopsis* and tomato. In total, 9 putative DNA methyltransferease and 3 DNA demethylases were identified in grape (Table II-3). The structure of the putative grape MTases and DMLs proteins revealed the presence of highly conserved domains in the grape MTase and DML (see supplementary Figure II-32, page 121)

Gene name	Gene identifier	Genomic location	No. of intron/exons	Protein length(aa)
VvMET1	VIT_207s0130g00380	chr7: 20683940 -20689960	10/11	1424
VvMET2	VIT_207s0130g00390	chr7: 20695315 - 20704766	10/11	1549
VvCMT1	VIT_208s0007g06800	chr8: 20455686 - 20461727	18/19	736
VvCMT2	VIT_202s0033g00610	chr2: 14943456 - 14983872	18/19	706
VvCMT3	VIT_206s0004g01080	chr6: 1171054 - 1183851	20/21	821
VvCMT4	VIT_216s0039g02470	chr16: 2677332 - 2694276	8/9	412
VvDRM2A	VIT_214s0066g01040	chr14: 27478222 - 27491561	7/8	498
VvDRM2B	VIT_205s0020g00450	chr5: 2361314 - 2376608	8/9	466
VvDNMT2	VIT_204s0008g05060	chr4: 4545234 - 4550231	9/10	393
VvDML1	VIT_208s0007g03920	chr8: 17913972 - 17925002	18/19	1470
VvDML2	VIT_213s0074g00450	chr13: 8239147 - 8251127	17/19	1621
VvDML3	VIT_206s0061g01270	chr6: 19096083 - 19101208	16/17	931

Table II-3. Identification of DNA Methyltransferases and demethylases in grape.

To study the evolutionary relationship of grape MTase with that of *Arabidopsis* and tomato, two Phylogenetic trees were generated using the full length protein sequence (see methods) (Figure II-10). All identified MTases in grape belong to the four clades of MTases already described in plants (Law & Jacobsen, 2011). The DRM clade was separated first and contains two grape DRMs, named VvDRM2A and VvDRM2B. Of note, grape DMRs appeared more homologous to tomato proteins than to those of Arabidopsis. For example, the grape VvDRM2A showed greater similarity to the tomato SlDRM7 proteins (65%) and to AtDRM2 (52% similarity) whereas VvDRM2B shared 53% similarity to the tomato SlDRM8 protein, compared to 38% homology to AtDRM3. A single putative VvDNMT2 gene was found in grape, and its product shows 71% and 67% similarity to *Arabidopsis* and tomato DNMT2, respectivaly. Two closely related MET proteins (82% similarity) were identified in grape that showed significant similarity to the corresponding tomato protein. The tomato SlMET1 shared 67% similarity to VvMET1 and 60% to VvMET2. VvMET1 and VvMET2 showed 61% and 59% similarity to AtMET1. Upon phylogenetic analysis, grape VvCMT1 is likely orthologous to the Arabidopsis AtCMT1 (53% similarity), VvCMT3 appeared closely related to the tomato SlCMT2 (72% similarity) and SlCMT3 (72% similarity) that are groups with AtCMT3 (53% similarity), whereas VvCMT2 and VvCMT4 are grouped with AtCMT2 and SlCMT4.

In addition, three DNA demethylase genes were identified in grape. The VvDML1 protein shared a high level of similarity with the tomato SlDML1-2 (77%) and AtROS1 (58%), VvDML3 with the tomato SlDML3 (55%), and VvDML1 was found form subclade with the Arabidopsis AtDEM protein (64% homology). Supplementary table II-17 (page 119) summarizes the similarity of DNA methyltransferase and demethylase protein between grape, *Arabidopsis* and tomato.

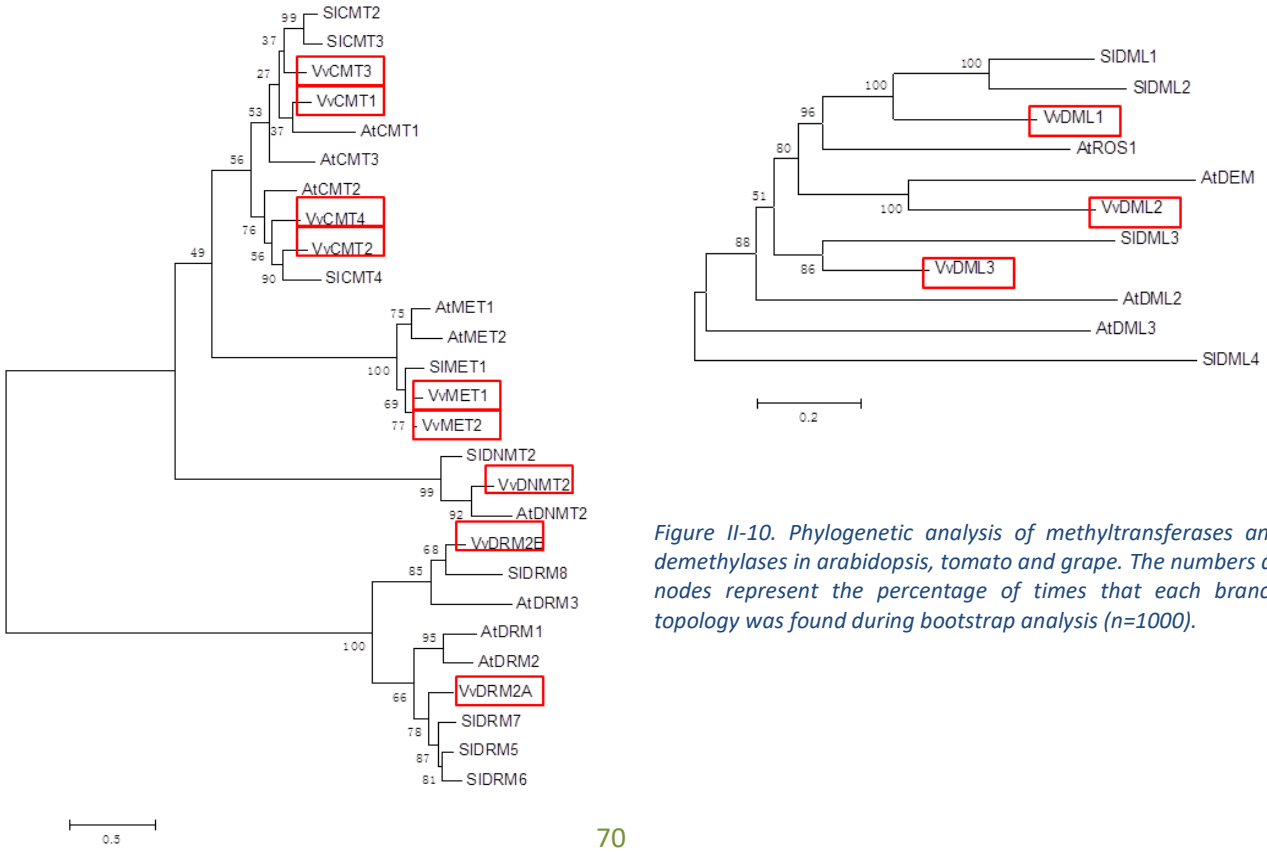

Figure II-10. Phylogenetic analysis of methyltransferases and demethylases in arabidopsis, tomato and grape. The numbers at nodes represent the percentage of times that each branch topology was found during bootstrap analysis (n=1000).

MTase and DML genes present similar expression patterns during grape berry development with RNA seq and RT QPCR

In order to compare expression profiles obtained after RNA seq to those determined by absolute quantification real-time PCR (RT-PCR) analysis, expression profiles of the 11 genes encoding the different MTAses and DMLs were extracted from the RNA seq data, together with those of the gene encoding the transcription factor VvMYBA1, which is involved in regulating anthocyanin synthesis and is typically induced at the onset of grape fruit ripening (Kobayashi et al., 2004). Data presented in Figure II-11 indicate that whereas *VvMET1* shows a progressive increase in expression all through fruit development and ripening in the pulp. In the skin the *VvMET1* genes shows a progressive increase up to 3 weeks after the véraison stage, before decreasing at later stages of berry ripening. Expression *VvMET2* does not show major changes in expression level between stages and is similar in both tissues analyzed. In contrast both the *VvDML1* and *VvDML2* genes are significantly down-regulated in pulp and skin during ripening (Figure II-11). The other five genes, including VvCMT1-4 and VvDML3 are weakly expressed at all stages and in both tissues and were hardly detectable (RPKM<1.4) (supplementary Figure II-33, page 122). In addition we also extracted expression data of the MYBA1 gene that has been widely described. The expression of this gene which is specific to the skin is induced during the Véraison stage and increases during ripening as shown in Figure II-11. Surprisingly, a weak expression peak is found in the pulp at the Véraison plus 1 week (V1P) stage in the pulp that could be explained by a slight tissue contamination during fruit dissection. As VvMYBA1 is expressed at very high levels in the skin at this stage, a slight contamination of the pulp by the skin would be visible. To control the RNA seq data, all genes cited above were analyzed at the four analyzed stages of pulp and skin by absolute quantification RT-PCR (see materials and methods). Absolute qPCR verified that VvCMT1-4 and VvDML3 are expressed at very low levels during development and berry in both tissues analyzed, consistent with RNA seq results. However, due to the very low expression levels of these gene it is difficult conclude that they present the exact same expression profile with the two methods (see supplementary Figure II-33).

Comparing the expression of genes with higher expression levels, namely *VvMET1, VvMET2*, *VvDML1, VvDML2* and VvMYBA1, showed that they present very similar expression patterns to those obtained using RNA seq data.

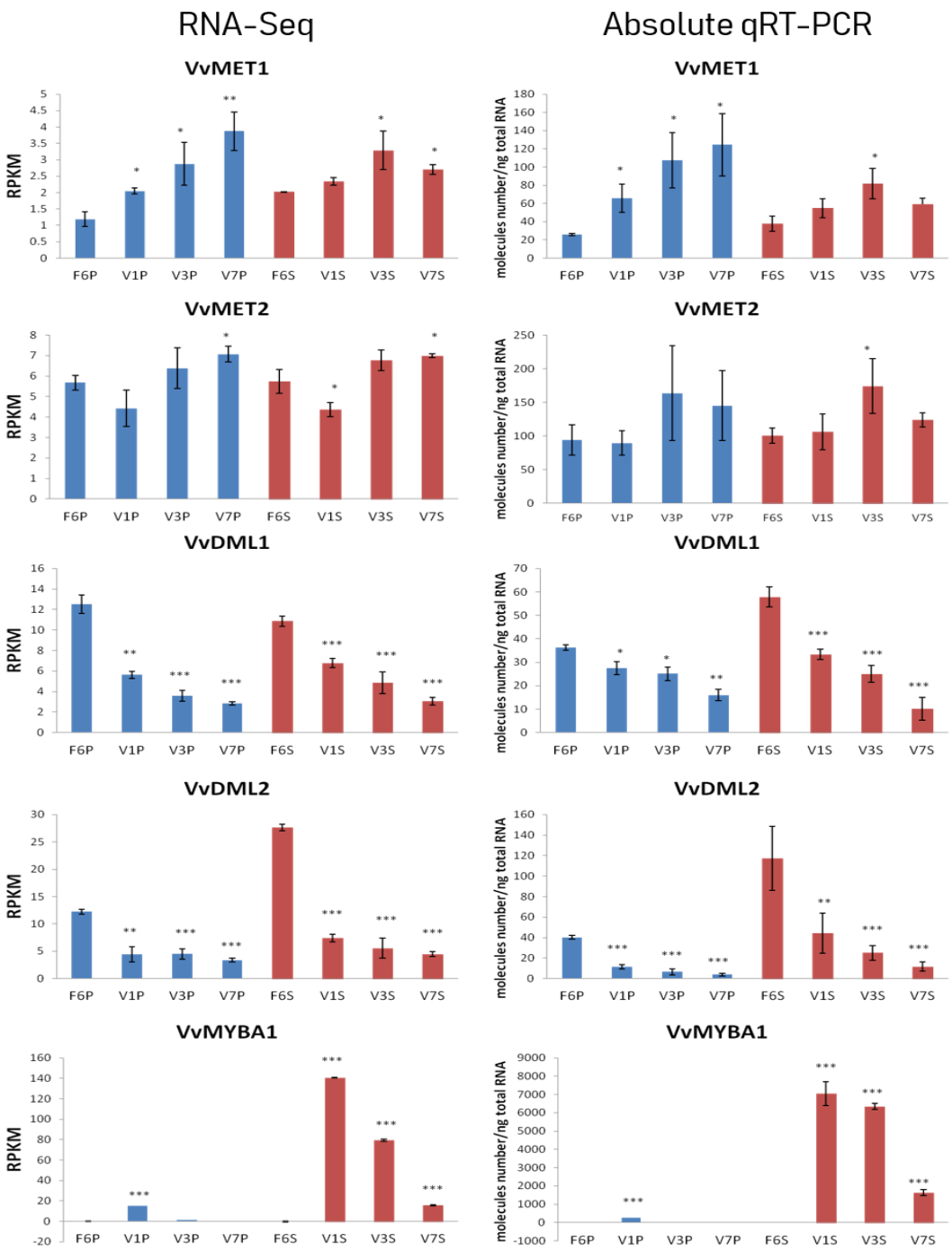

*Figure II-11 Validation of RNA seq data by absolute qRTPCR. Expression profile of VvMET1, VvMET2, VvDML1, VvDML2 and VvMYBA1 determined by RNA- seq (left panels) and absolute RT qPCR (right panels). Asterisks indicate significant difference [Student's t test (n = 3)] between SlDML2 and all other SlDML genes: *P < 0.05;**P < 0.01; ***P < 0.001. Error bars indicate means ± SD. Blue, pulp; red, skin.*

e. Transcriptomic variations in skin and pulp during berry ripening

To investigate the expression profiles of the DEGs identified in the pulp and in the skin during berry development, a clustering analysis was performed in each tissue separately using all the selected DEGs (8788 and 9023 in pulp and skin, respectively). A total of twelve clusters were generated in both the skin and pulp that were named from 1 to 12 in each tissue. The skin and the pulp clusters that have the same name contain genes that present similar expression profile (Figure II-12A). The gene composition of the clusters was also analyzed to determine whether clusters grouping genes with same expression profiles (clusters with same number) in the skin and in the pulp contained the same genes. As shown in Figure II-12A, the gene composition of similar clusters differs between the two tissues.

Among the 6328 DEGs found in both pulp and skin (referred to as "common DEGs"), only 3675, approximately 45% are found in the equivalent clusters in pulp and skin. This indicates that even though similar regulatory processes are operating in both tissues, they don't target the exact same genes, as would be expected with tissues that present clear developmental and metabolic differences.

A

	pulp(2700)	852	615	273	112	59	222	345	64	99	23	12	24
skin(2465)	Tissue	PC1-3406 37,7%	PC2-1920 21,2%	PC3-794 8,8%	PC4-462 5,1%	PC5-152 1,7%	PC6-691 7,7%	PC7-895 9,9%	PC8-152 1,7%	PC9-363 4%	PC10-87 1%	PC11-32 0,4%	PC12-69 0,8%
628	SC1-2899 33%	**1778**	5	6	73	0	204	185	3	5	7	5	0
493	SC2-1979 22,6%	12	**1054**	247	6	52	2	22	22	56	1	0	12
176	SC3-514 5,8%	19	40	**160**	21	3	9	5	2	65	12	1	1
99	SC4-661 7,5%	369	2	3	**142**	0	18	4	0	14	8	2	0
67	SC5-205 2,3%	2	58	23	4	**23**	0	1	4	22	0	0	1
295	SC6-780 8,9%	210	1	8	11	0	**158**	74	0	2	14	0	7
429	SC7-915 10,4%	90	38	13	4	1	60	**226**	29	1	5	3	16
68	SC8-240 2,7%	6	99	13	2	7	0	17	**24**	0	0	0	4
142	SC9-412 4,7%	36	5	30	73	6	4	6	3	**95**	5	7	0
27	SC10-96 10,9%	19	0	9	14	0	12	4	0	2	**9**	0	0
5	SC11-27 0,3%	11	1	0	0	1	0	4	1	2	0	**2**	0
36	SC12-60 0,7%	2	2	9	0	0	2	2	0	0	3	0	**4**

B

peel specific DEGs
pulp specific DEGs
Common DEGs
cluster1
'not assigned' 203
'signalling' 73
'misc' 74
'stress' 55
'hormone metabolism' 24
'secondary metabolism' 27
'lipid metabolism' 22
'not assigned' 241
'protein' 118
'C1-metabolism' 6
'redox' 18
'lipid metabolism' 32
'PS' 18
'not assigned' 465
'transport' 86
'cell' 78
'signalling' 147
'RNA' 114
'misc' 158
'redox' 29
'hormone metabolism' 67
'cell wall' 71
'PS' 58
cluster2
'not assigned' 173
'RNA' 62
'secondary metabolism' 38
'not assigned' 259
'signalling' 18
'protein' 93
'RNA' 86
'not assigned' 409
'signalling' 44
'protein' 156
'DNA' 41
'RNA' 144
'stress' 29
cluster3
'RNA' 19
'secondary metabolism' 17
'amino acid metabolism' 5
'stress' 14
'redox' 7
cluster4
'not assigned' 31
'misc' 13
'not assigned' 29
'amino acid metabolism' 2
'not assigned' 29
'nucleotide metabolism' 2
cluster5
'protein' 8
'protein' 11
'RNA' 8
'secondary metabolism' 2
'metal handling' 2
cluster6
'not assigned' 80
'signalling' 57
'stress' 42
'lipid metabolism' 17
'not assigned' 77
'not assigned' 51
'stress' 56
cluster7
'signalling' 56
'RNA' 56
'stress' 46
'hormone metabolism' 14
'not assigned' 98
'development' 18
'protein' 45
'PS' 12
'not assigned' 67
'RNA' 32
cluster8
'not assigned' 19
'transport' 3
'protein' 7
'amino acid metabolism' 2
'lipid metabolism' 2
cluster9
'not assigned' 36
'hormone metabolism' 12
'secondary metabolism' 16
'N-metabolism' 2
'not assigned' 27
'not assigned' 26
'transport' 11
cluster10
'protein' 1
'lipid metabolism' 3
'cell wall' 1
'stress' 4
'TCA / org transformation' 1
cluster11
'transport' 2
'cell wall' 1
'minor CHO metabolism' 1
'secondary metabolism' 1
cluster12
'not assigned' 6
'secondary metabolism' 18
'minor CHO metabolism' 1

FigureII-12: Cluster and GO enrichment analyses of DEGs identified in the pulp and skin of developing berries. (A) Clustering analysis of DEGs identified in the pulp and skin during berry development. The 9023 and 8788 DEGs identified in the pulp and skin, respectively, are distributed in 12 clusters both in the skin (red) and pulp (blue). In each tissue clusters present the number and proportion of DEGs in each cluster is indicated and is highlighted in light pink (skin) and light green (pulp). Among the DEGs, 6323 are found in the pulp and skin and were defined as common DEGs. Their distribution among the 12 clusters is indicated. The number of DEGs found in clusters with equivalent expression patterns is indicated (diagonal highlighted in grey), together with those found in different clusters between tissues. The number of DEGs specific to one of the tissue is also indicated for each of the cluster and is highlighted in dark pink (skin) and dark green (pulp). (B) GO enrichment and overrepresentation analysis of tissue specific and common DEGs in 12 clusters. Gene numbers in each category are shown on the right side.

f. Go Analysis of DEGs

To investigate the distribution of DEGs in biological processes, gene enrichment analysis was performed for each cluster, using the Mefisto software that has ranked genes in 35 functional categories (Usadel et al., 2005) as indicated in the material and methods. DEGs belonging to clusters 1, 4, 6 and 11 (referred to as group A clusters here below) representing 3406, 462, 691 and 32 DEGs respectively in the pulp, and 2899, 661, 780, and 27 DEGs respectively in the skin, are in general repressed in the grape berry tissues analyzed during all the ripening process (clusters 1) or more specifically from the véraison stage (clusters 4 and 11) or in a stepwise manner (cluster 6). Inversely, DEGs in cluster 2, 3, 5 and 12 (referred to as group B clusters here below), which correspond to 1920, 794, 152, and 69 DEGs respectively in the pulp, and 1979, 514, 205, and 60 DEGs respectively in the skin, are overexpressed during the ripening process with some differences between clusters though. In cluster 2 DEGs the pulp show a progressive increase of transcript abundance during berry ripening, whereas those of cluster 3 are characterized by a transient increase in mRNA abundance from F6 to V3 before a slight decline at V7, whereas DEGs in cluster 5 present an stepwise increase from V1 to V7. Finally DEGs in cluster 12 increase from V1 to V3. Clusters 7 to 9 present more complex expression pattern. Clusters 7 contain DEGs (345 in the pulp and 295 in the skin) that present a rapid decrease in expression from F6 to V1 followed by a moderate increase at after stages, whereas cluster 8 groups DEGs (64 in the pulp, 68 in the skin) that present a slight decrease from F6 to V3 and are induced at later stages of ripening. In cluster 9 DEGs (99 in the pulp and 142 in the skin) are expressed at a similar level from F6 to V3 and present a rapid reduction in mRNA abundance at later stages of ripening.

Taken together these results indicate that most genes will range in two main categories, those presenting an increased expression level during fruit ripening (Group A clusters), and those repressed (group B clusters). A few DEGs present more complex expression patterns reflecting variations in expression levels at specific development stages.

Functionnal Annotation of Group A DEGs

Gene enrichment was performed considering separately DEGs that were found in the same clusters in the skin and pulp (common DEGs) and those specific to the pulp and the skin, as they may reflect tissue specific processes occurring during ripening. GO annotation of the common DEGs identified in clusters 1 (1778 DEGs), 4 (142 DEGs), 6 (158 DEGs) and 11 (2 DEGs), referred here below to as Goup A clusters, are over-represented in genes belonging to 9 main functional categories (Figure II-12B). Although many genes were either not assigned, or ranked in the misc category, common group A DEGs were ranked in nine main functional categories including 'transport', 'cell', 'RNA'(RNA Processing, Transcription factors), 'signaling' (including light signaling, calcium, receptor kinase etc..), 'redox', 'stress', 'cell wall'(expansin, cellulose synthesis, and proteins involved in cell wall synthesis)' hormone metabolism' (Synthtesis and response to various hormones including auxin, ABA, cytokinins) and Photosynthesis (PS, Rubisco). This indicates that several important physiological and cellular processes are similarly down regulated in both the pulp and the skin during berry ripening. The first 20 DEGs are listed in Table4.

In addition, many DEGs specific to each tissue were identified in Group A clusters. Pulp specific DEGs (cluster 1: 852; Cluster 4: 112; cluster 6: 222; cluster 11: 12) were essentially enriched in C1- metabolisms, redox, lipid metabolisms and Photosynthesis functional categories. Those specific to the skin in the same clusters (cluster 1: 628; Cluster 4: 99; cluster 6: 295; cluster 11:5) were in contrast mainly enriched in signaling', 'stress', secondary metabolites, 'hormone metabolism and lipid metabolism'. A diversity of reasons could explain why these genes were classified as tissue specific DEGs. For example, the tissue specific DEGs related to PS (18 genes in total specific to the pulp cluster 1), are repressed in the pulp but their expression is maintained in the skin. A similar observation is made for genes involved in lipid metabolism in the pulp (32 genes specific to the pulp cluster 1). In contrast skin specific DEGs of group A clusters reflect a different situation. For example, skin specific DEGs corresponding to the lipid metabolism functional category are indeed repressed in the skin during ripening (22 DEGs in peel cluster 1), but these genes are barely expressed in the pulp at any stage. Their skin specific expression in young fruits may therefore reflect metabolic pathways operating only in the skin of young fruits. A similar observation is made for DEGs of the secondary metabolism functional category.

As a conclusion, skin specific DEGs of group A clusters may represent specific processes occurring in the skin of young fruits, whereas pulp specific DEGs of the group A clusters may rather represent processes that are maintained, at least partially in the skin of ripening fruits, but not in the pulp.

cluster	identier	name	category
cluster1	Vitvi17g00320	RuBisCOsmallsubunitF1	PS, calvincycle, rubiscosmallsubunit
cluster1	Vitvi05g01266	xyloglucanendotransglucosylase/hydrolase15	Cell wall, modification
cluster1	Vitvi07g03060	xyloglucanendotransglycosylase-relatedprotein(XTR7)	Cell wall, modification
cluster1	Vitvi11g01268	xyloglucanendotransglycosylase6(XTR6)	Cell wall, degradation,mannan-xylose-arabinose- fucose
cluster1	Vitvi14g01977	expansinA1	Cell wall, modification
cluster1	Vitvi08g00135	5-methyltetrahydropteroyltriglutamate	Amino acid metabolism,synthesis,aspartatefamily,methionine
cluster4	Vitvi07g03077	NAD-dependentmannitoldehydrogenase	Secondary metabolism,phenylpropanoids,ligninbiosynthesis,CAD
cluster1	Vitvi18g01019	cytokinin oxidase5(CKX5)	Hormone metabolism,cytokinin,synthesis-degradation
cluster1	Vitvi16g00713	Beta-fructofuranosidase	Major CHO metabolism,degradation,sucrose,invertases,vacuolar
cluster1	Vitvi02g00532	lipid-transfer	misc,proteaseinhibitor/seedstorage/lipidtransferprotein(LTP)familyprotein
cluster1	Vitvi04g01389	beta-galactosidase3	misc,gluco-,galacto-andmannosidases,beta-galactosidase
cluster1	Vitvi10g00100	peroxidases	misc,peroxidases
cluster4	Vitvi13g01760	Leucine-rich repeat(LRR)family protein	DNA,repair
cluster1	Vitvi06g00321	Elongationfactor1-alpha	protein,synthesis,elongation
cluster1	Vitvi18g00590	tubulinalpha-2chain	cell,organisation,cytoskeleton,mikrotubuli
cluster1	Vitvi07g01893	Auxineffluxcarrierfamilyprotein	transport,misc
cluster1	Vitvi15g01110	water transport PIP	transport,Major Intrinsic Proteins,PIP
cluster4	Vitvi02g00310	water transport PIP	transport,Major Intrinsic Proteins,PIP
cluster4	Vitvi08g01602	water transport PIP	transport,Major Intrinsic Proteins,TIP
cluster4	Vitvi13g00255	water transport PIP	transport,Major Intrinsic Proteins,TIP

Table II-4. List of the top 20 highly expressed co regulatory DEGs in group A.

Functionnal Annotation of Group B DEGs

DEGs ranked in group B clusters correspond to genes induced or upregulated during the ripening of berries suggesting that the corresponding porteins could be involved during this developmental process. As for group A clusters, several DEGs were found in similar clusters in the pulp and the skin, indicating that they present an equivalent expression patterns in both tissues. They may therefore fulfill similar roles in both tissues. These DEGs, referred to as “common group B DEGs”, represent 1054, 160, 23 and 4 DEGs in clusters 2, 3, 5 and 12 respectively. They are mainly enriched in 7 functional categories, ‘stress’ (29 genes), ‘RNA’ (144 genes), ‘DNA’ (41 genes), ‘protein’ (156 genes), ‘signaling’ (44 genes), redox (7 genes) and secondary metabolism (2 genes). Indeed, as for group A clusters many genes were not assigned or ranked in the misc subcategories. Most of the DEGs identified in group B clusters belong to cluster 2 which contains the higher number of genes in this group. The 144 genes related to ‘RNA’ include several genes encoding transcription factors, such as *NAC25 (Vitvi10g00437), NAC2 (Vitvi19g00271), MYB24 (Vitvi14g01750), WRKY75 (Vitvi17g00102), VvbHLH75 (Vitvi01g01946)* but also to others aspects of RNA metabolisms, including RNA binding, maturation and polyadenylation. DEGs belonging to the ‘DNA’ functional category, include genes encoding histone such as Vitvi04g01432 (histoneH1-3), Vitvi10g02198 (histoneH2A2), Vitvi13g00706 (histone2B), Vitvi18g01064 (HistoneH3) but also genes involved in DNA synthesis. DEGs ranked in the ‘protein’ functional category, include genes involved in a diversity of protein synthesis and degradation processes. These results indicate that several regulatory processes, notably those involving gene transcription are co-regulated in the skin and the pulp

at the Véraison stage and during ripening. A list of the top 20 common DEGs of group B clusters, selected based on their expression level is provided in table 5.

As for group A, tissue specific DEG in group B clusters were identified, most of them belonging to the cluster 2, though. The 493 skin specific DEGs, most (4/5th) were enriched in 4 main functionnal categories, secondary metabolism (38 genes in cluster 2, 17 in cluster 3 and 18 in cluster 12) and RNA (62 genes cluster 2, and 19 in cluster 3), amino acid metabolism (5 genes in cluster 3) and protein (8 genes in cluster 5). Noteworthy, all secondary metabolism related genes induced in the skin during ripening, remained silent or weakly expressed in the pulp at the same stages. They include the gene coding for the 1 Flavonone-3-hydroxylase （F3H) and those, 9 and 17, respectively, encoding the Phenyl-alanine-ammonia- lyase （PAL） and the naringenin- chalconesynthase (CHS) enzymes involved in the polyphenols synthesis pathway. Within the 62 DEGs related to the RNA functional category, several additional transcription factors were identified, including WRKYs, 5 MYBs, SNF2 and the methyl-CPG-bindingdomain11 (MBD11) that seem specifically induced in the skin. A list of the 20 DEGs that are the most highly induced is provided in Table II-5. The group B pulp specific DEGs, were essentially enriched in 5 functional categories namely, signaling (18 genes cluster 2), protein (93 genes cluster 2 and 11 cluster 5), RNA (86 genes cluster 2 and 8 cluster 5), stress (14 genes cluster 3) and minor CHO metabolism (1 gene cluster 12). The most highly expressed genes in the pulp are shown in Figure II-12. Although it is difficult to infer from this result a general view of tissue specialization, an obvious observation is that several genes associated with secondary metabolites, and in particular with anthocyanin accumulation were specifically induced in the skin, and remained at very low expression levels or silent in the pulp. This is consistent with the analysis of the anthocyanins that only accumulate in the skin and reflects the tissue specialization that is observed at this stage. Of note transcription factors specific to each of these tissues were identified in line with the specific upregulation of several hundreds of genes.

cluster	identier	name	category
cluster2	Vitvi15g00643	expansinB2	cellwall,modification
cluster2	Vitvi13g01966	UDP-glucuronicacid decarboxylase	cellwall.precursorsynthesis.UXS
cluster3	Vitvi02g01171	Acyl-CoA-binding protein	lipidmetabolism,FAsynthesisandFAelongation,acyl-CoAbindingprotein
cluster5	Vitvi05g00020	Glyoxysomal fatty acid beta-oxidation protein MFP-a	lipidmetabolism.lipiddegradation.beta-oxidation.multifunctional
cluster2	Vitvi05g00560	Aci-reductonedioxygenase 2	metalhandling,regulation
cluster5	Vitvi03g00374	Isoprenoid biosynthesis HDR	secondarymetabolism.isoprenoids.non-mevalonatepathway.HDR
cluster2	Vitvi02g00333	glutathioneperoxidase6	redox,ascorbateandglutathione,glutathione
cluster2	Vitvi18g02775	Thioredoxin H-type	redox,thioredoxin
cluster2	Vitvi17g00484	CYP78A	misc,cytochromeP450
cluster3	Vitvi09g00436	Auxin-inducedprotein 22A	RNA,regulationoftranscription,Aux/IAAfamily
cluster3	Vitvi06g01114	Cystatin B	protein,degradation,cysteineprotease
cluster2	Vitvi08g00939	Cystatin B	protein,degradation,cysteineprotease
cluster2	Vitvi14g01748	ADP-ribosylationfactorA1B(ARFA1B)	protein,postranslationalmodification
cluster2	Vitvi15g01632	Translation initiation factor1A	protein,synthesis,initiation
cluster2	Vitvi18g00740	Granulin repeat cysteine protease	protein,degradation,cysteineprotease
cluster2	Vitvi08g01890	Glycoside hydrolase	minorCHOmetabolism,raffinosefamily,raffinosesynthases,putative
cluster2	Vitvi07g00595	Actin-depolymerizing factor(ADF)	cell,organisation,cytoskeleton,actin,actindepolymerizingfactors
cluster2	Vitvi01g01719	senescence-associatedgene29(SAG29)	development,unspecified
cluster2	Vitvi12g01880	RmlC-like cupins protein	development,storageproteins
cluster3	Vitvi17g00070	RAG1-activating protein1	development,unspecified

Table II-5. List of the top 20 highly expressed co regulatory DEGs in group B

Additional clusters present stage specific variations of gene expression

The 4 remaining clusters group genes that present stage specific variations in expression level. Although different, the clusters present some similarities. For example Clusters 7 and 8 both display a U shaped profile. DEGs in both clusters are down regulated between F6 and V1, and their expression increase again during ripening from V1 in clusters 7 and from V3 in clusters 8. In contrast both clusters 9 and 10 have an inversed-U shaped profile.DEGs in these clusters present an increased expression from F6 to V1 (Cluster 9) or to V3 cluster 10) before being repressed at later ripening stages. Clusters 7 and 8 represent a total of 1047 genes in the pulp and 1150 genes in the skin, and Clusters 9 and 10, 550 and 508. As for group A and B, common DEGs were identified for each of these clusters, further demonstrating coregulatory processes in both tissues (Figure II-12B).

In the case of cluster 7, 226 common DEGs were identified, that were enriched in only one functional category 'RNA' (32 genes), that includes 21 transcription factors encoding genes, such as, *Homeobox transcription factor (HB2,Vitvi02g01717), HB12(Vitvi16g01362) WRKY50(Vitvi04g001330) and WRKY11 (Vitvi04g00756)* were highly expressed at F6 and repressed after veraison. The 429 skin specific DEGs of cluster 7 were enriched in 4 categories hormone metabolism (14 genes), stress (46 genes), RNA (56 genes) and signaling (56 genes). However, most of these genes were expressed at low levels (RPKM<20). In addition, 345 pulp specific DEGs were identified that are overrepresented in 3 categories, photosynthesis (12 genes), protein (29 genes) and development (18 genes).

Clusters 8 contain 152 (pulp) and 240 (skin) DEGs, of which 24 were shared between pulp and skin. In addition, 64 and 68 of pulp and skin specific DEGs were identified, respectively, most of them being either expressed at low levels or unknown.

363 and 412 DEGs belong to clusters 9 of pulp and skin, respectively. Ninety five common DEGs identified between pulp and skin were enriched in transport category (11 genes). A total of 142 DEGs were uniquely found in skin and enriched in 3 functional categories, N-metabolisn (2 genes), secondary metabolism (16 genes), hormone metabolism (12 genes).

Clusters 10 contain 87 and 96 DEGs in pulp and skin, respectively. Nine common DEGs were found both pulp and skin. These common DEGs include 3 genes encoding Heat shock proteins, one a Carbonic anhydrase (Vitvi14g01763). In addition, 23 pulp specific and 27 skin specific DEGs were found in this cluster.

g. Photosynthesis related genes are more repressed in pulp and skin during ripening

Most fruits at early developmental stages, including grape berry, accumulate chlorophylls in chloroplasts and present a photosynthetic capacity (Aschan & Pfanz, 2003), whereas they lose this capacity along with the degradation of chlorophyll during ripening. Consistent with this view, the results obtained here indicate that 58 gene related to photosynthesis which were strongly expressed at F6, shown a gradual

decline in expression level during berry development and ripening irrespective to the tissue considered. However, their kinetic of repression differs between tissues. These 58 genes were barely detectable in the pulp at V7, but they remain at a significant expression level in skin. For example, *Vitvi17g00320* encoded a Ribulose 1,5-bisphosphate carboxylase/oxygenase (Rubisco) small subunit (RBCS) F1 orthologous to the Arabidopsis *RBCS1A (AT1G67090)* subunit which is involved in the first step of carbon fixation (Izumi et al., 2012). The *Vitvi17g00320* gene is highly expressed both in pulp and peel before veraison (pulp RPKM=1525; skin RPKM=1319, at F6), but its expression decrease 300 fold in the pulp and only 3 fold in the skin after veraison. Similarly, several genes involved in light harvest complexes and photosynthesis reaction including *Vitvi19g01479 (Photosystem II 10k Da polypeptide,PII10), Vitvi18g00272 (Photosystem II 22 kDa protein, CP22), Vitvi15g00004(photosystem I light harvesting complex 3, LHCA3), Vitvi12g02485 (photosystemII light harvesting complex 2.1, LHCB2.1), Vitvi12g00050 (light-harvesting chlorophyll-protein complex II subunitB1, LHB1B1), Vitvi10g01839 (light-harvesting complex,chlorophyll A/B binding protein1,CAB1), Vitvi09g00361 (Photosystem I reaction center subunit VI, PSI-H), Vitvi07g00035 (Photosystem II reaction center W protein, PSII6, 1kDa protein), Vitvi06g00513 (Ribulosebis phosphate carboxylase/oxygenaseactivase, RuBisCO activase)* were expressed at higher levels in the skin than the pulp (Figure II-13), although their expression seemed equivalent at F6. This suggests that their expression were more strongly repressed in the pulp than in the skin.

In addition, a total of 18 DEGs related to photosynthesis were uniquely repressed in pulp, whereas they remained stably expressed in the skin (Figure II-13). They include genes encoding a Rubisco activase *(Vitvi08g01245)* which is required for the light activation of RuBisCO, a fructose-bisphosphatealdolase2 (FBA2), 3 enzymes in calvin cycle, an aldolase *(Vitvi04g01421), Glyceraldehyde-3-phosphate dehydrogenase B (GAP,Vitvi18g00068), triosephosphate isomerase (TPI,Vitvi03g00097).* A similar observation is made for a Ferredoxin (*Vitvi12g01968*) encoding gene that is involved in electron transport (Minna M. Koskela, 2018).

Taken together, these observations are consistent with the idea that even though pulp and skin show reduced expression during ripening of genes related photosynthesis, repression of this category of genes is more intense in the pulp than the skin, as previously reported (Lijavetzky et al., 2012)(Marques et al., 2013).

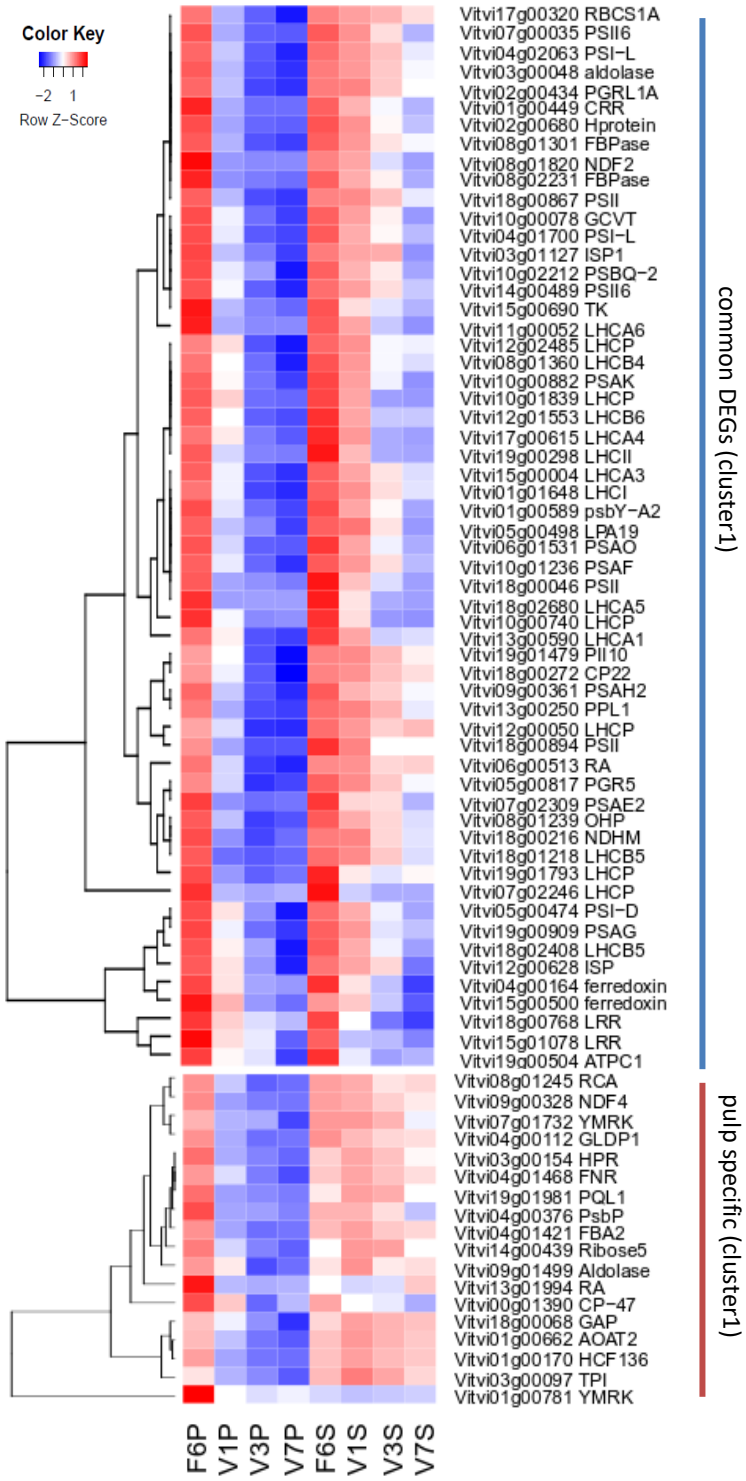

Figure II-13. Heatmap of photosynthesis related genes expression in pulp and skin during ripening. Details of gene names are indicated in the text. Tissue specific and common DEGs are indicated.

h. *Genes encoding enzymes involved in cell wall metabolism present complex expression patterns during ripening.*

Softening is an important process occurring during ripening in fleshy fruits. It involves a diversity of metabolic modification catalyzed by a number of cell wall modification enzymes. It involves a cooperative action between several different enzyme families, including expansins, endo-1,4-glucanases (EGase), xyloglucan endotransglycosylases/ hydrolases (XTH), polygalacturonases (PG) or pectate lyases (PL), esterase like pectin methylesterases (PME) and pectin acetylesterases (PAE), exo-acting hydrolases and other glycosidases such as -galactosidases (-gal) that were all identified in the DEGs here. Expansins mediated the loosening of cell walls in a pH-dependent manner. Expansins are encoded by a superfamily of genes of 29 genes in grape (Santo et al., 2013). In our study, 11 of the expansin genes were barely expressed (RPKM<1) in both tissues whereas 16 others identified as DEGs were clustered in clusters 2, 3, 4 and 9 with a maximal transcript accumulation at V1 and a progressive decrease during ripening. Among those, *Vitvi18g00189 (VvEXPA19)* and *Vitvi13g00172 (VvEXPA14)*, the two predominately expressed expansin genes exhibit similar expression pattern, peaking at V1 both in the pulp and the skin. Other expansin genes displayed a different behavior. For example *VvEXPA16* which peaks at F6 before veraison and decrease during ripening, in contrast to *VvEXPB4* that belongs to cluster 2 and shows a linear increase in expression during berry ripening in pulp and skin to reach a maximal level at V7 in pulp and skin. In addition, some expansin encoding genes are tissue specific DEGs. Transcript abundance of *Vitvi03g00209* (*VvEXA1*) and V*itvi06g00016* (*VvEXPA5*) is higher in pulp than in skin at V1 corresponding to the maximal accumulation level. In contrast *Vitvi01g01030* (*VvEXPA1*) is only expressed in the skin and peaks at V1.

Xyloglucan endo-trans-glycosylase/hydrolase (XTH), a xyloglucan modifying enzyme, has been proposed to be important for loosening the cell wall during fruit ripening (Muñoz-Bertomeu et al., 2013). *Vitvi06g01329* (*XTH32*), which is DEGs identified in cluster 9 of pulp and in cluster 5 of skin which remains highly expressed during ripening in both tissues. Interestingly, *Vitvi07g03060* (Vv*XTH7*) and *Vitvi05g01266* (*VvXTH15*) that show a tissue specific expression pattern and therefore were ranked in tissue specific DEGs, are both the most highly expressed at F6 in skin and pulp, respectively, but display different expression patterns between tissues at later stages of fruit ripening.

Pectin Methylesterase (PME) which removes the methyl groups from esterified pectin, was also suggested to be involved in cell wall softening, although inhibition of their activity, essentially in tomato fruits had limited effects on fruit softening (Phan et al., 2007). The role of PME is difficult to anticipate based on the expression patterns observed here. The *Vitvi12g02137* presents an enhanced expression level after veraison in both the pulp and the skin, whereas *Vitvi16g01418* which is highly expressed at F6 and declines rapidely during ripening in both tissues. Other PME encoding genes had contrasted expression patterns between tissues: hence *Vitvi03g00217* was more highly expressed in the pulp than the skin during ripening (Figure II-14). Similarly Polygalacturonses (PG) have limited effects on fruit softening in tomato fruits, although they are often dramatically upregulated in fruits (Smith et al., 1988). In the data presented here, *Vitvi08g02394* (*VvPG1*) displays tissue specific transcript accumulation in the pulp during ripening, but only a weak increase in expression level in the skin. An increased transcript

level of Xyloglucan endo-trans-glycosylase (*XET, Vitvi01g01805*) was also detected during early ripening, however preferentially in the skin. B-Galactosidase (BG), Vitvi18g01022 (BG1) transcripts accumulated to high levels abundance in immature berry both in the pulp and skin, and rapidly decreases during ripening.

The recent demonstration that Pectate lyase (PL), an enzyme that degrades de-esterified pectin in the primary wall, is an essential contributor to fruit softening in tomato (Uluisik et al., 2016), suggests that it may have a similar role in other fruits including grape. Consistent with this idea, *VvPL1* (*Vitvi05g00953*) and *VvPL5* (*Vitvi01g00593*) are strongly induced at the beginning of berry ripening, with slightly different expression patterns though. Hence *VvPL1* peaks in both tissues at the V1 stage, whereas, *VvPL5* peaks at V1 in the pulp but at F6 in the skin, before decreasing at later developmental stages in both tissues.

In conclusion, genes encoding enzymes potentially involved in cell wall modification were significantly up-regulated before or véraison or at early stages of ripening. However, in addition to the genes similarly regulated in both tissues, several genes also present contrasted expression patterns between tissues, suggesting that different enzymes participate to the regulation of cell wall metabolism in grape fruit tissues, suggesting tissue specific regulatory pathways controlling fruit softening.

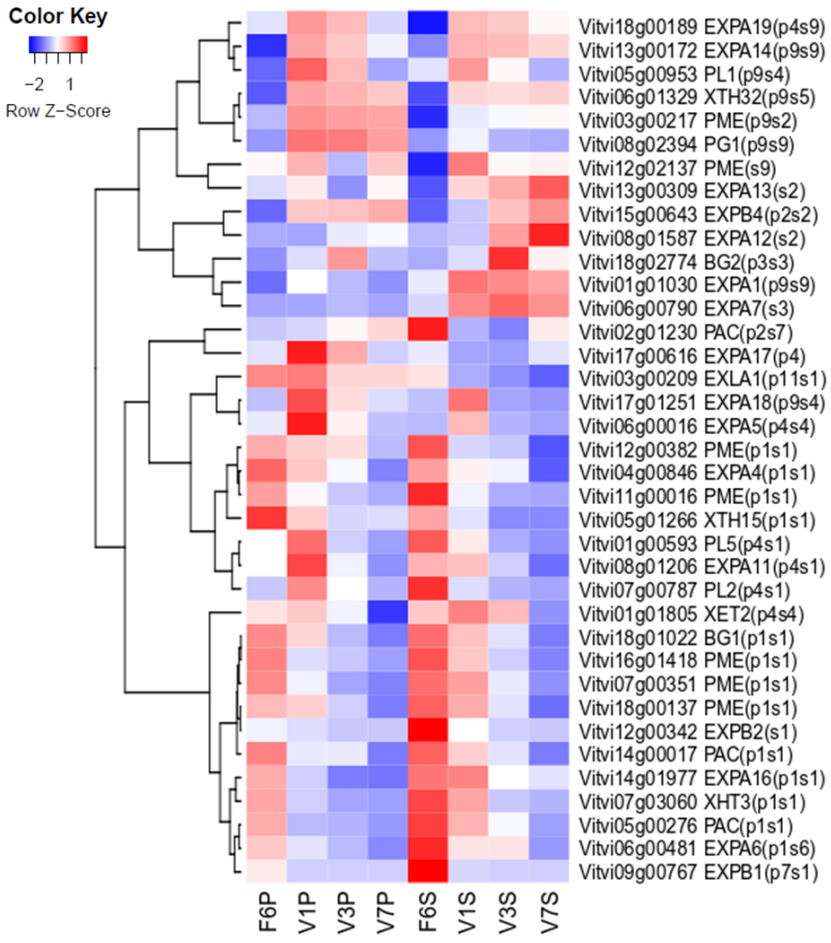

Figure II-14. Heatmap of gene expression related to cell wall modification in pulp and skin during ripening. Gene names are indicated in the text above. p, pulp, s, skin, number indicated the cluster number.

i. Genes involved in soluble sugar synthesis and transport are highly expressed in the pulp

The content of sugar in grape berry is of commercial importance in winemaking, not only because its fermentation by yeast produces alcohol, but because it augments the flavor profile of the final wine product. The concentration of hexoses, fructose and glucose, was previously shown to be lower in the skin than in the pulp (Coombe et al, 1987). Analysis of soluble sugar accumulation in the berries of Cabernet Sauvignon confirmed that during ripening the content of both fructose and glucose is higher in the pulp than in the skin. It also showed that accumulation of hexoses is initiated at F7 in the pulp and 4 weeks later at V2 in the skin.

RNA seq data obtained in this study indicates that 64 sugar syntheses related genes were DEGs, including synthesis and transport of hexoses, sucrose and starch.

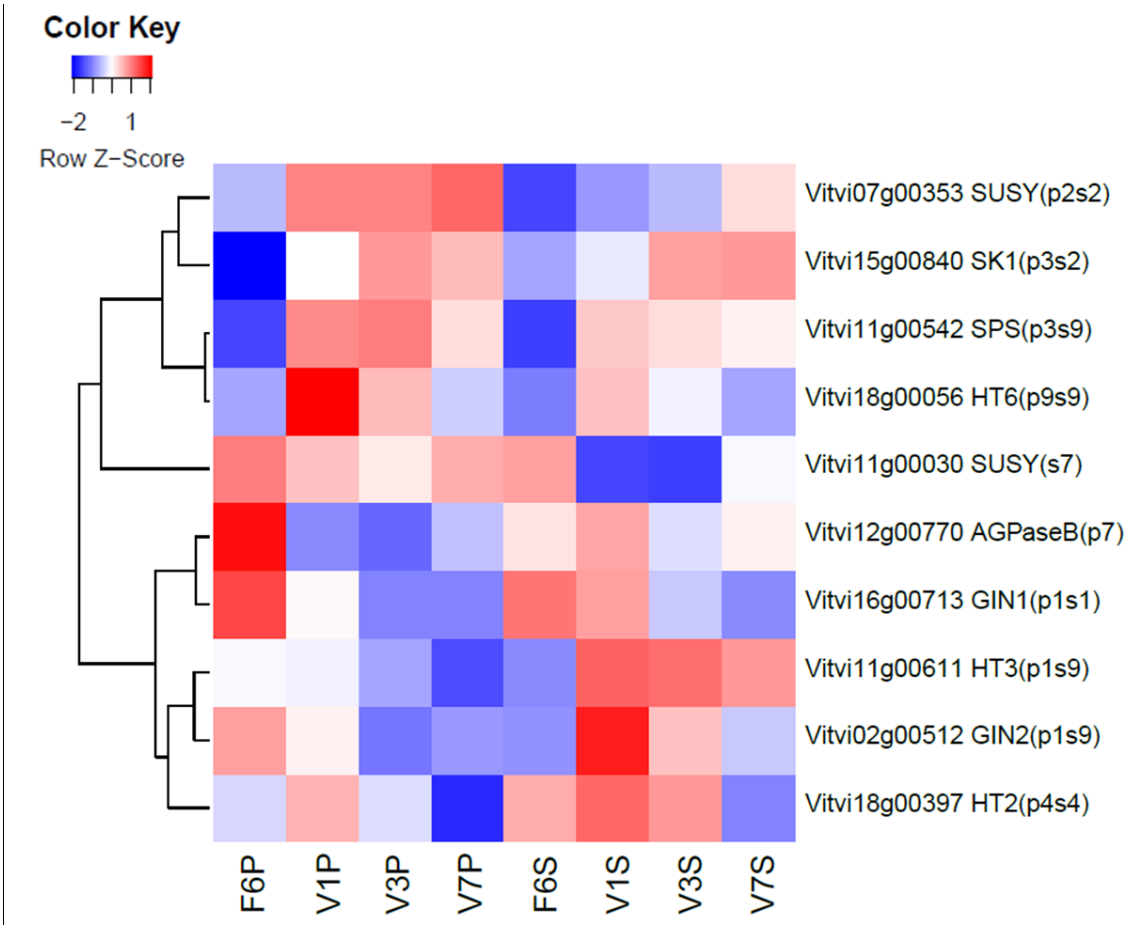

Figure II-15. Heatmap of gene expression related to sugar synthesis in pulp and skin during ripening. Gene names are indicated in the text above. p, pulp, s, skin, number indicated the cluster number.

Although we have not investigated sucrose accumulation in grape berry tissues, sucrose is the major form of carbohydrate loaded into the phloem at photosynthetic source leaves and distributed to heterotrophic sinks such as fruit. Sucrose is usually transported from leaves by phloem in a long distance transport and is cleaved into hexoses by invertase and reversible sucrose synthase. In CS berries, two sucrose invertase encoding genes, namely Vv*GIN1* (*Vitvi16g00713*) and *VvGIN2* (*Vitvi02g00512*), were identified among the DEGs. Yet they display distinct expression patterns: *VvGIN1* expression peaks in both tissues at F6 but decreases more rapidly in the pulp than in the skin. In contrast *VvGIN2* expression is not synchronized between tissues. *VvGIN2* transcript abundance peaks at F6 in the pulp ad decreases during ripening (from V1 to V7). *VvGIN2* gene expression is the highest at V1 in the skin and decreases progressively at later stages of ripening (Figure II-15). This suggest that whereas VvGIN1 is the key enzyme for sucrose mobilization in the pulp, VvGIN2 may be most important for the skin, as in both cases their expression precedes the accumulation of hexoses in pulp and skin, respectively. In addition, *VvSuSy* (*Vitvi07g00353*) which encodes a sucrose synthase is strongly induced during ripening, and present a higher expression levels in the pulp than in the skin. Differential regulation of *Vitvi07g00030* that also encodes a sucrose synthase, also shows that *SuSy* transcript are more abundant in the pulp than in the skin (Figure II-15). These data are consistent with earlier and higher accumulation of hexoses in the pulp as compared to the skin. Finally, among the 6 hexose transporter (tonoplast hexose transporters) encoding gene identified in grape, only Vv*HT2* (*Vitvi18g00397*), *VvHT3* (*Vitvi18g00611)* and Vv*HT6* (*Vitvi18g00056*) were induced during ripening, with different expression patterns. *VvHT6* which is preferentially expressed in the pulp, peaks in both tissues at the V1 stage. In contrast *VvHT2* is preferentially expressed in the skin and is only repressed at V7 in this tissue. Finally *VvHT3* is barely expressed in the pulp and present high expression levels in the skin at all ripening stages.

j. Organic acid related genes reflect the differential accumulation of organic acid in berry tissues

At harvest, the ratio of sugar / acid is an important quality trait of grape berries. Malic and tartaric acid are the two major organic acids accumulating in grape berry, accounting for 90% of total fruit acidity (Kliewer, 1967)(Lamikanra et al., 1995a)(Conde et al., 2007). Tartaric acid accumulates in berries at early developmental stages in both tissues analyzed (part 2.3.2b, page 62), and gradually decreases during ripening both in pulp and skin concomitantly to hexoses accumulation. In contrast malic acid presents a tissue specific accumulation profile. It increases from F4 to F7 and is rapidly mobilized in the pulp to reach very low levels at V2, whereas in the skin its accumulation starts at F7 peaks at V2 before decreasing during ripening. Figure II-16 displays the simplifed metabolite pathway of malate and tartrate in grape berry. Before veraison, sucrose is transported from the leaves to the berries where it is broken down to glucose and fructose. Glucose and fructose enter glycolysis and enable malate synthesis. In plants, malate can be synthesized through carboxylation of phosphoenolpyruvate (PEP) provided from glycolysis, to oxaloacetate (OAA) by phosphoenolpyruvate carboxylase (PEPC) and further reduction into malate by cytosolic NAD-dependent malate dehydrogenase (NAD-MDH), or following the conversion of PEP to pyruvate by pyruvate kinase (PK), then to malate by NADP dependent malic enzyme (NADP-ME).

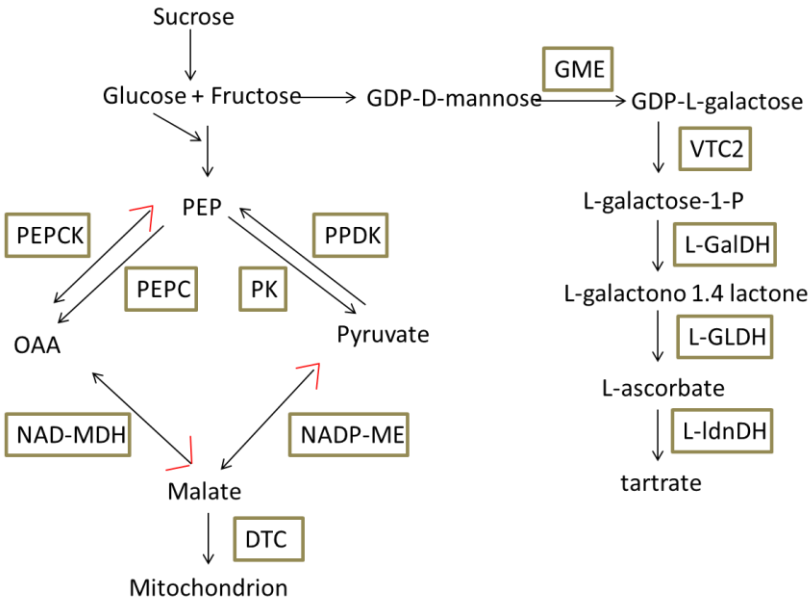

FigureII-16. Simplifed biosynthesis pathway of malate and tartrate (Cholet et al., 2016)(Sweetman, 2009b). NAD-MDH, NAD-linked malate dehydrogenase; NADP-ME,NADP-linked malic enzyme; PEPC, phosphoenolpyruvate carboxylase; PEPCK, phosphoenolpyruvate carboxykinase; PK, pyruvate kinase; PPDK, pyruvate orthophosphate dikinase. GME, GDP-D-mannose 3,5epimerase; VTC2, GDP-L-galactose phosphorylase; L-GalDH, L-galactose dehydrogenase; GLDH, L-galactono-1,4-lactone dehydrogenase; L-IdnDH, L-idonate dehydrogenase;PEP, phosphoenolpyruvate; OAA, oxaloacetate. For reversible reactions is indicated by larger red arrowhead.

It should be noticed that NAD-MDH can catalyze the reversible conversion between malate and OAA depending on the abundance of malate in cytosol. If malate is transported to vacuole, then NAD-MDH tends to drive malate synthesis. Alternatively, if malate is abundant, it preferentially catalyzes the conversion from malate to OAA. Similarly, NADP-ME is also involved in malate synthesis and degradation, depending on the isoform present and cellular condition and the content of substrate. So the decrease in malate content resulted from the increase of cytoplasmic malate dehydrogenase NAD-MDH and NADP-ME. Pyruvate orthophosphate dikinase (PPDK) control the synthesis of PEP directly from pyruvate.

In the present study, genes coding for PEPC (*Vitvi01g00214, Vitvi12g00185*) were significantly down regulated following the induction of ripening (Figure II-17). However the kinetic of repression was delayed in the skin as expected from the delay in malate accumulation observed in the skin. Surprisingly, one of the genes encoding a PEPC isoform (*Vitvi19g00112*) exhibited an opposite expression patterns, characterized by an increased transcript level during ripening in the pulp while remaining stable in the skin. The possible role of this isoform remains unclear. NAD-MDH transcripts encoded by the gene *Vitvi19g0013*8 were also up-regulated throughout development irrespective to the tissue considered. Three other NAD-MDHs (*Vitvi13g00700, Vitvi15g00628, Vitvi17g00607*) showed very variable patterns throughout development, transitent increase during ripening, making difficult any correlation between their expression patterns and malate synthesis in berry tissues.

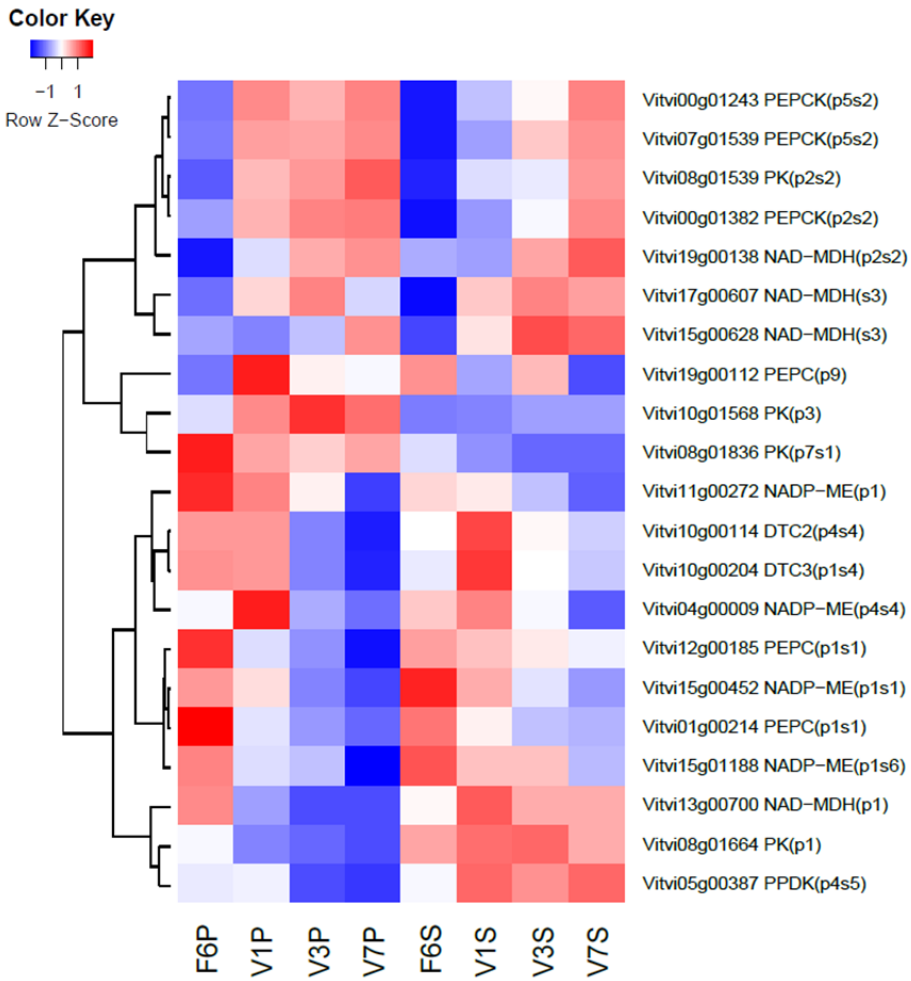

Figure II-17. Heatmap of gene expression related to malate metabolite in pulp and skin during ripening. Gene names are indicated in the text above. p, pulp, s, skin, number indicated the cluster number.

Malate degradation occurs following oxidation by the Krebs cycle, gluconeogenesis, and fermentation reactions that produce ethanol, anthocyanin synthesis, and amino acid interconversions. Degradation takes place both in the cytosol, by oxidation into pyruvate and PEP via the malic enzyme (ME) and phosphoenol-pyruvate-carboxykinase (PEPCK), respectively, and in the mitochondria, where malate is a substrate for the citrate cycle. It should be noted that mitochondria purified from ripening berries cannot oxidize malate in the absence of added pyruvate, exactly as if the plant-specific mitochondrial ME was lacking. Ruffner et al reported an increase in PEPCK activity in ripening grapes which coincides with two PEPCK transcripts found by (Terrier et al., 2005).

Three *PEPCK* genes were consistently up-regulated throughout berry development (*Vitvi07g01539, Vitvi00g01243, Vitvi00g01382*). Their induction was delayed in the skin as compared to the pulp consistent with the delayed metabolization of malate in this tissue. Malate degradation may also be promoted by the increased expression of dicarboxylate transporters (Sweetman, 2012). Four NADP-ME encoding genes *(Vitvi04g00009, Vitvi11g00272, Vitvi15g00452, Vitvi15g01188)* were differentially expressed during berry ripening. Transcript production of *Vitvi11g00272* was the key NADP-ME linear

down regulated in pulp during ripening located in cluster 1, while it was slightly decreased in skin. The other three *NADP-ME* genes gradually declined in two tissues. There were four PK encoding genes *(Vitvi08g01539, Vitvi08g01664, Vitvi08g01836, Vitvi10g01568)* were identified as DEGs in present RNA seq data. *Vitvi08g01539* located in cluster 2 was the highest expressed PK, but with more abundance at all stage in pulp than skin. PPDK *(Vitvi05g00387)* was significantly induced in skin but weakly repressed in pulp during ripening, suggest it play different roles in pulp and skin.

Regalado et al., (2013) recently characterized three *V. vinifera* mitochondrial dicarboxylate/ tricarboxylate carriers (VvDTC1–VvDTC3) putatively involved in the transport of mitochondrial malate, citrate, and other di/tricarboxylates. The two genes encoding VvDTC2 (*Vitvi10g00114*) and VvDTC3 (*Vitvi10g00204*) were allocated to cluster 1 and 4 (maximum expression at F6) and decreased 7-fold between F6 and V3 in pulp, but their peak of expression was delayed to V1 in the skin. These results are consistent with the delayed accumulation and degradation patterns of malic acid in the skin that could result from the decrease inmalic transport into the vacuole, combined with the increase of PEPCK and MDH activity, leading to the decline of malic accumulation during berry ripening.

The highest concentration of tartaric acid was detected in very young berry shortly after fruit set and gradually decrease during berry development and ripening. So tartaric acid synthesis occurs at early stages of berry development immediately after fruit set. Ascorbate has been proposed to be a precursor of tartaric acid (DeBolt et al., 2006). In grape berries, previous studies have shown that both ascorbate and tartrate accumulate rapidly after fruit set (Melino et al., 2009). Ascorbate is mainly synthesized by the Smirnoff-Wheeler pathway. Briefly, the ascorbate precursor L-galactono-1,4-lactone is produced from GDP-L-mannose by the sequential action of GDP-mannose-3,5-epimerase (GME), GDP-L-galactosephosphorylase (VTC2), L-galactose-1-phosphate phosphatease and L-galactose dehydrogenase (L-GalDH). The L-idonate dehydrogenase (L-IdnDH) catalyzes ascorbate degradation generating tartarte. Recently an alternative pathway for ascorbate biosynthesis was proposed that involves the production of L-galactono-1.4-lac-tone from D-galacturonic acid by the enzyme galacturonic acid reductase (GalUR)(Agius et al., 2003).

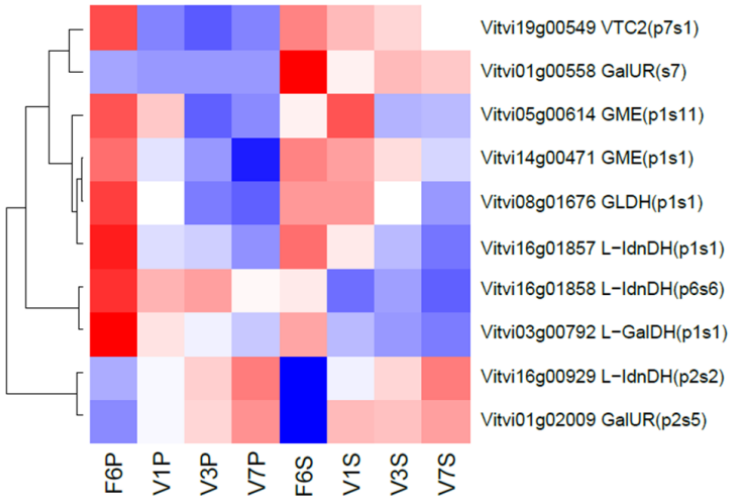

Figure II-18. Heatmap display the expression of genes related to tartrate biosynthesis. Gene names are indicated in the text above. p, pulp, s, skin, number indicated the cluster number.

In our data, the GME (*Vitvi14g00471, Vitvi05g00614), VTC2 (Vitvi19g00549), L-galactose-1,4-lactone dehydrogenase (GLDH, Vitvi08g01676), L-GalDH (Vitvi03g00792), L-IdnDH (Vitvi16g01858, Vitvi16g01857)* encoding genes were mainly expressed in immature green berries before veraison. Their expression rapidly decreased after veraison and during ripening. Noteworthy their expression is higher in in the pulp than in the peel. These results are consistent with the accumulation kinetic of tartrate during berry development and ripening. In contrast, genes encoding *L-IdnDH (Vitvi16g00929)* and *GalUR (Vitvi01g02009)* present opposite expression profile with increase during ripening and peak at V7, with similar expression levels in the pulp and the skin (Figure II-18).

k. Hormones

Hormones are involved in the regulation of many important physiological and developmental processes in plants including fruit development and ripening (see general introduction part 1.4.3, page 44). For example, ethylene plays a crucial role in the ripening of tomato, a climacteric fruit, which display a sharp increase in ethylene production and respiratory activity at the onset of ripening (Yokotani et al., 2009). Grape berry is a non-climacteric fruit and as such lacks a respiration and ethylene accumulation peaks profile prior to ripening induction (Chervin et al., 2004). However, ethylene was also suggested to play an important role in berry development and anthocyanin accumulation (Chervin et al., 2004)(Chervin et al., 2008).

Ethylene synthesis and signaling related genes: A total of 81 DEGs related to ethylene synthesis and signaling were identified during berry development and ripening, Most of them are expressed prior to veraison and are repressed during ripening. Among these genes, *Vitvi10g02409, Vitvi05g01929* and *Vitvi12g00445* which encode ACC oxidase (ACO), a key enzyme in the biosynthesis of ethylene, were highly expressed at F6, and rapidly decline to their lowest level at V1, before a new and moderate increase at later stages of ripening. However these genes present different levels of transcript abundance in pulp and skin, *Vitvi10g02409* preferentially expressed in the pulp, *Vitvi05g01929* in the skin, whereas *Vitvi12g00445* present similar expression profiles in both tissues, but it was 3.5 fold higher in skin at F6. One ACC synthase gene (ACS, *Vitvi02g00032*) is also repressed after veraison in both pulp and skin. Five ethylene response factor (ERF) related genes (*Vitvi04g00533, Vitvi05g00715, Vitvi07g01702, Vitvi12g00274, Vitvi16g00380*) were significantly induced during ripening, but *Vitvi12g00274, Vitvi16g00380* preferentially expressed in pulp while Vitvi07g01702 higher induced in pulp after veraison, and *Vitvi04g00533, Vitvi05g00715* were up-regulated in both tissue during ripening. It suggested different proteins respond to ethylene signaling in pulp and skin during ripening. Genes involved in ethylene synthesis and signaling expressed at higher levels in the skin than the pulp (Figure II-19).

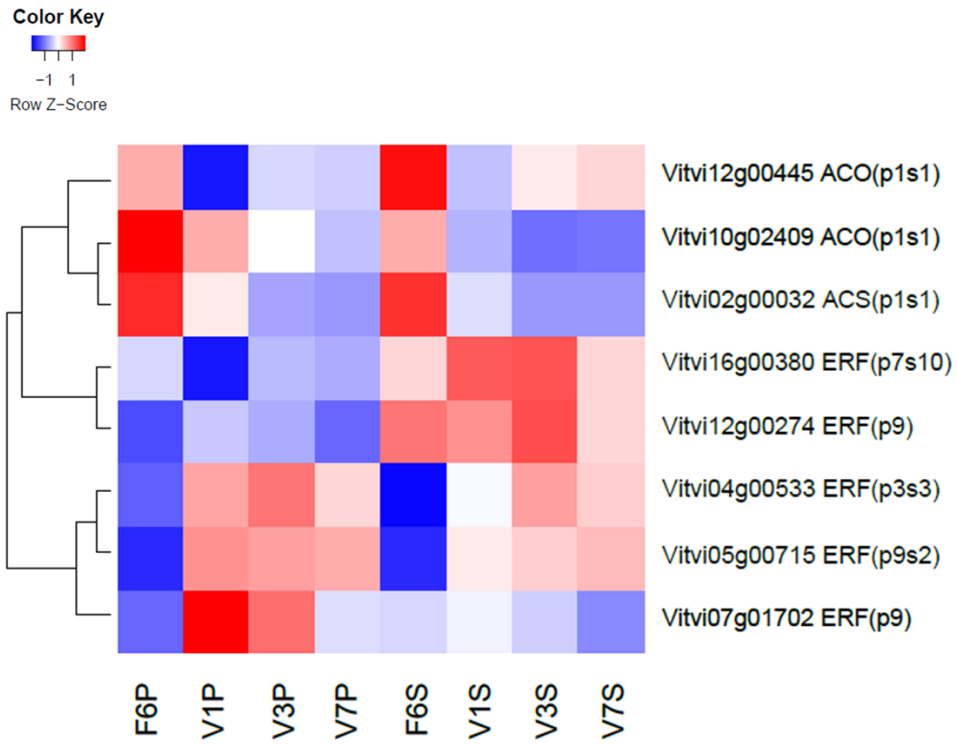

Figure II-19. Heatmap of the 7 top expressed genes related to ethylene in pulp and skin during ripening. Gene names are indicated in the text above. p, pulp, s, skin, number indicated the cluster number.

ABA synthesis: ABA is considered as an important signal triggering berry ripening (Koyama et al.,2010), because a strong increase in ABA content is observed in grape berry at the initiation of ripening, and berry treatment with exogenous ABA induced more sugar and anthocyanin accumulation in grape berry (Gambetta et al., 2010)(Koyama et al., 2010). Fifty eight DEGs corresponding to genes involved in ABA synthesis and response were differential expressed during berry ripening. For example, 9-*cis*-epoxycarotenoid dioxygenases (NCED) which catalyzes the first step in ABA biosynthesis, and is rate-limiting.Five NCED encoding genes, *Vitvi10g00821*, *Vitvi02g01288*, *Vitvi02g01286*, *Vitvi05g00963* and *Vitvi19g01356* were found induced at higher levels in pulp than skin after verasion. Among them, *Vitvi05g00963* gene that encodes NCED transcript is specifically expressed in skin during ripening, but at very low level in pulp. The other four NCED encoding genes showed similar expression pattern and levels in the two tissues. These data indicate that different enzymes of ABA synthesis are involved in pulp and skin of grape berries. Genes encoding proteins involved in ABA signaling, such as, highly ABA-induced PP2C gene (*HAI, Vitvi06g00533)*, ABA-INSENSITIVE1 (ABI1, Vitvi11g00270), HVA22 homologue D (HVA22D) were strongly upregulated during ripening. Most genes showed higher expression levels in the skin than in pulp (Figure II-20).

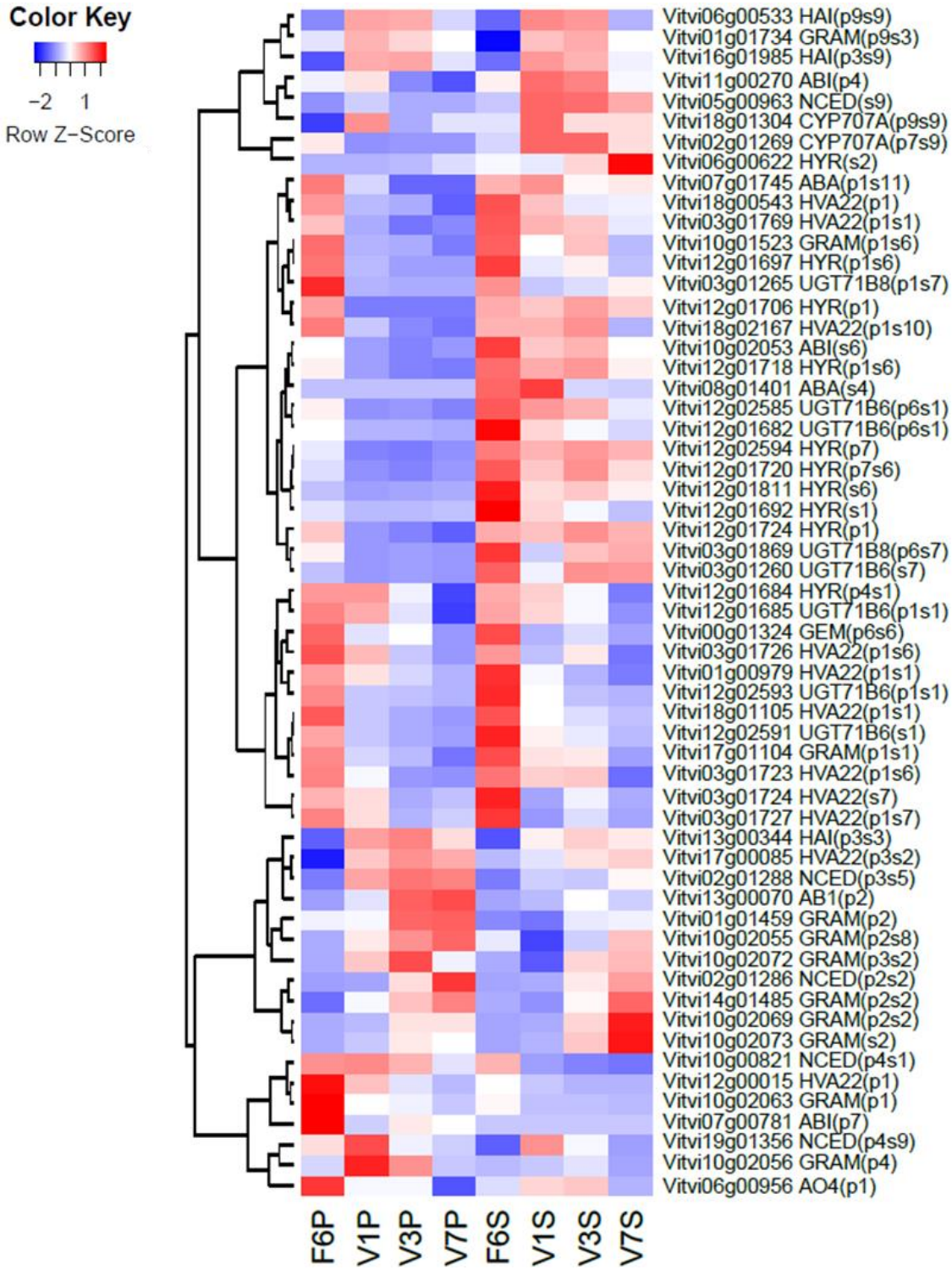

Figure II-20. Heatmap of 58 DEGs related to ABA metabolite in pulp and skin during ripening. Gene names are indicated in the text above. p, pulp, s, skin, number indicated the cluster number.

I. Genes involved in Secondary metabolite accumulation are specifically induced in the skin during berry ripening

Phenolic compounds are considered as the most important secondary metabolites in grape. They have a pivotal role as they contribute to the color and astringency of beery and wine and provide health benefit to humans (Xia et al., 2010). In plants, phenolic compounds are divided into two groups: non-flavonoid (hydroxybenzoic and hydroxycinnamic acids and stilbenes) and flavonoid compounds (anthocyanins, flavan-3-ols and flavonols). In grape berry, phenolic compounds are mainly accumulating in the skin and seeds of berry, but also in the stems and leaves. Phenolic compounds including stilbene, flavonol, tannin and anthocyanin share common precursors in the phenylpropanoid pathway. A simplified scheme of the pathway is shown in Figure II-21.

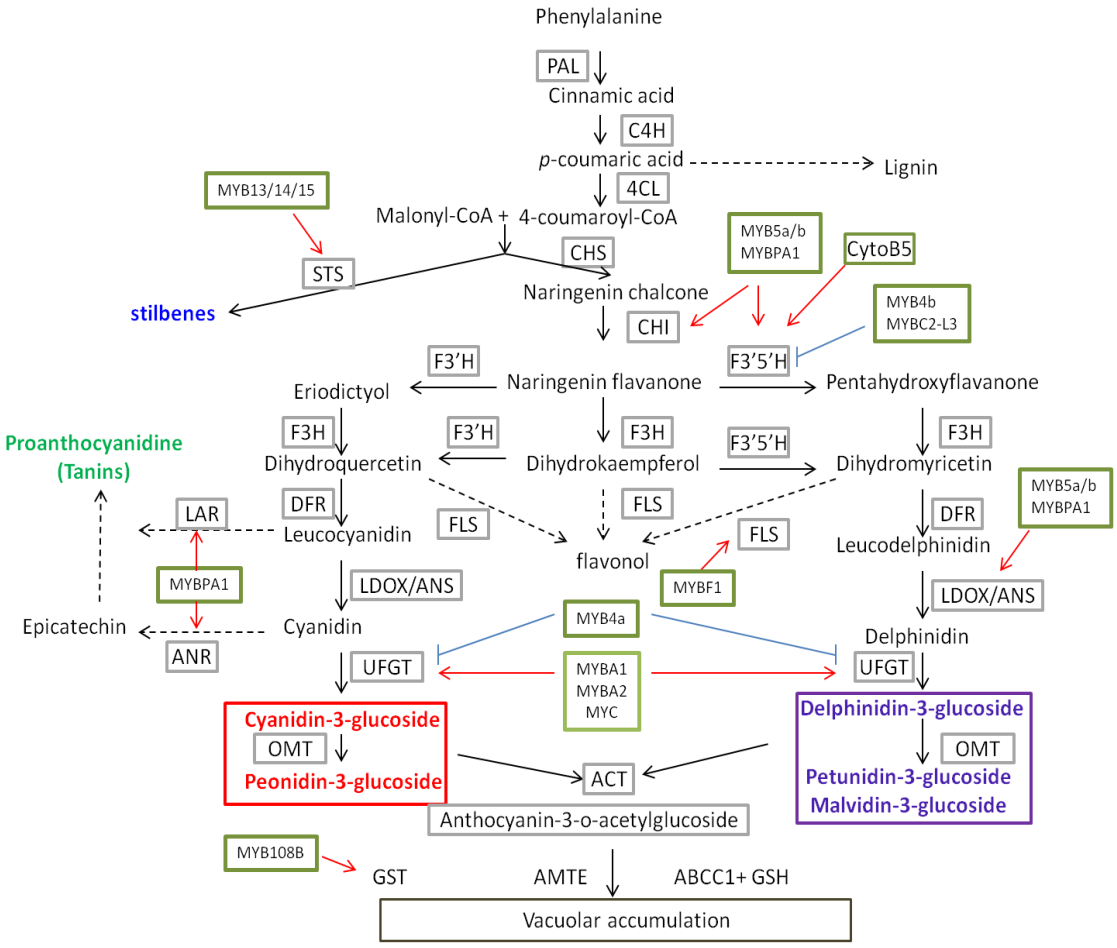

Figure II-21. Phenylpropanoid and flavonoid biosynthesis pathways. PAL, Pheammonia-lyase; C4H, cinnamate 4-hydroxylase; 4CL, 4-coumarate-CoA ligase; CHS, chalcone synthase; CHI, chalcone isomerase; F3H, flavanone 3-hydroxylase; DFR, dihydroflavonol 4- reductase; ANS, anthocyanidin synthase; UFGT, UDPG-flavonoid-3-O-glucosyltransferase; ANR, anthocyanidin reductase; LAR, leucoanthocyanidin reductase; FLS, flavonol synthase; ACC, acetyl CoA carboxylase; CCR, cinnamyl-CoA reductase; C3H, 4-coumarate 3-hydroxylase.

Genes involved in Anthocyanin biosynthesis: Phenylalanine Ammonia Lyase (PAL) which is the first enzyme in the synthesis of phenylpropanoids is encoded by 19 genes in the grape genome (Sparvoli et al., 1994)(Canaguier et al., 2017b).Four *PAL (PAL6, Vitvi11g00115; PAL7, Vitvi11g00126;PAL8, Vitvi11g01361; PAL19, Vitvi18g01463)* were barely expressed in both pulp and skin (RPKM<1 at the four stages analyzed). The remaining 15 PAL genes differently expressed in pulp and skin during berry ripening (located in cluster2). In pulp, twelve of the *15 PAL* genes were expressed at very low levels (RPKM<1 at the four stages analyzed), and three of them present relative highly expression, including *PAL2 (Vitvi13g00622)* up-regulated 1.4 fold during berry ripening whereas two others (*PAL1, Vitvi06g00256 and PAL5, Vitvi08g01022)* were significantly down-regulated after veraison. By contrast, in skin the *15 PALs* were clearly up-regulated during berry ripening. Specifically *PAL1, Vitvi06g00256 and PAL2*, *Vitvi13g00622* displayed the highest expression level, suggesting these two PALs play key role in phenylpropanoid biosynthesis. It is consistent with previous reports indicating these two PAL genes presented an increased transcript abundance at late ripening stages (Guillaumie et al., 2011).

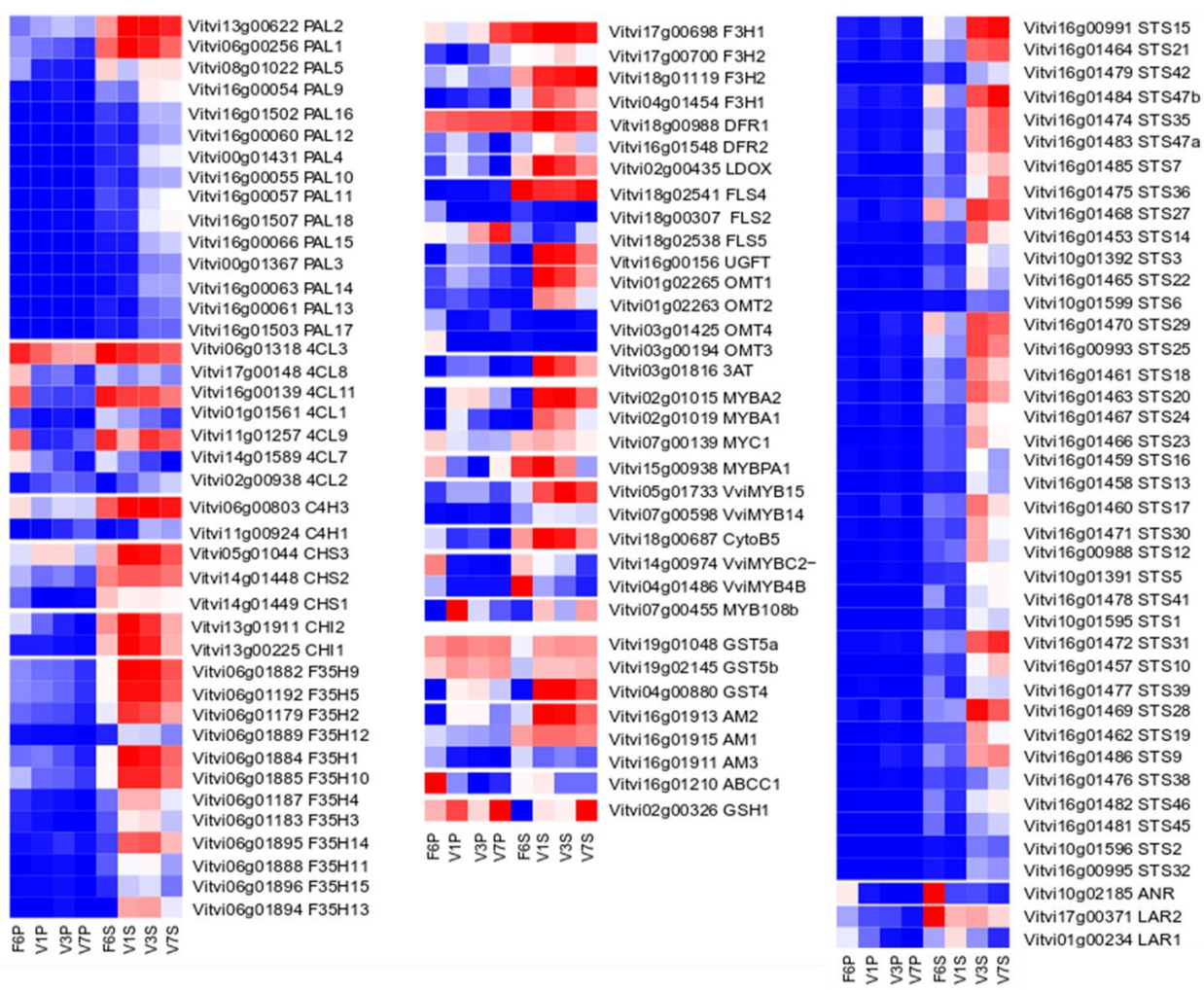

Figure II-22. Heatmap shown the expression of genes related to phenylpropanoid synthesis. Gene names are indicated in the text above.

As shown in the biosynthetic pathway (Figure II-21) the cinnamate-4-hydroxylase (C4H), 4-coumaratel-coA ligase (4CL) convert cinnamic acid to phenolic precursors. Compared to other genes encoding enzymes of this pathway, little is known about the impact of C4H, 4CL on anthocyanin synthesis. In strawberry, these two genes do not seem to have an essential role in determining the final amount of anthocyanin accumulation in fruits, but they were rather involved in the synthesis of lignin monomers(Salvatierra et al., 2010). In grape, C4H and 4CL are encoded by multigenic families composed of 3 and 11 genes, respectively. In the present study, among the three *C4H* genes, *VvC4H2 (Vitvi11g01045)* was expressed at a low level in both pulp and skin (RPKM<1 at the four stages analyzed), while *VvC4H1 (Vitvi11g00924)* and *VvC4H3* (Vitvi06g00803) were differentially expressed between tissues. Compared to *VvC4H3*, the expression of *VvC4H1* was relatively low and increased during ripening in both the pulp and the skin. In contrast, *VvC4H3* expression was repressed in the pulp but enhanced in the skin during berry ripening. Transcripts encoded by the *4CL4 (Vitvi08g01625), 4CL5(Vitvi13g00701), 4CL6(Vitvi14g01588)* and *4CL10 (Vitvi11g01258)* genes could not be detected in our RNA seq data, whereas the 7 other genes belonged to DEGs that were differentially expressed in skin and pulp. The expression of *4CL1(Vitvi01g01561), 4CL2(Vitvi02g00938), 4CL7(Vitvi14g01589)*, and *4CL8 (Vitvi17g00148)* were repressed and low expressed in pulp and skin during ripening. The *Vv4CL3, Vv4CL9* and *Vv4CL11* genes are highly expressed green berries at F6, and repressed in pulp but remain relative high expression in skin (Figure II-22).

CHSs catalyze the condensation of 4-hydroxycinnamoyl- CoA and three malonyl-CoA molecules to form the chalcone derivative, naringenin chalcone, which is the first committed step in the phenylpropanoid pathway of plants, leading to the biosynthesis of flavonoids, isoflavonoids, and anthocyanins (Ferrer et al., 1999). Three CHS encoding genes were identified in grape genome(Jeong et al., 2008). *CHS3 (Vitvi05g01044)* is predominantly expressed in the skin of red cultivar berry during coloration, while *CHS1(Vitvi14g01449)* and *CHS2(Vitvi14g01448)* are expressed in the leaves and berry skin of both white and red cultivars (Yamamoto et al., 2003) (Harris et al., 2013). *CHS3* expression correlates with anthocyanin accumulation, whereas C*HS1* and *CHS2* were related to the accumulation of other metabolites, including flavonol. In our RNA seq data *CHS1*, *CHS2* and *CHS3* are expressed at low level in the pulp of young berries. Expression of *CHS1* and *CHS2* decreases during ripening, whereas *CHS3* expression level increases after veraison with a maximum level at V1 and V3. All the three CHSs displayed higher expressed in skin than pulp in young fruits (Figure II-22). During véraison and ripening the *CHS1* was repressed. When comparing the transcript abundance from V1 to F6, *CHS2* and CHS3 mRNA levels increased 2 and 12 fold, respectively, indicating that CHS3 was the key enzyme to control the anthocyanin accumulation in skin during berry ripening (Yamamoto et al., 2003).

Chalcone is isomerized to flavanone by the chalcone isomerase (CHI). Two copies of the *CHI* genes were identified in grape (Jeong et al., 2004), and the expression of *CHI2* was higher than *CHI1* in all organs. *CHI1* expression was related anthocyanin and *CHI2* to flavonol (Jeong et al., 2008). In CS berries, both *CHI1 (Vitvi13g00225)* and *CHI2 (Vitvi13g01911)* are expressed at higher levels in the skin than the pulp, and sharply increase during ripening in skin to a maximum level at the V1 stage. *CHI2* is expressed in the pulp of in young berry and gradually decreased during ripening whereas *CHI1* expression remains low and stable.

Flavonoid 3',5'-hydroxylases (F3'5'Hs) and flavonoid 3'-hydroxylases (F3'Hs) compete for the same substrate naringenin flavanone and deliver their 3'5'- or 3'-OH products into the synthesis of delphinidin and cyanidin which eventually lead to blue and red pigments (Iwashina, 2000)(Mazza et al., 1999). In grape, F3'5'Hs are highly redundant with 16 genes encoding this enzyme (Falginella et al., 2010). In the new annotation of the grape genome (Canaguier et al., 2017b), only 15 F3'5'Hs were identfied. Three of are not expressed in berry (F3'5'H6, *Vitvi06g01194; F3'5'H7, Vitvi06g01199; F3'5'H8, Vitvi06g01206*,). The 12 F3'5'Hs are significantly induced after veraison and peaked at V1 or V3, the latest corresponding to the maximal content of anthocyanins. In the pulp, all these F3'5'Hs were low or not detectable in 4 stages analyzed. Grapevine contains two copies F3'Hs (Falginella et al., 2010), both F3'Hs are highly expressed in skin when compared with pulp, and present a slight increase towards ripening in both pulp and skin. No difference was found between tissues. Two flavanone 3-hydroxylase (*F3H*) genes were identified in grape, and expression analysis revealed that F3H1, and F3H 2 coincided with flavonol, while F3H2 with anthocyanin biosynthesis (Jeong et al., 2004)(Jeong et al., 2008).In pulp, only *F3H2* was up-regulated during berry ripening and declined again at V3. In skin, both *F3H1* and F3H2 were highly expressed rapid increased after veraison, however the maximal expression level of F3H1 and F3H2 were detected at different stages, the peak of *F3H1* was detected at V1whereas *F3H2* was detected at V7.

FLS is a key enzyme in flavonol biosynthesis that control the last step, from dihydroflavonol to flavonol (Holton et al.,1993). Five *FLS* genes were identified in grape (Fujita et al., 2006). The expression of *FLS1* (*Vitvi18g02542*), *FLS2* (*Vitvi18g00307*), and *FLS3* (*Vitvi18g02543*) were too low to be detected in berries. *FLS 4* (*Vitvi18g02541*) and *FLS5* (*Vitvi18g02538*) displayed a differential expression between pulp and skin: *FLS4* is expressed in skin and decrease after veraison while *FLS 5* is specifically expressed in the pulp and gradually increases during ripening.

The dihydroflavonols are reduced to leuco-anthocyanidins by the dihydroflavonol 4-reductase (DFR). There are 2 *DFR* genes present in the grape genome (Jeong et al., 2004). Transcript abundance is higher for *DFR1* (*Vitvi18g00988*) than *DFR2* (*Vitvi16g01548)* in both skin and pulp at all stages. During ripening, the expression of *DFR1* and *DFR2* increase and peaked at V1. Leucoanthocyanidin dioxygenase (LDOX) catalyzes the conversion of the colorless leucoanthocyanidin to blue delphidin and red cyanidin. Only one copy of LDOX (Vitvi02g00435) was identified in grape genome, the expression level of LDOX in skin was higher than in pulp and increased to a maximal level at V1.

The anthocyanidin aglycones are further modified through glycosylation, methylation (Fournier-level et al., 2011) and acylation (Nakayama et al., 2003), through the action of 3-O-glucosyltransferase (3-GT), O-methyltransferases (OMTs) and acyltransferases (ACTs), respectively, that contribute to increase stability and water solubility and to the production of a wide variety of anthocyanin compounds.

The grapevine genome contains as many as 240 flavonoid 3-O-glucosyltransferase (3-GT) genes (The French-Italian Public Consortium for Grapevine Genome Characterization, 2007). Among them, GT1 has been functionally characterized as VvUGFT, which controls the last step of anthocyanin synthesis. It forms anthocyanidin 3-O-glucoside from the 3-O-specific glucosylation of anthocyanidin (Ford et al., 1998). In skin, after veraison the expression of UGFT (*Vitvi16g00156*) sharply increases to a maximal level

at the V1 stage. The other GTs are expressed at low levels and function unknown. Four OMTs were identified in grape. OMT1 (*Vitvi01g02265*) and OMT2 (*Vitvi01g02263*) were reported to modulate the anthocyanin 3'- and 3',5'-O-methylation (Hugueney et al.,2009; Lücker et al.,2010;Fournier-Level et al.,2011). The *OMT3* gene (*Vitvi03g00194*) was highly specific for 2-hydroxy-3- isobutylpyrazine methylation (Guillaumie et al., 2013). *OMT1* and *OMT2* are highly expressed in skin during ripening, while *OMT3* and *OMT4* are mainly expressed in the pulp of young berry.

Anthocyanins are synthesized in the cytoplasm at the cytoplasmic surface of the endoplasmic reticulum and eventually accumulated into the vacuole. Before being transported to the vacuole, anthocyanins will be acylated by acyltransferases, which produce 3-O-acetyl-, 3-O-coumaroyl-, and 3-O-caffeoyl-monoglucosides by attaching acyl groups to the C6' position of the Glc moiety (Nakayama et al., 2003). In grape, an acyltransferases *Vv3AT* (*Vitvi03g01816*) was shown to be the key enzyme associated to anthocyanin acylation (Rinaldo et al., 2015). The corresponding gene is s induced in pulp and skin during berry ripening, but its abundance in skin is 42 times higher than in pulp.

Genes involved in Anthocyanin transport: Three proteins are considered as transporters of anthocyanin, glutathione-S-transferases (GST), ATP binding cassette 1 (ABCC1) and antho-MATE transporters (AM). In grape, 26 ABCC genes were identified, and ABCC1(Vitvi16g01210) was proved to preferentially transport malvidin 3-Oglucoside strictly depending on the presence of Glutathione (GSH) (Francisco et al., 2013). ABCC1 is mainly expressed in the pulp of young berry and declined during ripening, and presents relative low expression levels in the skin. Two GSHs were identified in grape: *GSH1* (*Vitvi02g00326*) is expressed at higher levels than *GSH2* (*Vitvi14g00291*) both in pulp and skin at all stages, and is up-regulated during ripening.

Three tonoplast-localized grapevine MATEs, AM1 (V*itvi16g01915*), AM2 (*Vitvi16g01913*) and AM3 (Vitvi16g01911), were described as specifically transport acylated anthocyanins but not glucosylated ones (Gomez et al., 2009). In the present study, *AM1* and *AM2* expression increased whereas *AM3* was repressed during ripening in skin. In pulp, *AM2* was up-regulated while *AM1* and *AM3* were down regulated during ripening.

Arabidopsis tt19 mutant allowed demonstrating that GST is the central transport and required for transport of all types of flavonoids (Kitamurs et al., 2004). The grape genome contains 5 GST genes (Kitamurs et al., 2004; Conn et al., 2008). However, in the new genome annotation 6 *GST* genes were identified (Canaguier et al., 2017). *GST4* (Vitvi04g00880) was proved have the pivotal role in anthocyanin transport (Conn et al., 2008). Consistently, no transcript of *GST4* was detected before veraison at F6 but their quantity rapidly increased during ripening and peaked at V1 at different levels in pulp and skin (65 fold higher in skin than pulp). *GST5a* (*Vitvi19g01048*) and *GST5b* (*Vitvi19g02145*) were also induced during ripening but much lower than *GST4*. *GST2* (Vitvi07g00286) was repressed during ripening in two tissues. *GST1* (*Vitvi19g01328*) and *GST3* (*Vitvi12g00080*) were not transcribed in grape berries in our conditions.

Genes involved in Stilbene and tannins biosynthesis: Stilbene and tannin also shared this pathway. Stilbene synthases (STSs), which catalyze the biosynthesis of the stilbene back bone compete the same substrate malonyl-CoA and p-coumaryl-CoA with CHS. STSs, belonging to a large family of 48 genes have been suggested to derive from CHSs (Parage et al., 2012). In the present data, 8 STSs transcript were not detected in both pulp and skin, including STS3 (Vitvi10g01392), STS4 (Vitvi10g01598), STS8 (Vitvi16g01456), STS11 (Vitvi16g01452), STS34 (Vitvi16g01454), STS40 (Vitvi16g01455), STS43 (Vitvi16g01480), and STS44 (Vitvi16g00998). Also the other 40 STSs did not detected in pulp, whereas were up-regulated in skin during ripening (Figure II-22). It is consistent with previous studies (Lijavetzky et al., 2012)(Parage et al., 2012). Leucoanthocyanidin reductase (LAR) and anthocyanidin reductase (ANR) contribute to synthesis of tannin, LAR catalysis flavan-3.4-diol converted to catechin directly, and epicatechin is produced from cyanidin by the action of an enzyme ANR (xie et al.,2003)(Bogs et al., 2005). Two copies of LAR (Vitvi01g00234, Vitvi17g00371) and one copy of ANR (Vitvi10g02185) were identified in grape, and highly expressed in young berry which is in agreement with that tannin synthesis in the skin and seed of young berry (Bogs et al., 2005; 2007).

F genes encoding TFs involved in the control of flavonol and anthocyanins: The flavonol biosynthesis pathway is regulated by a MYB–bHLH–WDR (MBW) complex. Transcription factors, MYB primarily determine the activation or repression role of the MBW complex, by binding to the promoters of synthesis genes, together with the common bHLH and WD40 factors. Activators of anthocyanin accumulation include MYAB1 (Vitvi02g01019), MYAB2 (Vitvi02g01015), MYBPA1 (Vitvi15g00938), MYB108B (Vitvi07g00455), MYB5a (Vitvi08g01797), MYB5b (Vitvi06g00059). There active regulators control the expression of different target genes. For instance, MYBA1-A2 positively regulated anthocyanin accumulation by activing the expression of UFGT (Kobayashi et al., 2002, Walker et al., 2007). MYB13/ 14/ 15 have been demonstrated related to the stilbene pathway (Cavallini et al., 2015) (Wong et al., 2016). And *MYB108B* was co-expressed with *GST4*. MYB5a/5b and MYBPA1 positively modulate the expression *of CHI, F3'5'H* and *LDOX/ANS* (Deluc et al., 2006, Deluc et al., 2008). In addition, MYBPA1 regulated the expression of LAR and ANR (Bogs et al., 2007). Besides, 3 repressors were also revealed, MYB4a (Vitvi03g00136) and MYBC2-L3 (Vitvi14g00974) were reported as the negative regulator of UGFT, PAL, C4H and 4CL (Jin et al.,2000, Colguhoun et al.,2011, Gavallini et al., 2015). MYB4b (Vitvi04g01486) and MYBC2-L3 repressed the expression of F3'5'H (Jin et al., 2000, Colguhoun et al., 2011, Gavallini et al.,2015). In the present data, positive MYB regulators exhibit high expression and up-regulated in skin during ripening. While the negative MYB predominately expressed in the pulp and skin of young berry.

MYC1 (Vitvi07g00139), a bHLH transcription factor, interacts with MYB transcription factors to regulate the expression of genes in flavonoid pathway (Hichri et al., 2010). It is highly expressed in the pulp of young berry and decline after veraison, whereas presented similar expression pattern in skin at 4 analyzed stages. WD40 proteins provide a stable platform for MYBA and bHLH to form the MBW complex, and their expression levels did not affect the transcript levels of structural genes or anthocyanin content (Stommel and Dumm, 2015). One WD40 protein was revealed in grape, exhibiting similar expression level between two tissues at four stages as other species.

In addition to MBW complex, cytochrome b5 (CytoB5, Vitvi18g00687) was another regulator which modulate the expression of F3'5'H, and the transcript abundance of CytoB5 was associated with the content of anthocyanin (de Vetten et al., 1999, Guan et al., 2016). In this RNA sequence data, CytoB5 was found highly expressed in the skin and significantly increased during ripening.

Taken together, compared to pulp, all the structural and regulatory genes related to anthocyanin biosynthesis were specifically and significantly induced in skin after veraison, which is constant with the accumulation of anthocyanin.

2.3.4 Analysis of changes in the DNA methylation landscape in fruits tissues during ripening

a. Summary of DNA Methylation analysis

To characterize the variations in DNA methylation level and distribution in grape berry tissues during ripening, whole-genome bisulfite sequencing (WGBS) was performed to generate single-base resolution maps of DNA methylation for skin and pulp of grape berry at 2 developmental stages, one before véraison, FS+6w (6 weeks after fruit set), and a second one after véraison, Ver+3w (3 weeks after véraison), using two biological replicates corresponding to two of the samples previously analyzed by RNA seq (Figure II-4, page 61).

The genome of grape is 450 Mb (2n=38). For each sample, more than 100 M paired-end reads (read length = 150 bp) were produced of which between 61% and 73.8 % depending on the samples (see table II-6), were mapped to the grape reference genome using BSMAP. Unique mapping ranged between 54% and 65% covering in average more than 93% of grape genome (Canaguier et al., 2017). In each bisulfite-treated library, 4 to 19% of the total reads were mapped to the unmethylated chloroplast genome and were used to calculate the conversion rate of non-methylated cytosines, it was found above 99.2% in all cases.

All of our sequenced methylomes had a ~12.5-fold average coverage (minimum 9.71, and maximum 14.39) per DNA strand (Table II-6). The coverage and depth of the sequenced methylomes are comparable to those of the published methylomes from Arabidopsis (Lister et al., 2008) and tomato (Lang et al., 2017, Zhong et al., 2013).

Sample name	total_reads	Clean_reads	mapping_rate	unique_mapping	C coverage_ratio	Average_coverage	Conversion_rate
FS-6W_pulp-1	107374735	102314293	65681164 (64.2%)	58290515(57.0%)	93.42%	9.71	99.80%
FS-6W_pulp-3	111420220	106857510	65410079 (61.2%)	58385731(54.6%)	93.87%	10.78	99.79%
Ver_3W_pulp-1	110718644	104338469	73709131 (70.6%)	65773690(63.0%)	94.28%	12.59	99.20%
Ver_3W_pulp-2	124906251	119562914	83738215 (70.0%)	75011417(62.7%)	94.59%	14.39	99.68%
FS-6W_peel-1	121959446	102563323	72783379 (71.0%)	64315912(62.7%)	94.19%	12.52	99.77%
FS-6W_peel-2	129520198	110882913	78229209(70.6%)	69056949(62.3%)	94.39%	13.34	99.76%
Ver_3W_peel-1	116110873	115471555	85166675(73.8%)	75045443(65.0%)	94.00%	12.13	99.74%
Ver_3W_peel-2	109337579	108836138	77756894(71.4%)	68666187(63.1%)	93.71%	11.1	99.76%

Table II-6. Quality assessment of the WGBS Data.

To evaluate the consistency among biological replicates at each stage and in both tissue, a principal component analysis (PCA) was performed (Figure II-23). Noteworthy, the two biological replicates of pulp at V3, skin at F6 and V3 stage were grouped together. However, the two biological replicates corresponding to the pulp at F6W were separated from each other, suggesting these two samples had some differences that may reflect biological diversity of samples. Whether such difference reflects variations between biological replicate is so far unclear. However, result indicate that PCA1 mainly separate skin samples and pulp samples as a function of developmental stages, and to lower extend tissues at a given stage. In contrast the PCA2 dimension mainly explains differences between tissues, and for the pulp samples part of the stage dependent differences.

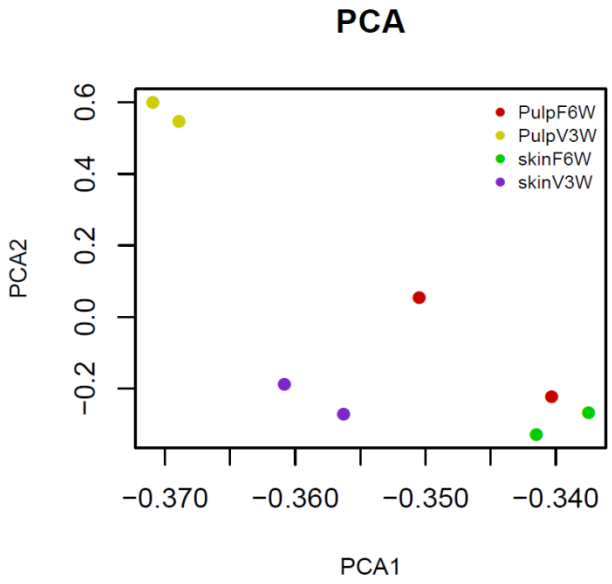

Figure II-23. Principal component analysis of WGBS data. PCA1 explains the variability between samples and separate tissues as a function of their developmental stages. PCA2 separates skin samples from pulp samples, as a function of stage. Except for pulp F6W samples that show some difference reflecting biological variations, all other samples are were grouped indicating a high level of similarity between samples.

b. *Features of grape berry DNA methylomes*

The average methylation level found in immature fruit (F6W) was 11.05% in the pulp and 9.95% in the skin. This is much lower than the methylation of immature tomato fruits that was found to be 30% using HPLC analysis (Teyssier et al, 2008) or 22% by WGBS (Zhong et al, 2013). In young orange fruits the methylation level was 13% slightly above the one of immature grape fruits (Huang et al., 2019). Strawberry fruits had the lowest methylation level, with an average value of 7.5% (Cheng et al, 2018). Globally the average methylation level is correlated with the genome size: tomato has the largest genome (900Mb, the tomato genome consortium, 2008), whereas orange and grape have fairly similar genome size 380 Mb and 450Mb respectively, (Xu et al., 2013)(Jaillon et al., 2007), and strawberry has the smallest genome (240Mb, Shulaev et al., 2011).

Average methylation level in the CG, CHG and CHH context were 56.4%, 29.98% and 4.8% respectively in the pulp and 52.4%, 26.65% and 3.92% respectively in the skin. Values were systematically lower in the skin than in the pulp in all C contexts, consistent with the lower average methylation level found in this tissue. Interestingly methylation level in all sequence contexts followed the same trend (Figure II-24).

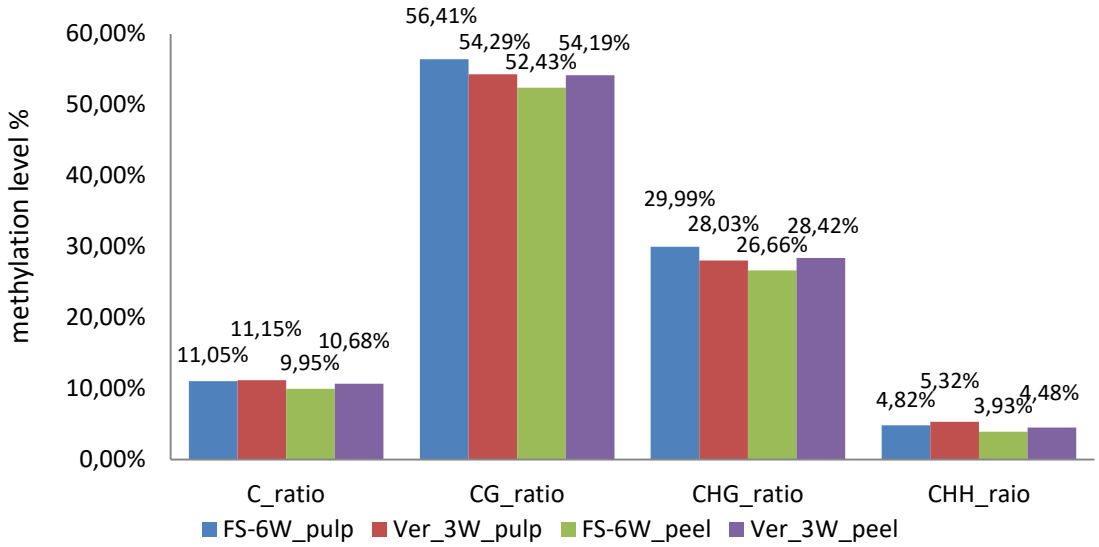

Figure II-24. Methylation level of pulp and skin at the two stages. Data indicates that methylation is slightly higher in the pulp than in the skin at each stage.

In order to further analyze the difference in methylation levels between the skin and the pulp at each developmental stage, the two biological replicates were merged and used to calculate the number of differentially methylated C region between tissues at each stage, using a fisher test. Data presented in table 7 show that at both stages there are approximately 3 times more hypomethylated C than hypermethylated C in the skin versus pulp.

Sample	DMR type	CG	CHG	CHH	All contexts
SkinvsPulp_F6W	hyper	30474	27518	63518	121510
SkinvsPulp_F6W	hypo	64206	66119	228379	358704
SkinvsPulp_V3W	hyper	27580	24343	66212	118135
SkinvsPulp_V3W	hypo	64529	69928	300364	434821

Table II-7. Number of DMRs between pulp and skin at two stages.

Although this does not take into account exact differences in methylation level at each C, it clearly suggests a lower methylation level in the skin than in the pulp.

As the genome size is correlated with the genome transposon (TE) content (Tenaillon et al., 2011), we also examined the correlation between DNA methylation distribution and transposon distribution. As shown in Figure II-25 methylation distribution was correlated with TE abundance, irrespective to the C context and was rather low in gene rich regions. Indeed, the CG type methylation is the most abundant in TE rich region. No major difference between tissue and stages could be found as far as the general distribution along chromosomes is considered (Figure II-25). We further examined the distribution of methylation in each sequence context considering genes and TEs separately. In all cases (stages and tissues) TE are enriched in CG and non-CG methylation as compared to gene rich region that are preferentially located in chromosomes arms (Figure II-25). No difference between tissues was detected.

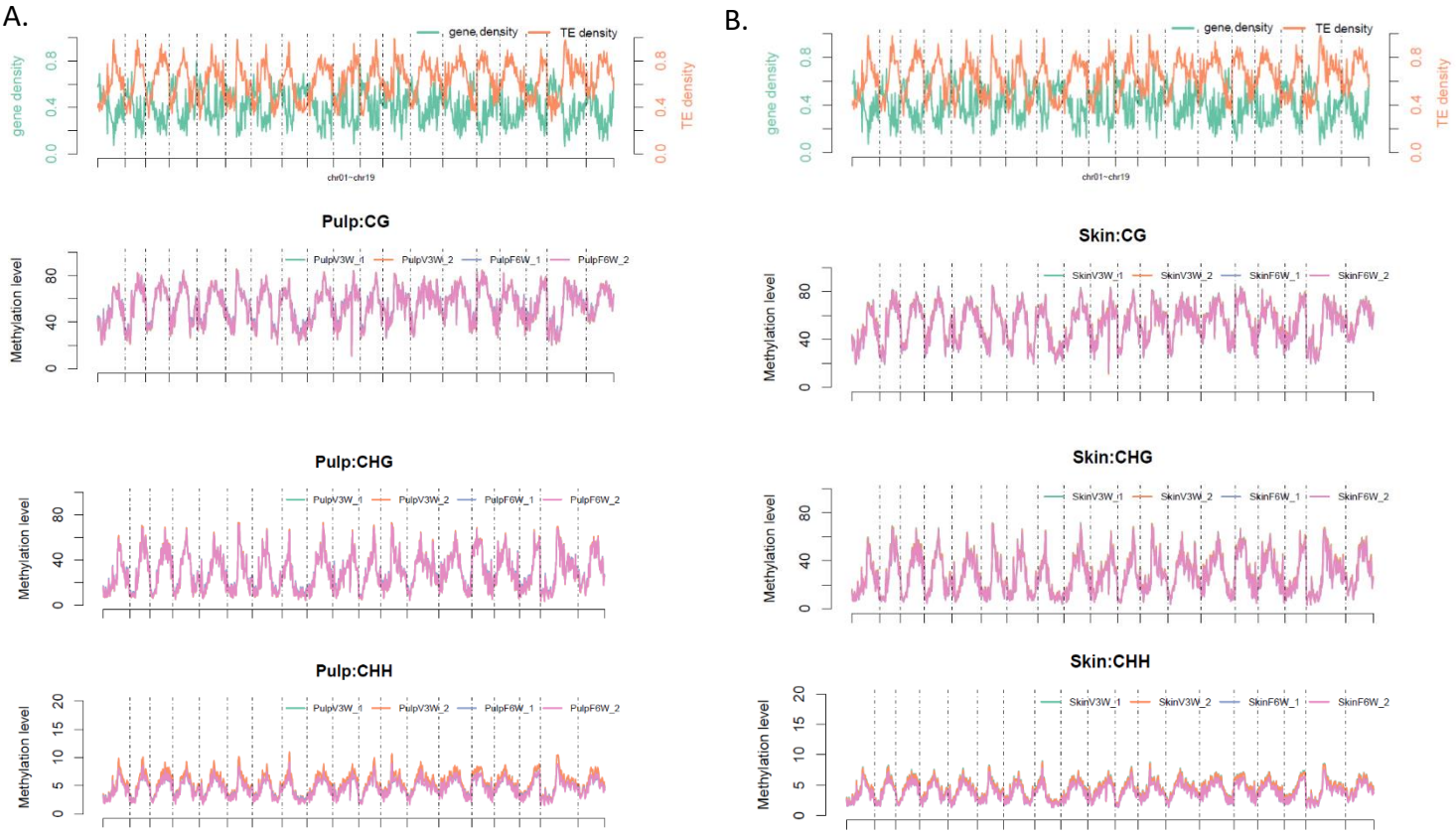

Figure II-25. DNA methylation distribution along chromosomes in the pulp (A) and in the skin (B)

Methylation distribution was also analyzed in transposons. Methylation levels increased in the body of transposons as compared to the 5' and 3' regions in all sequence contexts (Figure II-26, and Table II-9). The pattern was similar in both tissues at the two developmental stages. However, the methylation level in the CHH context was slightly higher in the pulp than in the skin.

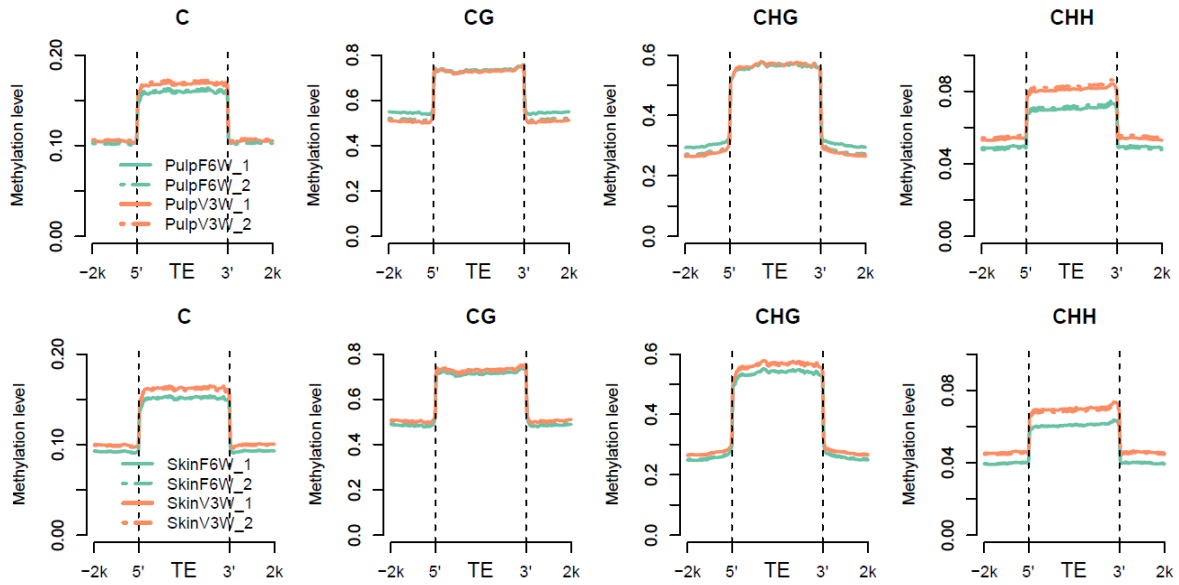

Figure II-26. DNA methylation distribution in TEs in the different C contexts in the pulp and skin at 2 developmental stages

The distribution of methylation was also analyzed in gene regions. As expected, the average methylation level of genes, which is below 10%, is lower than the one of TEs, as already suggested by the distribution of cytosine methylation along chromosomes (Figure II-25). When considering methylation contexts, genes are also enriched in CG type of methylation, although their methylation level remained lower than that of TEs. Of note, genes contain significant CHG methylation levels close to 30% in the promoter region and maintain a significant level in CHG methylation within their body, approximately to 20% in their body (Figure II-27).

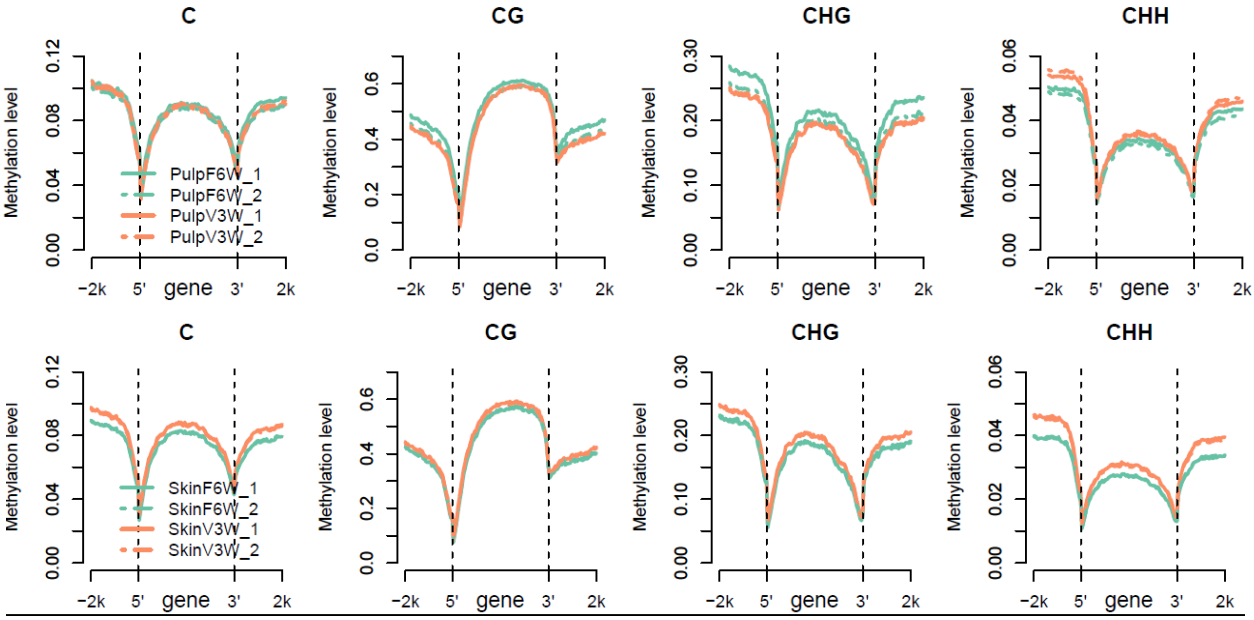

Figure II-27. DNA methylation distribution in genes in the different C contexts in the pulp and skin at 2 developmental stages

Hence, DNA methylation distribution within genes differs from Arabidopsis or tomato where CHG and CHH methylation are at very low levels in gene bodies (Lister et al., 2008)(Lang et al., 2017b).

c. DNA Methylation changes during berry ripening

DNA methylation was shown to decrease at the onset of fruit ripening in tomato and strawberry (Teyssier et al., 2008; Zhong et al., 2013; Cheng et al., 2019), and inversely to increase during sweet orange fruit ripening (Huang et al., 2018). To determine DNA methylation changes in grape, we calculated the average DNA methylation levels in all samples. The average DNA methylation level remained stable in the pulp with an average methylation of 11.05% in immature green fruits and of 11.15% ripening fruits. The situation was different in the skin, with a slight increase from 9.95% to 10.7%. Although this resembles the evolution of methylation observed in sweet orange fruits, the increase observed in grape berries skin is much less (0.75% for grape versus 1.5%, in sweet orange, from 13 to 14.5%) and was only detectable in the skin of grape berries. General tendencies were similar in both biological replicates at each stage and in each tissue, even though some discrepancies were found between the two F6W-pulp samples. The pulp-F6W-2 replicate presented in general slightly lower methylation levels in the CG and CHG context at genes and transposons than the pulp-F6W-1 replicate, with little impact on average methylation levels though. Globally, these results differ significantly from previous observations in tomato and strawberry that are both showing an important loss of DNA methylation during ripening (Teyssier et al., 2008; Zhong et al., 2013; Cheng et al., 2018).

When analyzing ripening induced changes in DNA methylation levels in each sequence context, the average methylation levels increased in the skin from 52.43% to 54.19%, from 26.665 to 28.42%, and from 3.93% to 4.48%, in the CG, CHG and CHH sequence contexts, respectively, consistent with the weak increase in global DNA methylation level observed in this tissue. By contrast, in the pulp only CHH methylation level increased from 4.82% to 5.32% (+0.5%) whereas cytosine methylation in the CG and CHG contexts decreased moderately at Ver-3w as compared to immature berry F6 (Table II-8). The opposite tendency is observed in the CG and CHG contexts *versus* the CHH context may explain the absence of significant DNA methylation changes observed in the pulp between F6W and V3W stages.

Sample name	C_ratio	CG_ratio	CHG_ratio	CHH_ratio
FS-6W_pulp-1	11.23%	57.66%	31.12%	4.89%
FS-6W_pulp-3	10.87%	55.16%	28.85%	4.75%
Ver_3W_pulp-1	11.06%	54.08%	27.89%	5.25%
Ver_3W_pulp-2	11.24%	54.49%	28.17%	5.38%
FS-6W_peel-1	9.95%	52.22%	26.54%	3.91%
FS-6W_peel-2	9.95%	52.63%	26.77%	3.94%
Ver_3W_peel-1	10.73%	54.38%	28.50%	4.52%
Ver_3W_peel-2	10.63%	53.99%	28.34%	4.44%

Table II-8. Global methylation changes in berry tissues during ripening.

We then analyzed the difference in methylation levels between stages and tissues in genes and TEs (Table II-9). As mentioned above, TE bodies present a higher methylation level than the surrounding regions. No major difference in the general distribution of methylation was found in and around TEs. However, in both tissues, the average methylation level within TEs increases between F6W and V3W. This increase remained moderate (from 15.08% to 16.10%) in the skin, and from 15.98% to 16.87% in the pulp and was essentially observed in the CHH context (Figure II-26). As shown in Figure II-27, the body of genes is enriched in CG methylation as compared to CHG and CHH methylation.

sample	region	C_ratio	CG_ratio	CHG_ratio	CHH_ratio
pulp_f6w_gene	2k upstream	9,17%	39,10%	24,18%	4,53%
	5'-3'	7,78%	51,72%	16,90%	2,90%
	2k downstream	8,46%	41,66%	20,61%	3,93%
pulp_v3w_gene	2k upstream	9,18%	36,29%	22,19%	5,00%
	5'-3'	7,71%	50,36%	15,68%	3,10%
	2k downstream	8,35%	38,72%	18,61%	4,27%
skin_f6w_gene	2k upstream	7,93%	34,68%	20,70%	3,61%
	5'-3'	7,08%	48,27%	15,09%	2,35%
	2k downstream	7,29%	37,04%	17,41%	3,11%
skin_v3w_gene	2k upstream	8,58%	35,93%	22,10%	4,16%
	5'-3'	7,51%	49,95%	16,21%	2,63%
	2k downstream	7,89%	38,48%	18,69%	3,58%
pulp_f6w_TE	2k upstream	10,31%	53,14%	29,14%	4,87%
	5'-3'	15,98%	73,27%	56,25%	7,10%
	2k downstream	10,38%	53,22%	29,35%	4,89%
pulp_V3w_TE	2k upstream	10,54%	50,86%	27,47%	5,43%
	5'-3'	16,87%	73,05%	56,46%	8,20%
	2k downstream	10,61%	50,95%	27,67%	5,45%
skin_f6w_TE	2k upstream	9,22%	48,77%	25,75%	3,97%
	5'-3'	15,08%	71,66%	53,73%	6,08%
	2k downstream	9,29%	48,88%	25,96%	3,99%
skin_v3w_TE	2k upstream	9,88%	50,27%	27,25%	4,52%
	5'-3'	16,10%	72,92%	56,16%	6,92%
	2k downstream	9,95%	50,39%	27,47%	4,55%

Table II-9. Methylation levels in TE and genes in the two stages of two tissues

However, gene body is not depleted in CHG methylation as was shown in other plant systems including arabidopsis and tomato (Lister et al., 2008)(Zhong et al., 2013). Of note, in the skin, a very weak increase in methylation level was found in the body of genes (0.05%), whereas no difference could be observed in the pulp. When analyzing the context of methylation, CG and CHG methylation seemed to decrease very slightly in the 5' and 3' part of genes in the pulp. Yet this should be considered with caution, because the two F6W replicates were different with respect to this observation, and this tendency was only observed with one of them. In contrast when considering the CHH methylation level within and around genes, a

weak increase was observed in all part of genes, consistently between replicates. A similar trend is observed at genes in the skin in the CHH context. In addition methylation also showed a consistent but very limited increase in the CHG and CG context in the skin, in all part of genes. Taken together these results suggest a weak increase in methylation in the CHH context in both transposons and genes, whereas other types of methylation showed different behaviors depending on position and tissues.

We further controlled variation in DNA methylation between stages in each tissue by calculating dmCs using merged samples and a fisher test. Results indicate that a 3 (pulp) and a 2.5 (skin) fold difference between hyper and hypomethylated Cs in both tissues. Little difference is found in the number of hyper and hypo Cs in the CG context (1.2 fold difference in the pulp and 1.1 in the skin) in each tissue. The number of hyper Cs is 2.45 (pulp) and 2.1 (skin) times higher than of hypo Cs in the CHG context, and 4.1 (pulp) and 3.4 (skin) in the CHH context. This is consistent with an increase in DNA methylation during ripening, with differences in the control of C methylation depending on the context though. Of note, the same trend is observed in both tissues (Table II-10).

Sample	dmC type	CG	CHG	CHH	All contexts
PulpV3WvsF6W	hyper	28096	50656	214702	293454
PulpV3WvsF6W	hypo	22746	20712	52315	95773
SkinV3WvsF6W	hyper	32789	63682	212617	309088
SkinV3WvsF6W	hypo	30431	30388	63112	123931

Table II-10. Number of dmCs between two stages in pulp and skin. dmCs were calculated using Methylkit. dmCs in different context were calculated using the same parameters (q value=0.01 and % of methylation difference=10).

d. Analysis of differentially methylated regions

Methylation located in promoter regions has been shown to be involved in the regulation of gene expression. We therefore determined differentially methylated regions (DMRs) in genes and transposons comparing different stages in the same tissue. Analysis of methylation variations was performed using the Methykit package in R (win.size= 500bp, step.size= 500bp and qvalue= 0.01, Akalin et al., 2012) as described in the methods, in collaboration with Dr Huan Huang (Shanghai, China).

As shown in Table II-11, a total of 42000 and 59928 DMRs were found in the skin and in the pulp, respectively, when comparing F6W to V3W. Interestingly, a slightly higher number of DMRs was identified in the pulp as compared to skin. However, the same trends were observed in both tissues irrespective to the sequence context considered. In the CHG and CHH contexts hyper DMRs are more numerous than hypo DMRs whereas these numbers are fairly identical in the CG context. This is in line with the previous observation that variation in the methylation status Cs was more frequent in the CHG and CHH context than in the CG context (Table II-10). Globally, considering the higher number of hyper DMRs as compared to the hypo DMRs, this is also consistent with the global and limited increase in DNA methylation previously observed during fruit ripening in both tissues.

We then ranked the DMRs based on the variations of the DNA methylation level. As the threshold for DMR identification was a 10% variation, we grouped DMRs in three categories, those with a methylation change above 30%, those with a methylation change between 30% and 15% and those with a methylation change between 15% and 10%. In all cases most of the DMRs presented a rather modest change in DNA methylation level (10 to 30%), whereas those with the highest change in DNA methylation represented at most 12% of the total DMRs. This indicates that changes in DNA methylation in all contexts and irrespective to their location (genes, TEs, intergenic regions) remain quite limited.

Peel V3W vs F6W DMRs								
	C_hyper	C_hypo	CG_hyper	CG_hypo	CHG_hyper	CHG_hypo	CHH_hyper	CHH_hypo
Gene body	1740	981	2970	2764	2360	1494	714	132
Gene_promoter	2208	993	1482	1822	1068	1047	1664	382
TE	8385	3914	5586	5312	6277	3971	5229	891
Intergenic	1718	764	1495	1673	1139	859	1246	246
Total	14051	6652	11533	11571	10844	7371	8853	1651
Pulp V3W vs F6W DMRs								
	C_hyper	C_hypo	CG_hyper	CG_hypo	CHG_hyper	CHG_hypo	CHH_hyper	CHH_hypo
Gene body	1945	1219	3293	3537	3026	1696	777	263
Gene_promoter	2781	1104	1666	2034	1486	982	2092	493
TE	10224	4004	6152	5418	8153	3561	6197	1387
Intergenic	2096	802	1673	1950	1377	877	1472	366
Total	17046	7129	12784	12939	14042	7116	10538	2509

Table II-11 Number of DMRs in C, CG, CHG and CHH context, in the pulp and the skin. DMR were calculated using Methylkit. DMRs in different context were calculated using the same parameters (q value=0.01 and % of methylation difference=10).

We then analyzed the distribution of DMRs in gene and transposons. Results indicate that a majority of DMRs are found in TEs (between 45 and 59% of total DMRs) depending on tissue and sequence contexts. No major difference in the distribution of DMRs between tissues was found. However, whereas DMRs in TE represent 45% to 47 % of total DMRs in the CG context they represent above 55% of all DMRs in all other contexts. Inversely, DMRs in promoter regions represent a higher percentage in the CHH context (20% of total DMRs) than in all other contexts (12 to 16%; Figure II-28). Noteworthy, hyper DMRs are much more abundant than hypo DMR in this context. A similar observation is made in the CHG context whereas in the CG context hypo and hyper DMRs are similarly abundant.

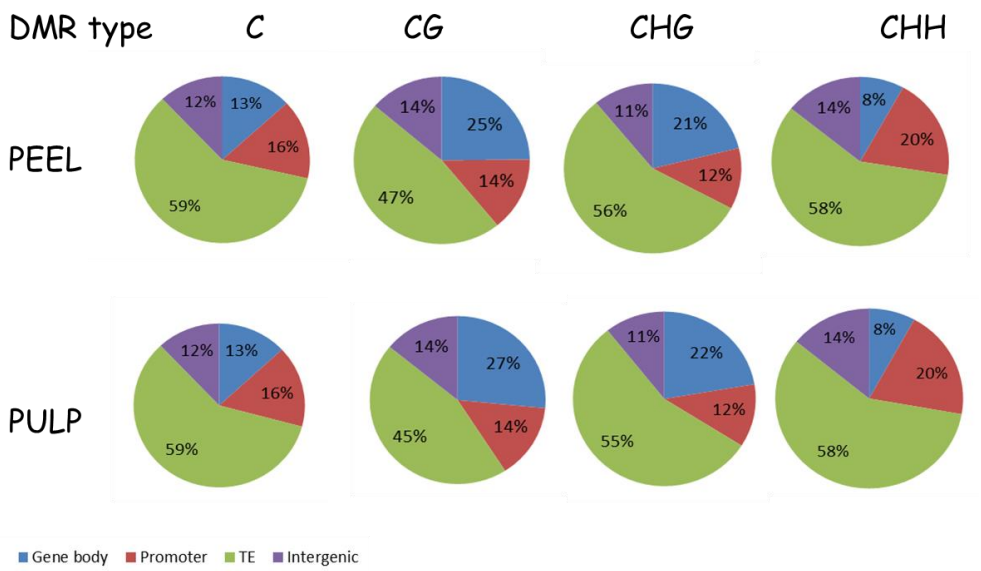

Figure II-28. Distribution of DMRs in the different sequence context and tissues at two developmental stages. Percentages have been calculated based on data presented in table 11.

To determine whether promoter regions were enriched in DMRs (hyper or hypo), we compared their distribution as determined experimentally to a calculated random distribution using a fisher test. Results indicate that the frequency of DMRs in promoters is higher than what would be expected in the case of a random distribution, except for hyper DMRs in the CG context, suggesting that they could be involved in gene regulation during fruit ripening (Table II-12).

DMR context	DMR type	DMR in pro	DMR in pro: random	total number of DMRs	p_value
PulpV3WvsF6W_C	hyper	2781	2108	10535	4.7526e-28
PulpV3WvsF6W_C	hypo	1014	833	4216	2.1163e-06
PulpV3WvsF6W_CG*	hyper	1666	1617	7953	3.4704e-01*
PulpV3WvsF6W_CG	hypo	2033	1566	7844	8.1346e-19
PulpV3WvsF6W_CHG	hyper	1486	1730	8810	1.9341e-06
PulpV3WvsF6W_CHG	hypo	982	822	4174	2.3377e-05
PulpV3WvsF6W_CHH	hyper	2092	1212	6325	1.9198e-71
PulpV3WvsF6W_CHH	hypo	493	299	1450	6.8977e-16
SkinV3WvsF6W_new2_C	hyper	2208	1626	8631	1.6599e-26
SkinV3WvsF6W_new2_C	hypo	993	796	4087	1.5477e-07
SkinV3WvsF6W_new2_CG	hyper	1482	1324	7148	9.4460e-04
SkinV3WvsF6W_new2_CG	hypo	1822	1352	7114	3.1450e-21
SkinV3WvsF6W_new2_CHG	hyper	1560	1838	9394	1.3548e-07
SkinV3WvsF6W_new2_CHG	hypo	1047	877	4481	1.3639e-05
SkinV3WvsF6W_new2_CHH	hyper	1664	1039	5323	3.4813e-44
SkinV3WvsF6W_new2_CHH	hypo	475	245	1320	7.4290e-24

Table II-12. Analysis of the distribution of DMRs in promoters as compared to a random distribution. As showed, in all cases except for CG DMRs in the pulp, a significant difference in found between the values found experimentally and the theorical values, indicating that DMRs in promoter region are more frequent that expected. The p values were calculated by two-sided Fisher's exact test.

e. Methylation and gene expression.

In order to evaluate possible links between gene expression and variations of methylation in promoters, we selected the genes presenting DMRs in their promoter region and analyzed their expression, first using a pairwise comparison between V3W and F6W, or using the clusters previously described (page73). The rationale of these two complementary analyses is that RNA quantities may vary more rapidly than DNA methylation patterns. A two stage comparison may therefore hide transient changes in expression that could however be related to changes in DNA methylation patterns.

Among the 14052 hyper-DMRs and 6652 hypo-DMRs (C-DMRs) identified in the skin, 2208 and 993 are located in promoter regions and could therefore be potentially be involved in regulating gene expression. These DMRs correspond to 2347 and 1081 genes in the grape genome. A similar analysis performed for CG, CHG, ad CHH DMRs showed a slightly higher number of genes potentially associated with DMRs than the number of DMRs itself. This indicates that in some cases, DMRs are located in the vicinity of more than one gene. Similarly, 17046 and 7129 hyper-DMR and hypo-DMRs (C-DMRs) were found in pulp. Among them, 2781hyper-DMRs and 1104 hypo-DMRs are located in promoter regions, corresponding to 2884 and 1124 genes. Similar results were found for DMRs in other sequence contexts.

As previously mentioned, both in pulp and in skin, more hyper- than hypo DMRs (C Types) were found in the promoter region of genes. This result is in line with the observation that methylation levels are slightly increased during ripening. To assess the potential effect of DNA methylation on gene expression, a pairwise comparison was performed to identify DEGs between V3W and F6W in the skin and in the pulp. A total of 3358 and 1816 DEGs in the skin, and 3953 and 2215 DEGs in the pulp were identified that are down- and up- regulated respectively in V3W versus F6W berries. Correlation analysis was then performed to determine the possible relationships between these DEGs and genes having C-DMRs in their promoters.

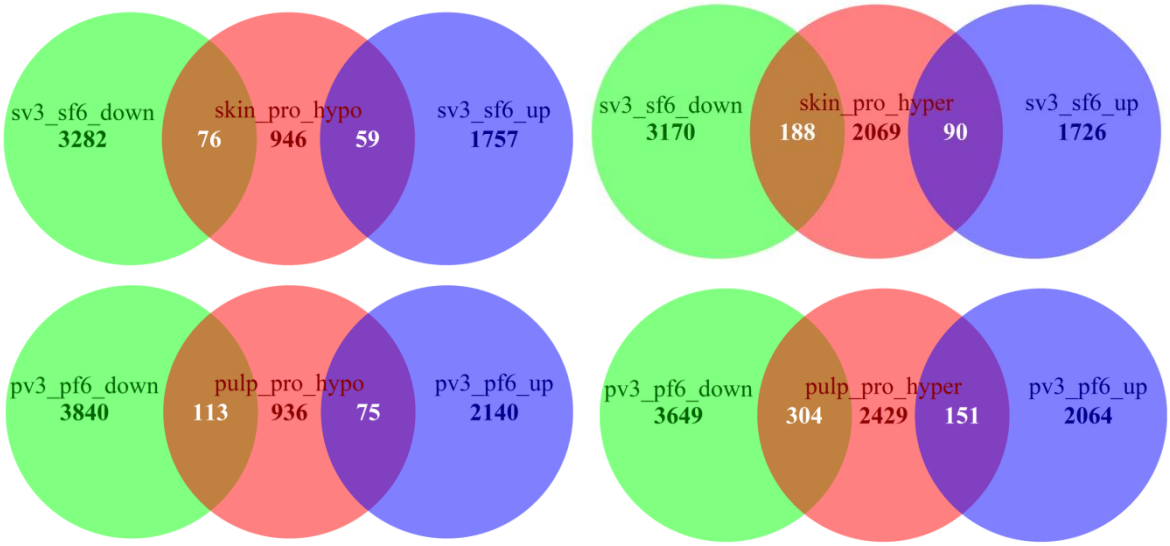

Figure II-29. Vennplot displays the number of DEGs associated with DMRs in pulp and skin.

Among all DEGs identified in the skin, 135 have hypo- and 278 hyper-DMRs in their promoter region However, most genes, 946 and 2069 genes with hypo- and hyper-DMRs in their promoter, are not DEGs. In addition, among the 135 genes with hypo-C-DMRs in their promoters, 76 were downregulated and 59 were up-regulated in the skin of V3W berries as compared to F6W berries. Similarly, the 278 genes with hyper-C-DMRs include 188 and 90 down and up regulated DEGs respectively. Similar analysis performed in the pulp showed that, 113 and 75 genes with hypo-C-DMRs methylated are down and up-regulated, respectively, whereas 304 down- and 151 up-regulated DEGs corresponded to genes with hyper-C-DMRs in their promoter. These results indicate that there is no strict relationship between DNA methylation variations and gene expression.

As mRNA levels are more prone to rapid variations than DNA methylation, we investigated whether a different type of correlations could be found considering in addition to V3W and F6W berries, the V1W and V7W samples, for which RNA seq analyses were also performed (page 61).

As explained above, DEGs identified by analyzing these four developmental stages are organized in 12 clusters that were themselves classified in 3 groups A, B, C based on their global expression profile (page 73). In addition C-DMRs in promoter region were also separated in three groups based on the difference in methylation level between the two developmental stages: above 30%, between 15-30% and less than 15%. DEGs corresponding to genes with C-DMRs are found in all three groups of clusters. Inversely, each type of DMR was distributed along the different DEG expression groups (Table II-13).

		Pulp_C_hyper			Pulp_C_hypo			Peel_C_hyper			Peel_C_hypo		
group	v3f6 expression	>30%	15%-30%	<15%	>30%	15%-30%	<15%	>30%	15%-30%	<15%	>30%	15%-30%	<15%
group A (cluster1,4,6,11)	down,stable	10	115	238	16	49	73	9	88	155	5	47	58
group B (cluster2,3,5,12)	up,stable	9	72	128	8	35	47	4	37	95	9	26	52
group C (cluster7,8,9,10)	down,up ,stable	2	36	63	1	13	26	3	37	52	2	20	31

Table II-13. Distribution of DMR in different group of expression clusters

For example, genes with the highest difference in methylation level (hyper or hypo) correspond to DEG that belong to any of the expression groups. In the pairwise comparisons these genes are also either up or down regulated or do not present differences between the two stages analyzed. Similar observations are done in the pulp and skin. Indeed more genes with hypermetylated promoter regions seem down regulated, but this was not statistically significant.

As for DEGs, we analyzed whether DEGs with C-DMRs in their promoters were enriched in the specific specific functional categories. GO analysis was therefore performed with DEGs that are differentially methylated (Table II-14). In the pulp, DEGs with hyper-C-DMRs were enriched in 3 functional categories, 'PS' (13 genes), 'misc' (59 genes), 'transport' (42 genes), whereas no specific enrichment was found for

those associated with hypo-C-DMRs. In the skin, four DEGs with hypo-C-DMRs in their promoters were ranked in the category 'secondary metabolite', whereas no specific enrichment was identified for DEGs with promoter containing hyper-C-DMRs.

	Bin	Bin name	contingency	Pvalue	Adj.Pvalue(Bonf)
pulp C hyper	1	PS	13 220 660 39725	1.56E-04	6.16E-02
	1.1	PS.lightreaction	11 141 662 39804	5.01E-05	1.98E-02
	26	misc	59 1931 614 38014	1.89E-05	7.48E-03
	34	transport	42 1258 631 38687	5.33E-05	2.11E-02
	35	not assigned	187 19766 486 20179	8.85E-30	3.51E-27
	35.2	not assigned.unknown	138 17554 535 22391	8.87E-37	3.51E-34
pulp C hypo	35	not assigned	85 19868 183 20482	8.66E-09	1.94E-06
	35.2	not assigned.unknown	67 17625 201 22725	2.81E-10	6.31E-08
skin C hyper	35	not assigned	149 19804 331 20334	9.55E-16	3.24E-13
	35.2	not assigned.unknown	111 17581 369 22557	8.31E-21	2.82E-18
skin C hypo	16.8.4	secondary metabolism.flavonoids.flavonols	4 67 246 40301	9.85E-04	2.10E-01
	35	not assigned	86 19867 164 20501	3.11E-06	6.63E-04
	35.2	not assigned.unknown	70 17622 180 22746	4.89E-07	1.04E-04

Table II-14. Enrichmen of mapman functional categories (BINs) of the DEGs that different methylated. The Contingency column shows the number of genes (i) in the BIN in the input list, (ii) in the background, (iii) not in the BIN in the input list, and (iv) not in the background. P-values were adjusted with a Bonferroni correction. Values were filtered with an adjusted P-value threshold <0.05(Usadel et al., 2005).

As described previously in chapter 2 (part2.3.3g, page 79), young berries express several genes involved in photosynthesis, which are subsequently repressed during ripening along with chlorophyll degradation and the loss of photosynthetic activity. As shown in Figure II-13 (page 81), genes related to photosynthesis were more repressed in the pulp than in the skin during berry ripening. Among them, 13 PS related DEGs identified in the pulp, were hyper methylated in their promoter region (Table II-15), whereas only two of the 13 genes, *Vitvi03g01127* and *Vitvi05g00474*, show difference in methylation levels in the skin. Furthermore they do not show and increase but a decrease in their methylation level, eventhough they are also down regulated in the skin.

We also analyzed the link between genes with DMRs involved in flavonoids biosynthesis a key process in the skin during berry ripening. Four of the genes were hypo methylated and repressed during ripening, including the flavonol synthase (FLS5, Vitvi18g02538) and 3 Fe(II)/ascorbate oxidase (Vitvi02g00620, Vitvi10g00697, Vitvi10g01832).

gene	function	cluster	group	pvalue	qvalue	meth_diff
Vitvi06g01265	ELONGATEDHYPOCOTYL2(HY2)	ps6com	A	1.53E-34	9.00E-32	19.2424202
Vitvi07g02309	photosystemIsubunitE-2(PSAE-2)	ps1com	A	1.69E-38	1.38E-35	13.6596941
Vitvi09g00361	PhotosystemIreactioncentersubunitVI,chloroplastprecursor(PSI-H	ps1com	A	2.46E-32	1.17E-29	13.3529878
Vitvi12g00092	PhotosystemIIoxygenevolvingcomplexproteinPsbP	p1s4	A	1.26E-10	3.41E-09	10.1818506
Vitvi12g00475	photosystemIIrepair	p1s4	A	4.37E-14	2.32E-12	19.9879554
Vitvi13g00254	PsbP-likeprotein2(PPL2)	p1s4	A	3.93E-12	1.44E-10	10.9235123
Vitvi14g00489	PhotosystemIIreactioncenterWprotein	ps1com	A	1.31E-34	7.77E-32	10.3888237
Vitvi15g00004	photosystemIlightharvestingcomplexgene3(LHCA3)	ps1com	A	2.35E-26	6.21E-24	11.7316053
Vitvi19g01352	Aldolase-typeTIMbarrelfamilyprotein	p1s4	A	2.87E-06	2.45E-05	10.619684
Vitvi19g01692	Phosphoglyceratekinasefamilyprotein	p1s4	A	4.39E-08	6.40E-07	10.7680114
Vitvi19g01981	subunitoftheNAD(P)Hcomplexlocated PsbQ-like1(PQL1)	pulpsc1	A	2.14E-28	6.97E-26	15.2384755
Vitvi03g01127	Plastohydroquinone:plastocyaninoxidoreductaseiron-sulfurprotein1)(ISP1)	ps1com	A	4.05E-08	5.96E-07	19.8257713
Vitvi05g00474	PhotosystemIreactioncentersubunitII,PsaD	ps1com	A	4.33E-15	2.70E-13	17.3299945

Table II-15. List of DEGs related to photosynthesis that down regulated with hyper-methylation.

To study the relationship of all DEGs associated with DMRs, a correlation analysis was preformed (Figure II-30). Between log2 fold change of gene expression (comparing V3 to F6) and the variation of methylation (comparing V3 to F6). No clear correlation could be identified with R2 value being very low, 2.83e-5, 2.5e-5, 2.6e-4 and 0.0012 of pulp _hyper_C, pulp _hypo_C, skin _hyper_C, and skin _hypo_C, respectively. Overall, the changes of gene expression appear independent of methylation variations in the promoter of gene in grape berry during ripening.

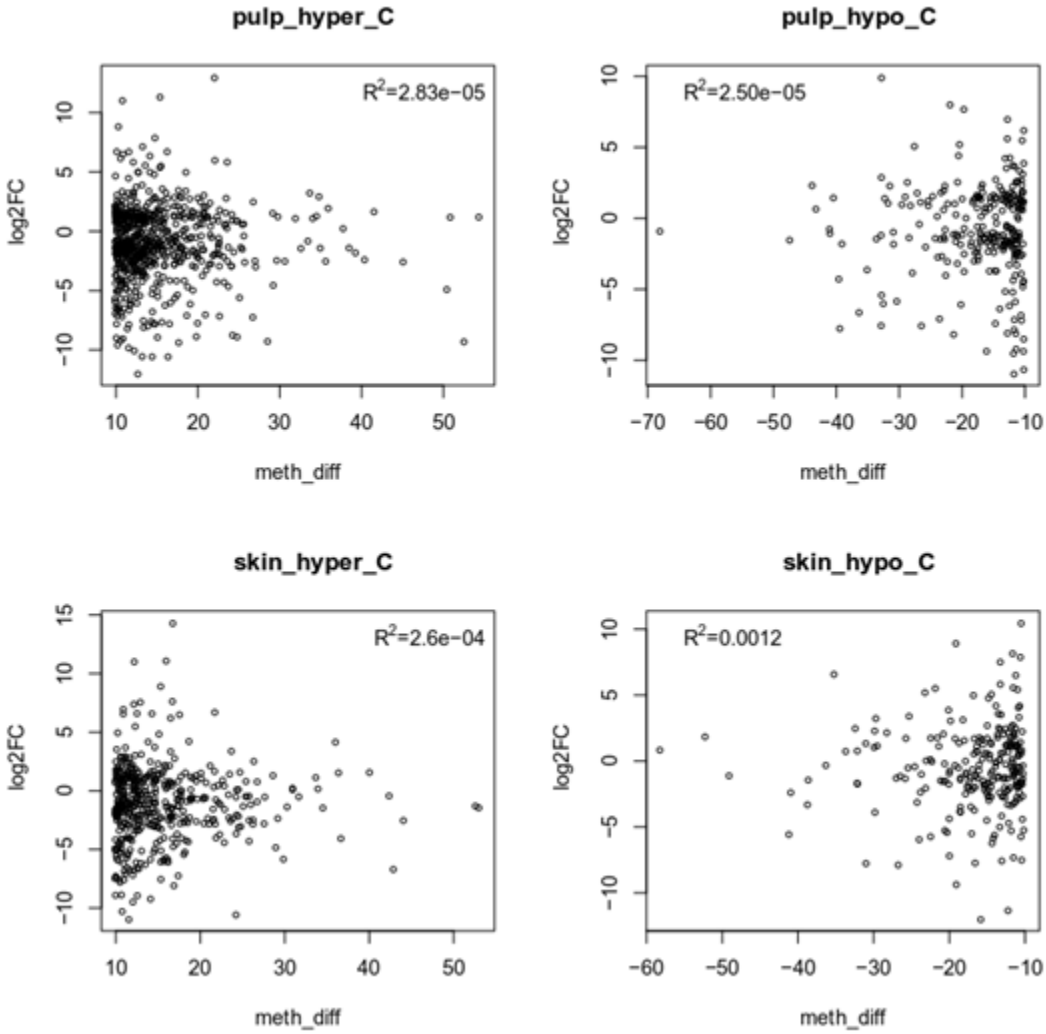

Figure II-30. Correlation analysis of gene expression and methylation variation of DEGs associated with DMRs. The logarithm of fold change values in the RNA-seq and the variation of methylation, log2FC represent the gene expression change of V3 to F6.

Discussion

DNA methylation has been shown to play important roles in the control of fruit ripening in tomato (Lang et al., 2017), strawberry (Cheng et al., 2019) and orange (Huang et al., 2019), and citrus (Xu et al., 2017). In the present work we have investigated the potential role of DNA methylation in the control of grape berry ripening using a combination of approaches:

- We used DNA methylase inhibitors to interfere with DNA methylation control during berries ripening, using an in vitro ripening system.

- We have analyzed the DNA methylation changes occurring during ripening by comparing at a base pair resolution DNA methylation in berry tissues before and after véraison. This was performed using hand dissected fruit tissues harvested a selected developmental stages that were carefully analyzed at the metabolic level. DNA methylation changes were then correlated with gene expression variations in order to evaluate potential relationships between both processes.

2.4.1 In vitro treatment with DNA methyltransferase inhibitors affected grape berry ripening

In the present work, DNA methyltransferase inhibitors, zebularine and RG108 have been used to evaluate the potential role of DNA methylation on grape berry ripening *in vitro*. DNA methyltransferase inhibitors were already used to investigate the function of DNA methylation in plant development, including fruit ripening, such as tomato (Zhong et al, 2013), orange (Huang et al., 2019), strawberry (J. Cheng et al., 2018) or citrus (Xu et al., 2017). For example, the exogenous application of 5-azacytidine, a cytosine analog, induced premature fruit ripening in tomato (Zhong et al., 2013), and strawberry (Cheng et al., 2018). In our work, we have chosen to use zebularine and RG108, because both molecules were shown to be more stable and to have lower toxicity than of 5-AzaC (Pecinka and Liu, 2014). As the experimental system in use here (Dai et al., 2014) requires that the treatment is performed *in vitro* in sterile conditions. Additional manipulation of the incubation plates that would have been necessary if using less stable molecules, to renew the treatment may have resulted in high contamination rates. However both zebularine and RG108 also have demethylation activities that make them suitable to analyze the role of DNA methylation *in vivo.* For example, a comparative analysis of 5-azacytidine and zebularine demonstrated that treatment of *A. thaliana* with either of these drugs results in similar changes in DNA methylation across the genome (Patrick T. Griffin et al., 2016). RG108, is a novel small molecule that effectively blocks DNA methyltransferases *in vitro* and did not cause covalent enzyme trapping (Brueckner et al., 2005). Intriguingly, RG108 causes demethylation, but it does not affect the methylation of centromeric satellite sequences and displays greater demethylation activity when used at the same concentration than 5-azacytidine (Brueckner et al., 2005).

Experiments were performed using either 2 or 7 week-old berries. The rationale of this choice was based on the assumption that zebularine may be more efficient when using berries still containing dividing cells such as young berries as compared to berries harvested just prior to véraison (Zhou et al.,

2002). Indeed, treatments with zebularine had very different impacts depending on the age of berries: treatment of 2 week-old berries with zebularine severely limited the number of berries that changed color after 8 weeks as compared to control, whereas a similar experiments performed with 7 week old berries did not block berry ripening. In this context it is tempting to suggest that differences between both experiments is due to the fact zebularine impact is limited on 7 week-old berries because of low DNA replication activity.

To account for this limitation we also used the DNA methyltransferase inhibitors, RG108 which directly binds to active sites of DNA methyltransferases. RG108 which acts independently of DNA replication would therefore be expected to be similarly efficient at both developmental stages (Brueckner et al., 2005). As zebularine, RG108 inhibits ripening of 2 weeks old berries, to a lower extend though. Of note, 7 week old berries were separated in two groups based on their softness, which marks the first step of véraison. Hard berries could not ripen *in vitro* in the absence of ABA. Indeed, ABA has been described as the key hormone controlling berry ripening: exogenous application of ABA induced early grape berry ripening, and triggered the accumulation of sugar and anthocyanin (Pilati et al., 2017). Addition of RG108 with ABA had a synergetic effect on berry ripening and promoters ripening even more efficiently that ABA alone. This result seems however contradictory with the inhibition of ripening observed with 2 week-old berries cultured in the presence of zebularine and RG108, suggesting that DNA methylation may play different roles depending on berry age. In line with this observation, neither RG108 nor ABA did affect the ripening of 7 week-old soft berries. This suggests that the role of DNA methylation occurs before ripening induction. So far, results indicate that at early stages of development, the use of DNA demethylation agents result in ripening inhibition, whereas an opposite effects is observed at later developmental stages prior to Véraison. In addition, how does demethylation and ABA interact is still unclear.

2.4.2 Pulp and skin present specific metabolite, transcriptomic and methylation characteristics.

In order to determine the potential role of DNA methylation at the onset of fruit ripening, we have analyzed the methylation at the Whole Genome level. In order to obtain suitable biological replicates and to minimize eventual developmental variations between berries within and between clusters, clusters were labelled at flowering and berries were marked at the véraison stage. Indeed both metabolic and RNA seq analyses indicated that biological replicates have very similar features. Focusing on RNA seq experiments, PCA indicated that all biological replicates were grouped (page 67). Samples were clearly separated as a function of their developmental stages (PC1), but also at each developmental stage as a function of tissues (PC2). A total of 8788 and 9023 DEGs were identified in the skin and the pulp during berry development, respectively, accounting for 20.7% and 21.3% of all grape genes (Canaguier 2017). In both tissues, more DEGs were down-regulated than up-regulated in both pulp and skin as observed in previous studies (Lijavetzky et al., 2012). Of note, among the DEGs, 2700 and 2465 are pulp and skin specific, respectively, representing approximately 30% of total DEGs. Taken together these results indicate that whereas many genes are likely co-regulated between tissues during berry development, the expression of several of them seems to be controlled in a tissue specific manner

consistent with each tissue bearing specialized features, as previously described by (Lijavetzky et al., 2012). This is also consistent with the analyses of metabolites showing that both primary and secondary metabolites presented tissue specific accumulation patterns (chapter2, pages 60-63). Indeed, in some cases, such as tartaric acids, the kinetic of accumulation was very similar between tissues. However, when considering malic acid or hexoses significant differences in either the kinetic of accumulation or the final accumulation levels were found. As expected, this was even more pronounced with secondary metabolites, such as anthocyanin accumulation a specific characteristic of the skin in most red grape cultivars, including Cabernet sauvignon (Ananga et al., 2013).

Analysis of DNA methylation distribution leads to similar conclusions. When considering the distribution of methylation along chromosomes (Figure II-25), or within genes and transposons (Figure II-26-27, and supplementary Figure II-34), a similar trend is observed in both tissues. In addition, changes in methylation levels were nearly similar between tissues with a global but very limited increase in DNA methylation during ripening. The distribution of DMRs in genes, intergenic regions and transposons (Figure II-29), was also similar between tissues at all stages and in all sequence contexts. These observations are consistent with DNA methylation being similarly controlled in the skin and the pulp. However, differences between tissues were also observed: (1) whereas, changes in global DNA methylation are very limited and comparable in both tissues during ripening differences were observed between contexts. In the pulp the CG and CHG ratios decreased during ripening, whereas they increased in the skin. The CHG methylation ratio behaved similarly in both tissues during ripening. (2) A similar number of DMRs (hypo and hyper) is observed during berry ripening in each tissue. However, analysis of the targeted regions indicates that most DMRs are different and do not target the same genes (sup data Fig36). This should allow defining methylation signatures that are specific to the skin and the pulp.

2.4.3 There is no clear link between DNA methylation variations at promoters and changes in gene expression.

As previously mentioned, several genes are differentially regulated during ripening within and between tissues. For example genes involved in photosynthesis are expressed at higher level in the skin than in the pulp. In addition, at véraison, the regulation of PS related genes differs between tissues: their repression is much stronger in the pulp than in the skin, suggesting distinct regulatory processes (Richard Breia., 2013). In tomato, orange and strawberry (Lang et al., 2017; Cheng et al., 2018; Huang et al., 2019) the repression of PS related genes was suggested to be associated with changes in DNA methylation levels, with distinct mechanisms between plants though. In tomato and strawberry, repression of these genes was associated with their demethylation, and the converse in sweet orange. In the present study, 13 DEGs related to photosynthesis that are repressed in pulp present a hypermethylated promoter in the pulp at V3 versus F6. In the skin, these genes are also repressed, although with different kinetics and intensity. However, only two of them are associated with changes in methylation levels or patterns in their promoter region. Additionally, these two genes become hypomethylated in the skin instead of hypermethylated as observed in the pulp. This would suggest that methylation participate to the regulation of these genes in the pulp only (Table II-14, page110). Analysis of genes related to

anthocyanin biosynthesis did not reveal a clear link between stage and tissue specific gene expression and changes in methylation levels in their promoter regions. At a more global scale, correlation studies between C-DMRs and variations in expression levels in the pulp and the skin did not reveal clear relationship between changes in DNA methylation and changes in gene expression levels (Figure II-30, page 112).

Hence, whereas our studies showed that the treatment of young berries with two different DNA methylase inhibitors resulted in a severe inhibition of ripening, DNA methylation analysis at a genome wide scale did not allow identifying a clear link between variations in gene expression and changes in DNA methylation levels in promoters. This is clearly different from previous observation in tomato, where DNA demethylation mediated by the DNA demethylase DML2 was shown to be necessary for ripening to occur (Liu et al., 2015; Lang et al., 2017). Recent studies in citrus (Xu et al., 2017), orange (Huang et al., 2019) and strawberry (J. Cheng et al., 2018) also clearly indicated that variation of DNA methylation is associated with gene expression and ripening controls. Indeed, specific mechanisms were identified in these different plants. For example, in sweet orange, the global increase in DNA methylation level observed during ripening was associated with a decrease of the expression genes encoding the DNA demethylase (Huang et al., 2019), whereas loss methylation in strawberry occurred along with the downregulation of genes involved in RNA-directed DNA methylation (J. Cheng et al., 2018).

As far as grape is concerned, unlike other fruits described so far, variations of DNA methylation in fruit tissues were very limited during ripening: the global methylation level was 11.05%, 11.15% in the pulp, and 9.95% and 10.68% in the skin at F6 and V3, respectively. In addition, no clear correlation between gene expression and methylation changes was found suggesting that DNA methylation might not be of primary importance in grape for the control of gene expression during ripening. However, the stage dependent effect of zebularine and RG108 in vitro might indicate that DNA methylation changes are critical at earlier stages that the one analyzed in this study.

Conclusion

In the present study, transcriptional and metabolite analysis were carried in the pulp and skin at four developmental stage of grape berry revealing that approximately 32% of the transcriptional program operating during ripening is shared between pulp and skin, about 68% transcriptional variation were tissue specific. This analysis provides a number of candidate genes that account for the regulation of tissue-specific ripening events. *In vitro* treatment with DNA methyltransferase inhibitor indicated that DNA methylation is involved in berry ripening. Subsequently, whole bisulfite sequencing suggested no significantly variation in methylation level during grape berry ripening. Moreover gene expression were not associated with the change of methylation as we expected suggested methylation modulated gene expression is more complex, both methylation and demethylation can both active and repress gene expression.

Chapter II Supplementary Material

name	12Xv2 VCOST.v3	12Xv1 VIT code	primer	Sequence 5'-3'
VvMET1	Vitvi07g02047	VIT_207s0130g00380	VvMET1-F	AACACAAGCACAGGCAGATAG
			VvMET1-R	CAACCTCACAACTGACCTTCTAC
VvMET2	Vitvi07g02048	VIT_207s0130g00390	VvMET2-F	TGCTGGTAACATTCAACAC
			VvMET2-R	TGCTAATACATACAACCTATATCC
VvCMT1	Vitvi08g01767	VIT_208s0007g06800	VvCMT1-F	CCAAGGACTCTGTGATGAC
			VvCMT1-R	TGGCTTCACCTTCAACTG
VvCMT2	Vitvi02g01050	VIT_202s0033g00610	VvCMT2-F	GCCAATACGACTTTCCCAGA
			VvCMT2-R	CCAGTTGACATTCCACCACA
VvCMT3	Vitvi06g00102	VIT_206s0004g01080	VvCMT3-F	GTGGTTTATGCCTTGGTGCT
			VvCMT3-R	TTTCTCACCTGGGTCTCTGG
VvCMT4	Vitvi16g00174	VIT_216s0039g02470	VvCMT4-F	CTCCCATTCTACTACTGCC
			VvCMT4-R	CCAGGTTCCTAGCGTAGTA
VvDRM2A	Vitvi14g01743	VIT_214s0066g01040	VvDRM2A-F	CACACATTTGGTGGATTTGAT
			VvDRM2A-R	ACTGATTTCTACCCATTATACACT
VvDRM2B	Vitvi05g00215	VIT_205s0020g00450	VvDRM2B-F	GTCTCCACCAACAACTATTCTG
			VvDRM2B-R	AGTTTAGTCATTGATGCCATTACA
VvDML1	Vitvi08g01515	VIT_208s0007g03920	VvDML1-F	GAGAACTAGGTATTGTGCTTGATG
			VvDML1-R	ACTCACTTGTCATGGAATCTTAGA
VvDML2	Vitvi13g00747	VIT_213s0074g00450	VvDML2-F	AGCACCCCGACCTCTGAT
			VvDML2-R	ACTTAGCAATCTCCATCTCCTCCA
VvDML3	Vitvi06g01402	VIT_206s0061g01270	VvDML3-F	TGTGTGCGAGGGTTCAAT
			VvDML3-R	AGGTGGACTAGACAATATGAAGTT
VvMYBA1	Vitvi02g01019	VIT_02s0033g00410	VvMYBA1-F	AAGCCATCATCCACTTCACC
			VvMYBA1-R	TCTCTCCAGAAGCCGAAAAG
VvGAPDH	Vitvi16g00258	VIT_16s0013g00080	VvGAPDH-F	CCACAGACTTCATCGGTGACA
			VvGAPDH-R	TTCTCGTTGAGGGCTATTCCA
VvEF1	Vitvi12g02055	VIT_12s0035g01130	VvEF1-F	CAAGAGAAACCATCCCTAGCTG
			VvEF1-R	TCAATCTGTCTAGGAAAGGAAG

Table II-16. List of prime sequences used in qRT-PCR analysis.

grape	Arabidopsis				tomato			
	AtMET1	AtMET2			SlMET1			
VvMET1	61%	575			67%			
VvMET2	59%	54%			60%			
	AtDRM1	AtDRM2	AtDRM3		SlDRM5	SlDRM6	SlDRM7	SlDRM8
VvDRM2A	52%	54%	44%		66%	63%	65%	47%
VvDRM2B	27%	26%	38%		35%	28%	29%	53%
	AtCMT1	AtCMT2	AtCMT3		SlCMT2	SlCMT3	SlCMT4	
VvCMT1	53%	51%	54%		58%	685%	52%	
VvCMT2	46%	63%	515%		52%	50%	66%	
VvCMT3	59%	60%	53%		72%	72%	61%	
VvCMT4	46%	57%	48%		52%	49%	60%	
	AtDEM	AtDML2	AtDML3	AtROS	SlDML1	SlDML2	SlDML3	SlDML4
VvDML1	74%	43%	50%	58%	77%	65%	69%	54%
VvDML2	64%	51%	48%	68%	75%	74%	71%	45%
VvDML3	58%	50%	40%	57%	56%	56%	55%	46%

TableII-17. Similarity of DNA methyltransferase and demethylase protein between grape, Arabidopsis and tomato.

		Pulp_C_hyper			Pulp_C_hypo			Peel_C_hyper			Peel_C_hypo		
group	v3f6 expression	>30%	15%-30%	<15%	>30%	15%-30%	<15%	>30%	15%-30%	<15%	>30%	15%-30%	<15%
group A (cluster1,4,6,11)	down,stable	10	115	238	16	49	73	9	88	155	5	47	58
group B (cluster2,3,5,12)	up,stable	9	72	128	8	35	47	4	37	95	9	26	52
group C (cluster7,8,9,10)	down,up ,stable	2	36	63	1	13	26	3	37	52	2	20	31

TableII-18. Distribution of DMR in different methylation variation.

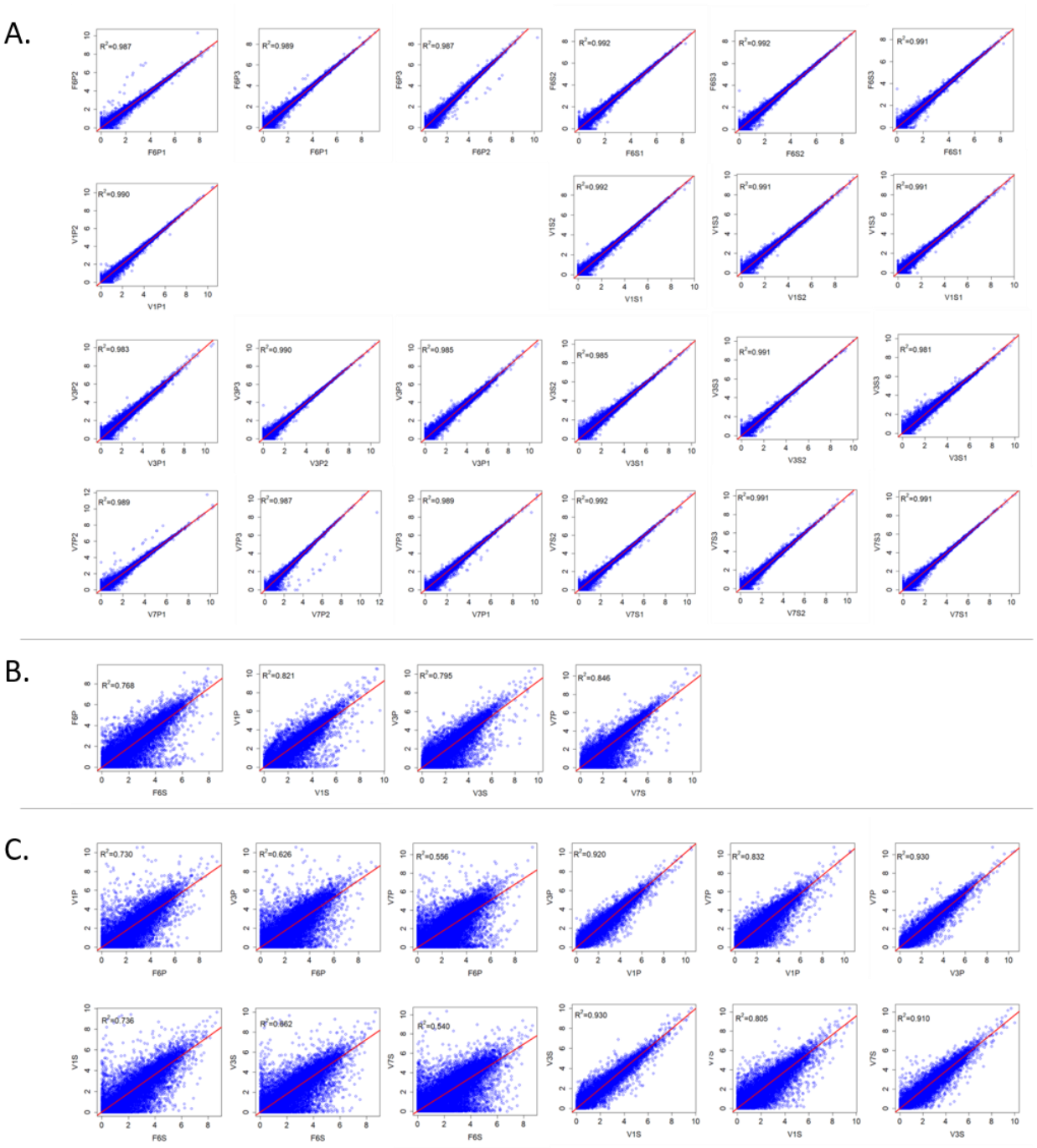

Figure II-31. Correlation analysis of RNA seq data.between 3 replicates (A), tissues at equivalent stage (B), each pairwise comparison (C)

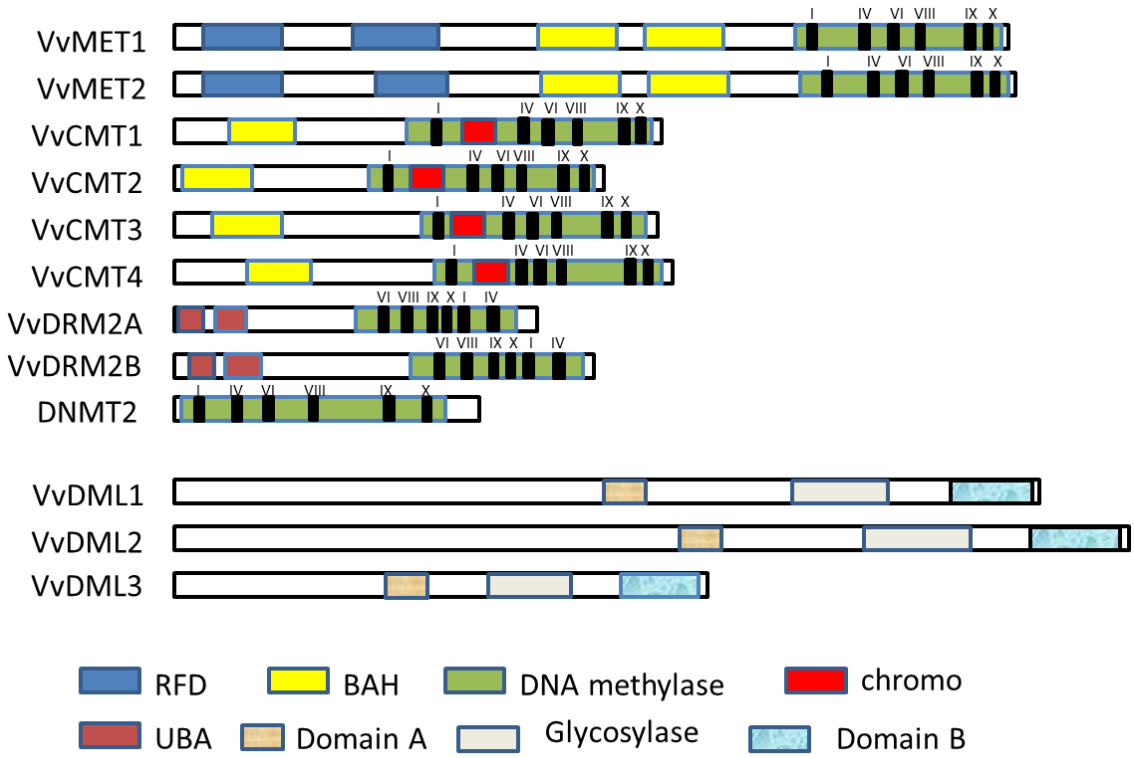

Figure II-32. Structure and conserved domains of grape DNA methyltransferase and demethylase

Based on the presence of conserved domain in the amino-terminus, such as ubiquitin-associated domain (UBA), bromo adjacent homology (BAH) domain, chromodomain (Chr) and replication foci domain (RFD), MTases were grouped into four subfamilies. MTases containing RFD, BAH and methyltransferase domains were classified as MET family members, whereas members with Chr along with BAH and methyltransferase domain were placed in CMT family. Members harboring both UBA and methyltransferase domains were grouped into DRM family. BAH domain appears to act as a protein-protein interaction module specialized in gene silencing (Callebaut et al., 1999), while RFD domain may have a role in inhibiting the binding of DNA to the catalytic motif of unmethylated CpG dinucleotides that emerge from the replication complex. UBA domain unique located in DRM members, suggests a link between DNA methylation and ubiquitiny proteasome pathways (Cao et al., 2000).There are six highly conserved motifs in the catalytic domain that transfer of methyl group from Sadenosyl-methionine onto cytosine, motif I,IV,VI,VIII,IX and X. The order of these six conserved motifs in MTases are subfamily specific. In MET subfamily is I,IV,VI,VIII,IX and X, but a Chr domain insert between the motif I and IV in the CMT subfamily. And in the DRM and DNMT subfamily, they were re-arranged, in a new arrangement: VI, VIII, IX, X, I and IV. DNMT2 gene codes a shorter protein product compared with other DNA methyltransferase subfamilies, which only contain DNA methylase domain with six conserved motifs. DNMT2 has been reported to be a highly specific tRNA methyltransferase in eukaryotic (Steffen Kaiser et al., 2017). Three conserved domains—domain A, glycosylase domain, and domain B—which are necessary and sufficient for catalyzing DNA demethylation through a base excision-repair pathway were identified in DMLs (Gong et al., 2002; Gehring et al., 2005)

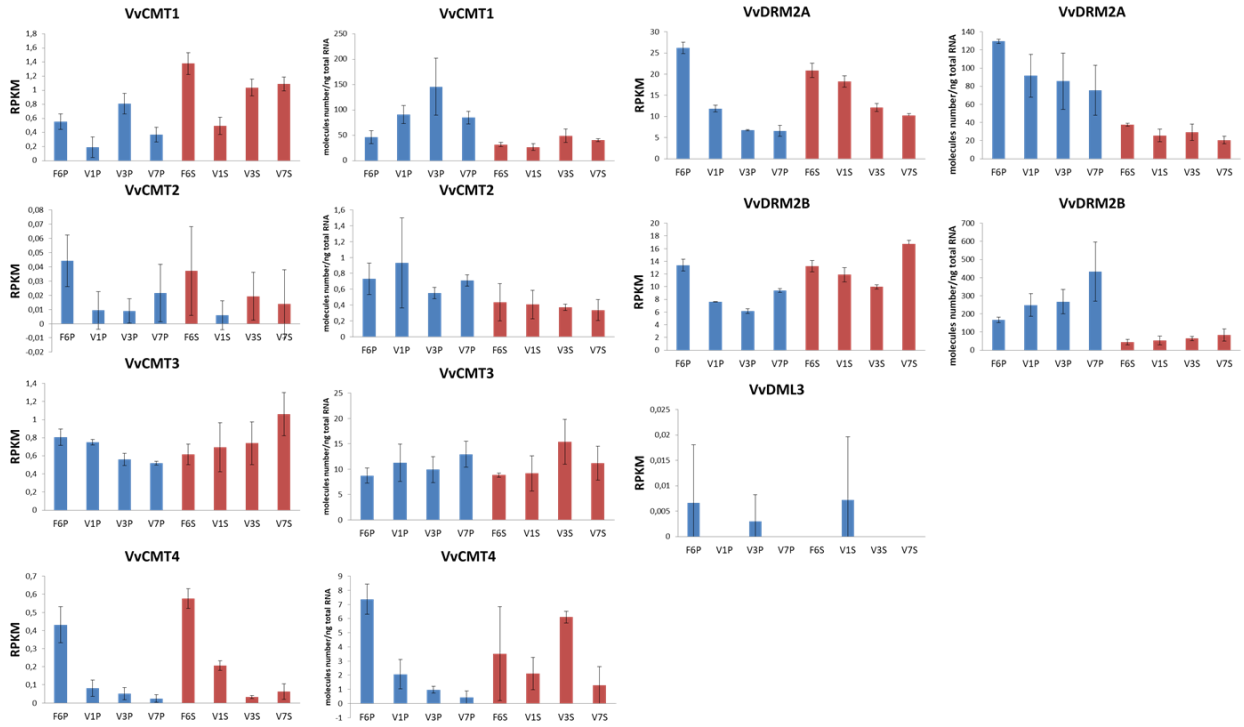

*FigureII-33. Expression profile of grape CMTs, DRMs and DML3.Expression profile of CMTs, DRMs and DML3and determined by RNA- seq (left panels) and absolute RT qPCR (right panels). Asterisks indicate significant difference [Student's t test (n = 3)] between SlDML2 and all other SlDML genes: *P < 0.05;**P < 0.01; ***P < 0.001. Error bars indicate means ± SD*

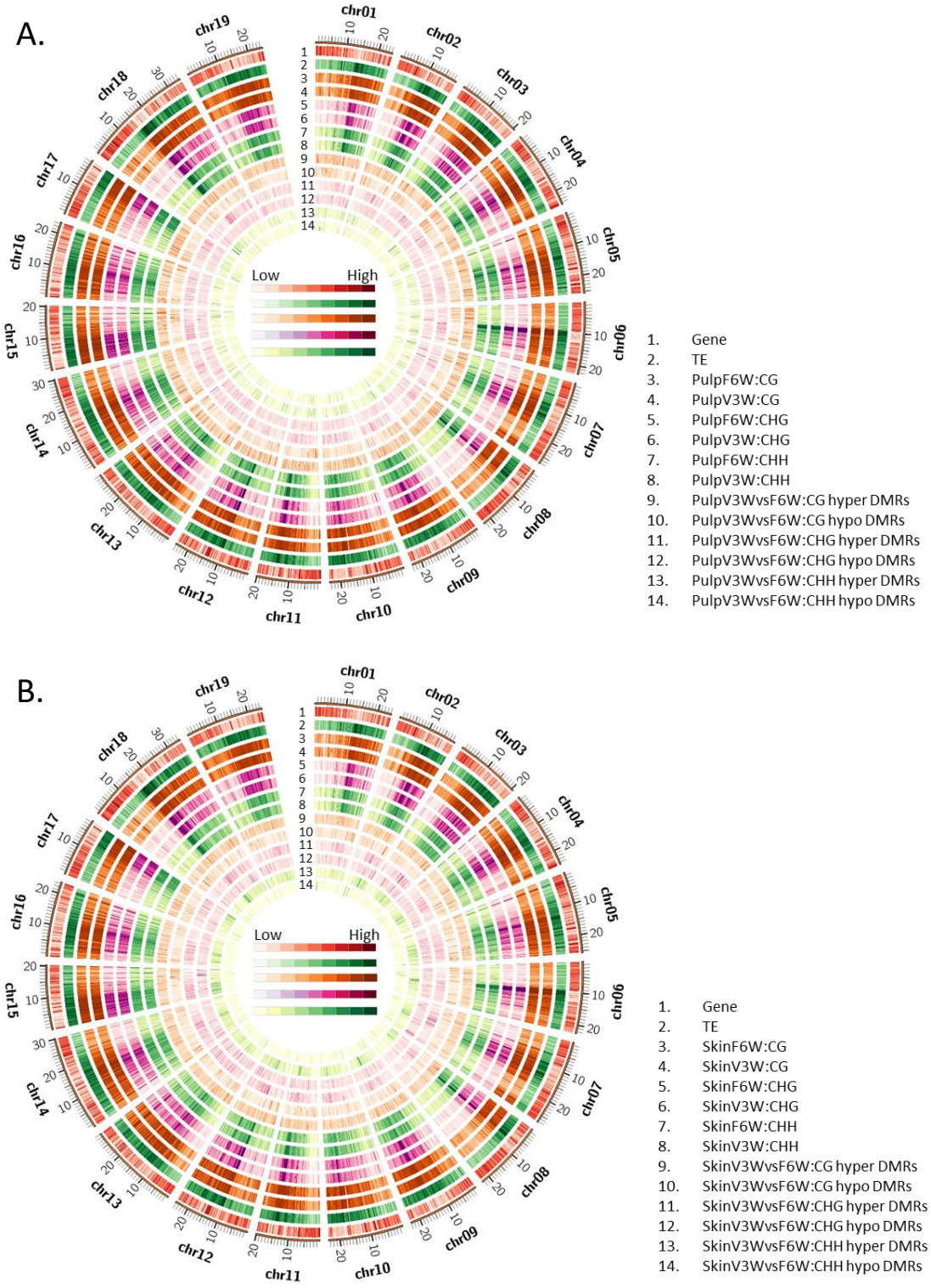

Figure II-34. Density plots of DNA methylation, transposable elements (TEs), genes,methylated cytosine in three context and DMRs comparing between two stage(A,pulp,B,skin) and two tissues(C,F6,D,V3). The results shown that methylation was enriched in TEs, while gene rich regions were characterized by reduction methylcytosine density

C

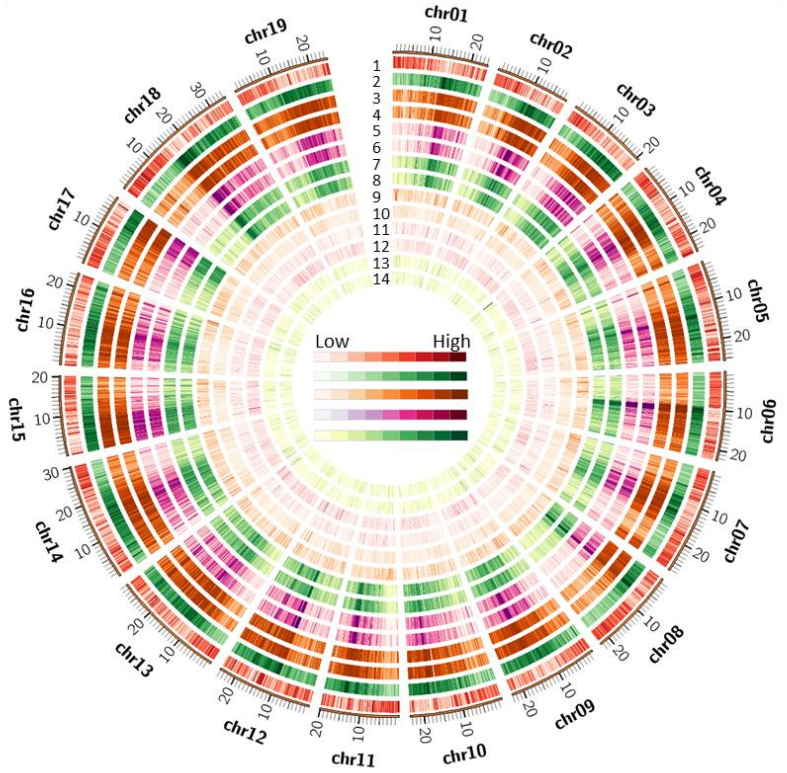

1. Gene
2. TE
3. PulpF6W:CG
4. SkinF6W:CG
5. PulpF6W:CHG
6. SkinF6W:CHG
7. PulpF6W:CHH
8. SkinF6W:CHH
9. SkinvsPulp_6W:CG hyper DMRs
10. SkinvsPulp_6W:CG hypo DMRs
11. SkinvsPulp_6W:CHG hyper DMRs
12. SkinvsPulp_6W:CHG hypo DMRs
13. SkinvsPulp_6W:CHH hyper DMRs
14. SkinvsPulp_6W:CHH hypo DMRs

D

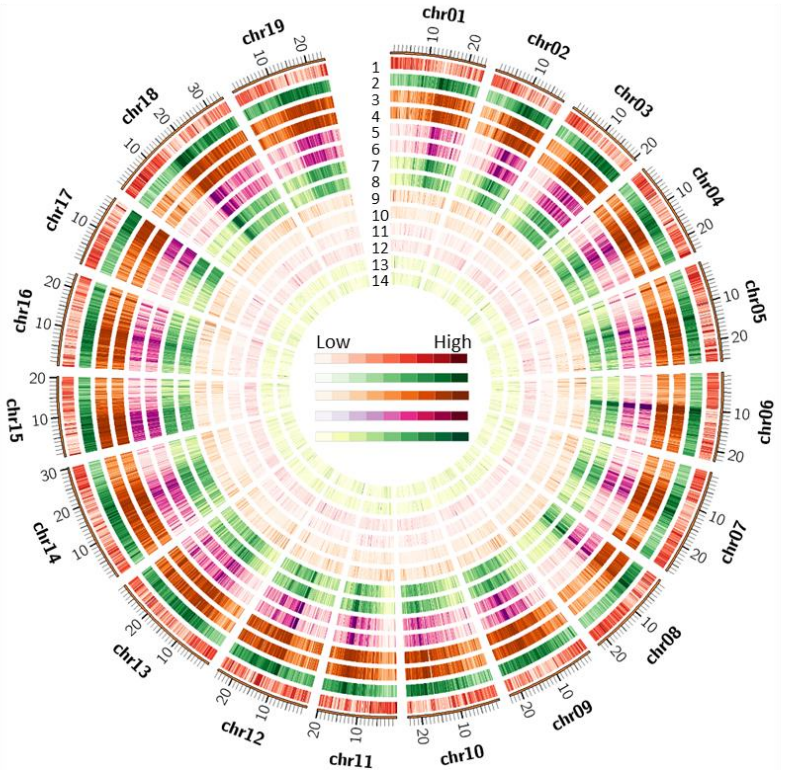

1. Gene
2. TE
3. PulpV3W:CG
4. SkinV3W:CG
5. PulpV3W:CHG
6. SkinV3W:CHG
7. PulpV3W:CHH
8. SkinV3W:CHH
9. SkinvsPulp_11W:CG hyper DMRs
10. SkinvsPulp_11W:CG hypo DMRs
11. SkinvsPulp_11W:CHG hyper DMRs
12. SkinvsPulp_11W:CHG hypo DMRs
13. SkinvsPulp_11W:CHH hyper DMRs
14. SkinvsPulp_11W:CHH hypo DMRs

	C_DMR in the promoter	corresponding gene
skin vs pulp-6w_hyper	1352	1455
skin vs pulp-6w_hypo	2632	2809
skin vs pulp-11w_hyper	1119	1217
skin vs pulp-11w_hypo	2895	3029

Table II-19. C-DMR identified in the promoter compared between pulp and skin.

1352 hyper and 2632 hypo DMR indetified between skin and pulp at F6 stage, corresponding to 1455 and 2809 genes. Similarly, 1119 and 2895 hyper and hypo DMR were identified between skin and pulp at V,corresponding to 1217 and 3029 genes,respectively.Results indicated that 2 and 2.6 fold hyper DMRs than hypo DMRs were identified between skin and pulp at F6 and V3 stages,respectively.Compared skin to pulp at two stages, more hypo DMRs than hyper DMRs were found which suggested higher methylation level in pulp than skin.

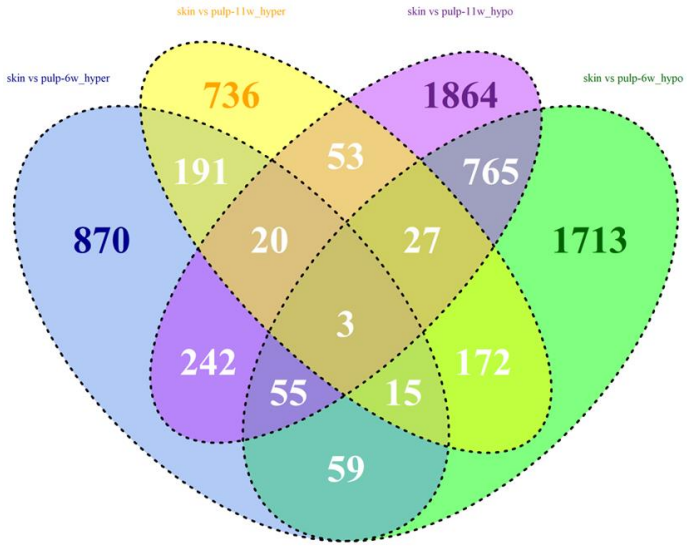

Figure II-35. Vennplot displaying the number of common and specific C-DMR located in the promoter between pulp VS skin.

Chapter II References

Agius, F., Kapoor, A., & Zhu, J.-K. (2006). Role of the Arabidopsis DNA glycosylase/lyase ROS1 in active DNA demethylation. *Proceedings of the National Academy of Sciences*, *103*(31), 11796–11801. https://doi.org/10.1073/pnas.0603563103

Agius, Fernanda, González-Lamothe, R., Caballero, J. L., Muñoz-Blanco, J., Botella, M. A., & Valpuesta, V. (2003). Engineering increased vitamin C levels in plants by overexpression of a D-galacturonic acid reductase. *Nature Biotechnology*, *21*(2), 177–181. https://doi.org/10.1038/nbt777

Akalin, A., Kormaksson, M., Li, S., Garrett-Bakelman, F. E., Figueroa, M. E., Melnick, A., & Mason, C. E. (2012). MethylKit: a comprehensive R package for the analysis of genome-wide DNA methylation profiles. *Genome Biology*, *13*(10), R87. https://doi.org/10.1186/gb-2012-13-10-R87

Aschan, G., & Pfanz, H. (2003). Flora Review Non-foliar photosynthesis – a strategy of additional carbon acquisition, 81–97.

Bapat, V. A., Trivedi, P. K., Ghosh, A., Sane, V. A., Ganapathi, T. R., & Nath, P. (2010). Ripening of fleshy fruit: Molecular insight and the role of ethylene. *Biotechnology Advances*, *28*(1), 94–107. https://doi.org/https://doi.org/10.1016/j.biotechadv.2009.10.002

Berries, G., Dai, Z., Meddar, M., & Delrot, S. (2015). http://www.bio-protocol.org/e1510, *5*(1981), 1–8.

Bogs, J., Jaffe, F. W., Takos, A. M., Walker, A. R., & Robinson, S. P. (2007). The Grapevine Transcription Factor VvMYBPA1 Regulates Proanthocyanidin Synthesis during Fruit Development. *Plant Physiology*, *143*(3), 1347–1361. https://doi.org/10.1104/pp.106.093203

Bolger, A. M., Lohse, M., & Usadel, B. (2014). Genome analysis Trimmomatic : a flexible trimmer for Illumina sequence data, *30*(15), 2114–2120. https://doi.org/10.1093/bioinformatics/btu170

Brueckner, B., Boy, R. G., Siedlecki, P., Musch, T., Kliem, H. C., Zielenkiewicz, P., … Lyko, F. (2005). Epigenetic Reactivation of Tumor Suppressor Genes by a Novel Small-Molecule Inhibitor of Human DNA Methyltransferases, (14), 6305–6312.

Bucher, E., Kong, J., Teyssier, E., & Gallusci, P. (2018). Chapter Ten - Epigenetic Regulations of Fleshy Fruit Development and Ripening and Their Potential Applications to Breeding Strategies. In M. Mirouze, E. Bucher, & P. B. T.-A. in B. R. Gallusci (Eds.), *Plant Epigenetics Coming of Age for Breeding Applications* (Vol. 88, pp. 327–360). Academic Press. https://doi.org/https://doi.org/10.1016/bs.abr.2018.09.015

Callebaut, I., Courvalin, J. C., & Mornon, J. P. (1999). The BAH (bromo-adjacent homology) domain: A link between DNA methylation, replication and transcriptional regulation. *FEBS Letters*, *446*(1), 189–193. https://doi.org/10.1016/S0014-5793(99)00132-5

Canaguier, A., Grimplet, J., Di Gaspero, G., Scalabrin, S., Duchêne, E., Choisne, N., … Adam-Blondon, A.-F. (2017a). A new version of the grapevine reference genome assembly (12X.v2) and of its annotation (VCost.v3). *Genomics Data*, *14*(September), 56–62. https://doi.org/10.1016/j.gdata.2017.09.002

Canaguier, A., Grimplet, J., Di Gaspero, G., Scalabrin, S., Duchêne, E., Choisne, N., … Adam-Blondon, A.-F. (2017b). A new version of the grapevine reference genome assembly (12X.v2) and of its annotation

(VCost.v3). *Genomics Data*, *14*(September), 56–62. https://doi.org/10.1016/j.gdata.2017.09.002

Cao, X., & Jacobsen, S. E. (2002). Locus-specific control of asymmetric and CpNpG methylation by the DRM and CMT3 methyltransferase genes. *Proceedings of the National Academy of Sciences*, *99*(Supplement 4), 16491–16498. https://doi.org/10.1073/pnas.162371599

Castellarin, S. D., Gambetta, G. A., Wada, H., Krasnow, M. N., Cramer, G. R., Peterlunger, E., … Matthews, M. A. (2016). Characterization of major ripening events during softening in grape: Turgor, sugar accumulation, abscisic acid metabolism, colour development, and their relationship with growth. *Journal of Experimental Botany*, *67*(3), 709–722. https://doi.org/10.1093/jxb/erv483

Cavallini, E., Matus, J. T., Finezzo, L., Zenoni, S., Loyola, R., Guzzo, F., … Tornielli, G. B. (2015). The Phenylpropanoid Pathway Is Controlled at Different Branches by a Set of R2R3-MYB C2 Repressors in Grapevine 1, *167*(April), 1448–1470. https://doi.org/10.1104/pp.114.256172

Cheng, G., Zhou, S., Zhang, J., Huang, X., Bai, X., Xie, T., … Xie, L. (2019). Comparison of transcriptional expression patterns of phenols and carotenoids in 'Kyoho' grapes under a two-crop-a-year cultivation system. *PLoS ONE*, *14*(1), 1–17. https://doi.org/10.1371/journal.pone.0210322

Cheng, J., Niu, Q., Zhang, B., Chen, K., Yang, R., Zhu, J.-K., … Lang, Z. (2018). Downregulation of RdDM during strawberry fruit ripening. *Genome Biology*, *19*(1), 212. https://doi.org/10.1186/s13059-018-1587-x

Chervin, C., El-kereamy, A., Roustan, J., Lamon, J., Bouzayen, M., & Latche, A. (2004). Ethylene seems required for the berry development and ripening in grape , a non-climacteric fruit, *167*, 1301–1305. https://doi.org/10.1016/j.plantsci.2004.06.026

Chervin, C., Tira-Umphon, A., Terrier, N., Zouine, M., Severac, D., & Roustan, J. P. (2008). Stimulation of the grape berry expansion by ethylene and effects on related gene transcripts, over the ripening phase. *Physiologia Plantarum*, *134*(3), 534–546. https://doi.org/10.1111/j.1399-3054.2008.01158.x

Choi, Y., Gehring, M., Johnson, L., Hannon, M., Harada, J. J., Goldberg, R. B., … Fischer, R. L. (2002). DEMETER, a DNA glycosylase domain protein, is required for endosperm gene imprinting and seed viability in Arabidopsis. *Cell*, *110*(1), 33–42. https://doi.org/10.1016/S0092-8674(02)00807-3

Cholet, C., Claverol, S., Claisse, O., Rabot, A., Osowsky, A., Dumot, V., … Gény, L. (2016). Tartaric acid pathways in Vitis vinifera L. (cv. Ugni blanc): A comparative study of two vintages with contrasted climatic conditions. *BMC Plant Biology*, *16*(1), 1–18. https://doi.org/10.1186/s12870-016-0833-1

Cokus, S. J., Feng, S., Zhang, X., Chen, Z., Merriman, B., Haudenschild, C. D., … Jacobsen, S. E. (2008). Shotgun bisulphite sequencing of the Arabidopsis genome reveals DNA methylation patterning. *Nature*, *452*(7184), 215–219. https://doi.org/10.1038/nature06745

Colquhoun, T. A., Kim, J. Y., Wedde, A. E., Levin, L. A., Schmitt, K. C., Schuurink, R. C., & Clark, D. G. (2011). PhMYB4 fine-tunes the floral volatile signature of Petunia×hybrida through PhC4H. *Journal of Experimental Botany*, *62*(3), 1133–1143. https://doi.org/10.1093/jxb/erq342

Conde, C., Paulo Silva, B., Natacha Fontes, B., Alberto P Dias, B. C., Rui Tavares, B. M., Maria Sousa, B. J., … Hernâni Gerós, B. (2007). Biochemical Changes throughout Grape Berry Development and Fruit and Wine Quality.

Conesa, A., Madrigal, P., Tarazona, S., Gomez-cabrero, D., Cervera, A., Mcpherson, A., … Zhang, X. (2016). A survey of best practices for RNA-seq data analysis, 1–19. https://doi.org/10.1186/s13059-016-0881-8

Conn, S., Curtin, C., Bézier, A., Franco, C., & Zhang, W. (2008). Purification, molecular cloning, and characterization of glutathione S-transferases (GSTs) from pigmented Vitis vinifera L. cell suspension cultures as putative anthocyanin transport proteins. *Journal of Experimental Botany*, *59*(13), 3621–3634. https://doi.org/10.1093/jxb/ern217

Coombe, B. G. (1987). Distribution of Solutes within the Developing Grape Berry in Relation to Its Morphology , Iii. *American Journal of Enology and Viticulture*, *38*(2), 120–126.

Coombe, B. G. (1995). Adoption of a system for identifying grapevine growth stages, (1994), 104–110.

Coombe, B. G., & Mccarthy, M. G. (n.d.). Dynamics of grape berry growth and physiology of ripening, 131–135.

D.Y., X., S.B., S., N.L., P., D., F., & R.A., D. (2003). Role of anthocyanidin reductase, encoded by BANYULS in plant flavonoid biosynthesis. *Science*, *299*(January), 396–399.

Dai, Z. W., Ollat, N., Gomès, E., Decroocq, S., Tandonnet, J. P., Bordenave, L., … Delrot, S. (2011). Ecophysiological, genetic, and molecular causes of variation in grape berry weight and composition: A review. *American Journal of Enology and Viticulture*, *62*(4), 413–425. https://doi.org/10.5344/ajev.2011.10116

de Vetten, N., ter Horst, J., van Schaik, H.-P., de Boer, A., Mol, J., & Koes, R. (2002). A cytochrome b5 is required for full activity of flavonoid 3',5'-hydroxylase, a cytochrome P450 involved in the formation of blue flower colors. *Proceedings of the National Academy of Sciences*, *96*(2), 778–783. https://doi.org/10.1073/pnas.96.2.778

DeBolt, S., Cook, D. R., & Ford, C. M. (2006). L-Tartaric acid synthesis from vitamin C in higher plants. *Proceedings of the National Academy of Sciences*, *103*(14), 5608–5613. https://doi.org/10.1073/pnas.0510864103

Deluc, L., Bogs, J., Walker, A. R., Ferrier, T., Decendit, A., Merillon, J., & Robinson, S. P. (2008). The Transcription Factor VvMYB5b Contributes to the Regulation of Anthocyanin and Proanthocyanidin Biosynthesis in Developing Grape Berries 1 , 2 [W], *147*(August), 2041–2053. https://doi.org/10.1104/pp.108.118919

Deluc, L. G., Grimplet, J., Wheatley, M. D., Tillett, R. L., Quilici, D. R., Osborne, C., … Cramer, G. R. (2007a). Transcriptomic and metabolite analyses of Cabernet Sauvignon grape berry development. *BMC Genomics*, *8*, 429. https://doi.org/10.1186/1471-2164-8-429

Destrac-irvine, A., & Leeuwen, C. Van. (n.d.). in order to optimize the use of genetic diversity within the Vitis vinifera species as a tool for adaptation to a changing environment, 165–171.

El-Sharkawy, I., Liang, D., & Xu, K. (2015). Transcriptome analysis of an apple (Malus × domestica) yellow fruit somatic mutation identifies a gene network module highly associated with anthocyanin and epigenetic regulation. *Journal of Experimental Botany*, *66*(22), 7359–7376. https://doi.org/10.1093/jxb/erv433

Falginella, L., Castellarin, S. D., Testolin, R., Gambetta, G. A., Morgante, M., & Gaspero, G. Di. (2010). Expansion and subfunctionalisation of flavonoid 3 ' , 5 ' -hydroxylases in the grapevine lineage. *BMC Genomics*, *11*(1), 562. https://doi.org/10.1186/1471-2164-11-562

Fang, M. Z., Wang, Y., Ai, N., Hou, Z., Sun, Y., Lu, H., … Yang, C. S. (2003). Tea polyphenol (-)-epigallocatechin-3-gallate inhibits DNA methyltransferase and reactivates methylation-silenced genes in cancer cell lines. *Cancer Research*, *63*(22), 7563–7570. Retrieved from http://www.ncbi.nlm.nih.gov/pubmed/14633667

Fasoli, M., Dal Santo, S., Zenoni, S., Tornielli, G. B., Farina, L., Zamboni, A., … Pezzotti, M. (2012). The Grapevine Expression Atlas Reveals a Deep Transcriptome Shift Driving the Entire Plant into a Maturation Program. *The Plant Cell*, *24*(9), 3489–3505. https://doi.org/10.1105/tpc.112.100230

Fasoli, Marianna, Richter, C. L., Zenoni, S., Bertini, E., Vitulo, N., Dal Santo, S., … Tornielli, G. B. (2018). Timing and Order of the Molecular Events Marking the Onset of Berry Ripening in Grapevine. *Plant Physiology*, *178*(3), 1187–1206. https://doi.org/10.1104/pp.18.00559

Ferrer, J. L., Jez, J. M., Bowman, M. E., Dixon, R. A., & Noel, J. P. (1999). Structure of chalcone synthase and the molecular basis of plant polyketide biosynthesis. *Nature Structural Biology*, *6*(8), 775–784. https://doi.org/10.1038/11553

Ford, C. M., Boss, P. K., & Hæj, P. B. (1998). Cloning and characterization of Vitis vinifera UDP-glucose. Flavonoid 3- O-Glucosyltransferase, a homologue of the enzyme encoded by the maize Bronze- 1 locus that may primarily serve to glucosylate anthocyanidins in vivo. *Journal of Biological Chemistry*, *273*(15), 9224–9233. https://doi.org/10.1074/jbc.273.15.9224

Fortes, A. M., Teixeira, R. T., & Agudelo-romero, P. (2015). Complex Interplay of Hormonal Signals during Grape Berry Ripening, 9326–9343. https://doi.org/10.3390/molecules20059326

Fournier-level, A., Hugueney, P., Verriès, C., This, P., & Ageorges, A. (2011). Genetic mechanisms underlying the methylation level of anthocyanins in grape (Vitis vinifera L .). *BMC Plant Biology*, *11*(1), 179. https://doi.org/10.1186/1471-2229-11-179

Francisco, R. M., Regalado, A., Ageorges, A., Burla, B. J., Bassin, B., Eisenach, C., … Nagy, R. (2013). ABCC1, an ATP Binding Cassette Protein from Grape Berry, Transports Anthocyanidin 3- O -Glucosides . *The Plant Cell*, *25*(5), 1840–1854. https://doi.org/10.1105/tpc.112.102152

Fujita, A., Goto-Yamamoto, N., Aramaki, I., & Hashizume, K. (2006). Organ-specific transcription of putative flavonol synthase genes of grapevine and effects of plant hormones and shading on flavonol biosynthesis in grape berry skins. *Bioscience, Biotechnology, and Biochemistry*, *70*(3), 632–638. Retrieved from http://www.ncbi.nlm.nih.gov/pubmed/16556978

Gallusci, P., Hodgman, C., Teyssier, E., & Seymour, G. B. (2016). DNA Methylation and Chromatin Regulation during Fleshy Fruit Development and Ripening. *Frontiers in Plant Science*, *7*(June), 1–14. https://doi.org/10.3389/fpls.2016.00807

Gambetta, G. A., Matthews, M. A., Shaghasi, T. H., McElrone, A. J., & Castellarin, S. D. (2010). Sugar and abscisic acid signaling orthologs are activated at the onset of ripening in grape. *Planta*, *232*(1), 219–234. https://doi.org/10.1007/s00425-010-1165-2

Gapper, N. E., Giovannoni, J. J., & Watkins, C. B. (2014). Understanding development and ripening of fruit

crops in an “omics” era. *Horticulture Research*, *1*, 14034. https://doi.org/10.1038/hortres.2014.34

Gehring, M., Huh, J. H., Hsieh, T. F., Penterman, J., Choi, Y., Harada, J. J., … Fischer, R. L. (2006). DEMETER DNA glycosylase establishes MEDEA polycomb gene self-imprinting by allele-specific demethylation. *Cell*, *124*(3), 495–506. https://doi.org/10.1016/j.cell.2005.12.034

Gomez, C., Terrier, N., Torregrosa, L., Vialet, S., … Klein, M. (2009). Grapevine MATE-Type Proteins Act as Vacuolar, *150*(May), 402–415. https://doi.org/10.1104/pp.109.135624

Gong, Z., Morales-Ruiz, T., Ariza, R. R., Roldán-Arjona, T., David, L., & Zhu, J. K. (2002). ROS1, a repressor of transcriptional gene silencing in Arabidopsis, encodes a DNA glycosylase/lyase. *Cell*, *111*(6), 803–814. https://doi.org/10.1016/S0092-8674(02)01133-9

Goto-Yamamoto, N., Wan, G. H., & Kobayashi, S. (2003). Structure and transcription of three chalcone synthase genes of grapevine (Vitis vinifera). *Acta Horticulturae*, *603*, 571–579. https://doi.org/10.17660/ActaHortic.2003.603.76

Grimplet, J., Deluc, L. G., Tillett, R. L., Wheatley, M. D., Schlauch, K. A., Cramer, G. R., & Cushman, J. C. (2007). Tissue-specific mRNA expression profiling in grape berry tissues, *23*, 1–23. https://doi.org/10.1186/1471-2164-8-187

Guan, L., Dai, Z., Wu, B. H., Wu, J., Merlin, I., Hilbert, G., … Delrot, S. (2016). Anthocyanin biosynthesis is differentially regulated by light in the skin and flesh of white-fleshed and teinturier grape berries. *Planta*, *243*(1), 23–41. https://doi.org/10.1007/s00425-015-2391-4

Guillaumie, S., Ilg, A., Rety, S., Brette, M., Trossat-Magnin, C., Decroocq, S., … Gomes, E. (2013). Genetic Analysis of the Biosynthesis of 2-Methoxy-3-Isobutylpyrazine, a Major Grape-Derived Aroma Compound Impacting Wine Quality. *Plant Physiology*, *162*(2), 604–615. https://doi.org/10.1104/pp.113.218313

Guillaumie, Sabine, Fouquet, R., Kappel, C., Camps, C., Terrier, N., Moncomble, D., … Delrot, S. (2011). Transcriptional analysis of late ripening stages of grapevine berry. *BMC Plant Biology*, *11*(1), 165. https://doi.org/10.1186/1471-2229-11-165

Harris, N. N., Luczo, J. M., Robinson, S. P., & Walker, A. R. (2013). Transcriptional regulation of the three grapevine chalcone synthase genes and their role in flavonoid synthesis in Shiraz. *Australian Journal of Grape and Wine Research*, *19*(2), 221–229. https://doi.org/10.1111/ajgw.12026

Hichri, I., Heppel, S. C., Pillet, J., Léon, C., Czemmel, S., Delrot, S., … Bogs, J. (2010). The basic helix-loop-helix transcription factor MYC1 is involved in the regulation of the flavonoid biosynthesis pathway in grapevine. *Molecular Plant*, *3*(3), 509–523. https://doi.org/10.1093/mp/ssp118

Hoballah, M. E., Gubitz, T., Stuurman, J., Broger, L., Barone, M., Mandel, T., … Kuhlemeier, C. (2007). Single Gene-Mediated Shift in Pollinator Attraction in Petunia. *The Plant Cell Online*, *19*(3), 779–790. https://doi.org/10.1105/tpc.106.048694

Holton_et_al-1993-The_Plant_Journal (1).pdf. (n.d.).

Hugueney, P., Provenzano, S., Verries, C., Ferrandino, A., Meudec, E., Batelli, G., … Ageorges, A. (2009). A Novel Cation-Dependent O-Methyltransferase Involved in Anthocyanin Methylation in Grapevine. *Plant Physiology*, *150*(4), 2057–2070. https://doi.org/10.1104/pp.109.140376

Iwashina, T. (2006). The Structure and Distribution of the Flavonoids in Plants. *Journal of Plant Research*, *113*(3), 287–299. https://doi.org/10.1007/pl00013940

Izumi, M., Tsunoda, H., Suzuki, Y., Makino, A., & Ishida, H. (2012). RBCS1A and RBCS3B , two major members within the Arabidopsis RBCS multigene family , function to yield sufficient Rubisco content for leaf photosynthetic capacity, *63*(5), 2159–2170. https://doi.org/10.1093/jxb/err434

Jaillon, O., Aury, J.-M., Noel, B., Policriti, A., Clepet, C., Casagrande, A., … French-Italian Public Consortium for Grapevine Genome Characterization. (2007). The grapevine genome sequence suggests ancestral hexaploidization in major angiosperm phyla. *Nature*, *449*(7161), 463–467. https://doi.org/10.1038/nature06148

Jeong, S. T., Goto-Yamamoto, N., Hashizume, K., & Esaka, M. (2006). Expression of the flavonoid 3'-hydroxylase and flavonoid 3',5'-hydroxylase genes and flavonoid composition in grape (Vitis vinifera). *Plant Science*, *170*(1), 61–69. https://doi.org/10.1016/j.plantsci.2005.07.025

Jeong, S. T., Goto-Yamamoto, N., Hashizume, K., & Esaka, M. (2008). Expression of multi-copy flavonoid pathway genes coincides with anthocyanin, flavonol and flavan-3-ol accumulation of grapevine. *Vitis - Journal of Grapevine Research*, *47*(3), 135–140.

Jeong, S. T., Goto-Yamamoto, N., Kobayashi, S., & Esaka, M. (2004). Effects of plant hormones and shading on the accumulation of anthocyanins and the expression of anthocyanin biosynthetic genes in grape berry skins. *Plant Science*, *167*(2), 247–252. https://doi.org/10.1016/j.plantsci.2004.03.021

Jochen Bogs, Mark O.Downey2, John S.Harvey3, Anthony R. Ashton, Gregory J. Tanner, and S. P. R. (2005). Proanthocyanidin Synthesis and Expression of Genes Encoding Leucoanthocyanidin Reductase and Anthocyanidin Reductase in Developing Grape Berries and Grapevine Leaves. *Plant Physiology*, *139*(October), 652–663. https://doi.org/10.1104/pp.105.064238.disease

Kaiser, S., Jurkowski, T. P., Kellner, S., Schneider, D., Jeltsch, A., & Helm, M. (2017). The RNA methyltransferase Dnmt2 methylates DNA in the structural context of a tRNA. *RNA Biology*, *14*(9), 1241–1251. https://doi.org/10.1080/15476286.2016.1236170

Kankel, M. W., Ramsey, D. E., Stokes, T. L., Flowers, S. K., Haag, J. R., Jeddeloh, J. A., … Richards, E. J. (2003). Arabidopsis MET1 cytosine methyltransferase mutants. *Genetics*, *163*(3), 1109–1122.

Kennedy, J. A., Matthews, M. A., & Waterhouse, A. L. (2000). Changes in grape seed polyphenols during fruit ripening, *55*, 77–85.

Kennedy James. (2002). Understanding grape berry development. *Practical Winery & Vineyard*, (August).

Kim, D., Langmead, B., & Salzberg, S. L. (2016). HHS Public Access, *12*(4), 357–360. https://doi.org/10.1038/nmeth.3317.HISAT

Kliewer, W. M. (1967). The glucose-fructose ratio of Vitis Vinifera grapes. *American Journal of Enology and Viticulture*, *18*(1), 33–41. Retrieved from http://www.ajevonline.org/cgi/content/abstract/18/1/33

Kobayashi, S., Goto-Yamamoto, N., & Hirochika, H. (2004a). Retrotransposon-Induced Mutations in Grape Skin Color. *Science*, *304*(5673), 982. https://doi.org/10.1126/science.1095011

Kobayashi, S., Goto-Yamamoto, N., & Hirochika, H. (2004b). Retrotransposon-Induced Mutations in

Grape Skin Color. *Science*, *304*(5673), 982. https://doi.org/10.1126/science.1095011

Koskela, M. M., Dahlström, K. M., Goñi, G., Lehtimäki, N., Nurmi, M., Velazquez-Campoy, A., … Mulo, P. (2018). Arabidopsis FNRL protein is an NADPH-dependent chloroplast oxidoreductase resembling bacterial ferredoxin-NADP+ reductases. *Physiologia Plantarum*, *162*(2), 177–190. https://doi.org/10.1111/ppl.12621

Koyama, K., Sadamatsu, K., & Goto-Yamamoto, N. (2010). Abscisic acid stimulated ripening and gene expression in berry skins of the Cabernet Sauvignon grape. *Functional and Integrative Genomics*, *10*(3), 367–381. https://doi.org/10.1007/s10142-009-0145-8

Lamikanra, O., Inyang, I. D., & Leong, S. (1995). Distribution and Effect of Grape Maturity on Organic Acid Content of Red Muscadine Grapes. *Journal of Agricultural and Food Chemistry*, *43*(12), 3026–3028. https://doi.org/10.1021/jf00060a007

Lang, Z., Wang, Y., Tang, K., Tang, D., Datsenka, T., Cheng, J., … Zhu, J.-K. (2017a). Critical roles of DNA demethylation in the activation of ripening-induced genes and inhibition of ripening-repressed genes in tomato fruit. *Proceedings of the National Academy of Sciences of the United States of America*, *114*(22), E4511–E4519. https://doi.org/10.1073/pnas.1705233114

Lang, Z., Wang, Y., Tang, K., Tang, D., Datsenka, T., Cheng, J., … Zhu, J.-K. (2017b). Critical roles of DNA demethylation in the activation of ripening-induced genes and inhibition of ripening-repressed genes in tomato fruit. *Proceedings of the National Academy of Sciences*, *114*(22), E4511–E4519. https://doi.org/10.1073/pnas.1705233114

Lauvergeat, V., Decendit, A., Richard, T., & Deluc, L. (2006). Characterization of a Grapevine R2R3-MYB Transcription Factor That Regulates the Phenylpropanoid Pathway 1 [W], *140*(February), 499–511. https://doi.org/10.1104/pp.105.067231.ered

Law, J. A., & Jacobsen, S. E. (2010). Establishing, maintaining and modifying DNA methylation patterns in plants and animals. *Nature Reviews Genetics*, *11*(3), 204–220. https://doi.org/10.1038/nrg2719

Law, J. A., & Jacobsen, S. E. (2011). Patterns in Plants and Animals. *Nature Reviews Genetics*, *11*(3), 204–220. https://doi.org/10.1038/nrg2719.Establishing

Lijavetzky, D., Carbonell-Bejerano, P., Grimplet, J., Bravo, G., Flores, P., Fenoll, J., … Martínez-Zapater, J. M. (2012). Berry flesh and skin ripening features in Vitis vinifera as assessed by transcriptional profiling. *PLoS ONE*, *7*(6). https://doi.org/10.1371/journal.pone.0039547

Lindroth, A. M. (2001). Requirement of Chromomethylase 3 for Maintenance of Cpxpg Methylation. *Science*, *292*(5524), 2077–2080. Retrieved from http://www.sciencemag.org/cgi/doi/10.1126/science.1059745%5Cnpapers2://publication/doi/10.1126/science.1059745

Lister, R., O'Malley, R. C., Tonti-Filippini, J., Gregory, B. D., Berry, C. C., Millar, A. H., & Ecker, J. R. (2008). Highly Integrated Single-Base Resolution Maps of the Epigenome in Arabidopsis. *Cell*, *133*(3), 523–536. https://doi.org/10.1016/j.cell.2008.03.029

Liu, R., How-Kit, A., Stammitti, L., Teyssier, E., Rolin, D., Mortain-Bertrand, A., … Gallusci, P. (2015). A DEMETER-like DNA demethylase governs tomato fruit ripening. *Proceedings of the National Academy of Sciences*, *112*(34), 10804–10809. https://doi.org/10.1073/pnas.1503362112

Lücker, J., Martens, S., & Lund, S. T. (2010). Characterization of a Vitis vinifera cv. Cabernet Sauvignon 3',5'-O-methyltransferase showing strong preference for anthocyanins and glycosylated flavonols. *Phytochemistry*, *71*(13), 1474–1484. https://doi.org/10.1016/j.phytochem.2010.05.027

Lyko, F., & Brown, R. (2005). DNA Methyltransferase Inhibitors and the Development, *97*(20). https://doi.org/10.1093/jnci/dji311

Manning, K., Tör, M., Poole, M., Hong, Y., Thompson, A. J., King, G. J., … Seymour, G. B. (2006). A naturally occurring epigenetic mutation in a gene encoding an SBP-box transcription factor inhibits tomato fruit ripening. *Nature Genetics*, *38*(8), 948–952. https://doi.org/10.1038/ng1841

Marques, J., & Cunha, A. (2013). Mapping Grape Berry Photosynthesis by Chlorophyll Fluorescence Imaging : The Effect of Saturating Pulse Intensity in Different Tissues, 579–585. https://doi.org/10.1111/php.12046

Massonnet, M., Fasoli, M., Tornielli, G. B., Altieri, M., Sandri, M., Zuccolotto, P., … Pezzotti, M. (2017). Ripening Transcriptomic Program in Red and White Grapevine Varieties Correlates with Berry Skin Anthocyanin Accumulation. *Plant Physiology*, *174*(4), 2376–2396. https://doi.org/10.1104/pp.17.00311

Mattivi, F., Guzzon, R., Vrhovsek, U., Stefanini, M., & Velasco, R. (2006). Metabolite profiling of grape: Flavonols and anthocyanins. *Journal of Agricultural and Food Chemistry*, *54*(20), 7692–7702. https://doi.org/10.1021/jf061538c

Mazza, G., Fukumoto, L., Delaquis, P., Girard, B., & Ewert, B. (1999). Anthocyanins, phenolics, and color of Cabernet Franc, Merlot, and Pinot Noir wines from British Columbia. *Journal of Agricultural and Food Chemistry*, *47*(10), 4009–4017. https://doi.org/10.1021/jf990449f

Melino, V. J., Soole, K. L., & Ford, C. M. (2009). Ascorbate metabolism and the developmental demand for tartaric and oxalic acids in ripening grape berries. *BMC Plant Biology*, *9*, 1–14. https://doi.org/10.1186/1471-2229-9-145

Michael, I., Huber, W., Anders, S., Love, M. I., Huber, W., & Anders, S. (2014). Moderated estimation of fold change and dispersion for RNA-seq data with DESeq2 Moderated estimation of fold change and dispersion for RNA-seq data with DESeq2. https://doi.org/10.1186/s13059-014-0550-8

Muñoz-Bertomeu, J., Miedes, E., & Lorences, E. P. (2013). Expression of xyloglucan endotransglucosylase/hydrolase (XTH) genes and XET activity in ethylene treated apple and tomato fruits. *Journal of Plant Physiology*, *170*(13), 1194–1201. https://doi.org/10.1016/j.jplph.2013.03.015

Nakayama, T., Suzuki, H., & Nishino, T. (2003). Anthocyanin acyltransferases: Specificities, mechanism, phylogenetics, and applications. *Journal of Molecular Catalysis B: Enzymatic*, *23*(2–6), 117–132. https://doi.org/10.1016/S1381-1177(03)00078-X

Oa, G. B. W., Czemmel, S., Stracke, R., Weisshaar, B., Cordon, N., Harris, N. N., … Germany, S. C. (2009). The Grapevine R2R3-MYB Transcription Factor VvMYBF1 Regulates Flavonol Synthesis in Developing, *151*(November), 1513–1530. https://doi.org/10.1104/pp.109.142059

Ollat, N., and Gaudillère, J. P. (1998). The effect of limiting leaf area during stage I of berry growth on development and composition of berries ofVitis vinifera L. cv. Cabernet Sauvignon. Am. J. Enol. Vitic. 49, 251–258.

Parage, C., Tavares, R., Rety, S., Baltenweck-Guyot, R., Poutaraud, A., Renault, L., … Hugueney, P. (2012). Structural, Functional, and Evolutionary Analysis of the Unusually Large Stilbene Synthase Gene Family in Grapevine. *Plant Physiology*, *160*(3), 1407–1419. https://doi.org/10.1104/pp.112.202705

Phan, T. D., Bo, W., West, G., Lycett, G. W., & Tucker, G. A. (2007). Silencing of the Major Salt-Dependent Isoform of Pectinesterase in Tomato Alters Fruit Softening. *Plant Physiology*, *144*(4), 1960–1967. https://doi.org/10.1104/pp.107.096347

Pilati, S., Bagagli, G., Sonego, P., Moretto, M., Brazzale, D., Castorina, G., … Moser, C. (2017). Abscisic Acid Is a Major Regulator of Grape Berry Ripening Onset: New Insights into ABA Signaling Network. *Frontiers in Plant Science*, *8*(June), 1–16. https://doi.org/10.3389/fpls.2017.01093

Regalado, A., Pierri, C. L., Bitetto, M., Laera, V. L., Pimentel, C., Francisco, R., … Agrimi, G. (2013). Characterization of mitochondrial dicarboxylate/tricarboxylate transporters from grape berries. *Planta*, *237*(3), 693–703. https://doi.org/10.1007/s00425-012-1786-8

Reid, K. E., Olsson, N., Schlosser, J., Peng, F., & Lund, S. T. (2006). An optimized grapevine RNA isolation procedure and statistical determination of reference genes for real-time RT-PCR during berry development. *BMC Plant Biology*, *6*, 1–11. https://doi.org/10.1186/1471-2229-6-27

Rinaldo, A., Cavallini, E., Jia, Y., Moss, S. M. A., McDavid, D. A. J., Hooper, L. C., … Walker, A. R. (2015). A grapevine anthocyanin acyltransferase, transcriptionally regulated by VvMYBA, can produce most acylated anthocyanins present in grape skins. *Plant Physiology*, *169*(November), pp.01255.2015. https://doi.org/10.1104/pp.15.01255

Robinson, S. P., Davies, C., Industry, C. P., Box, P. O., & Osmond, G. (1992). Molecular biology of grape berry ripening, (Coombe).

Salvatierra, A., Pimentel, P., Moya-Leon, M. A., Caligari, P. D. S., & Herrera, R. (2010). Comparison of transcriptional profiles of flavonoid genes and anthocyanin contents during fruit development of two botanical forms of Fragaria chiloensis ssp. chiloensis. *Phytochemistry*, *71*(16), 1839–1847. https://doi.org/10.1016/j.phytochem.2010.08.005

Santi, D. V, Norment, A., & Garrett, C. E. (1984). Covalent bond formation between a DNA-cytosine methyltransferase and DNA containing 5-azacytosine. *Proceedings of the National Academy of Sciences of the United States of America*, *81*(22), 6993–6997. Retrieved from http://www.ncbi.nlm.nih.gov/pubmed/6209710%0Ahttp://www.pubmedcentral.nih.gov/articlerender.fcgi?artid=PMC392062

Santo, S. D., Vannozzi, A., Tornielli, G. B., Fasoli, M., Venturini, L., Pezzotti, M., & Zenoni, S. (2013). Genome-Wide Analysis of the Expansin Gene Superfamily Reveals Grapevine-Specific Structural and Functional Characteristics, *8*(4). https://doi.org/10.1371/journal.pone.0062206

Shulaev, V., Sargent, D. J., Crowhurst, R. N., Mockler, T. C., Folkerts, O., Delcher, A. L., … Folta, K. M. (2011). The genome of woodland strawberry (Fragaria vesca). *Nature Genetics*, *43*(2), 109–116. https://doi.org/10.1038/ng.740

Smith, S., Watson, C. F., Birdt, C. R., & Morris, C. (1988). No Title, (July), 4–6.

Sparvoli, F., Martin, C., Scienza, A., Gavazzi, G., Tonelli, C., & Celoria, V. (1994). (Vitis vinifera, *75969*, 743–755.

Stommel, J. R., & Dumm, J. M. (2019). Coordinated Regulation of Biosynthetic and Regulatory Genes Coincides with Anthocyanin Accumulation in Developing Eggplant Fruit. *Journal of the American Society for Horticultural Science*, *140*(2), 129–135. https://doi.org/10.21273/jashs.140.2.129

Stroud, H., Do, T., Du, J., Zhong, X., Feng, S., Johnson, L., … Jacobsen, S. E. (2014). Non-CG methylation patterns shape the epigenetic landscape in Arabidopsis. *Nature Structural and Molecular Biology*, *21*(1), 64–72. https://doi.org/10.1038/nsmb.2735

Sun, Y., Li, H., & Huang, J. R. (2012). Arabidopsis TT19 functions as a carrier to transport anthocyanin from the cytosol to tonoplasts. *Molecular Plant*, *5*(2), 387–400. https://doi.org/10.1093/mp/ssr110

Sweetman, C., Deluc, L. G., Cramer, G. R., Ford, C. M., & Soole, K. L. (2009). Regulation of malate metabolism in grape berry and other developing fruits. *Phytochemistry*, *70*(11–12), 1329–1344. https://doi.org/10.1016/j.phytochem.2009.08.006

Sweetman, C., Wong, D. C. J., Ford, C. M., & Drew, D. P. (2012). Transcriptome analysis at four developmental stages of grape berry (Vitis vinifera cv. Shiraz) provides insights into regulated and coordinated gene expression. *BMC Genomics*, *13*(1), 1. https://doi.org/10.1186/1471-2164-13-691

Tenaillon, M. I., Hufford, M. B., Gaut, B. S., & Ross-Ibarra, J. (2011). Genome size and transposable element content as determined by high-throughput sequencing in maize and Zea luxurians. *Genome Biology and Evolution*, *3*(1), 219–229. https://doi.org/10.1093/gbe/evr008

Terrier, N., Glissant, D., Grimplet, J., Barrieu, F., Abbal, P., Couture, C., … Hamdi, S. (2005). Isogene specific oligo arrays reveal multifaceted changes in gene expression during grape berry (Vitis vinifera L.) development. *Planta*, *222*(5), 832–847. https://doi.org/10.1007/s00425-005-0017-y

Teyssier, E., Bernacchia, G., Maury, S., How Kit, A., Stammitti-Bert, L., Rolin, D., & Gallusci, P. (2008). Tissue dependent variations of DNA methylation and endoreduplication levels during tomato fruit development and ripening. *Planta*, *228*(3), 391–399. https://doi.org/10.1007/s00425-008-0743-z

Uluisik, S., Chapman, N. H., Smith, R., Poole, M., Adams, G., Gillis, R. B., … Seymour, G. B. (2016). Genetic improvement of tomato by targeted control of fruit softening. *Nature Biotechnology*, *34*(9), 950–952. https://doi.org/10.1038/nbt.3602

Usadel, B. (2005). Extension of the Visualization Tool MapMan to Allow Statistical Analysis of Arrays, Display of Coresponding Genes, and Comparison with Known Responses. *Plant Physiology*, *138*(3), 1195–1204. https://doi.org/10.1104/pp.105.060459

Waters, D. L. E., Holton, T. A., Ablett, E. M., Lee, L. S., & Henry, R. J. (2005). cDNA microarray analysis of developing grape (Vitis vinifera cv . Shiraz) berry skin, 40–58. https://doi.org/10.1007/s10142-004-0124-z

Whelan, J. A., Russell, N. B., & Whelan, M. A. (2003). Recombinant Technology A method for the absolute quantification of cDNA using real-time PCR, *278*, 261–269. https://doi.org/10.1016/S0022-1759(03)00223-0

Wong, D. C. J., Schlechter, R., Vannozzi, A., Höll, J., Hmmam, I., Bogs, J., … Matus, J. T. (2016). A systems-oriented analysis of the grapevine R2R3-MYB transcription factor family uncovers new insights into the regulation of stilbene accumulation. *DNA Research*, *23*(5), 451–466. https://doi.org/10.1093/dnares/dsw028

Woodward, G., Kroon, P., Cassidy, A., & Kay, C. (2009). Anthocyanin stability and recovery: Implications for the analysis of clinical and experimental samples. *Journal of Agricultural and Food Chemistry*, *57*(12), 5271–5278. https://doi.org/10.1021/jf900602b

WuDai, Z., Meddar, M., Renaud, C., Merlin, I., Hilbert, G., Delro, S., & Gomès, E. (2014). Long-term in vitro culture of grape berries and its application to assess the effects of sugar supply on anthocyanin accumulation. *Journal of Experimental Botany*, *65*(16), 4665–4677. https://doi.org/10.1093/jxb/ert489

Xi, Y., & Li, W. (2009). BSMAP: Whole genome bisulfite sequence MAPping program. *BMC Bioinformatics*, *10*(May). https://doi.org/10.1186/1471-2105-10-232

Xia, E., He, X., Li, H., Wu, S., Li, S., & Deng, G. (2013). Biological Activities of Polyphenols from Grapes. *Polyphenols in Human Health and Disease*, *1*, 47–58. https://doi.org/10.1016/B978-0-12-398456-2.00005-0

Xu, J., Wang, X., Cao, H., Xu, H., Xu, Q., & Deng, X. (2017). Dynamic changes in methylome and transcriptome patterns in response to methyltransferase inhibitor 5-azacytidine treatment in citrus. *DNA Research*, *24*(5), 509–522. https://doi.org/10.1093/dnares/dsx021

Xu, Q., Chen, L. L., Ruan, X., Chen, D., Zhu, A., Chen, C., … Ruan, Y. (2013). The draft genome of sweet orange (Citrus sinensis). *Nature Genetics*, *45*(1), 59–66. https://doi.org/10.1038/ng.2472

Yokotani, N., Nakano, R., Imanishi, S., Nagata, M., Inaba, A., & Kubo, Y. (2009). Ripening-associated ethylene biosynthesis in tomato fruit is autocatalytically and developmentally regulated. *Journal of Experimental Botany*, *60*(12), 3433–3442. https://doi.org/10.1093/jxb/erp185

Zemach, A., Kim, M. Y., Hsieh, P. H., Coleman-Derr, D., Eshed-Williams, L., Thao, K., … Zilberman, D. (2013). The arabidopsis nucleosome remodeler DDM1 allows DNA methyltransferases to access H1-containing heterochromatin. *Cell*, *153*(1), 193–205. https://doi.org/10.1016/j.cell.2013.02.033

Zhong, S., Fei, Z., Chen, Y. R., Zheng, Y., Huang, M., Vrebalov, J., … Giovannoni, J. J. (2013a). Single-base resolution methylomes of tomato fruit development reveal epigenome modifications associated with ripening. *Nature Biotechnology*, *31*(2), 154–159. https://doi.org/10.1038/nbt.2462

Zhong, S., Fei, Z., Chen, Y. R., Zheng, Y., Huang, M., Vrebalov, J., … Giovannoni, J. J. (2013b). Single-base resolution methylomes of tomato fruit development reveal epigenome modifications associated with ripening. *Nature Biotechnology*, *31*(2), 154–159. https://doi.org/10.1038/nbt.2462

Zhong, X., Du, J., Hale, C. J., Gallego-bartolome, J., Feng, S., Vashisht, A. A., … Jacobsen, S. E. (2014). Molecular Mechanism of Action of Plant DRM De Novo DNA Methyltransferases. *Cell*, *157*(5), 1050–1060. https://doi.org/10.1016/j.cell.2014.03.056

Zhou, L., Cheng, X., Connolly, B. A., Dickman, M. J., Hurd, P. J., Hornby, D. P., … Bank, W. (2002). Zebularine : A Novel DNA Methylation Inhibitor that Forms a Covalent Complex with DNA Methyltransferases, *2836*(02), 591–599. https://doi.org/10.1016/S0022-2836(02)00676-9

CHAPTER III

Zebularine, a DNA methyltransferase inhibitor, impacts the biosynthesis of anthocyanins in grape cells culture.

Abstract

Anthocyanins are flavonoid compounds responsible for the color of many flowers and fruits including red grape berries. Their biosynthesis in grape has drawn much attention, because anthocyanins play an important role in red wine color and quality. Their biosynthesis is regulated by many nutritional, developmental and environmental factors including sugars, abscisic acid, temperature and light, and a complex network involving several transcription factors and regulatory proteins is being progressively deciphered. In particular MYB transcription factors have been shown to play a key role through the control of the expression of the UDP glucose: flavonoid-3-O-glucosyltransferase encoding genes (UFGT), which are critical for anthocyanin biosynthesis. Indeed in different species specific MYB transcription factors are expressed in a correlated manner with anthocyanin accumulation. Interestingly in apple and pear fruits the expression of MYB10, as well as anthocyanin accumulation, were correlated with the DNA methylation status in MYB10 promoter region, suggesting that DNA methylation could play a role in the regulation of anthocyanin biosynthesis. To determine the role of DNA methylation in anthocyanin accumulation in grape, zebularine, a DNA methyltransferase inhibitor, was used to treat cell suspensions (*vitis vinifera L*. cv Gamay teinturier). Anthocyanin accumulation was stimulated by zebularine, the drug inducing an increase in anthocyanin quantities in the light, and eliciting their accumulation in the dark. Accordingly RNA-seq analyses revealed that several genes coding for anthocyanin biosynthetic enzymes were upregulated by zebularine. However, the analysis of DNA methylation by McrBC-PCR revealed that the methylation level was not changed significantly in the promoter region of three anthocyanin-related genes known to be under transcriptional control (UGFT, MYBA1, and MYBA2). This suggests that a decrease in DNA methylation may not be the primary cause for anthocyanin accumulation in response to zebularine. The metabolic and transcriptomic characterization of the Gamay teinturier cells 12 days after sub-culturing revealed that zebularine indeed globally impacts cell physiology. Notably the nutritional status of light grown cells appeared to be deeply modified by zebularine. In addition many stress-related genes were specifically up-regulated by zebularine in the light and in the dark, especially genes linked to genotoxic stress. Therefore the induction of anthocyanin production could be part of a stress response elicited by zebularine.

Introduction

Anthocyanins are flavonoid colored compounds found in the vacuoles of cells from diverse plant tissues. Because they contribute to flower and fruit colors, they are responsible for the attraction of pollinators and herbivores, therefore facilitating pollen and seed dispersal. In addition anthocyanins have been associated with photoprotection and free radical scavenging (Hatier and Gould, 2009). It is also speculated that they contribute to stress tolerance since their synthesis is upregulated in response to many different abiotic stresses including drought, salinity, excess light , sub- or supra-optimal temperatures, and nitrogen and phosphorus deficiency (Chalker-Scott, 1999). However the potential mechanisms underlying anthocyanin function during these stress responses are not clearly established.

In red grapes anthocyanins accumulate in the berries at véraison and throughout the ripening process, primarily in the skin but also in the flesh for a few varieties. Although the grape anthocyanins all correspond to monoglucosides of five anthocyanidins, namely, delphnidin, cyaniding, petunidin, peonidin and malvidin, the proportion between these five structures is cultivar specific, so that grape anthocyanin composition can be used as a cultivar fingerprint (Mattivi et al.,2006; Dimitrovska et al., 2011). Because they are responsible for the grape color and play a key role in wine quality, their synthesis has drawn much attention. It has been characterized in a number of species, revealing very well conserved features. Briefly, anthocyanin biosynthesis is divided into two main parts: phenylalanine is first converted to 4-coumaroyl-CoA through the phenylpropanoid pathway. The flavonoid pathway is then initiated by the coupling of 4-coumaroyl-CoA with malonyl-CoA, leading to the production of flavonols, tannins and anthocyanins. Anthocyanins ultimately derive from the unstable anthocyanidins by glycosylation and eventually acylation (Figure III-1) (Kuhn et al., 2014; Liu et al., 2018). The genes coding for the different biosynthetic enzymes have been identified in grape (review: He et al., 2010), many of them belonging to multigene families specially those corresponding to early steps of the biosynthesis pathway (Kunst et al., 2014). Interestingly gene expression analyses have revealed that the induction or repression of anthocyanin biosynthesis is primarily regulated at the transcriptional level (Kunst et al., 2014, Liu et al., 2018). In particular the expression of UFGT (UDP glucose:flavonoid-3-O-glucosyltransferase), which is responsible for the conversion of anthocyanidins into anthocyanins, was shown to be critical for anthocyanin biosynthesis (Boss 1996). Moreover the relative activity of the two enzymes F3’H (flavonoid 3’-hydroxylase) and F3’5’H (flavonoid 3’,5’-hydroxylase), which determines the proportion of dihydroxylated and trihydroxylated anthocyanins is also under transcriptional regulation (Falginella et al., 2012). A complex network involving different regulatory genes coding for MYB, basic helix-loop-helix (bHLH) and WD40 repeat proteins, has been characterized (review: He et al., 2010). Among the transcription factors, MYBA1 was shown to play a central role, as an inducer of UGFT transcription. Its importance was further supported by the demonstration that MYBA1 loss of function through the insertion of a retrotransposon in its promoter correlates with the loss of pigmentation in the skin of grape white cultivars (Walker et al., 2007).

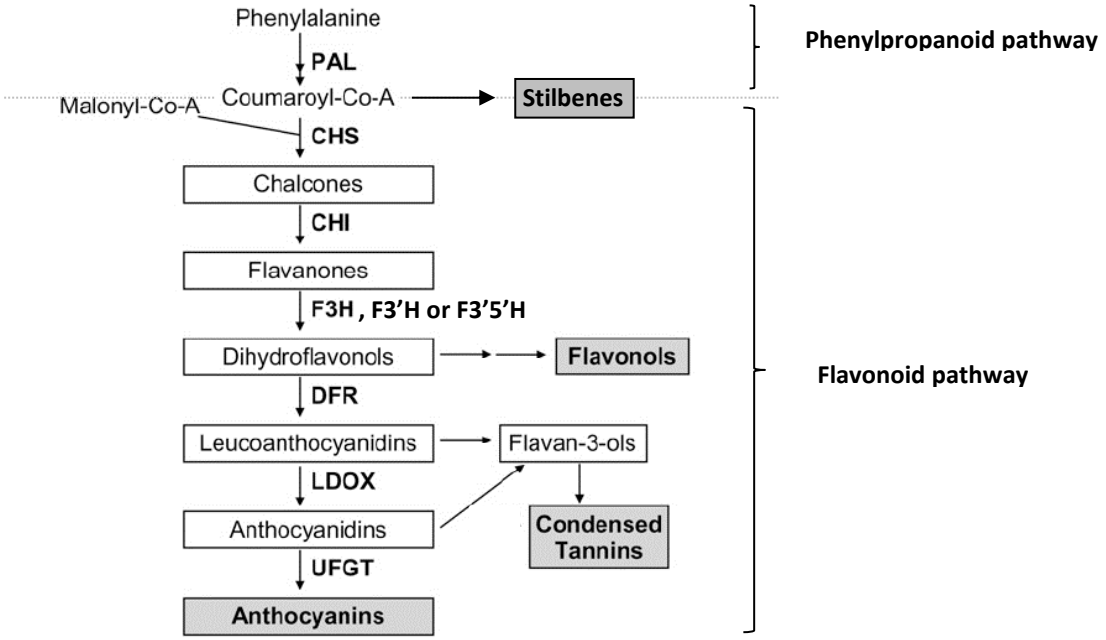

Figure III-1. Simplified anthocyanin biosynthesis pathway. Adapted from Takos et al. Plant physiol 2006. CHS, chalcone synthase; CHI, chalcone isomerase; F3H, flavanone 3-hydroxylase; F3'H, flavonoid 3'-hydroxylase; F3'5'H, flavonoid 3' ,5'-hydroxylase; DFR, dihydroflavonol 4-reductase; LDOX, leucoanthocyanidin dioxygenase; UFGT, UDP glucose : flavonoid-3-0-glucosyltransferase

Different factors regulate anthocyanin production and accumulation. First anthocyanin biosynthesis is determined by the plant genotype, as demonstrated by the genotype dependent anthocyanin composition (Mattivi et al., 2006; Dimitrovska et al., 2011). Moreover, several internal and external factors control anthocyanin accumulation (review: He et al., 2010). Among the internal factors, sugars and ABA play a major role. Indeed anthocyanin accumulation in the grape berry skin occurs in a coordinated manner with an increase in sugar concentration and ABA content during the ripening process (for a review see Agasse 2009), and both compounds were shown to stimulate anthocyanin biosynthesis in different models, such as in vitro intact detached berries or grape cell cultures (Agasse et al., 2009, Gambetta et al., 2010; Gagnéet al., 2011; Dai et al., 2014; Ferrero et al., 2018). Interestingly Dai et al (2014) showed that the sugar-dependent increase in anthocyanin production in detached berries occurs whereas the concentration of its synthesis precursor (phenylalanine) decreases, suggesting that the induction of anthocyanin accumulation by sugars does not correspond to a metabolic effect but to a true signaling process. Indeed the sugar-dependent increase in anthocyanin was correlated with modification in the expression of regulatory and structural genes of the flavonoid biosynthesis pathway together with a genome-wide reprogramming of the transcriptome (Dai et al., 2014). In addition to sugar, ABA also induces anthocyanin production, as it was first demonstrated through the application of exogenous ABA on field grown clusters. Such treatments lead to earlier véraison and increase anthocyanin content in the grape skin (Ban et al., 2003; Jeong et al., 2004; Ferrero et al., 2018) (see also

ref in Gao et al., 2018), concomitantly with the induction of anthocyanin biosynthetic and regulatory genes (Ban et al., 2003; Jeong et al., 2004). The impact of ABA on anthocyanin production was further confirmed by genetic manipulation of grape sensitivity to ABA: transient overexpression of the ABA receptor PYL1 in grape berries enhances the expression of ABA-responsive genes and promotes anthocyanin accumulation (Gao et al., 2018).

Anthocyanin accumulation is not only sensitive to internal factors, but also to external factors, with temperature and light the two major environmental cues known to control anthocyanin quantity and composition (Azuma et al., 2012; Lecourieux et al., 2017). Light positively regulates anthocyanin accumulation in many fruit species, including litchi, apple, Chinese bayberry and grape, as demonstrated by bagging and shading treatments. Light exclusion systematically leads to a strong decrease in total anthocyanin content together with a down regulation of anthocyanin biosynthesis relevant genes (Yong et al., 2011; Feng et al., 2013; Niu et al., 2010). Interestingly the impact of shading on anthocyanin biosynthesis is cultivar dependent (Guan et al., 2016). For instance, light exclusion from fruit set to maturity was associated with a complete lack of anthocyanin in the cultivar jingxiu while the jingyan cultivar still produced a high quantity of anthocyanins. This difference was correlated with a differential impact on UGFT gene expression (Zheng et al., 2013). In addition light exclusion also alters anthocyanin composition, in a cultivar dependent manner (Guan et al., 2016; Downey et al., 2004; Spayd et al., 2002). For instance, in Shiraz shading was shown to induce a decrease in the proportion of delphinidin petunidin and malvidin, while the proportion of peonidin was increased (Downey et al., 2004), whereas in Merlot, it was associated with a decrease in delphinidin and cyanidin proportion and an increase in malvidin proportion (Spayd et al., 2002).

Finally several results suggest that DNA methylation may be involved in the complex regulatory network underlying anthocyanin biosynthesis. In apple and pear, DNA hypermethylation was detected in the promoter of MYB10 in red defective fruits, suggesting that anthocyanin biosynthesis is regulated by DNA methylation via a control on the transcription of MYB10 (El-Sharkawy et al., 2015; Wang et al., 2013). Furthermore variations in DNA methylation were observed during the ripening process in diverse fruits, such as tomato, apple, pear, strawberry, orange, citrus and grape *Vitis amurensis Rupr*(Liu et al., 2015; Lang et al., 2017; Cheng et al., 2018; Huang et al., 2019; Xu et al., 2017; Tyunin et al., 2013). More particularly, in tomato, DNA demethylation was shown to be essential for fruit ripening and carotenoid accumulation (Liu et al., 2015; Lang et al., 2017). On the contrary in citrus cell, the induction of global DNA demethylation by a DNA methyltransferase inhibitor (5-azacytidin) lead to carotenoid degradation (Xu et al., 2017). Altogether these results suggest that DNA methylation plays a role in the control of the biosynthesis of secondary metabolites, in a species dependent manner.

In order to analyze the functional relationship between DNA methylation and anthocyanin biosynthesis in grape, we chose to use a drug known to inhibit DNA methylation, i.e. the zebularine. Indeed for a number of crop species, like grapevine, the production of transgenic plants is still challenging and this chemical approach appears as a useful alternative to the genetic approach which requires the production of mutants or transgenic plants affected in DNA methylation homeostasis. Zebularine (1-(β-d-ribofuranosyl)-1, 2-dihydropyrimidin-2-one) is a nonmethylable nucleoside analog of cytidine, that is incorporated into DNA. The interaction between DNA methyltransferases and zebularine produce a

stable complex. Hence DNA methyltransferases become trapped and inactivated in the form of covalent protein – DNA adducts (Champion et al., 2010). As a result, DNA methyltransferases are rapidly depleted, and genomic DNA becomes demethylated when DNA replication occurs (Pecinka and Liu, 2014). Zebularine treatment causes global genome demethylation, as revealed by whole genome bisulfite sequencing of *Arabidopsis* seedlings grown on zebularine containing media (Griffin et al., 2016; Baubec et al., 2009). Compared to other DNA methyltransferase inhibitors, zebularine is more stable (Pecinka and Liu, 2014) and earlier studies suggested that its toxicity was reduced (J.C. et al., 2003).

To investigate the role of DNA methylation in anthocyanin biosynthesis in grape, we have analyzed the effects of zebularine treatments on Gamay teinturier cells. Indeed plant cell suspension cultures have proven to be good models for the analysis of secondary metabolite production under controlled conditions. In particular, Gamay teinturier cell suspensions are used to gain a better understanding of the regulation of anthocyanin biosynthesis in response to abiotic and biotic factors (Ananga et al., 2013). In this model, zebularine treatments were correlated with an increase in anthocyanin accumulation both in light and dark. Metabolic and gene expression analyses were undertaken in order to decipher this impact of zebularine on the biosynthesis of anthocyanins and more globally on cell physiology. The integration of both data provided comprehensive insights into the DNA methylation regulation of anthocyanin accumulation in grape cell.

Material and Methods

3.2.1 Plant material

Vitis vinifera (L.) cv. “Gamay Fréaux” var. Teinturier (Vitaceae) cell suspensions were established from berries as described previously (Decendit et al., 1996). GT cell suspension culture were initiated from fresh friable call in a modified MS liquid medium (M0221, Duchefa) supplemented with 20g/L sucrose (S0809, Duchefa), 0.25 g/L N-Z-Amine A (C7290,SIGMA), 0.5 mg/L auxin, 0.1 mg/L cytokinin and vitamins (100mg/L myo-inositol, 1.0 mg/L nicotinic acid, 1.0 mg/L pantothenic acid, 0.01 mg/L biotin, 1.0 mg/L pyridoxine HCl, and 1.0 mg/L thiamine HCl), pH 5.8 (Decendit et al., 1996). Cells were sub-cultured in 50 mL of MS liquid medium with a 1/5 (v/v) ratio every 12 days using 250 mL Erlenmeyer flasks and maintained at 25+/-1°C with constant shaking (120 rpm) under continuous fluorescent light (5000 lx) at 24 +/- 1°\u0001C or in dark condition (light off and Erlenmeyer flasks wrapped with aluminum foil). Treatment with the DNA methyltransferase inhibitor zebularine (Selleckchem, S7113) was performed the 3rd day after culture at the end of the lag phase. The MS medium was supplemented with zebularine at a final concentration of 25 µM, 50 µM and 75 µM or with 75 µM DMSO, which was used as a solvent for zebularine. An additional control with water was performed. Cells were harvested the 12th day after inoculation by vacuum filtration, quickly washed twice with MS medium and immediately frozen in liquid nitrogen. Frozen grape cell samples were ground into fine powder in liquid nitrogen and stored at –80°C for further analysis.

3.2.2 Growth curve and Metabolite analyses

Growth curve were established in triplicate for each condition using a final volume of 125ml by measuring the fresh weight (FW) of 10ml samples after vacuum filtration.

3.2.3 Quantification of anthocyanin

Anthocyanins were extracted and analyzed using freeze-dried powders prepared from cell samples, essentially as described in Soubeyrand et al., (2014). Briefly, 20mg of freeze-dried powder were resuspended in 300 µL of methanol (0.1% HCl) to extract anthocyanin before filtering through a 0.2 µM syringe filters, before injecting 3 µL for HPLC analysis. The integrated absorbance at 520 nm was used to determine the concentration of individual anthocyanin expressed as malvidin 3-glucoside equivalents (Extrasynthese, Genay, France) calculated from a calibration function obtained on the commercial standard.

3.2.4 Quantification of stilbenes

Stilbenes extraction was performed from freeze-dried cells (10-20 mg DW) overnight at 4°C with 3 mL MeOH. After centrifugation (5 min) at 3500 rpm, 2 mL of supernatant were recovered and a second extraction was carried out on cells with 3 mL MeOH for 1h30 at room temperature. Tubes were centrifuged as previously (5 min, 3500 rpm) and 3 mL of supernatant were recovered. Cells were extracted a third and final time with 3 mL MeOH (1h30, RT), and 3 mL of supernatant were recovered. The three recovered supernatant were pooled and speed-vacuum evaporated. Dried extract was resuspended in 500 µL MeOH/H2O (50/50, v/v) and filtered (0.45 µm PTFE) before HPLC analysis.
Stilbenes from the culture medium (5 mL) were obtained by a triple ethyl acetate extraction. Extracts were dry-evaporated and resuspended in 1 mL of MeOH/H_2O (50/50, v/v). Analysis of stilbene content was performed by HPLC (Agilent 1100 Series, (Agilent Technologies, Santa Clara, CA, USA), on a 250 x 4 mm Prontosil C18 (5 mm) reverse-phase C18 column (Bischoff Chromatography, Leonberg, Germany) protected by a guard column of the same material. Separation was performed at a flow rate of 1 mL/min with a mobile phase composed of (A) H_2O: TFA 1% (97.5/2.5, v/v) and (B) Acetonitrile: A (80/20, v/v).
The run was set as follows: 0–1 min, 20% (B), 1–8 min, from 20% (B) to 24% (B), 8–10 min, from 24% (B) to 25% (B), 10–13 min, 25% (B), 13–18 min, from 25% (B) to 30% (B), 18–35 min, from 30% (B) to 50% (B), 35–37 min, from 50% (B) to 100% (B), 37–41 min, 100% (B), 41–42 min, from 100% (B) to 20% (B), and 20% (B) for 4 min. The chromatogram was monitored at 286 and 306 nm using a UV-visible-DAD detector (Agilent Technologies, Santa Clara, CA, USA). Stilbene contents were determined from calibration curves of pure standards (injected concentrations ranging from 2 to 500 µg/mL). The linearity of the response of the standard molecules was checked by plotting the peak area versus the concentration of the compounds (Cooperation with Stéphanie Cluzet).

3.2.5 Quantification of sugar and organic acids

Four hundred milligrams of fresh powder prepared from cell samples were extracted at 80 °C with 2 mL of decreasing concentrations of ethanol successively 80%, 50% (v/v) and finally ultrapure water. Supernatants were pooled and evaporated in a Speed-Vac concentrator (Savant Instruments,Inc., Hicksville, NY) before resuspension in 1 mL of ultra-pure water (Millipore, Billerica, MA, USA) and stored at -20°C for subsequent analysis of sugar, organic acid and amino acid. Glucose and fructose were measured enzymatically with an automated micro-plate reader (Elx800UV, Biotek Instruments Inc., Winooski, VT, USA) as described in Gomez et al (2007). Tartaric and malic acids were determined using the autoanalyser TRAACS 800 (Bran & Luebbe, Plaisir, France) as described by (Pereira et al., 2006). Amino acids were determined using HPLC (Waters, Milford, MA,USA) after derivation with 6-aminoquinolyl-N-hydroxysuccinimidylcarbamate (AccQ-Fluor Reagent Kit, Waters), as described in (Pereira et al., 2006) using Waters 2695 HPLC system equipped with a Waters 474 fluorescence detector (Waters, Milford, MA, United States). All the amino acids were identified and quantified with external chemical standards purchased from Sigma (St Louis, MO, USA).

3.2.6 Nucleic acid extraction

Total RNA was isolated as described in (Reid et al., 2006). The quantity of the RNA were determined using a Nanodrop 2000 spectrophotometer (Thermo Scientific), the quality of the RNA was evaluated on 1.2% agarose gels. Total RNA was treated with DNase I (Turbo DNA-freeTM kit, Ambion, Austin, TX, USA) according to manufactures instructions. To control the eventual genomic DNA contamination, PCR was performed using primers of VvEF1.

Genomic DNA was isolated with modified CTAB protocol. The CTAB extraction buffer contain 0,5 M Tris–HCl pH 8, 1.4 M NaCl, 20 mM EDTA, 3% CTAB and 2% Polyvinylpolypyrrolidone(PVPP). Add 1% β-mercaptoethanol in the extraction buffer prior to add into sample powder. Then samples were incubated at 65 °C for 90 minutes, centrifuge 6500 rpm, 4 °C for 15 min, collect the supernatant and wash twice with 1 volume of chloroform/isoamyl alcohol (24:1). The final aqueous layer was add 0.6 volume cold isopropanol and NaAc 3 M pH 5.2 to precipitate out genomic DNA. Total DNA was quantified using a 2000 nanodrop, and the quality was evaluated on 0.8% agarose gels.

3.2.7 McrBC-PCR Analysis

For McrBC-PCR methylation analysis, 1 µg of genomic DNA was digested with McrBC (NEB) for 5h according to manufacturer instructions with or without GTP as a negative control. PCR amplification was performed with 50 ng of genomic DNA with the relevant primers shown in Table III-7, page 175.

3.2.8 RNA-seq analysis

The paired-end reads were cleaned and trimmed with Trimmomatic (Bolger et al., 2014) version 0.38 (with the options PE, LEADING:3, TRAILING:3, SLIDINGWINDOW:4:15 and MINLEN:36). Hisat2 (version 2.2.0)(Kim, Langmead, & Salzberg, 2016) with default parameters was used to align filtered reads to the 12X.2 version of the grapevine reference genome sequence from the French-Italian Public Consortium (PN40024) with the associated structural annotation (VCost.v3) provided by URGI. (https://urgi.versailles.inra.fr/Species/Vitis/Data-Sequences/Genome-sequences). The count matrices were created by importing directly BAM alignments in DESEQ2 (Michael et al., 2014)(R version 3.5.1, DESEQ2 version 1.22.2) as well as the gene models described in the previously used gff file. Reads *per* gene were counted with the summarize Overlaps function with "Union" mode and transformed with the rlog function. Sample-to-sample distances were visualized with PCA plots. Differential gene expression analysis was carried out with the DESeq pipeline with a design formula including tissue, stage and the interaction term tissue: stage. All the contrasts of interest were extracted from the results and only items with an adjusted p-value > 0.05 and a log fold change threshold of 1 were selected for downstream analysis.

Results and discussion

3.3.1 Zebularine treatments lead to modified growth and metabolic status of cells in culture.

Fresh biomass accumulation kinetics were similar in water and DMSO controls irrespective to the light conditions (water or DMSO) and followed a typical sigmoid growth curve with a lag phase that lasts 3 days followed by a rapid increase in cell quantity to reach a plateau at day 10 after sub-culturing. Fresh weight increased from approximately 0.018 g/ml to 0.15 g/ml and remained stable until sub-culturing. Addition of zebularine had a significant effect on FW accumulation kinetics both in the presence and absence of light in a dose dependent manner. Addition of 25, 50 or 75 µM Zeb resulted in a 30, 40 and 46% reduction in FW accumulation, respectively for cells grown in light and in a 34, 45 and 50% reduction for those grown in the dark (Figure III-2A).

Noteworthy, in light conditions, the color intensity of the Zeb treated cells appeared more intense than the one of controls, suggesting a stimulatory effect of the treatment on anthocyanin synthesis (Figure III-2B). Furthermore, in dark conditions Zeb treated cells appeared red whereas controls remained uncolored, indicating that Zeb treatment was sufficient to induce anthocyanin accumulation (Figure III-2C).

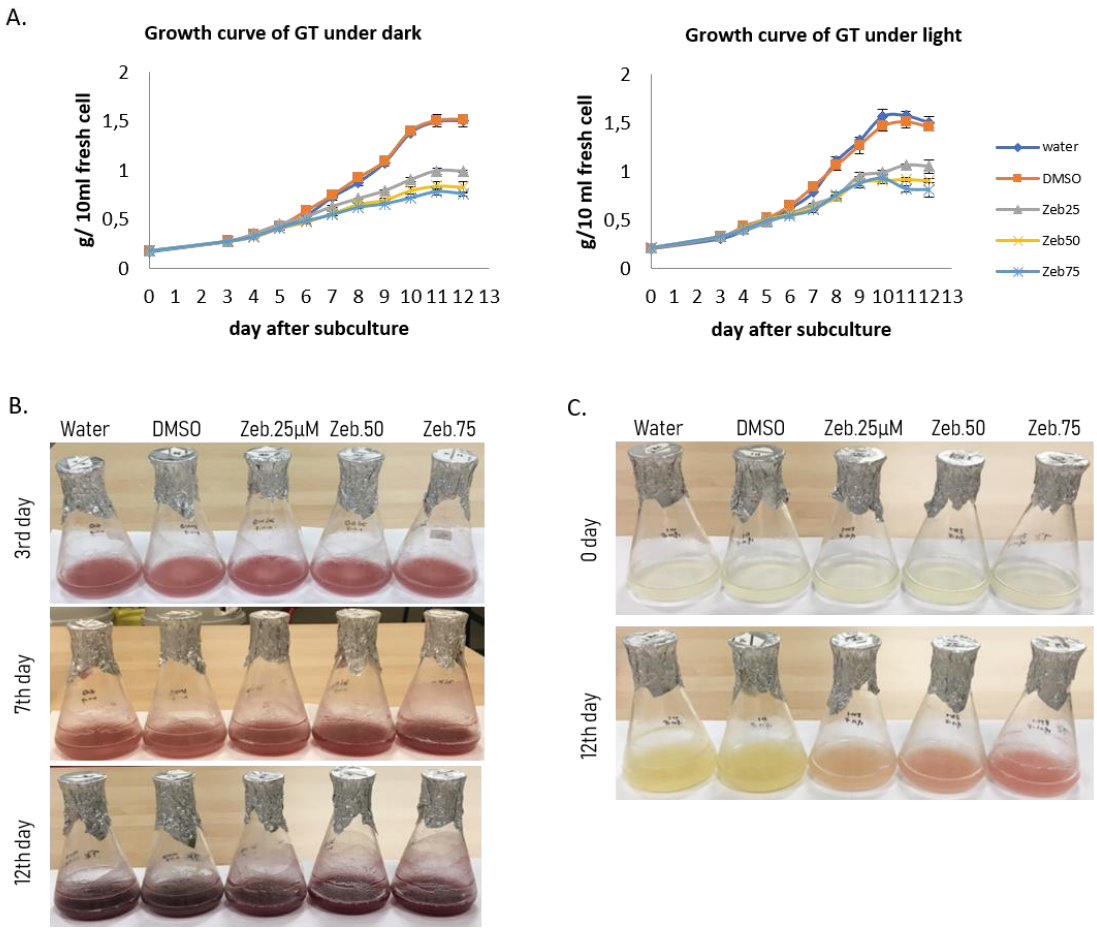

Figure III-2. Zebularine treatments affect GT cell growth and anthocyanin accumulation. (A) Growth curves of GT cell grown under light and dark condition, with or without zebularine treatment. Zebularine was added at the 3rd day after subculturing. Each day, 10 ml of cells were harvested and filtered by vacuum before determination of the corresponding fresh weight. Values are the mean ± SE of three biological replicates. (B) Effect of zebularine on GT cells cultured in light condition. Photo were taken 3,7 and12 days after subculture. (C) Effect of zebularine on GT cells grown under dark. To avoid light exposure, photo were only taken at the first (0 day) and last day (12th day) after subculturing.

3.3.2 Zebularine treatment stimulates anthocyanin accumulation in light conditions and induces their synthesis in dark conditions.

Potential effects of zebularine on anthocyanin accumulation were analyzed in cells in light conditions 12 days after sub-culturing. Water and DMSO control cells accumulate approximately the same amount of total anthocyanins, close to 4.7 mg/g DW. Accumulation of anthocyanins was 130, 155 and 220 % higher than in controls in 25, 50 and 75 µM Zeb treated cells respectively (Figure III-3A). Peonidin is the most abundant anthocyanins identified in water treated cells and represents 76.6% of the total amount of anthocyanins, whereas cyanidin, malvidin, petunidin and delphinidin, count only for 16.9, 4.7, 1.1 and 0.8% respectively.

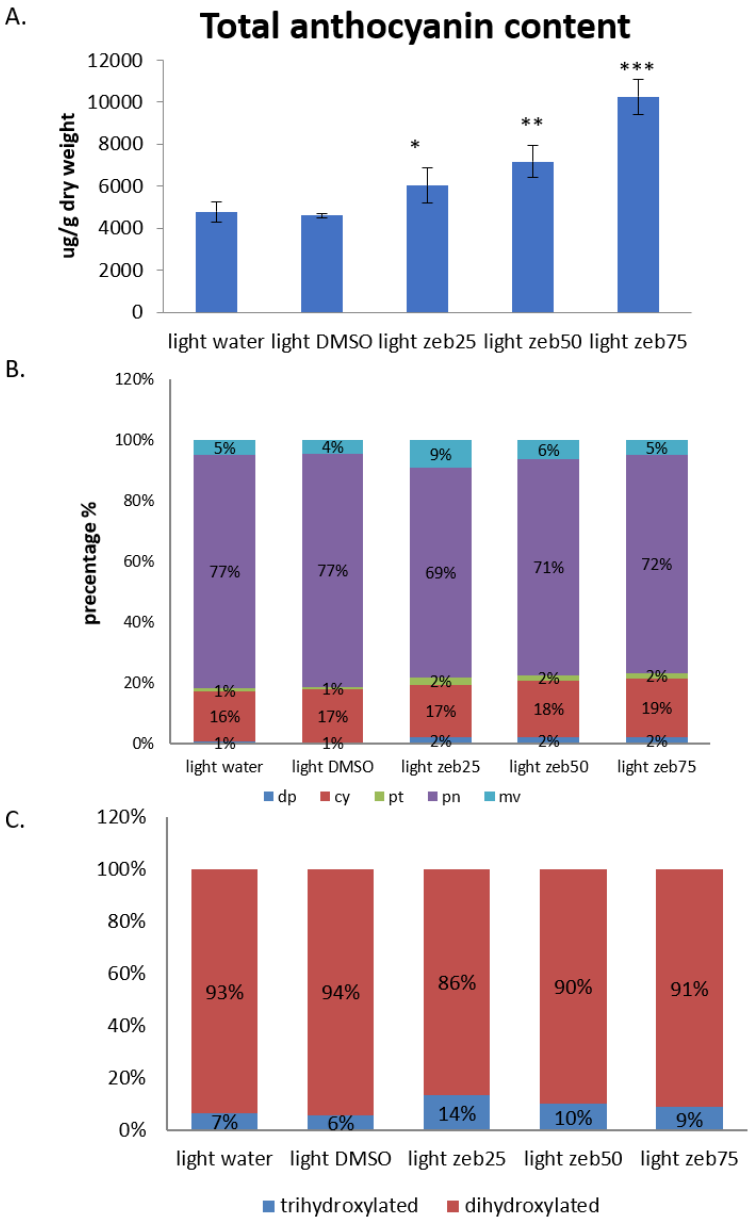

*Figure III-3. The anthocyanin profile of GT cells in response to zebularine. (A) Total anthocyanin content was increased after zebularine treatment of GT cell grown in light condition. Values are the mean ± SE of three biological replicates. Asterisks indicate significant difference, Student's t test (n = 3), *P < 0.05; **P < 0.01; ***P < 0.001. (B) The proportion of the 5 main anthocyanins varies after a treatment with zebularin in GT cell cultured under light. cy, cyanidin; pn, peonidin; de, delphinidin; pt, petunidin; mv, malvidin. (C) The proportion of tri-and di-hydroxylated anthocyanin in GT cell was affected by zebularine in light condition. delphinidin, petunidin and malvidin are trihydroxylated anthocyanins; cyanidin and peonidin belong to dihydroxylated anthocyanins.*

No significant difference was observed between water and DMSO treated cells. In contrast, zebularine treatment impacted the relative proportion of the different anthocyanins: peonidin remained the major compound, but its relative abundance decreased to approximately 71% whereas those of all other molecules increased (Figure III-3B). Concomitantly the proportion of di- and tri-hydroxylated anthocyanins increased from 6% in DMSO treated cell (7% in water treated cells) to 14%, 10% and 9% in 25, 50 and 75 µM zebularine treated cell respectively (Figure III-3C).

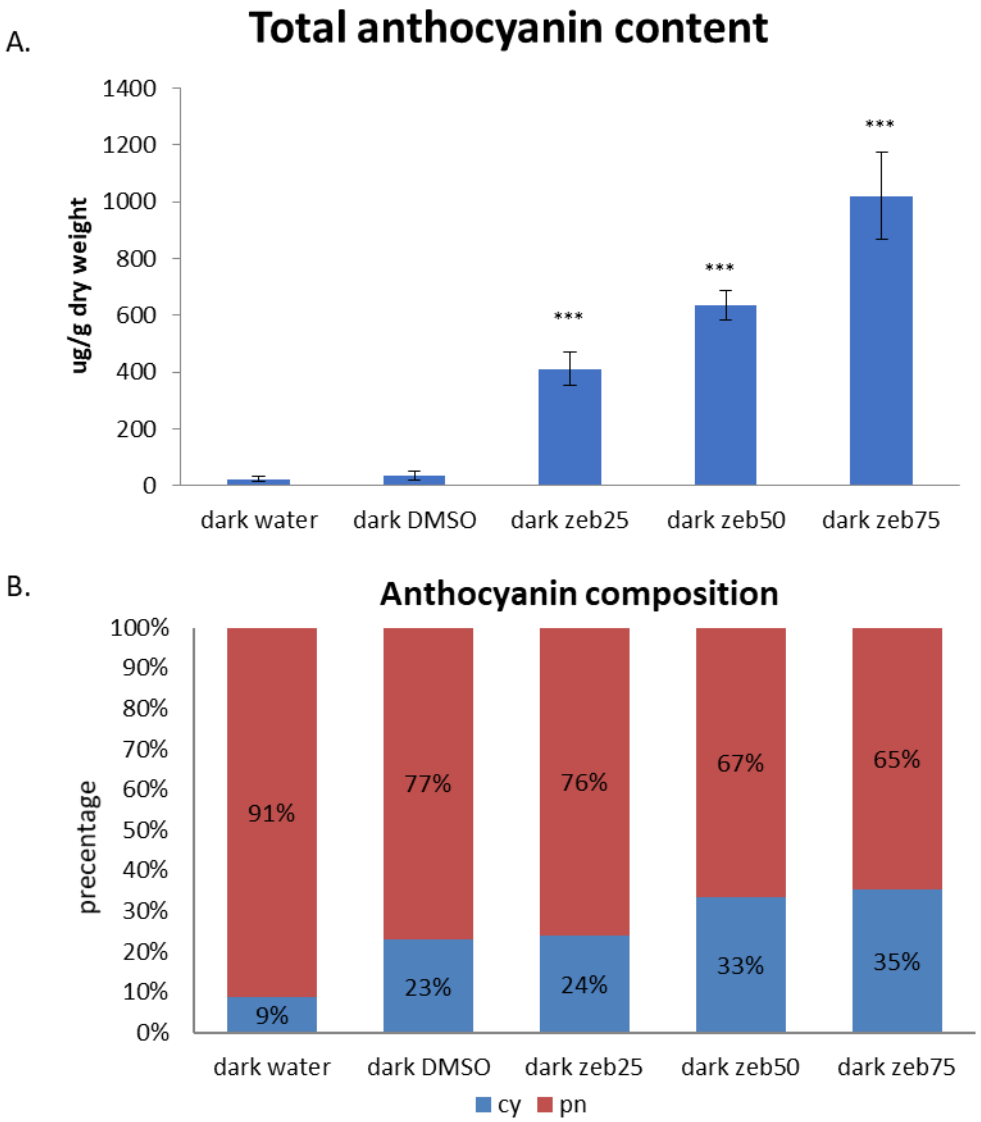

*Figure III-4. The effect of zebularine on the content and composition of anthocyanins for cells grown in dark conditions. (A) zebularine enhances anthocyanin accumulation in dark conditions. Values are the mean ± SE of three biological replicates. Asterisks indicate significant difference, Student's t test (n = 3),*P < 0.05;**P < 0.01; ***P < 0.001. (B) Proportion of 2 anthocyanins in dark condition. cy,cyanidin; pn,peonidin.*

It is well described that GT cells accumulate anthocyanins when cultured in light conditions, but do not in the absence of light (Ananga et al., 2013). In our growing conditions, both water and DMSO treated cells produce traces amount of total anthocyanin (below 40µg/g DW at 12 das, Figure III-4A).

However, zebularine treatments resulted in a dose dependent increase of total anthocyanin accumulation to reach 411.6, 634.9 and 1020 µg/g DW at 12 das in 25, 50 and 75 µM zeb treated samples, respectively. Interestingly, only cyanidin and penoidin and derivatives, the two most abundant compounds produced in light cultured cells were detected in dark grown cells. As a consequence no trihydroxylated compounds were detected in these conditions, suggesting that light is required for their accumulation.

Stilbenes were also analyzed as their synthesis derives from the same precursors as anthocyanins (see Figure III-1: show a scheme of the pathway). Irrespective to the light conditions small amount of stilbenes were found in control cultures that ranged between 200 µg/g DW and 300 µg/g DW both in light and dark conditions (Figure III-5). In both cases zebularine treatment resulted in a moderate increase in the total content of stilbenes in a dose dependent manner, and no significant increase when compared with control. Noteworthy whereas cis-piceid was the most abundant compound in light, the trans-isomer was the major one in dark conditions. As piceid isomerization is a spontaneous reaction that is enhanced by UV light (Julia López-Hernández et al., 2007), this most likely, simply reflects the growing conditions.

Taken together these results indicate that treating cells with a demethylation agent resulted either in an increase or in the induction of anthocyanin accumulation, depending on the light conditions. Similarly stilbene accumulation was enhanced in the presence of zebularine. This suggested a global effect of zebularine on phenolic pathway. We therefore analyzed other metabolic pathway to determine the impact of the treatment on primary metabolites.

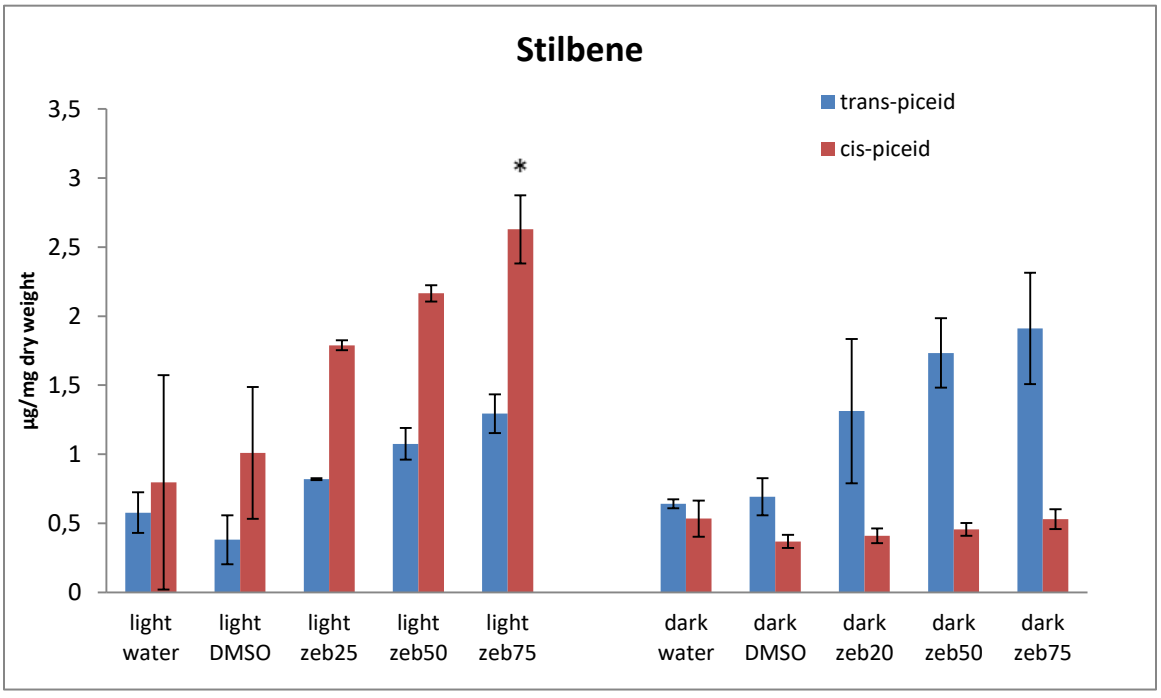

Figure III-5. Accumulation of stilbene in GT cell after zebularine treated. Values are the mean ± SE of three biological replicates.

3.3.3 Zebularine treatments impact the primary metabolite content of cells.

Analysis of hexoses showed that mainly glucose is detected in cells in light conditions to levels ranging between 2 and 3 mg/g FW. Glucose is the most abundant hexose with a ratio Glucose/Fructose of 34 and 23 in water and DMSO treated cells, respectively (Table III-1). The addition of zebularine resulted in an increase of both fructose and glucose. Glucose accumulation increased 4 to 5 fold for all zebularine treated samples used. Fructose content was 12 fold higher in cells treated with 25µM of Zeb than in the DMSO control, and 26 and 31 fold in those treated with 50 and 75 µM of zebularine, consistent with a dose dependent effect in this later case (Figure III-6A). This resulted in a significant change in the Glucose/Fructose ratio that dropped below to values below 10 depending on the zebularine concentration (Table III-1). Analysis of malate and tartrate, the two most abundant organic acids accumulating in grape fruits, showed that malate is the most abundant organic acid found in light conditions (between 0,65 and 0.85 mg/g FW) whereas tartrate remained below 0.1g/g FW. Zebularine treatment resulted in a 2 to 4 fold reduction in malate accumulation in contrast to tartarate that increased 2.5 to 5.4 fold compared to the DMSO control. In both cases effects were dependent on the concentration of zebularine added to the medium (Figure III-6B).

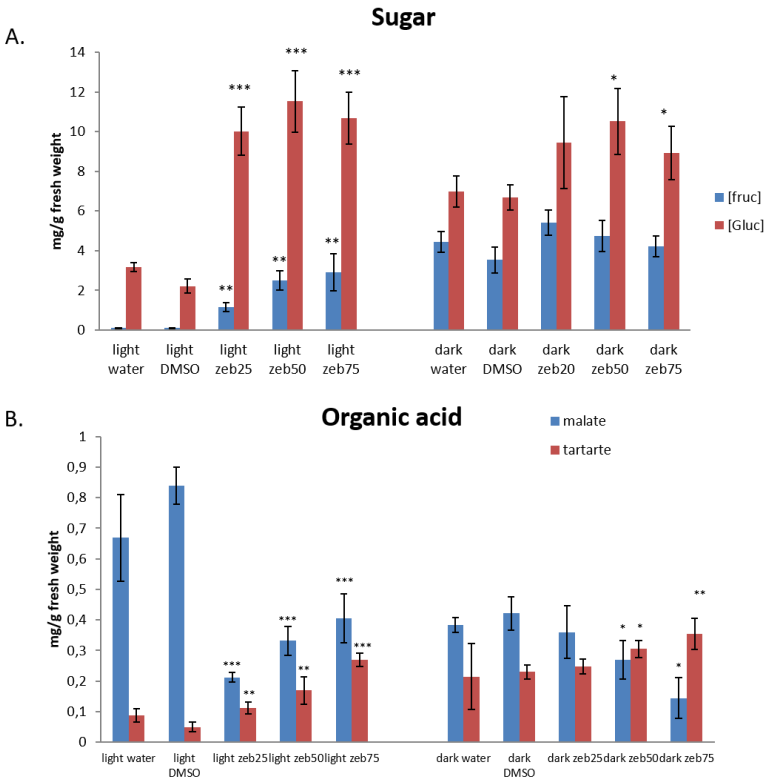

Figure III-6. The effect of zebularine on the accumulation of soluble sugar and organic acid in GT cell. (A) The accumulation of soluble sugar in GT cell after zebularine treatment. (B) The content of organic acid in zebularine- treated GT cell. Values are the mean ± SE of three biological replicates.

Similar analyses performed on dark grown cells indicate that in control conditions the total cell content in hexoses was in average 3 to 4 times higher that in light grown cells with Glucose being only 1.5 to 2-fold more abundant than fructose (Table III-1). Furthermore, zebularine treatment did not generate significant modification of fructose and only limited effects on glucose contents. Thus, Glucose/Fructose ratio was almost identical in control and zebularine treated cells, ranging from 1.6 to 2.2 (Table III-1).

These results suggest that in addition to differences in the cell metabolic status, light conditions also impact the cell response to the zebularine treatment. Similarly, the organic acid content of dark grown cells was very different from the one of light grown cells. In control conditions malate was in average twice lower than tartarate, this ratio reversing to values lower than 0.5 with increasing concentration of zebularine

Taken together, results indicate that metabolic status of cells differs between light and dark conditions, and that cells are differentially impacted by the presence of zebularine depending on their growing conditions.

Samples	Ratio of Glucose-Fructose
light water	34,159
light DMSO	23,528
light zeb25	8,770
light zeb50	4,610
light zeb75	3,669
dark water	1,577
dark DMSO	1,889
dark zeb25	1,745
dark zeb50	2,214
dark zeb75	2,117

Table III-1. The ratio of glucose and fructose in GT cell under light and dark condition.

3.3.4 Trasncriptome analysis reveals a global impact of zebularine on GT cell physiology

a. Summary of RNA seq data

With the aim to analyze the impact of zebularine treatments on gene expression in cells cultured in the presence and absence of light, RNA-seq analysis was performed using the exact same samples as those used for metabolic analysis, comparing two conditions, light (the DMSO control and Z50 treated cells) and dark (the DMSO control, Z25 and Z50 treated cells) as described in part 2. A total of 15 samples were analyzed (3 for each type of cells, sampling method see materials and methods) which generated between 9.5 to 16.8 million reads per sample (supplementary Table III-6, page 175). After filtering 9.0 to 16.1 million reads were obtained of which between 93.86% and 95.81%, which could be mapped to the grape reference genome (Canaguier et al., 2017, supplymentary Table III- 6, page 175).

To identify the differentially expressed genes between cell samples, data were analyzed using DESeq2, as described in the methods. A total of 32380 and 32960 genes were expressed in at least one sample of

light and dark, respectively, which represented approximately 76.3% genes in light and 77.7% genes in dark of all identified genes in the grape genome (https://urgi.Versailles.inra.fr/Species/Vitis.12X.v2, Canaguier et al., 2017). There were little variations of the total number of genes expressed in each samples.

Genes with low expression levels (RPKM below 1) were eliminated letting in total 21955 in light and 22010 genes in dark treated cells for further analysis. As expected, normalized read counts from independent biological replicates within one cell condition was highly correlated at each stage (R2>0.96, supplementary Figure III-17, page 176). On the contrary, correlation between different samples was variable depending on the comparisons, ranging from 0.708 to 0.988, as shown in supplementary Figure III-17, page 176. The lowest correlation coefficient (R2= 0.708) was detected between light DMSO versus dark DMSO, illustrating the great impact of light conditions on gene expression. In contrast, relatively high correlation coefficients were obtained for comparisons involving zebularine treated versus DMSO treated conditions (between 0.816 and 0.988) suggesting that zebularine effect on cell transcriptome is very moderate. Finally the higher correlation coefficient (R2= 0.988) was detected between dark zeb25 versus dark zeb50 indicating that zebularine had very similar effect, whatever the concentration used, 25µM or 50µM.

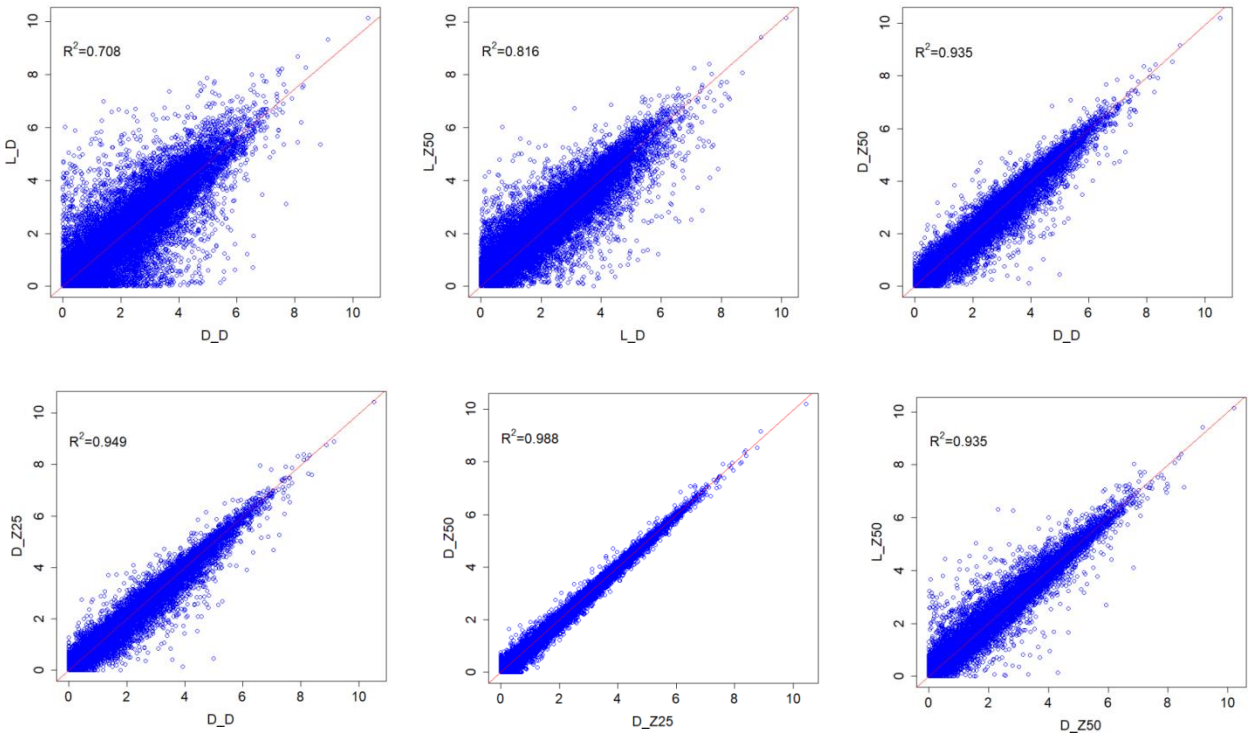

Figure III-7. Correlation analysis of RNA seq data between different treatments, light DMSO and dark DMSO, light zeb50 and light DMSO, dark DMSO and dark zeb50, dark DMSO and dark zeb25, dark zeb25 and dark zeb50, light zeb50 and dark zeb50. L, light; the letter D before underscore, dark; the letter D after underscore, DMSO; Z, zebularine; 25, 25 µM; 50, 50 µM.

The predominant effect of light conditions on GT cell transcriptomes was further confirmed by principal component analysis (PCA) (Figure III-8). Indeed the first principal component (PC1) explains 46.51% of total variability and clearly separates light DMSO control cells from dark DMSO cells and from all other

samples. Dark grown cells treated with zebularine or not, have very similar PC1. Noteworthy the comparison of PC1 reveals more similarity between light zeb cells and dark cells (with or without zeb treatment) than between light zeb and light DMSO cells, suggesting that a treatment by zebularine has a similar effect as continuous darkness on gene expression. PC2 represents 17.04% of total variability and it separates mainly the dark DMSO cells from all other samples: all zebularine treated cells are characterized by very similar PC2, whether they are grown in dark or light. Moreover light DMSO cell PC2 is also very similar to zebularine treated cell PC2.

In summary, all zebularine treated samples group closed to each other, whereas control samples were well separated in function of the illumination conditions. In other words, zebularine treatments mask the transcriptomic differences between light and dark grown cells, and make the light grown cells resemble dark grown cells.

Finally dark zeb25 and dark zeb50 could not be clearly distinguished according to the PCA analysis, which was consistent with the correlation analysis (supplementary Figure III-17, page 176), and revealed similar gene expression profile between these two conditions. As a consequence, for clarity purpose, only one concentration of zebularine (50µM) from the two tested (25 and 50µM) was considered for the following analysis.

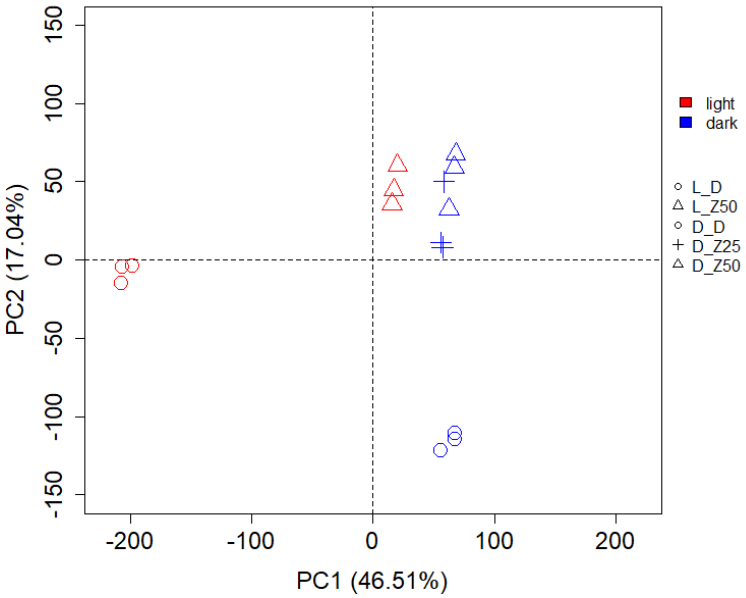

Figure III-8. Principal component analysis of RNA seq data. The color indicates the illumination conditions (red: cells grown in the light); blue: cells grown in the dark. The shape indicates the treatments: ○, DMSO; △, zeb50 ; +, zeb25. PC1 and PC2 explain 63.55% of the variability. PC1 represents the variation between light control and other treatments. PC2 separates sample according to control and zeb treated cells

Taking into consideration the 4 selected conditions, Light DMSO, Light zeb50, Dark DMSO and Dark Zeb50, all possible pairwise comparisons of RNA-SEQ results were made in order to determine the differentially expressed genes (DEGs). DEGs associated with a $\log_2$-fold change > 1 or <-1, in at least one comparison (p-value adj. < 0.05) were selected for further analysis. They represented a total of 7576 DEGs, accounting for 17.9% of all grape genes (Canaguier et al., 2017). As expected from the PCA analysis (Figure III-8), the highest number of DEGs was found for the Light DMSO / Dark DMSO comparison with 6282 DEGs, representing 82.9% of all DEGs (Figure III-9). These Light-dependent DEGs included 3456

down-regulated genes and 2826 up-regulated genes, representing 45.6% and 37.3% of all DEGs, respectively (Figure III-9). In contrast, the comparison of Light Zeb and Dark Zeb revealed a much lower number of DEGs (1166 DEGs), corroborating the PCA analysis, which suggested the convergence of light and dark g rown cell transcriptomes after zebularine treatments.

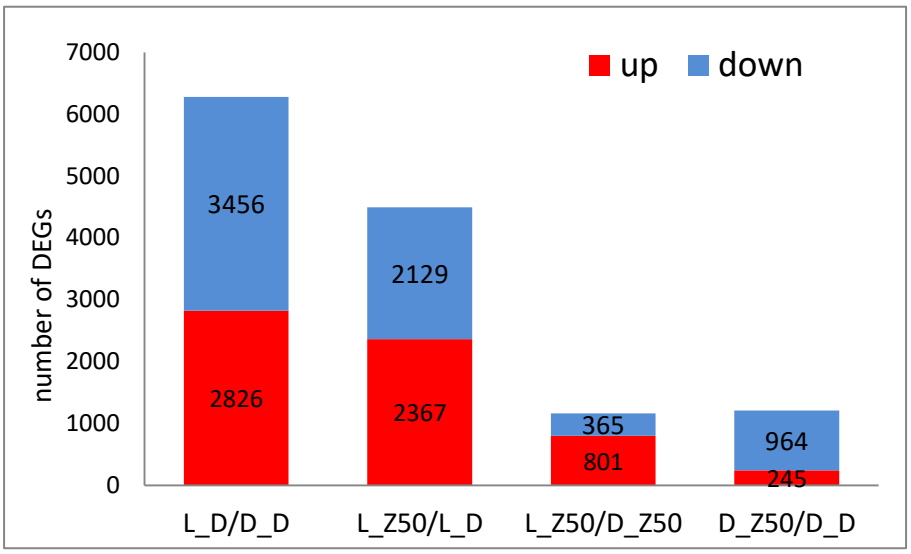

Figure III-9. Number of DEGs in each pairwise comparison

Whereas, in light, the zebularine treatment alters the expression of 4496 genes (accounting for 59.3% of all DEGs), much less genes were identified as zebularine-dependent in the dark (1209 DEGs, representing 16% of all DEGs). Interestingly each pairwise comparison revealed both up-regulated and down-regulated genes (Figure III- 9). Surprisingly, the comparison of zebularine-treated and control cells do not reveal much more up-regulated than down-regulated genes in the presence of the methylation inhibitor. On the contrary, in dark conditions, 964 genes were down-regulated by the treatment whereas only 245 genes were upregulated, whereas in the light, the numbers of up- and down-regulated genes were similar (2367 up-regulated genes and 2129 down-regulated genes).

As shown on the Venn diagram presented in Figure III-10, many DEGs are shared between two or more comparisons. For example, 3593 DEGS were similarly found when comparing the effect of light (in the DMSO control condition), and the effect of zebularine in the light condition. More interestingly, this analysis allowed the identification of condition-specific DEGs. For instance, 2021 DEGs (26.7%) were specifically deregulated in a light-dependent manner and only 144 genes were specifically affected by zebularine both in light and dark.

The RNA seq data were analyzed with two different objectives. First a global analysis was undertaken in order to describe the general effects of zebularine on grape cell gene expression, in an attempt to better understand its impact on cell metabolism and physiology. Second the expression of genes specifically

related to anthocyanin accumulation was studied in order to unveil the mechanisms leading to the zebularine-dependent increase in anthocyanin in grape cells.

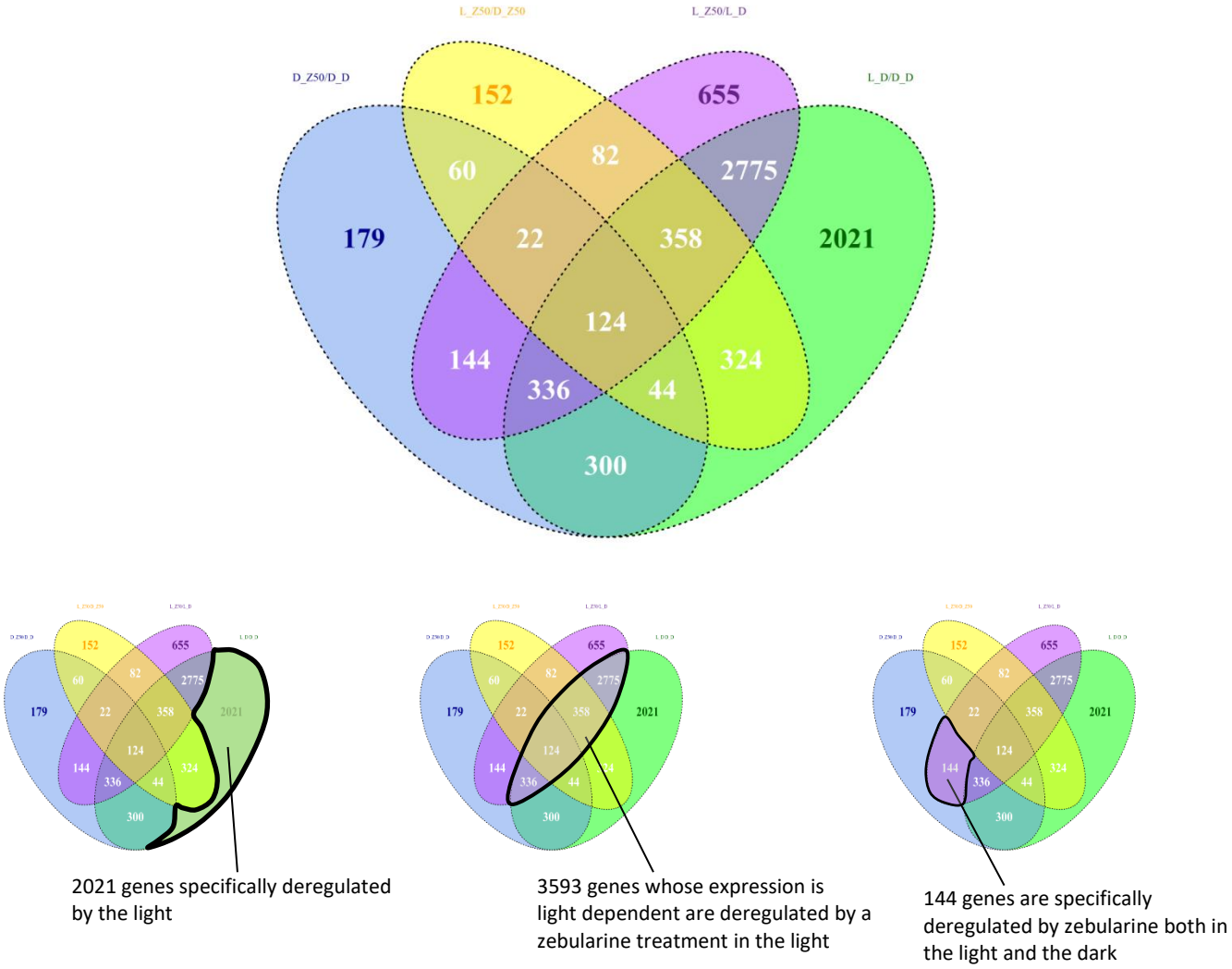

Figure III-10. Venn diagrams displaying the numbers of DEGs shared in different conditions, and treatments

b. *Many stress-related genes are highly and specifically induced by Zebularine*

In order to characterize the effects of zebularine, our study was first focused on the 144 genes specifically deregulated by zebularine both in light and dark (Figure III-10). The analysis of the genes the most induced by zebularine (log2FC>2) revealed a high proportion of stress-related genes (Table III-2): out of 26 genes with a functional annotation, there are 19 stress-related genes.

First there are several genes which have been reported to be induced by DNA damage in *Arabidopsis thaliana*. Among these genes, one gene is directly involved in DNA repair: Vitvi04g01692 (11.3 and 6.4

fold increase in light and dark, respectively) is homologous to at1g19025 coding for a DNA repair metallo-beta-lactamase family protein. In addition Vitvi05g01355 homologous to atKU70, a key player in non-homologous end-joining pathway that repairs DNA double-strand breaks, is also induced although to a lesser extent (2.7 and 2.9 fold in light and dark, respectively).The other genes related to genotoxicity include Vitvi13g01990 (14.3 and 3.6 fold increase in light and dark respectively), homologous to AtSMR4 which belongs to a SIAMESE/SIAMESE-RELATED (SIM/SMR) class of cyclin-dependent kinase inhibitors and is induced by DNA stress (Yi et al., 2014). Finally Vitvi12g02472 which is the most highly induced gene in the dark (19 fold increase), was considered by Yi et al (2014) as a transcriptional hallmark of the DNA damage response regardless of the type of DNA stress, together with 21 other genes (Yi et al., 2014).

gene	dark		light		function	homologous gene(s)
	log2FC	padj	log2FC	padj		
Vitvi12g02472	4,2	3,00E-79	3,6	8,00E-39	GEX1 (unknown function)	at5g55490
Vitvi13g01990	1,8	2,00E-03	3,6	8,00E-18	Cyclin-dependent protein kinase inhibitor	At5g02220 (SMR4)
Vitvi04g01692	2,6	3,00E-49	3,3	1,00E-74	DNA repair	at1g19025
Vitvi17g01550	3,3	2,00E-17	4,3	6,00E-12	brassinosteroid-signaling kinase	at5g59010 (ATBSK5)
Vitvi19g02101	2,9	1,00E-09	4,2	4,00E-08	Ferredoxin-fold anticodon-binding domain protein	at1g55790
Vitvi17g00593	2,3	1,00E-02	4,1	2,00E-03	glutathione S transferase	at1g74590 (GSTU10)
Vitvi17g01381	3,8	2,00E-27	3,2	1,00E-19	glutathione S transferase	at2g29420
Vitvi08g01112	3,2	4,00E-05	2,7	4,00E-05	ABC transporters and multidrug resistance system	at2g37360 ; at3G53510
Vitvi12g00272	2,8	5,00E-34	2,9	1,00E-27	tyrosine transaminase	at5g36160
Vitvi01g01572	2,8	2,00E-02	2,4	3,00E-02	AAA-ATPase	at3g50940 ; at2g18193*
Vitvi14g00163	2,5	3,00E-08	2,6	6,00E-09	heavy metal-associated isoprenylated protein	at5g27690
Vitvi08g00076	2,4	5,00E-16	1,8	2,00E-06	detoxification efflux carrier	at1g33110 *
Vitvi14g00332	2,4	1,00E-02	2,4	4,00E-05	geranylgeranyl diphosphate reductases	Q9ZS34 (*N. tabacum*)
Vitvi05g02234	1,5	3,00E-02	2,2	5,00E-04	Disease resistance RPP8-like protein	at5g35450 (RPP8L3)
Vitvi03g01650	1,3	5,00E-03	2,1	4,00E-20	Pathogenesis-related protein	at2g14580
Vitvi03g01542	1,9	3,00E-08	2,1	3,00E-19	2-oxoglutarate and Fe-dependent oxygenase	at3g19000
Vitvi09g00559	1,3	5,00E-03	2,1	3,00E-10	Glyoxalase I family protein	at1g80160*
Vitvi02g01446	1,5	2,00E-12	2,1	1,00E-07	heat shock protein	at4g25200 (HSP23.6)
Vitvi14g01439	2	2,00E-16	1,7	1,00E-12	retinoblastoma related protein	at3g12280 (RBR1)
Vitvi09g00768	4	2,00E-24	6,9	1,00E-19	ubiquitin E3 SCF FBOX	at5g07610
Vitvi12g00255	2	2,00E-05	3,2	5,00E-09	NAC transcription factor	at4g28500
Vitvi12g01880	3	2,00E-63	3	2,00E-70	cupin (storage protein)	at1g07750
Vitvi10g02406	2,2	3,00E-02	3	3,00E-02	MYB domain transcription factor	at2g02060
Vitvi05g00582	2,2	1,00E-38	1,8	9,00E-17	calcium transporting ATPase	at3g22910
Vitvi18g01607	1,9	5,00E-05	2,1	6,00E-06	protein kinases	at1g54610; at5G50860
Vitvi06g00621	1,6	8,00E-04	2	3,00E-13	UDP-glycosyltransferase	at1g07250 and homologous genes
Vitvi18g01244	2,2	2,00E-03	5,2	5,00E-06	unknown function	at1g77160
Vitvi16g01823	2	9,00E-03	4	8,00E-10	unknown function	
Vitvi06g00244	2	7,00E-06	3,6	4,00E-19	unknown function	at5g60720
Vitvi16g01566	1,7	1,00E-02	3,5	5,00E-18	unknown function	
Vitvi03g00886	2,3	1,00E-13	1,9	9,00E-08	unknown function	
Vitvi12g02199	2,1	7,00E-04	2,5	3,00E-04	unknown function	
Vitvi19g01877	1,6	1,00E-02	2,4	7,00E-10	unknown function	
Vitvi12g02197	1,7	2,00E-23	2,1	6,00E-39	unknown function	
Vitvi09g01611	1,6	6,00E-03	2,1	4,00E-06	unknown function	
Vitvi07g00538	1,4	1,00E-07	2,1	2,00E-06	unknown function	at2g47010
Vitvi00g02272	1,2	2,00E-02	2	1,00E-16	unknown function	
Vitvi16g00528	1,4	1,00E-05	2	5,00E-24	unknown function	

*Table III-2. Genes up-regulated by zebularine (log2FC>2) both in light and dark grown cells. The indicated functions correspond to the function associated with the closest Arabidopsis homologous gene(s). The grey color indicate genes with no associated function. The homologous genes were not functionally characterized and present no known functional domain. The orange color indicates genes related to genotoxic stress, and/or DNA repair processes. The blue color indicates stress-related genes. * indicated Arabidopsis genes induced by the herbicide atrazine (Ramel et al BMC genomics 2007).*

Second, there are several genes that can be linked to antioxidant response. Two genes could be functionally related to the biosynthesis of tocopherol, which constitutes a major plant antioxidant (Munne-Bosch et al.,2007): Vitvi12g00272 (15 and 7 fold induction in the light and dark respectively) is homologous to at5g36160 coding for a tyrosine transaminase which has been shown to be play a role in tocopherol biosynthesis(Wang et al.,2019). Vitvi14g00332 (6.4 and 5.6 fold induction in the light and dark condition, respectively) codes a Geranylgeranyl diphosphate reductase known to provide phytol for tocopherol synthesis (Tanaka et al., 1999). Finally, three genes correspond to genes also identified by Ramel et al (2007), as genes upregulated by atrazine, an herbicide which acts through induction of oxidative stress: Vitvi09g00559 (Glyoxalase); Vitvi01g01572 (AAA-ATPase) and Vitvi08g00076 (efflux carrier).

Moreover several genes related to cell detoxification were identified, including two genes coding for glutathione S-transferases (Vitvi17g01381 and Vitvi17g00593) and two genes coding for detoxification-related transporters (Vitvi08g01112 and Vitvi08g00076).

Finally, a few up-regulated genes code for proteins with a broad range spectrum of functions, including the stress response. For example, Vitvi17g01550 codes a brassinosteroid-signaling kinase, and Vitvi14g01439 for a retinoblastoma related protein, whose *Arabidopsis* closest homologous, RBR1, plays an important role in the detoxification response to DNA damage (Bouyer et al., 2018).
Altogether this transcriptional profile demonstrates that the zebularine treatments, in the light and in the dark, triggers a stress response. More precisely, it suggests that zebularine induces genomic lesions and oxidative injuries.

c. Zebularine reduces the difference between light and dark grown cells

As mentioned above, according to the PCA analysis, and to the number of DEGs, the two conditions which were associated with the most divergent transcriptomes are ‘light DMSO’ and ‘dark DMSO’. Indeed the presence of light greatly affects plant cell physiology, hence it is not surprising to identify a high number of DEGs when these two samples are compared. In contrast the two conditions which were associated with the most similar transcriptomes are ‘light zebularine’ and ‘dark zebularine’. In order to better understand why after a zebularine treatment light and dark grown cells present similar transcriptomes, we have first analyzed the DEGs between light and dark grown cells, in the absence of drug.

Dark grown and light grown cells are characterized by very divergent transcriptomes

A total of 6282 DEGs including 2826 up-regulated and 3456 down-regulated were identified when the transcriptomes of cells grown in light and dark were compared. This suggests that the light has a global impact on the GT cell physiology. To better understand the functional differences between light and dark grown cells, analyses of Gene Ontology (GO) enrichment and overrepresentation were performed. The distribution of the 6282 DEGs into the 35 Mapman functional categories, referred to as BIN (Usadel, 2005), were analyzed using Mefisto (see methods). This GO enrichment analysis indicates that the 2826 DEGs up-regulated in the light were overrepresented in 9 functionally annotated categories (Figure III-11), including PS (88 genes), minor CHO metabolism (36 genes), hormone metabolism (112 genes), stress (171 genes), RNA (230 genes), protein (321 genes), signaling (196 genes), development (83 genes), and transport (144 genes). In addition, there were 239 genes in the so called 'miscellaneous' category and 900 genes, that could not be assigned to any functional category (Figure III-11).

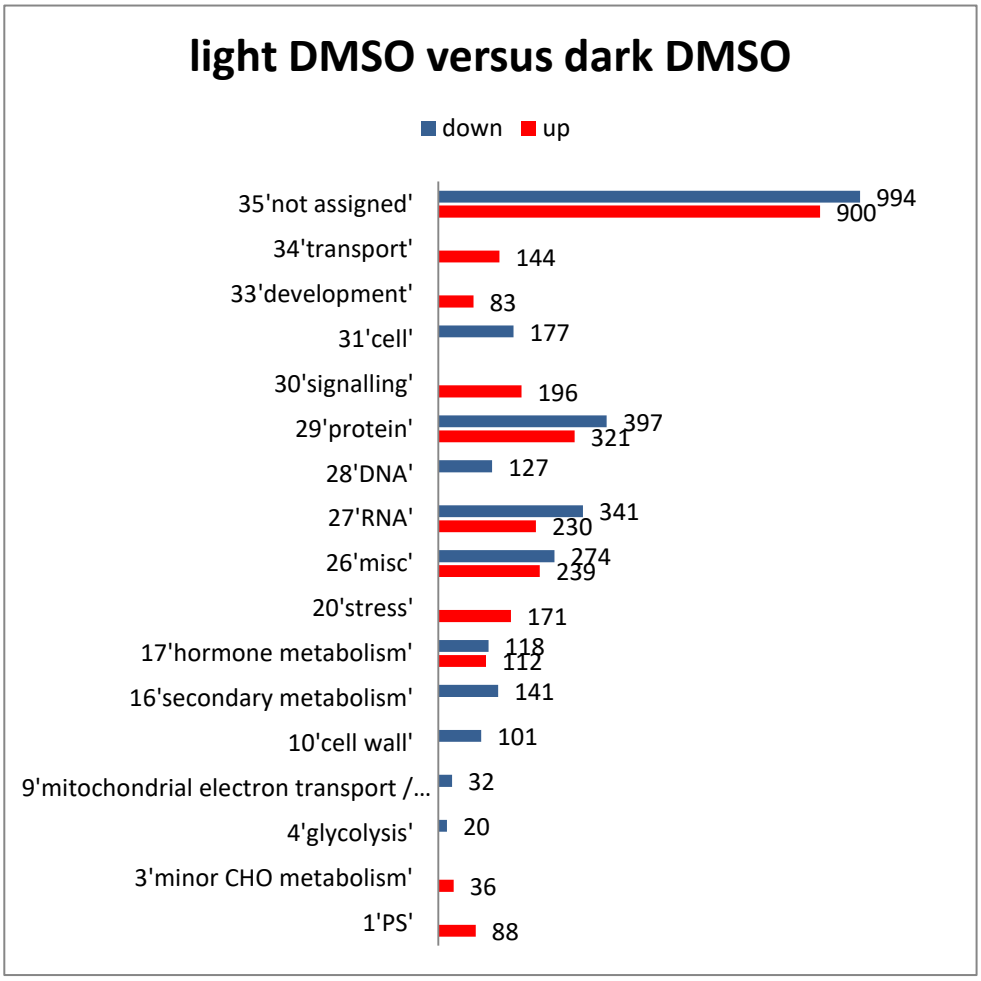

Figure III-11. Go enrichment and overrepresentation analysis of up- and down- regulated DEGs induced by light.

In the light, most zebularine-dependent genes (79%) were also identified as affected by light

In the light 2367 genes were induced by zebularine, whereas 2129 were repressed. Interestingly most of these genes were also identified as differentially expressed in the light compared to the dark (Figure III-9). More precisely 79% of the genes repressed by zebularine in the light were also repressed in the dark compared to the light. Similarly 79% of the genes induced by zebularine in the light were also more expressed in the dark than in the light (Figure III-12).

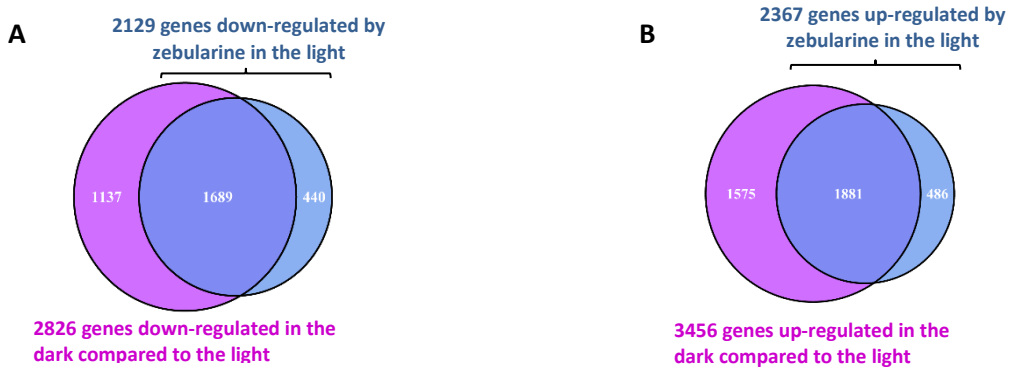

Figure III-12. Venn diagrams showing the overlap between (A) the genes down-regulated in the dark and the genes down-regulated by zebularine in the light; (B) the genes up-regulated in the dark and the genes up-regulated by zebularine in the light.

Accordingly with this observation, the GO categories associated with the genes differentially expressed in DMSO- and zebularine-treated light-grown cells (Figure III-13) are similar to the ones identified for the light-dependent DEGs (compare Figure III-13 and Figure III-11). Apart from the non-informative 'not assigned' and 'miscellaneous' GO categories, twelve functional categories are overrepresented (Figure III-13). Interestingly up- and down-regulated genes are found in different functional categories. Whereas up-regulated genes are found associated within the 'cell', 'DNA', 'RNA', and 'cell wall' categories, down-regulated genes are in the 'transport', 'signalling', 'protein', 'CHO metabolism' and 'photosynthesis' categories.

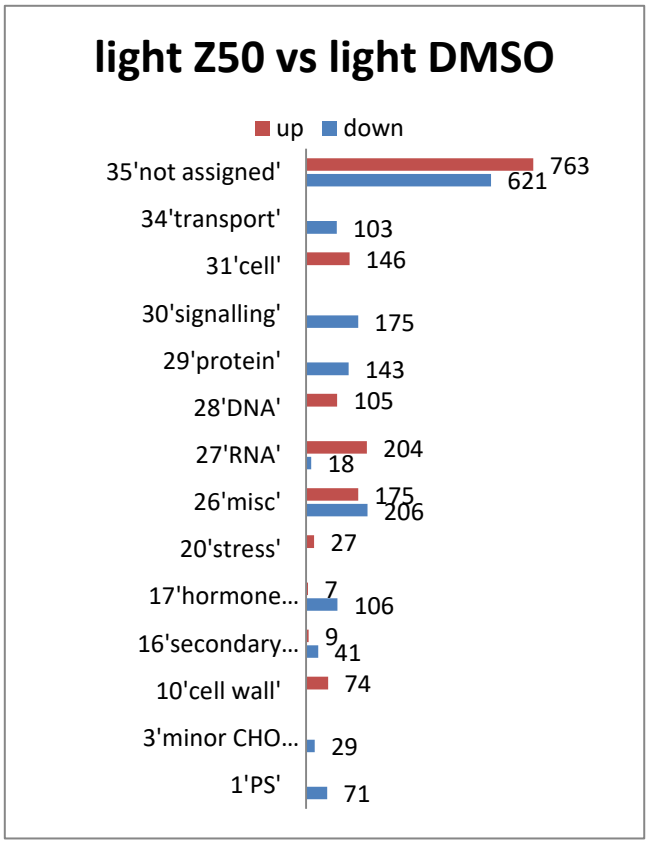

Figure III-13. Distribution of the GO functional categories of genes significantly down- and up-regulated in GT cells treated with zebularine 50µM in the light. Only the significantly enriched functional categories are shown. The numbers indicate the numbers of genes in each category.

Although the GO functional categories 'hormone metabolism' and 'secondary metabolism' are associated with both types of genes, up-regulated genes appear associated with jasmonate metabolism and down-regulated genes with abscisic acid, auxin and cytokinin metabolism (Table III-3). In a similar way, in the enriched 'secondary metabolism' GO category, induced and repressed genes are linked to different secondary metabolites (Table III-3).

	light Z50 vs light DMSO				
	Bin	**Bin name**	**contingency**	**Pvalue**	**Adj.Pvalue(Bonf)**
Up	10	cell wall	74 529 2276 37739	1.15E-09	7.34E-07
	10.7	cell wall.modification	21 62 2329 38206	7.10E-09	4.54E-06
	16.2.1.10	secondary metabolism.phenylpropanoids.lignin biosynthesis.CAD	9 22 2341 38246	4.50E-05	2.88E-02
	17.7.1.5	hormone metabolism.jasmonate.synthesis-degradation.12-Oxo-PDA-reductase	7 6 2343 38262	2.71E-06	1.73E-03
	20.1.7	stress.biotic.PR-proteins	27 977 2323 37291	3.92E-06	2.51E-03
	26	misc	175 1815 2175 36453	3.03E-08	1.94E-05
	27.3	RNA.regulation of transcription	204 2283 2146 35985	4.01E-07	2.56E-04
	28	DNA	105 547 2245 37721	1.64E-21	1.05E-18
	28.1	DNA.synthesis/chromatin structure	72 287 2278 37981	1.52E-20	9.69E-18
	28.1.3	DNA.synthesis/chromatin structure.histone	16 31 2334 38237	4.05E-09	2.59E-06
	28.1.3.2	DNA.synthesis/chromatin structure.histone.core	16 29 2334 38239	1.94E-09	1.24E-06
	28.1.3.2.4	DNA.synthesis/chromatin structure.histone.core.H4	5 2 2345 38266	1.23E-05	7.85E-03
	31	cell	146 939 2204 37329	1.94E-21	1.24E-18
	31.1	cell.organisation	85 531 2265 37737	1.76E-13	1.13E-10
	31.1.1	cell.organisation.cytoskeleton	23 114 2327 38154	3.89E-06	2.49E-03
	31.1.1.2	cell.organisation.cytoskeleton.mikrotubuli	18 50 2332 38218	3.89E-08	2.49E-05

	31.2	cell.division	23 115 2327 38153	4.42E-06	2.82E-03
	31.3	cell.cycle	30 105 2320 38163	1.51E-10	9.63E-08
	35	not assigned	763 19190 1587 19078	1.94E-63	1.24E-60
	35.2	not assigned.unknown	603 17089 1747 21179	1.85E-76	1.18E-73
Down	1	PS	71 162 2015 38370	2.42E-35	1.42E-32
	1.1	PS.lightreaction	54 98 2032 38434	5.25E-31	3.09E-28
	1.1.1	PS.lightreaction.photosystem II	24 28 2062 38504	1.05E-17	6.20E-15
	1.1.1.1	PS.lightreaction.photosystem II.LHC-II	11 2 2075 38530	4.53E-13	2.67E-10
	1.1.1.2	PS.lightreaction.photosystem II.PSII polypeptide subunits	13 24 2073 38508	1.86E-08	1.10E-05
	1.1.2	PS.lightreaction.photosystem I	16 12 2070 38520	3.74E-14	2.20E-11
	1.1.2.1	PS.lightreaction.photosystem I.LHC-I	5 2 2081 38530	6.84E-06	4.03E-03
	1.1.2.2	PS.lightreaction.photosystem I.PSI polypeptide subunits	11 8 2075 38524	3.29E-10	1.94E-07
	1.1.3	PS.lightreaction.cytochrome b6/f	6 7 2080 38525	2.29E-05	1.35E-02
	1.3	PS.calvin cycle	11 37 2075 38495	2.48E-05	1.46E-02
	3	minor CHO metabolism	29 165 2057 38367	2.42E-07	1.43E-04
	3.1	minor CHO metabolism.raffinose family	8 21 2078 38511	7.76E-05	4.57E-02
	3.2.3	minor CHO metabolism.trehalose.potential TPS/TPP	7 11 2079 38521	1.80E-05	1.06E-02
	16.2	secondary metabolism.phenylpropanoids	34 253 2052 38279	5.89E-06	3.47E-03
	16.2.1	secondary metabolism.phenylpropanoids.lignin biosynthesis	26 111 2060 38421	7.11E-09	4.19E-06
	16.2.1.1	secondary metabolism.phenylpropanoids.lignin biosynthesis.PAL	13 6 2073 38526	3.38E-13	1.99E-10
	16.5.1.3	secondary metabolism.sulfur-containing.glucosinolates.degradation	7 13 2079 38519	4.00E-05	2.36E-02
	17	hormone metabolism	106 862 1980 37670	2.82E-13	1.66E-10
	17.1	hormone metabolism.abscisic acid	20 129 2066 38403	8.14E-05	4.79E-02
	17.1.3	hormone metabolism.abscisic acid.induced-regulated-responsive-activated	13 47 2073 38485	8.92E-06	5.25E-03
	17.2	hormone metabolism.auxin	33 236 2053 38296	4.29E-06	2.53E-03
	17.2.1	hormone metabolism.auxin.synthesis-degradation	11 40 2075 38492	4.53E-05	2.67E-02
	17.4	hormone metabolism.cytokinin	20 68 2066 38464	1.59E-08	9.34E-06
	17.4.1	hormone metabolism.cytokinin.synthesis-degradation	18 52 2068 38480	1.03E-08	6.06E-06
	26	misc	206 1784 1880 36748	5.08E-22	3.00E-19
	26.1	misc.cytochrome P450	52 333 2034 38199	2.29E-10	1.35E-07
	26.2	misc.UDP glucosyl and glucoronyl transferases	50 287 2036 38245	1.71E-11	1.01E-08
	26.3	misc.gluco-, galacto- and mannosidases	21 110 2065 38422	3.43E-06	2.02E-03
	27.3.7	RNA.regulation of transcription.C2C2(Zn) CO-like, Constans-like zinc finger family	9 17 2077 38515	3.44E-06	2.03E-03
	27.3.40	RNA.regulation of transcription.Aux/IAA family	9 11 2077 38521	2.45E-07	1.44E-04
	29.4	protein.postranslational modification	81 906 2005 37626	3.87E-05	2.28E-02
	29.5.11.4	protein.degradation.ubiquitin.E3	62 655 2024 37877	7.48E-05	4.40E-02
	29.5.11.4.3.2	protein.degradation.ubiquitin.E3.SCF.FBOX	29 228 2057 38304	8.35E-05	4.92E-02
	30	signalling	175 2210 1911 36322	2.03E-06	1.19E-03
	30.2.8	signalling.receptor kinases.leucine rich repeat VIII	19 64 2067 38468	3.18E-08	1.87E-05
	30.2.8.2	signalling.receptor kinases.leucine rich repeat VIII.VIII-2	18 53 2068 38479	1.31E-08	7.73E-06
	30.3	signalling.calcium	42 251 2044 38281	2.00E-09	1.18E-06
	34	transport	103 1197 1983 37335	1.69E-05	9.93E-03
	35	not assigned	621 19332 1465 19200	1.01E-75	5.92E-73
	35.1.5	not assigned.no ontology.pentatricopeptide (PPR) repeat-containing protein	10 607 2076 37925	8.13E-06	4.79E-03
	35.2	not assigned.unknown	516 17176 1570 21356	6.25E-75	3.68E-72

Table III-3. Enriched Mapman functional categories (BINs) among the DEGs identified from the comparison of light Z50 and light DMSO. For each BIN, the Contingency column shows four numbers : from left to right : the number of genes (i) in the input list, (ii) in the background, (iii) not in the BIN in the input list, and (iv) not in the background. P-values were adjusted with a Bonferroni correction. Values were filtered with an adjusted P-value threshold <0.05 (Usadel et al.,2005).

88 genes related to photosynthesis were upregulated in the light. In particular a few genes coding for diverse proteins involved in light harvesting were highly expressed in light condition whereas they were not detected in the dark, such as Vitvi01g01648, Vitvi12g00050, Vitvi13g00590, Vitvi15g00004, Vitvi10g00740, Vitvi10g01839, Vitvi12g02485, and Vitvi18g02408. 71 photosynthesis-related DEGs whose expression was higher in the light than in the dark, were also down regulated by zebularine.

36 light up-regulated genes were enriched in the category 'minor CHO metabolism'. They include genes related to the biosynthesis of *myo*-inositol, raffinose family oligosaccharides (raffinose and stachyose), trehalose and xylose. 29 of these DEGS were also down-regulated by zebularine in light grown cells.

In particular, two genes coding for *myo*-inositol oxygenases (Vitvi09g00246, MIOX2 and Vitvi11g00231, MIOX4) were detected with 31 and 13 fold down-regulation in dark conditions compared to light conditions, and with 54 and 33 fold down-regulation in the presence of zebularine. *Myo*-inositol oxygenases catalyze the oxidation of myo-inositol to D-glucuronic acid. These enzymes play different roles in the plant through the control of *myo* inositol level. Indeed this molecule forms the structural basis of many lipid signaling molecules, and also participates in ascorbate and cell wall biosynthesis. In rice, OsMIOX was induced by drought, H_2O_2, salt, cold and abscisic acid, and OsMIOX overexpression was associated with enhanced resistance to drougth stress (Duan et al., 2012). In *Arabidopis*, expression of the MIOX2 and MIOX4 genes has been correlated with low energy/nutrient conditions, with a reduced expression in *in vitro* seedlings grown with exogenous glucose and reciprocally a high expression in seedlings grown in low nutrient conditions (Baena-Gonzalez et al., 2007; Alford et al, 2012). Hence the differential expression of MIOX genes in light and dark grown cells, could be linked to different nutritional status in these two types of cells. Indeed the sugar content in light grown cells was significantly lower than in dark grown cells (Figure III- 6A), concomitantly with a higher expression of MIOX genes. In a similar way, zebularine-treated cells were characterized by a higher sugar content and a lower expression of MIOX genes compared to the control light grown cells.

The raffinose family oligosaccharides are thought to protect the cells from the oxidative damage caused by a wide range of abiotic stresses (Taji *et al.*, 2002; Pennycooke *et al.*, 2003; Ayako Nishizawa et al., 2008). Galactinol synthase, catalyzing the first step of galactinol synthesis from myo-inositol and UDP-Galactose has been proposed to be the key enzyme of the biosynthesis pathway. Our analysis revealed that genes coding for four Galactinol synthases (Vitvi01g00714, Vitvi07g00457, Vitvi07g02242, Vitvi01g00714), 2 stachyose synthases（Vitvi05g00139, Vitvi07g00431 and 3 Raffinose synthase (Vitvi19g00768, Vitvi11g00513, Vitvi08g01890）were significantly repressed by zebularine and by the dark. Interestingly, DARK-INDUCIBLE10 (DIN10), which is annotated as a raffinose synthase was shown to be repressed by sugars in *Arabidopsis* (Fujiki et al., 2001). Accordingly in our analysis, its grape homolog, Vitvi11g00513, displays the highest expression level in the cells characterized by the lowest sugar content (light grown control cells).

Trehalose is a non-reducing disaccharide sugar that is widely distributed in nature (Elbein et al., 1974). Trehalose functions as a stress protection metabolite. Accordingly, trehalose metabolism is activated upon chilling in grape (O Fernandez et al., 2012). Besides trehalose acts as a sugar signaling molecule

integrating metabolism and development in relation to carbon supply (Goddijn and van Dun, 1999) (Schluepmann and Paul, 2009). In our analysis three genes linked to trehalose synthesis exhibited higher expression in light condition than in dark condition (Vitvi17g00778, Vitvi10g00625, Vitvi01g00793), whereas zebularine repressed 7 Trehalose-6-phosphate synthase genes, coding for the first enzyme of the trehalose biosynthesis pathway.

In addition genes coding for sorbitol dehydrogenases (Vitvi16g01858, Vitvi16g01857) and a xylose isomerase (Vitvi11g01300) were highly repressed by dark and a zebularine treatment, with a 4 to 12 fold expression decrease.

A total of 101 and 74 DEGs involved in the synthesis, modification and degradation of cell wall were up-regulated respectively in the dark and after a zebularine treatment. Nine cellulose synthase, 3 hemicellulose synthase, 6 cell wall protein, 8 xyloglucan endo-transglycosylase, 12 pectin lyase, 15 pectin methylesterase, 3 pectin acetylesterase and 12 expansin encoding genes were induced in the presence of zebularine. In contrast very few genes were associated with the 'cell wall' functional GO category among the genes repressed by zebularine. This suggests that after 12 days of culture, cell walls undergo much more remodelling in cells grown in the dark or in the presence of zebularine than in light grown control cells.

112 and 106 genes associated with the 'hormone' GO functional category were repressed respectively in the dark, and after a zebularine treatment. Although light- and zebularine-dependent DEGs are not completely identical, the same hormones appeared in the functional annotations linked to the 112 / 106 hormone-related genes: ethylene, auxin, cytokinin, salicylic acid, ABA, brassinosteroid, gibberellin and jasmonate. The light-dependent DEGs include 80 genes related to hormone metabolism and signal transduction, as well as 42 genes characterized as hormone-responsive. Concerning ABA-related genes, 23 genes were repressed in the dark, as for example four genes coding for HYR1 homologous genes (Vitvi12g02594, Vitvi12g01720, Vitvi12g01718 and Vitvi12g01811). These four genes were also identified among the zebularine repressed genes. HYR1 has a glycosyltransferase activity and can conjugate ABA with glucose to produce abscisic acid glucosyl ester, which is storage or transport form of ABA. Furthermore genes involved in ABA signaling were also affected. For instance ABA INSENSITIVE 1 (ABI1, Vitvi11g00270), a negative regulator of ABA signal, was 11 times more expressed in the light than in the dark, and 4 times more in the DMSO control than in the zebularine treated cells. Three genes related to auxin response were strongly repressed in the dark (Vitvi07g01644, Vitvi10g00451 and Vitvi19g00255). Vitvi07g01644 is a homolog of the auxin-responsive gene, GH3.1, which codes for an enzyme responsible for the conjugation of IAA with amino acids thereby limiting auxin activity. Vitvi10g00451 and Vitvi19g00255 are homologous to at4g27450 annotated as Aluminium induced protein with YGL and LRDR motifs. These three genes were furthermore strongly repressed by zebularine both in light and dark. VvGAI1, a negative regulator of gibberellin response which has been functionally characterized in Pinot Meunier (Boss and Thomas 2002), was 2.8 times less expressed in the dark than in the light, and 2.3 times less expressed in the presence of zebularine. Finally whereas 108 hormone-related genes were up-regulated in the dark, only 7 were induced by zebularine. These 7 genes all correspond to 12-oxophytodienoate reductases (ORP) that catalyze the conversion of oxylipin 12-oxophytodienoic acid

to jasmonic acid. Corresponding genes were also up-regulated in dark grown cells compared to light grown cells, suggesting that more jasmonic acid were synthesized after a zebularine treatment, and in the dark.

196 signaling related genes were up-regulated in the light, including 22 light signaling transduction genes, and 34 calcium signaling protein encoding genes.

'Protein' was the GO category containing the largest number of light-dependent DEG with 321 up-regulated, and 397 down-regulated genes. Most genes were related to protein modification (118 up, 85 down) and degradation (154 up, 90 down), with 96 up-regulated and 64 down-regulated genes linked to the ubiquitin system. In contrast, only 22 and 150 genes corresponding to protein synthesis were identified among the light up- and down- regulated genes respectively, suggesting that protein synthesis may be more active in dark grown cells than in light grown cells. Some genes coding for important translational factors were significantly induced by light, such as, Translational initiation factor 1 (Vitvi19g00436), Elongation factor Tu (Vitvi17g00928), whereas several ribosomal proteins were strongly repressed by light, including ribosomal protein S27 (Vitvi01g01792), Ribosomal protein L36e family protein (Vitvi16g01054), Ribosomal protein L35A (Vitvi13g00500), and Ribosomal protein L37ae (Vitvi02g00599).

Interestingly whereas in most GO enriched category genes down regulated in the dark and by zebularine coincide, this is not the case for the DEGs related to the 'stress' GO category. All 171 light-dependent DEGs which are enriched in the 'stress' GO category are down-regulated in the dark, but no zebularine-down-regulated DEG are identified as enriched in the same GO category. Indeed all 27 zebularine-dependent DEGs enriched in the 'stress' GO category are induced by the drug. This observation further confirms that zebularine specifically causes a stress response, as described in the above paragraph. Nevertheless a few stress-related genes are both down-regulated in the dark and repressed by zebularine; such as four Kunitz Trypsin Inhibitor genes which were highly expressed in the light, but nearly not detected in the dark (Vitvi17g01621, Vitvi17g01613, Vitvi04g00798, Vitvi17g01121). The Kunitz Trypsin Inhibitor gene family is a complex family composed by versatile protease inhibitors. Most of them inhibit serine proteases, but some of them are able to inhibit cysteine proteases as well as other hydrolases (Renko et al., 2012). Vitvi03g00119 and Vitvi18g02423 encoding heat shock proteins were also more expressed in the light, and in the absence of zebularine.

There were 50 genes related to secondary metabolism among the zebularine-dependent DEGs, including 9 up and 41 down regulated DEGs. Flavonol, stilbene, glucosinolate and lignin biosynthesis genes were found significantly down-regulated. As an example all 48 grape stilbene synthase (STS) genes were more expressed in dark than light, and were repressed by a zebularine treatment. In contrast, as described in more details in paragraph Figure III-15, anthocyanin biosynthesis genes were up-regulated, including Leucocyanidinoxygenase (LDOX), Glycosyltransferase (GT), chalconesynthase (CHS), Flavonone-3-hydroxylase(F3H), Flavonoid3,5-hydroxylase (F3'5'H), and Flavonolsynthase (FLS). This was consistent with the higher concentration of anthocyanin detected after zebularine treatment in the light.

d. *In dark grown cells, zebularine has predominantly a repressive effect on gene expression*

A total of 1209 DEGs were identified that responded to a treatment with zebularine 50µM in the dark. They included 964 down-regulated and 245 up-regulated DEGs, indicating that most genes were repressed by the treatment. The 245 actived genes were enriched in two functionally annotated GO categories, 'secondary metabolism' (7 DEGs) and 'hormone metabolism' (4 DEGs). Whereas the 'miscellaneous' and 'not assigned' categories contain respectively 38 and 77 DEGs. The 964 genes repressed in response to zebularine treatment ranged in 11 functional categories: 'fermentation' (4 DEGs),'cell wall' (50 DEGs), 'secondary metabolism' (56 DEGs), 'hormone metabolism' (48 DEGs), 'misc' (106 DEGs), 'RNA' (16 DEGs), 'protein' (1 DEGs), 'signaling' (93 DEGs), 'cell' (14 DEGs), 'transport' (7 DEGs) and 'not assigned' (268 DEGs) (Figure III-14, Table III-4).

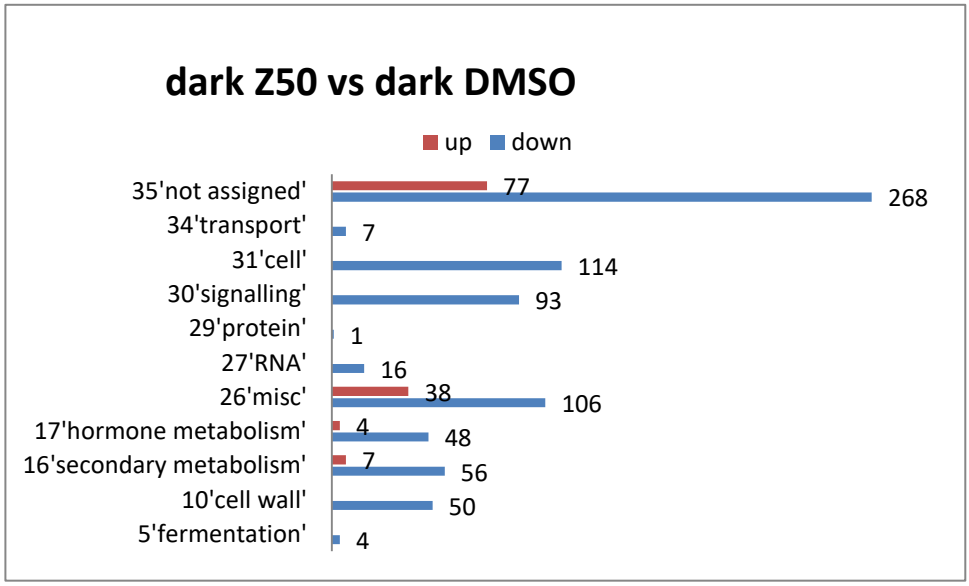

Figure III-14. Go enrichment and overrepresentation analysis of up- and down- regulated DEGs between dark Z50 and dark DMSO.

	dark Z50 vs dark DMSO				
	Bin	Bin name	contingency	Pvalue	Adj.Pvalue(Bonf)
up	16.2.1	secondary metabolism.phenylpropanoids.lignin biosynthesis	7 130 237 40244	2.05E-05	3.92E-03
	16.2.1.6	secondary metabolism.phenylpropanoids.lignin biosynthesis.CCoAOMT	3 9 241 40365	4.53E-05	8.64E-03
	17.8.1.1.5	hormone metabolism.salicylic acid.synthesis-degradation.synthesis.SA glucosyltransferase ester and ether bond making SGE, SAG	4 8 240 40366	6.06E-07	1.16E-04
	17.8.1.1.4	hormone metabolism.salicylic acid.synthesis-degradation.synthesis.SA glucosyltransferase ether bond making SAG	3 8 241 40366	3.41E-05	6.51E-03
	17.8.1.1	hormone metabolism.salicylic acid.synthesis-degradation.synthesis	4 27 240 40347	3.52E-05	6.72E-03
	26	misc	38 1952 206 38422	2.96E-10	5.66E-08
	26.2	misc.UDP glucosyl and glucoronyl transferases	10 327 234 40047	4.18E-05	7.99E-03
	26.9	misc.glutathione S transferases	9 114 235 40260	6.38E-08	1.22E-05
	35	not assigned	77 19876 167 20498	3.50E-08	6.69E-06
	35.2	not assigned.unknown	61 17631 183 22743	2.46E-09	4.70E-07

down	5.3	fermentation.ADH	4 5 948 39661	3.44E-05	1.29E-02
	10	cell wall	50 553 902 39113	1.79E-14	6.72E-12
	10.6	cell wall.degradation	17 169 935 39497	2.11E-06	7.94E-04
	10.6.3	cell wall.degradation.pectate lyases and polygalacturonases	12 83 940 39583	2.36E-06	8.86E-04
	10.7	cell wall.modification	17 66 935 39600	8.08E-12	3.04E-09
	16	secondary metabolism	56 1220 896 38446	8.19E-06	3.08E-03
	16.2.1	secondary metabolism.phenylpropanoids.lignin biosynthesis	13 124 939 39542	2.19E-05	8.23E-03
	16.2.1.1	secondary metabolism.phenylpropanoids.lignin biosynthesis.PAL	13 6 939 39660	1.42E-17	5.32E-15
	16.8	secondary metabolism.flavonoids	30 288 922 39378	1.44E-10	5.42E-08
	16.8.2	secondary metabolism.flavonoids.chalcones	25 47 927 39619	6.98E-23	2.62E-20
	16.8.2.1	secondary metabolism.flavonoids.chalcones.naringenin-chalcone synthase	24 26 928 39640	3.87E-26	1.46E-23
	17	hormone metabolism	48 920 904 38746	1.45E-06	5.45E-04
	17.1.3	hormone metabolism.abscisic acid.induced-regulated-responsive-activated	8 52 944 39614	7.70E-05	2.90E-02
	17.6.1.13	hormone metabolism.gibberelin.synthesis-degradation.GA2 oxidase	3 2 949 39664	1.24E-04	4.66E-02
	26	misc	106 1884 846 37782	3.78E-15	1.42E-12
	26.4	misc.beta 1,3 glucan hydrolases	12 53 940 39613	3.30E-08	1.24E-05
	26.4.1	misc.beta 1,3 glucan hydrolases.glucan endo-1,3-beta-glucosidase	8 37 944 39629	8.84E-06	3.32E-03
	26.12	misc.peroxidases	10 75 942 39591	3.05E-05	1.15E-02
	26.13	misc.acid and other phosphatases	12 66 940 39600	2.69E-07	1.01E-04
	26.21	misc.protease inhibitor/seed storage/lipid transfer protein (LTP) family protein	11 25 941 39641	3.89E-10	1.46E-07
	27.3.3	RNA.regulation of transcription.AP2/EREBP, APETALA2/Ethylene-responsive element binding protein family	10 73 942 39593	2.47E-05	9.31E-03
	27.3.8	RNA.regulation of transcription.C2C2(Zn) DOF zinc finger family	6 19 946 39647	1.97E-05	7.42E-03
	29.2	protein.synthesis	1 642 951 39024	8.26E-06	3.10E-03
	30	signalling	93 2292 859 37374	1.75E-06	6.58E-04
	30.3	signalling.calcium	28 265 924 39401	4.38E-10	1.65E-07
	31.3	cell.cycle	14 121 938 39545	3.80E-06	1.43E-03
	34.19	transport.Major Intrinsic Proteins	7 32 945 39634	3.04E-05	1.14E-02
	35	not assigned	268 19685 684 19981	1.83E-40	6.87E-38
	35.1.5	not assigned.no ontology.pentatricopeptide (PPR) repeat-containing protein	1 616 951 39050	1.13E-05	4.25E-03
	35.2	not assigned.unknown	236 17456 716 22210	5.31E-34	1.99E-31

Table III-4. Distribution of the GO functional categories of genes significantly down- and up-regulated in GT cells treated with zebularine 50µM in the dark. Only the significantly enriched functional categories are shown. The numbers indicate the numbers of genes in each category. The Contingency column shows the number of genes (i) in the BIN in the input list, (ii) in the background, (iii) not in the BIN in the input list, and (iv) not in the background. P-values were adjusted with a Bonferroni correction. Values were filtered with an adjusted P-value threshold <0.05(Usadel et al., 2005).

Anthocyanin biosynthesis related genes were induced by zebularine in dark

Seven genes related to the flavonoid biosynthesis pathway were induced by zebularine in the dark, including PAL (V*itvi13g00622*), 4CL (Vitvi02g00938), C4H (Vitvi06g00803), OMT (Vitvi01g02265, Vitvi01g02263, Vitvi01g01635), UGFT (Vitvi16g00156) and CHS (Vitvi16g00752) encoding genes. These genes are all putatively involved in anthocyanin biosynthesis, consistent with the induction of anthocyanin accumulation in these cells. The impact of the treatment on the expression of the complete set of genes identified as anthocyanin-related genes in grape will be described in the following part (part Table III-5 and Figure III-15).

In addition, 4 salicylic acid synthesis and degradation related genes were induced by zebularine. 'Misc' contained 38 up-regulated DEGs, 10 encoding glutathione S transferases (GTS) that are necessary to the transport of all type of anthocyanin from cytoplasmic to vacuole (Kitamurs et al.,2004), nine encoding cytochrome P450 superfamily proteins involved in oxidation reduction and 10 coding for UDP glucosyl and glucoronyl transferases superfamily proteins.

Zebularine repress a large number of genes in the dark

Compared to the 246 up –regulated DEGs due to zebularine in the dark, 964 DEGs were repressed after zebularine treatment. In the category 'fermentation', genes coding for a pyruvate decarboxylase and alcohol dehydrogenases (4 DEGs) were identified. Fifty DEGs were found in the category 'cell wall', including genes coding for cell wall proteins, a cellulose synthase (Vitvi07g00376), and hemicellulose synthesis related proteins (Vitvi04g01222, Vitvi18g00909), but also 41 DEGs related to the modification and degradation of cell wall, such as genes coding for pectin lyases (12 genes), expansins (12 genes), xyloglucan endotransglucosylase/hydrolases (4 genes), a pectin methylesterase, pectin methyl esterase inhibitors (6 genes), and a pectin lyase.

Fifty six DEGs related to the secondary metabolism were repressed by zebularine, mainly belonging to the biosynthesis of stilbenes (24 genes), lignins (13 genes) and isoprenoids (9 genes). The 48 repressed hormone related DEGs mainly corresponded to genes coding for proteins induced by ABA, auxin, brassinosteroid, ethylene and gibberellin. Six genes coding for C2C2 transcription factors and 10 genes coding for AP2/EREBR transcription factors were repressed by zebularine. Twenty and 43 genes related to protein modification and degradation, respectively, were down-regulated by zebularine. The 'signaling' category contained genes coding for leucine-rich repeat receptor-like protein kinase (61 genes) and proteins linked to calcium signaling transduction (28 genes). Genes related to cell organization (23 genes), cell cycle (14 genes) and cell division (6 genes) were also repressed by zebularine, which may be linked to the reduction of cell growth in the presence of the drug. In addition genes coding for sugar-, amino acid- and water-transport proteins were repressed by zebularine in the dark.

All grape genes related to anthocyanin biosynthesis were listed, including structural, transport and regulatory genes, using bibliographic data (Table III-5). Of note, several enzymes involved in anthocyanin biosynthesis are encoded by multigene families, especially enzymes of the phenylpropanoid pathway which is not exclusive to anthocyanin biosynthesis, but is also used for the synthesis of other isoprenoids, including lignins, stilbenes; flavonols and tannins (Figure III-15) (Boss et al., 1996). For some of these enzymes, specific isoforms have been associated with anthocyanin biosynthesis in grape berries (Table III-5). In such cases, only the genes coding for these specific isoforms were taken into consideration.

		number of genes in the grape genome		Genes associated with anthocyanin accumulation in the berries	
structural genes					
	phenylalanine ammonia lyase(PAL)	19	Sparvoli 1994, Sweetman et al.,2012	PAL1, PAL2	Guillaumie et al.,2011; Dinis et al.,2016; Belhadj et al.,2008
	cinnamate-4-hydroxylase(C4H)	3	Sweetman et al.,2012		
	4-coumaratel-coA ligase(4CL)	11	Sweetman et al.,2012		
	chalcone synthase(CHS)	3	Ferrer et al., 1999; Jeong et al.,2008	CHS3	Yamannto et al., 2002)
	chalcone isomerase(CHI)	2	Jeong et al.,2004 2008	CHI1	Feng et al., 2008, 2010)
	flavonoid 3',5'-hydroxylase(F3'5'H)	16	Falginella et al.,2010	F3'5'H1, 2, 5, 8	Falginella et al.,2010)
	flavonoid 3'-hydroxylase (F3'H)	2	Falginella et al.,2010	F3'H1	Falginella et al.,2010
	flavanone-3-hydroxylase (F3H)	2	Jeong et al.,2004 2008	F3H2	Jeong et al., 2008
	flavonol synthase (FLS)	5	Holton 1993; Fujita 2005	FLS4, FLS5	Fujita 2005
	dihydroflavanol reductase (DFR)	2	Jeong et al.,2004, TERRIER et al. 2008		
	Leucoanthocyanidin dioxygenase (LDOX)	1	Boss et al.,1996,		Boss et al.,1996
	O-methyltransferase (OMT)	4	Dunlevy et al.2010;Guillaumie et al,,2013	OMT1, OMT2	Hugueneyetal.,2009;Lückeretal.,2010;Fournier-Leveletal.,2011
	Acyltransferases (ACT)			3AT	Rinaldo et al., 2015
	leucoanthocyanidin reductase (LAR)	2	Bogs et al.,2005;2007		
	anthocyanidin reductase (ANR)	1	Bogs et al.,2005;2007		
	3-O-glucosyltransferase (GT)	240	Ono et al.,2010	GT1 = UGFT	Parageetal.,2012
transporter genes					
	glutathione S-transferase (GST)	6	Kitamurs et al.,2004; Conn et al.,2008	GST4	Conn et al.,2008
	anthoMATE (AM)	3	Gomez et al., 2009		
	ATP binding cassette (ABCC)	26	Francisco et al.,2013	ABCC1	Francisco et al.,2013
	Glutathione(GSH)	2	Francisco et al.,2013	GSH1,GSH2	Francisco et al.,2013

Table III-5. List of gene related to anthocyanin biosynthesis in grape.

RNA-SEQ results were then analyzed, focusing on these selected genes, in order to investigate the effect of zebularine on their expression. The expression of the anthocyanin-related genes identified as DEGs is illustrated in Figure III-15, revealing that a large number of structural genes are deregulated in the presence of zebularine.

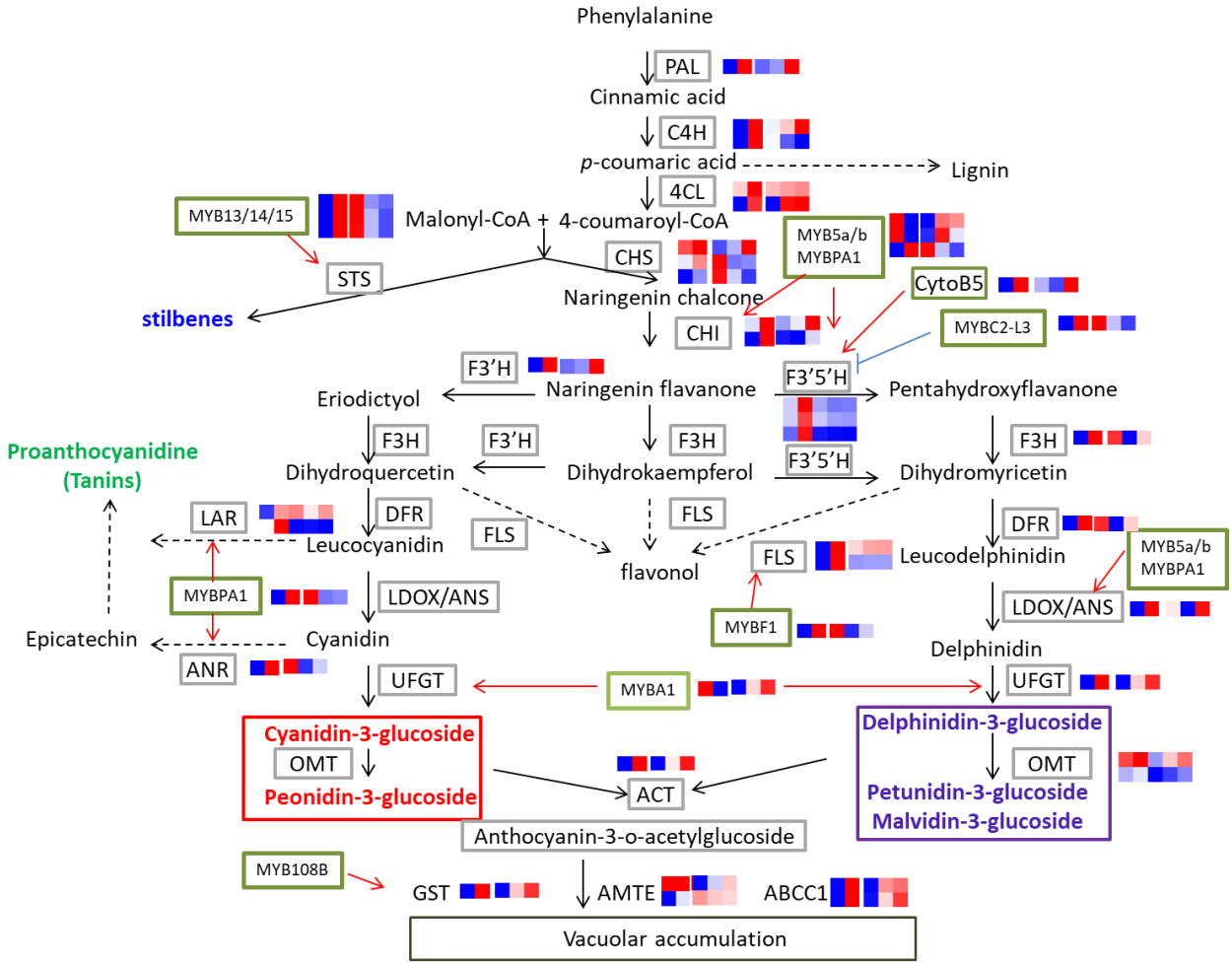

Figure III-15. Effect of zebularine on the transcript abundances of structural, regulatory, and transporter genes involved in anthocyanin biosynthesis grown in light and dark. Gene names are indicated in the text.

In the light, all structural genes are upregulated, although only part of them are induced in a significant manner (4CL2, CHS1, CHS2, CHI2, F3'5'H5, F3'5'H9, F3'5'H10, F3H1, LDOX). The other ones (PAL1, C4H1, C4H3, CHS3, DFR1, UFGT) were induced but not in a significant way (adj P value > 0.05). In addition two genes (out of three) coding for 4-CL (4CL3 and 4CL9) were down-regulated by zebularine. Only one regulatory gene, MYBPA1, was significantly induced by zebularine (log2FC=4) in the light. MYBPA1 which is highly expressed in grape berries, was shown to induce several genes of the flavonoid pathway (CHI, F3'5'H and LDOX/ANS), in addition to genes specifically involves in condensed tannins synthesis (ANR, LAR) (Bogs et al., 2007), therefore appearing as a main regulator of condensed tannins synthesis during fruit development. Interestingly, all the genes characterized as MYBPA1 targets (Bogs et al., 2007) are induced by zebularine in our experiment, suggesting that tannins are overproduced in response to zebularine treatment in the light. Intriguingly, MYBA1, which is known to directly up-regulate UFGT transcription, hence anthocyanin production, is not up-regulated. The comparison of the expression levels suggests on the contrary MYBA1 down-regulation by zebularine in the light, albeit in a non-significant manner. Accordingly UFGT expression was not dramatically induced (1.8 fold change).

Most of the structural genes upregulated in the light were also upregulated in the dark, except for two exceptions, F3'5'H and F3H encoding genes (Figure III-15), which are very lowly expressed in the dark without any substantial difference in the presence of zebularine. Interestingly these two enzymes are responsible for the synthesis of the tri-hydroxylated anthocyanins, at the expense of the di-hydroxylated forms. Accordingly, only di-hydroxylated anthocyanins were detected in dark (cyanidin and peonidin). In general, the expression increase was less marked in the dark than in the light, and only four genes were significantly upregulated in the dark (PAL1, C4H3, 4CL2, UFGT). Interestingly UFGT was highly induced by zebularine in the dark (13 fold increase), concomitantly with the up-regulation of the MYBA1 gene (4 fold change).

Another regulator of anthocyanin biosynthesis is cytochrome b5 (CytoB5) which was shown to modulate the expression of F3'5'H. Moreover CytoB5 gene expression was highly correlated to the content of anthocyanins, (de Vetten et al., 1999; Guan et al., 2016). In our RNA-seq data, CytoB5 was induced by zebularine in light and dark, although very weakly. Interestingly a few other transcription factors known to modulate flavonoid biosynthesis are deregulated by zebularine, but differently in the dark and in the light. Hence MYB13, MYB14, MYB15, related to the stilbene biosynthesis (Cavallini et al., 2015; Wong et al., 2016), MYBF1 and MYBC2-L3, regulating the expression of CHS, CHI and FLS4 (Fujita et al., 2006; Czemmel et al., 2009), and MYBC2-L3, repressing the expression of F3'5'H are all induced by zebularine in the light and repressed by zebularine in the dark.

O-methyltransferases (OMTs) have been shown to modulate the methylation of anthocyanins in grape.
As indicated in chapter 2, four OMT genes have been identified in the grape genome that encode proteins with different functions (chapter2, page93). The expression level of *OMT3* and *OMT4* was low and did not change after zebularine treatment. In contrast, both *OMT1* and *OMT2* were upregulated in zebularine treated cells, at different levels. After zebularine treatment, *OMT1* and *OMT2* expression level increased respectively, 1.9 and 1.6 fold in the light, and 10.5 and 6 fold in the dark.

Genes encoding enzymes involved in anthocyanin acylation (as indicated in chapter 2, page 93) were clearly impacted by zebularine treatments. The gene *Vv3AT* (*Vitvi03g01816*) which encodes a key enzyme associated to anthocyanin acylation in grape (Rinaldo et al., 2015), was significantly up-regulated by zebularine in light and dark grown cells. As for UGFT and OMT1/2, 3AT zebularine effect in dark grown cell was stronger (4.6 fold increase) than in light grown cell (1.6 fold increase). These observations suggested that the zebulairne impact on the expression of anthocyanin modifications related genes was stronger in the dark than in the light.But it also reflects two distinct stiuations: in the light the modification corresponds to an increase in th expression of genes which are also expressed without the drug, whereas in the dark it corresponds to the induction of the expression of genes which are barely expressed in the absence of zebularine.

Two main mechanisms, depending on species, have been suggested to be involved in the vacuolar transport of anthocyanins (Hao et al., 2015). They involve either ABCC1 or antho-MATE transporters (AM) that both seems to require glutathione-S-transferases (GST). Among the 26 ABCC genes identified in the grape genome, *ABCC1* encodes a protein involved in the transport of malvidin 3-Oglucoside in the

presence of GSH (Francisco et al., 2013). However, in GT cell only *ABCC14* (*Vitvi02g00081*) and *ABCC23* (*Vitvi19g00641*) were upregulated after zebularine treatment both in light and dark grown cells and the *GSH1* and G*SH2* were not affected by zebularine. Considering the MATE system, which was shown to specifically transport acylated forms of anthocyanins (Gomez et al., 2009), the AM2 gene was significantly induced in dark and AM3 in light. GST is required for the transport of all type of anthocyanin (see part 2). Finally, only *GST4* (*Vitvi04g00880*), among the 6 genes encoding GST in grape was significantly induced after zebularine treatment both in light and dark grown cells, suggesting it play a vital role in anthocyanin transport, as previously reported (Conn et al., 2008).

Altogether these results show that the stimulation of anthocyanin accumulation by zebularine corresponds to the up-regulation of several structural and regulatory genes. In particular *UFGT* expression was highly correlated with the cell anthocyanin content: in the light *UFGT* expression was multiplied by 1.8 for a 1.55 fold increase in the anthocyanin content; whereas in the dark *UFGT* expression was multiplied by 13 for a 16 fold increase in the anthocyanin content.

3.3.5 McrBC-PCR analyses suggest a low impact of zebularine on DNA methylation

The impact of zebularine treatments on DNA methylation levels was analyzed using an McrBC-PCR approach and targeting three selected loci, the retrotransposon GRET1 (Kobayashi 2004), and promoters of UFGT and MYBA2 (Figure III-15). These two genes were selected because they are related to anthocyanin biosynthesis and they were shown to be upregulated by zebularine and RG108 in preliminary experiments performed in the light. Furthermore a few genes coding for MYB transcription factors have been shown to be regulated by DNA methylation ((El-Sharkawy, Liang, & Xu, 2015b). Each promoter was analyzed using three to four different primer pairs (supplementary Table III-7) enabling the amplification of contiguous DNA fragments of 500 to 1000 base pairs.

GRET1 was entirely digested by McrBC both in dark and light grown cells: none of three GRET1 sequences could be amplified after digestion. This suggested that GRET1 is highly methylated, as expected for a repeated sequence.

UFGT promoter was partially digested by McrBC on a 999 bp long portion located 1779 bp upstream from the ATG initiator codon. Interestingly the digestion was more efficient for the dark grown cells, compared to the light grown cells, suggesting that UFGT methylation level is different depending on the light condition, with a lower methylation level in the presence of light. This difference in the level of methylation at UFGT promoter correlates well with the enhanced UFGT expression in the light (X30 in our RNA-SEQ experiment).

Whereas MYBA2 promoter could not be digested by McrBC on its most proximal region (from ATG to –1112 bp) (data not shown), our results demonstrated a susceptibility to McrBC for more distal regions (between –1112 and –1707 bp), with similar profiles for light and dark grown cells (Figure III-16).

Of note, the comparison of the different treatments (water, DMSO, RG108 or zebularine) did not show any clear difference in McrBC susceptibility for none of the loci tested, except for MYBA2 promoter. Indeed the results revealed a slight difference in the intensity of MYBA2 fragment after McrBC-PCR between the DMSO controls and the zebularine treated samples, with a higher amplification for zebularine treated samples (see the stars on Figure III-16). This difference suggests that MYBA2 promoter could be less methylated in zebularine treated cells. But this observation was made only in two replicates: one third replicate showed no difference between DMSO and zebularine treated cells, suggesting a stochastic effect of zebularine on this gene.

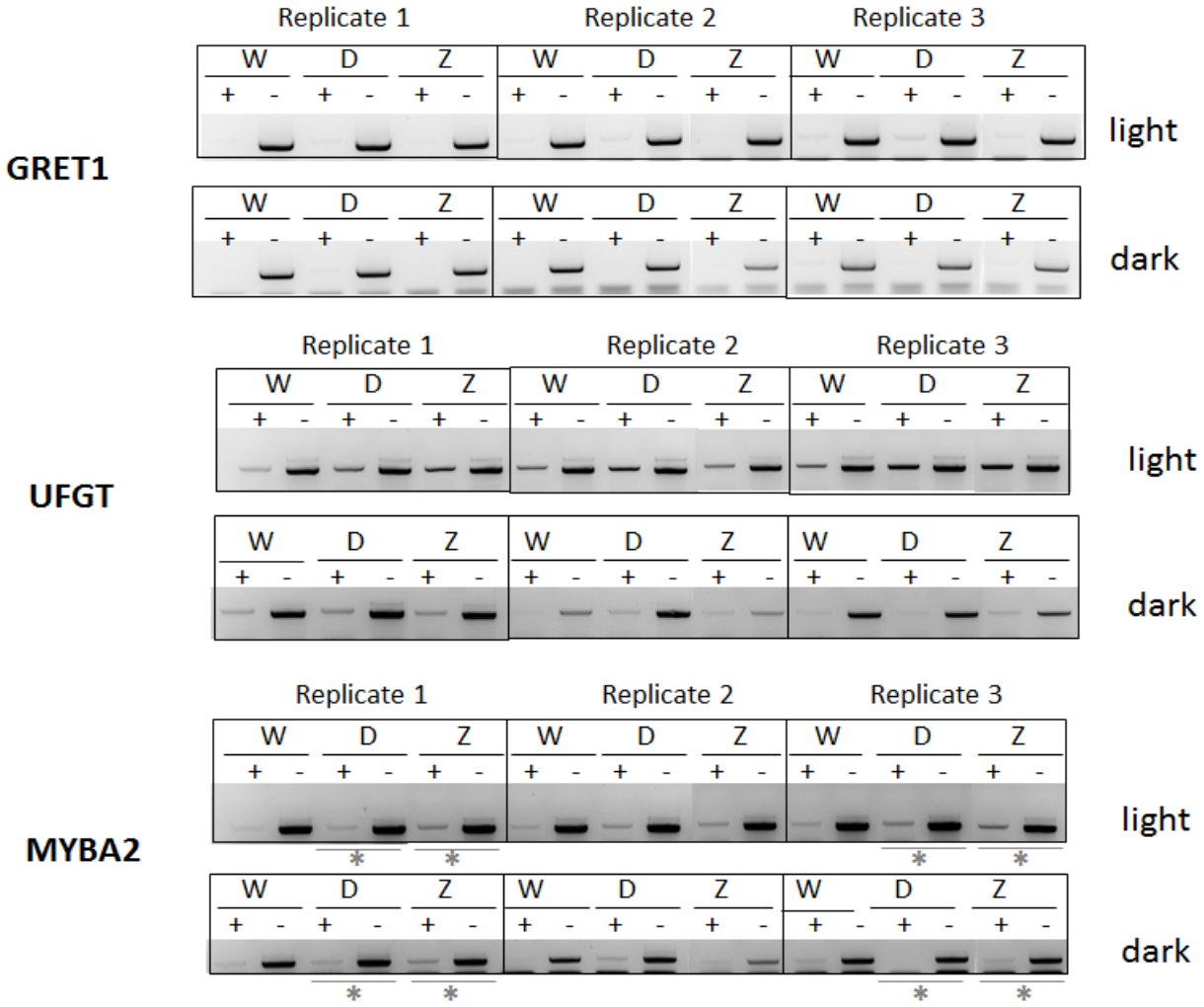

Figure III-16. McrBc-PCR analysis of the gDNA of Gamay teinturier cells grown in the light and in the dark, in the presence of zebularine. The results of three experiments performed on three independent cultures in the dark and three independent cultures in the light are presented. Three different loci were analyzed, GRET1 retrotransposon, UFGT promoter and MYBA2 promoter. For UFGT, the PCR primers were designed for the amplification of a 999 bp long portion of the promoter starting 1779 bases upstreaming from the ATG initiator codon. For MYBA2, the amplified fragment corresponds to a 648 bp long sequence starting 1058 bases upstream from the ATG initiator codon. The stars indicate the results which suggest a difference in methylation between the DMSO control and the corresponding zebularine-treated sample. W ; D and Z indicate the three different conditions used for the cell cultures : W : nothing was added to the growth medium; D : DMSO was added to the growth medium; Z : zebularine (solubilized in DMSO) was added to the growth medium.

Altogether these McrBC analyses suggest that the impact of zebularine on DNA methylation in GT cells is very limited. As an illustration no decrease in the methylation level of the GRET1 retrotransposon could be detected. Nevertheless these analyses also suggest that zebularine may reduce the methylation level at some loci, as for example MYBA2. However the identity of the loci affected by zebularine may not be the same in independent cell cultures, as its effects is random at the genomic level and all cells may not be affected similarly.

Conclusion

The present study provided new insights into the regulation of anthocyanin biosynthesis by light and zebularine.

Grape cell suspensions (vitis vinifera L. cv Gamay teinturier) were used in order to analyze the impact of a hypomethylating drug, zebularine, on anthocyanin biosynthesis in the light and in the dark. As expected, light was shown to be required for grape anthocyanin biosynthesis. Interestingly the analysis of the DNA methylation at the UFGT promoter revealed a difference in the methylation level depending on the light/dark conditions: the much higher expression of UFGT in the light was correlated with a lower methylation level at its promoter region, suggesting that DNA methylation may participate in the light-dependent regulation of this gene. Zebularine treatment furthermore increased anthocyanin accumulation in the light, whereas it induced anthocyanin accumulation in the dark. In both cases zebularine effect on anthocyanin production was correlated with the upregulation of different anthocyanin synthesis related genes. In contrast, no clear change in DNA methylation were detected by McrBC-PCR analyses, although three different loci linked to anthocyanin synthesis were tested: UFGT, MYBA1, and MYBA2 promoter regions. Only MYBA2 was associated with a slight decrease in DNA methylation. Although it cannot be excluded that other loci are associated with a significant decrease in DNA methylation, these results suggest that the upregulation of the anthocyanin biosynthesis pathway may not be directly linked to the hypomethylating effect of the zebularine. Indeed our analysis of the methylation status of the grape retrotransposon GRET1 suggests a rather low impact of zebularine on the global DNA methylation level. Indeed GRET1 methylation level was very high both in control and zebularine treated cells. The measure of the global genomic DNA methylation level would be however necessary in order to better assess zebularine hypomethylating effects in the gamay teinturier cells.

Whereas the impact of zebularine on the methylation state of anthocyanin-related genes appeared limited, the characterization of cell growth parameters and the analysis of cell metabolic content and transcriptomes suggested that the drug strongly impacts cell physiology especially in the light. Notably zebularine treatments impairs cell growth both in light and dark. But its impact on the cell metabolic status, as evaluated by the quantification of soluble sugars and major organic acids, is much stronger in the light than in the dark. Indeed in the light the addition of zebularine resulted in a strong increase in both fructose and glucose cell content, as well as major changes in malic and tartaric acid concentrations. In contrast in the dark only the content in malic and tartaric acid was modified. Furthermore malic and tartaric acid concentrations were modified to a lesser extent than in the light. These results suggest that the addition of zebularine in the light impacts the cell nutritional status. This conclusion was further

supported by the RNA-seq analysis. Indeed the transcriptome of the control light grown cells is reminiscent of the transcriptome of Arabidopsis suspension culture cells submitted to sucrose starvation, as described by Contento et al, 2004. Furthermore several genes highly expressed in the control light grown cells have been characterized as induced by low nutrient availability. Carbon starvation in light grown control cells would be consistent with the cell growth stage at the sampling point: the analysis was done 12 days after sub-culturing, at a time when the soluble sugars in the medium and the cells have been probably entirely consumed. By contrast light grown zebularine treated cells do not exhibit the same characteristics, suggesting that their carbon source has not been completely depleted. This would be consistent with the reduced cell growth kinetic in the presence of the drug. Interestingly our results suggest that the impact of zebularine on the cell nutritional status is much more limited in the dark than in the light. Indeed in the dark the metabolic and transcriptomic characteristics of control and zebularine treated cells are not so dissimilar. This could be linked to the lower number of cells growing in the dark than in the light which may result in a slower rate of sucrose consumption in the dark than in the light, so that dark grown cells may not suffer from carbon starvation at the harvest time with or without zebularine. Altogether these observations may explain why the PCA analysis of the transcriptomic data indicated that “zebularine makes light grown cells resemble dark grown cells”.

Another feature shared between light and dark grown cells treated with zebularine, is the specific induction of a large number of stress-related genes and more particularly of genes linked to oxidative stress and DNA damage responses. Zebularine genotoxic effects were previously reported by (Liu et al., 2015), although the exact nature of the DNA damages induced by zebularine are not known. Because anthocyanins were shown to be produced in response to a wide variety of environmental stress, it can be speculated that the induction of anthocyanin biosynthesis could be partly linked to the stress response elicited by zebularine.

Chapter III Supplementary Material

sample_name	Input Read Pairs	Both Surviving	Both Surviving%	Dropped	Dropped%
D_D-1	11704954	11047836	94.39	9714	0.08
D_D-2	12306562	11602603	94.28	11249	0.09
D_D-3	15312015	14665464	95.78	9668	0.06
D_Z20-1	11883040	11384925	95.81	8307	0.07
D_Z20-2	10198145	9742706	95.53	10319	0.1
D_Z20-3	12527731	11970228	95.55	9574	0.08
D_Z50-1	12353388	11748683	95.1	7655	0.06
D_Z50-2	13512700	12944461	95.79	9083	0.07
D_Z50-3	10919113	10401335	95.26	6716	0.06
L_D-1	9542594	9072106	95.07	9166	0.1
L_D-2	10456216	9946607	95.13	6498	0.06
L_D-3	10601470	10099169	95.26	5628	0.05
L_Z50-1	12335911	11578474	93.86	8642	0.07
L_Z50-2	14190093	13484245	95.03	9324	0.07
L_Z50-3	16833915	16110102	95.7	9403	0.06

Table III-6. Summary of RNA seq reads mapped to the reference genome

gene	ID	primer	sequence 5'-3'
VvUGFT	VIT_216s0039g02230	VvUGFT-F1	ACAGAGATTCGTTCACAGC
		VvUGFT-R1	CACCACGAATCTGTCCTA
		VvUGFT-F1	CCTAGGACAGATTCGTGGTG
		VvUGFT-R1	GTTGCCCTAGAGTGTGCTGA
		VvUGFT-F1	GGTTTACTTCGTCCCACCAC
		VvUGFT-R1	ATACAACACCCTCATGTGGAAT
		VvUGFT-F1	TTATTCCACATGAGGGTGTT
		VvUGFT-R1	GGTGAGTAGTAGCAAGAGCA
VvMYBA2	VIT_02s0033g00390	VvMYBA2-F1	AAGCGAAGACGGTCTGATTT
		VvMYBA2-R1	TTTTCGTGAGGCTTTTGAGA
		VvMYBA2-F2	CCTGCTTCTTTCTCACGG
		VvMYBA2-R2	CTAGTTGTAAGACTGTAGACCC
		VvMYBA2-F3	AATAACAACTCTCCGGGC
		VvMYBA2-R3	AATCGGCGTGTATTATTGGT
		VvMYBA2-F4	CCAAATAGGGTTTAACCCTCC
		VvMYBA2-R4	ATCTGTTGCTTGGGACGT
VvGRET1	AB242301	VvGRET1-F	GGATTCCCTTAAGGATACGCA
		VvGRET1-R	CCAGGTATTAAGAAGTTACCAGGA

Table III-7. List of primer sequences used in McrC-PCR analysis.

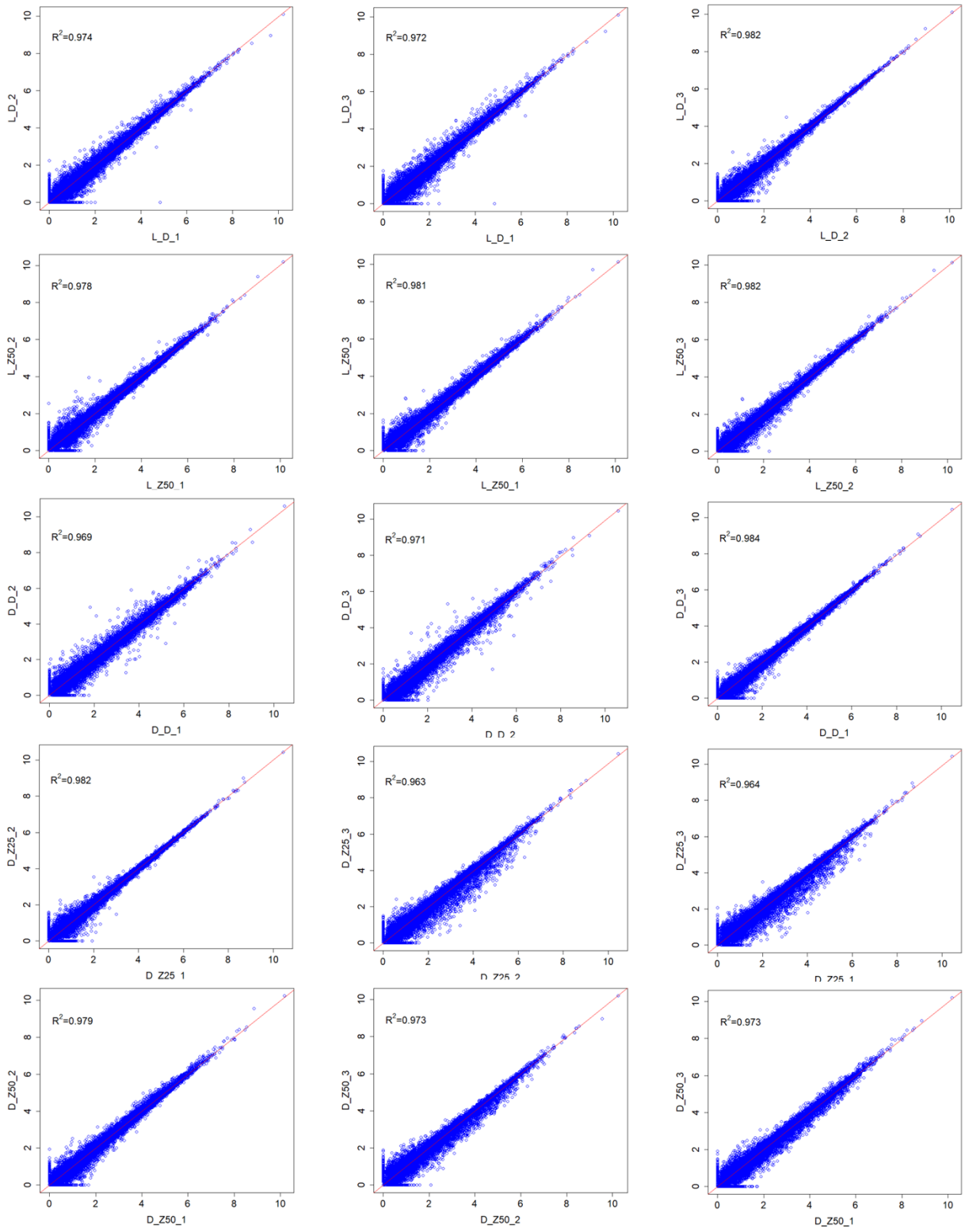

Figure III-17. correlation analysis of RNA seq data between 3 replicates

Chapter III References

Alford, S. R., Rangarajan, P., Williams, P., & Gillaspy, G. E. (2012). *myo -Inositol oxygenase is required for responses to low energy conditions in Arabidopsis thaliana*. *3*(April), 1–11. https://doi.org/10.3389/fpls.2012.00069

Azuma, A., & Yakushiji, H. (2012). *Flavonoid biosynthesis-related genes in grape skin are differentially regulated by temperature and light conditions*. 1067–1080. https://doi.org/10.1007/s00425-012-1650-x

Azuma, A., Yakushiji, H., Koshita, Y., & Kobayashi, S. (2012). Flavonoid biosynthesis-related genes in grape skin are differentially regulated by temperature and light conditions. *Planta*, *236*(4), 1067–1080. https://doi.org/10.1007/s00425-012-1650-x

Baena-González, E., Rolland, F., Thevelein, J. M., & Sheen, J. (2007). A central integrator of transcription networks in plant stress and energy signalling. *Nature*, *448*(7156), 938–942. https://doi.org/10.1038/nature06069

Baubec, T., Pecinka, A., Rozhon, W., & Scheid, O. M. (2009). *Effective , homogeneous and transient interference with cytosine methylation in plant genomic DNA by zebularine*. 542–554. https://doi.org/10.1111/j.1365-313X.2008.03699.x

Bouyer, D., Heese, M., Chen, P., Harashima, H., Roudier, F., Grüttner, C., & Schnittger, A. (2018). *Genome-wide identification of RETINOBLASTOMA RELATED 1 binding sites in Arabidopsis reveals novel DNA damage regulators*. *PLoS Genetics* (Vol. 14). https://doi.org/10.1371/journal.pgen.1007797

Bogs, J., Jaffe, F. W., Takos, A. M., Walker, A. R., & Robinson, S. P. (2007). The Grapevine Transcription Factor VvMYBPA1 Regulates Proanthocyanidin Synthesis during Fruit Development. *Plant Physiology*, *143*(3), 1347–1361. https://doi.org/10.1104/pp.106.093203

Bolger, A. M., Lohse, M., & Usadel, B. (2014). *Genome analysis Trimmomatic : a flexible trimmer for Illumina sequence data*. *30*(15), 2114–2120. https://doi.org/10.1093/bioinformatics/btu170

Boss, P, K, Davies, C, & Robinson, S, P. (1996). Expression of anthocyanin biosynthesis pathway genes in red and white grapes. *Plant Molecular Biology*, *32*(3), 565–569.

Boss, P. K., & Thomas, M. R. (2002). Association of dwarfism and floral induction with a grape "green revolution" mutation. *Nature*, *416*(6883), 847–850. https://doi.org/10.1038/416847a

Canaguier, A., Grimplet, J., Di Gaspero, G., Scalabrin, S., Duchêne, E., Choisne, N., … Adam-Blondon, A.-F. (2017). A new version of the grapevine reference genome assembly (12X.v2) and of its annotation (VCost.v3). *Genomics Data*, *14*(September), 56–62. https://doi.org/10.1016/j.gdata.2017.09.002

Champion, C., Guianvarc'h, D., Sénamaud-Beaufort, C., Jurkowska, R. Z., Jeltsch, A., Ponger, L., … Guieysse-Peugeot, A. L. (2010). Mechanistic insights on the inhibition of C5 DNA methyltransferases by zebularine. *PLoS ONE*, *5*(8). https://doi.org/10.1371/journal.pone.0012388

Cheng, J., Niu, Q., Zhang, B., Chen, K., Yang, R., Zhu, J.-K., … Lang, Z. (2018). Downregulation of RdDM during strawberry fruit ripening. *Genome Biology*, *19*(1), 212. https://doi.org/10.1186/s13059-018-1587-x

Dai, Z. W., Meddar, M., Renaud, C., Merlin, I., Hilbert, G., Delrot, S., & Gomès, E. (2014). *Long-term in vitro culture of grape berries and its application to assess the effects of sugar supply on anthocyanin accumulation*. *65*(16), 4665–4677. https://doi.org/10.1093/jxb/ert489

Dimitrovska, M., Bocevska, M., Dimitrovski, D., & Murkovic, M. (2011). Anthocyanin composition of Vranec, Cabernet Sauvignon, Merlot and Pinot Noir grapes as indicator of their varietal differentiation. *European Food Research and Technology*, *232*(4), 591–600. https://doi.org/10.1007/s00217-011-1425-9

DOWNEY, M. O., HARVEY, J. S., & ROBINSON, S. P. (2008). The effect of bunch shading on berry development and flavonoid accumulation in Shiraz grapes. *Australian Journal of Grape and Wine Research*, *10*(1), 55–73. https://doi.org/10.1111/j.1755-0238.2004.tb00008.x

Duan, J., Zhang, M., Zhang, H., Xiong, H., Liu, P., Ali, J., … Li, Z. (2012). OsMIOX, a myo-inositol oxygenase gene, improves drought tolerance through scavenging of reactive oxygen species in rice (Oryza sativa L.). *Plant Science*, *196*, 143–151. https://doi.org/10.1016/j.plantsci.2012.08.003

El-Sharkawy, I., Liang, D., & Xu, K. (2015a). Transcriptome analysis of an apple (Malus × domestica) yellow fruit somatic mutation identifies a gene network module highly associated with anthocyanin and epigenetic regulation. *Journal of Experimental Botany*, *66*(22), 7359–7376. https://doi.org/10.1093/jxb/erv433

El-Sharkawy, I., Liang, D., & Xu, K. (2015b). Transcriptome analysis of an apple (Malus × domestica) yellow fruit somatic mutation identifies a gene network module highly associated with anthocyanin and epigenetic regulation. *Journal of Experimental Botany*, *66*(22), 7359–7376. https://doi.org/10.1093/jxb/erv433

Falginella, L., Di Gaspero, G., & Castellarin, S. D. (2012). Expression of flavonoid genes in the red grape berry of "Alicante Bouschet" varies with the histological distribution of anthocyanins and their chemical composition. *Planta*, *236*(4), 1037–1051. https://doi.org/10.1007/s00425-012-1658-2

Feng, F., Li, M., Ma, F., & Cheng, L. (2013). Phenylpropanoid metabolites and expression of key genes involved inanthocyanin biosynthesis in the shaded peel of apple fruit in response to sun exposure. *Plant Physiology and Biochemistry*, *69*, 54–61. https://doi.org/10.1016/j.plaphy.2013.04.020

Fernandez, O., Vandesteene, L., Feil, R., Baillieul, F., Lunn, J. E., & Clément, C. (2012). Trehalose metabolism is activated upon chilling in grapevine and might participate in Burkholderia phytofirmans induced chilling tolerance. *Planta*, *236*(2), 355–369. https://doi.org/10.1007/s00425-012-1611-4

Francisco, R. M., Regalado, A., Ageorges, A., Burla, B. J., Bassin, B., Eisenach, C., … Nagy, R. (2013). ABCC1, an ATP Binding Cassette Protein from Grape Berry, Transports Anthocyanidin 3- O -Glucosides . *The Plant Cell*, *25*(5), 1840–1854. https://doi.org/10.1105/tpc.112.102152

Fujiki, Y., Yoshikawa, Y., Sato, T., Inada, N., Ito, M., Nishida, I., & Watanabe, A. (2001). Dark-inducible genes from Arabidopsis thaliana are associated with leaf senescence and repressed by sugars. *Physiologia Plantarum*, *111*(3), 345–352. https://doi.org/10.1034/j.1399-3054.2001.1110312.x

Gagné, S., Cluzet, S., Mérillon, J. M., & Gény, L. (2011). ABA Initiates Anthocyanin Production in Grape Cell Cultures. *Journal of Plant Growth Regulation*, *30*(1), 1–10. https://doi.org/10.1007/s00344-010-9165-9

Gambetta, G. A., Matthews, M. A., Shaghasi, T. H., McElrone, A. J., & Castellarin, S. D. (2010). Sugar and abscisic acid signaling orthologs are activated at the onset of ripening in grape. *Planta*, *232*(1), 219–234. https://doi.org/10.1007/s00425-010-1165-2

Gao, Z., Li, Q., Li, J., Chen, Y., Luo, M., Li, H., … Ma, C. (2018). Characterization of the ABA Receptor VlPYL1 That Regulates Anthocyanin Accumulation in Grape Berry Skin. *Frontiers in Plant Science*, *9*(May), 1–14. https://doi.org/10.3389/fpls.2018.00592

Gomez, C., Terrier, N., Torregrosa, L., Vialet, S., Fournier-Level, A., Verries, C., … Ageorges, A. (2009). Grapevine MATE-Type Proteins Act as Vacuolar H+-Dependent Acylated Anthocyanin Transporters. *Plant Physiology*, *150*(1), 402–415. https://doi.org/10.1104/pp.109.135624

Griffin, P. T., Niederhuth, C. E., & Schmitz, R. J. (2016). A Comparative Analysis of 5-Azacytidine- and Zebularine-Induced DNA Demethylation. *G3 (Bethesda, Md.)*, *6*(9), 2773–2780. https://doi.org/10.1534/g3.116.030262

Guan, L., Dai, Z., Wu, B. H., Wu, J., Merlin, I., Hilbert, G., … Delrot, S. (2016). Anthocyanin biosynthesis is differentially regulated by light in the skin and flesh of white-fleshed and teinturier grape berries. *Planta*, *243*(1), 23–41. https://doi.org/10.1007/s00425-015-2391-4

He, F., Mu, L., Yan, G. L., Liang, N. N., Pan, Q. H., Wang, J., … Duan, C. Q. (2010). Biosynthesis of anthocyanins and their regulation in colored grapes. *Molecules*, *15*(12), 9057–9091. https://doi.org/10.3390/molecules15129057

He, X. J., Chen, T., & Zhu, J. K. (2011). Regulation and function of DNA methylation in plants and animals. *Cell Research*, *21*(3), 442–465. https://doi.org/10.1038/cr.2011.23

Huang, H., Liu, R., Niu, Q., Tang, K., Zhang, B., Zhang, H., … Lang, Z. (2019). Global increase in DNA methylation during orange fruit development and ripening. *Proceedings of the National Academy of Sciences*, *116*(4), 1430 LP – 1436. https://doi.org/10.1073/pnas.1815441116

J.C., C., C.B., M., F.A., G., W., Y., S., G., V.E., M., … E.U., S. (2003). Inhibition of DNA methylation and reactivation of silenced genes by zebularine. *Journal of the National Cancer Institute*, *95*(5), 399–409. Retrieved from http://www.embase.com/search/results?subaction=viewrecord&from=export&id=L36395260

Jeong, S. T., Goto-Yamamoto, N., Kobayashi, S., & Esaka, M. (2004). Effects of plant hormones and shading on the accumulation of anthocyanins and the expression of anthocyanin biosynthetic genes in grape berry skins. *Plant Science*, *167*(2), 247–252. https://doi.org/10.1016/j.plantsci.2004.03.021

Kim, D., Langmead, B., & Salzberg, S. L. (2016). *HHS Public Access*. *12*(4), 357–360. https://doi.org/10.1038/nmeth.3317.HISAT

Kitamura, S., Shikazono, N., & Tanaka, A. (2004). TRANSPARENT TESTA 19 is involved in the accumulation of both anthocyanins and proanthocyanidins in Arabidopsis. *Plant Journal*, *37*(1), 104–114. https://doi.org/10.1046/j.1365-313X.2003.01943.x

Kobayashi, S., Goto-Yamamoto, N., & Hirochika, H. (2004a). Retrotransposon-Induced Mutations in Grape Skin Color. *Science*, *304*(5673), 982. https://doi.org/10.1126/science.1095011

Kobayashi, S., Goto-Yamamoto, N., & Hirochika, H. (2004b). Retrotransposon-Induced Mutations in Grape Skin Color. *Science*, *304*(5673), 982. https://doi.org/10.1126/science.1095011

Kuhn, N., Guan, L., Dai, Z. W., Wu, B. H., Lauvergeat, V., Gomès, E., … Delrot, S. (2014). Berry ripening: Recently heard through the grapevine. *Journal of Experimental Botany*, *65*(16), 4543–4559. https://doi.org/10.1093/jxb/ert395

Lang, Z., Wang, Y., Tang, K., Tang, D., Datsenka, T., Cheng, J., … Zhu, J.-K. (2017). Critical roles of DNA demethylation in the activation of ripening-induced genes and inhibition of ripening-repressed genes in tomato fruit. *Proceedings of the National Academy of Sciences of the United States of America*, *114*(22), E4511–E4519. https://doi.org/10.1073/pnas.1705233114

Lecourieux, F., Kappel, C., Pieri, P., Charon, J., & Pillet, J. (2017). *Dissecting the Biochemical and Transcriptomic Effects of a Locally Applied Heat Treatment on Developing Cabernet Sauvignon Grape Berries*. *8*(January). https://doi.org/10.3389/fpls.2017.00053

Liu, C.-H., Finke, A., Díaz, M., Rozhon, W., Poppenberger, B., Baubec, T., & Pecinka, A. (2015). Repair of DNA Damage Induced by the Cytidine Analog Zebularine Requires ATR and ATM in Arabidopsis. *The Plant Cell*, *27*(6), 1788–1800. https://doi.org/10.1105/tpc.114.135467

Liu, R., How-Kit, A., Stammitti, L., Teyssier, E., Rolin, D., Mortain-Bertrand, A., … Gallusci, P. (2015). A DEMETER-like DNA demethylase governs tomato fruit ripening. *Proceedings of the National Academy of Sciences*, *112*(34), 10804–10809. https://doi.org/10.1073/pnas.1503362112

Liu, Y., Tikunov, Y., Schouten, R. E., Marcelis, L. F. M., Visser, R. G. F., & Bovy, A. (2018). Anthocyanin Biosynthesis and Degradation Mechanisms in Solanaceous Vegetables: A Review. *Frontiers in Chemistry*, *6*(March). https://doi.org/10.3389/fchem.2018.00052

López-Hernández, J., Paseiro-Losada, P., Sanches-Silva, A. T., & Lage-Yusty, M. A. (2007). Study of the changes of trans-resveratrol caused by ultraviolet light and determination of trans- and cis-resveratrol in Spanish white wines. *European Food Research and Technology*, *225*(5–6), 789–796. https://doi.org/10.1007/s00217-006-0483-x

Mattivi, F., Guzzon, R., Vrhovsek, U., Stefanini, M., & Velasco, R. (2006). Metabolite profiling of grape: Flavonols and anthocyanins. *Journal of Agricultural and Food Chemistry*, *54*(20), 7692–7702. https://doi.org/10.1021/jf061538c

Michael, I., Huber, W., Anders, S., Love, M. I., Huber, W., & Anders, S. (2014). *Moderated estimation of fold change and dispersion for RNA-seq data with DESeq2 Moderated estimation of fold change and dispersion for RNA-seq data with DESeq2*. https://doi.org/10.1186/s13059-014-0550-8

Munné-Bosch, S. (2007). α-Tocopherol: A Multifaceted Molecule in Plants. *Vitamins and Hormones*, *76*(07), 375–392. https://doi.org/10.1016/S0083-6729(07)76014-4

Nishizawa, A., Yabuta, Y., & Shigeoka, S. (2008). Galactinol and Raffinose Constitute a Novel Function to Protect Plants from Oxidative Damage. *Plant Physiology*, *147*(3), 1251–1263. https://doi.org/10.1104/pp.108.122465

Pereira, G. E., Gaudillere, J. P., Pieri, P., Hilbert, G., Maucourt, M., Deborde, C., … Rolin, D. (2006). Microclimate influence on mineral and metabolic profiles of grape berries. *Journal of Agricultural and Food Chemistry*, *54*(18), 6765–6775. https://doi.org/10.1021/jf061013k

Ramel, F., Sulmon, C., Cabello-Hurtado, F., Taconnat, L., Martin-Magniette, M. L., Renou, J. P., … Gouesbet, G. (2007). Genome-wide interacting effects of sucrose and herbicide-mediated stress in Arabidopsis thaliana: Novel insights into atrazine toxicity and sucrose-induced tolerance. *BMC Genomics*, *8*, 1–20. https://doi.org/10.1186/1471-2164-8-450

Reid, K. E., Olsson, N., Schlosser, J., Peng, F., & Lund, S. T. (2006). An optimized grapevine RNA isolation procedure and statistical determination of reference genes for real-time RT-PCR during berry development. *BMC Plant Biology*, *6*, 1–11. https://doi.org/10.1186/1471-2229-6-27

Renko, M., Sabotič, J., & Turk, D. (2012). β-Trefoil inhibitors - From the work of Kunitz onward. *Biological Chemistry*, *393*(10), 1043–1054. https://doi.org/10.1515/hsz-2012-0159

Rinaldo, A., Cavallini, E., Jia, Y., Moss, S. M. A., McDavid, D. A. J., Hooper, L. C., … Walker, A. R. (2015). A grapevine anthocyanin acyltransferase, transcriptionally regulated by VvMYBA, can produce most acylated anthocyanins present in grape skins. *Plant Physiology*, *169*(November), pp.01255.2015. https://doi.org/10.1104/pp.15.01255

Soubeyrand, E., Basteau, C., Hilbert, G., Van Leeuwen, C., Delrot, S., & Gomès, E. (2014). Nitrogen supply affects anthocyanin biosynthetic and regulatory genes in grapevine cv. Cabernet-Sauvignon berries. *Phytochemistry*, *103*, 38–49. https://doi.org/10.1016/j.phytochem.2014.03.024

Spayd, S. E., Tarara, J. M., Mee, D. L., & Ferguson, J. C. (2002). *Separation of light and temp on Merlot*. *3*(December 2001), 171–182.

Taji, T., Ohsumi, C., Iuchi, S., Seki, M., Kasuga, M., Kobayashi, M., … Shinozaki, K. (2002). Important roles of drought- and cold-inducible genes for galactinol synthase in stress tolerance in Arabidopsis thaliana. *Plant Journal*, *29*(4), 417–426. https://doi.org/10.1046/j.0960-7412.2001.01227.x

Tanaka, R., Oster, U., Kruse, E., Rüdiger, W., & Grimm, B. (2002). Reduced Activity of Geranylgeranyl Reductase Leads to Loss of Chlorophyll and Tocopherol and to Partially Geranylgeranylated Chlorophyll in Transgenic Tobacco Plants Expressing Antisense RNA for Geranylgeranyl Reductase. *Plant Physiology*, *120*(3), 695–704. https://doi.org/10.1104/pp.120.3.695

Takos, A. M., Jaffe, F. W., Jacob, S. R., Bogs, J., Robinson, S. P., & Walker, A. R. (2006). Light-Induced Expression of a MYB Gene Regulates Anthocyanin Biosynthesis in Red Apples. *Plant Physiology*, *142*(3), 1216–1232. https://doi.org/10.1104/pp.106.088104

Tyunin, A. P., Kiselev, K. V., Karetin, Y.A. (2013). Differences in the methylation patterns of the VaSTS1 and VaSTS10 genes of Vitis amurensis Rupr. Biotechnol lett 35:1525-1532.OI 10.1007/S10529-013-1235-1

Usadel, B. (2005). Extension of the Visualization Tool MapMan to Allow Statistical Analysis of Arrays, Display of Coresponding Genes, and Comparison with Known Responses. *Plant Physiology*, *138*(3), 1195–1204. https://doi.org/10.1104/pp.105.060459

Wang, Z., Meng, D., Wang, A., Li, T., Jiang, S., Cong, P., & Li, T. (2013). The methylation of the PcMYB10 promoter is associated with green-skinned sport in Max Red Bartlett pear. *Plant Physiology*, *162*(2), 885–896. https://doi.org/10.1104/pp.113.214700

Wei, Y. Z., Hu, F. C., Hu, G. B., Li, X. J., Huang, X. M., & Wang, H. C. (2011). Differential expression of anthocyanin biosynthetic genes in relation to anthocyanin accumulation in the pericarp of litchi chinensis sonn. *PLoS ONE*, *6*(4). https://doi.org/10.1371/journal.pone.0019455

Xu, J., Wang, X., Cao, H., Xu, H., Xu, Q., & Deng, X. (2017). Dynamic changes in methylome and transcriptome patterns in response to methyltransferase inhibitor 5-azacytidine treatment in citrus. *DNA Research*, *24*(5), 509–522. https://doi.org/10.1093/dnares/dsx021

Yi, D., Alvim Kamei, C. L., Cools, T., Vanderauwera, S., Takahashi, N., Okushima, Y., … De Veylder, L. (2014). The Arabidopsis SIAMESE-RELATED Cyclin-Dependent Kinase Inhibitors SMR5 and SMR7 Regulate the DNA Damage Checkpoint in Response to Reactive Oxygen Species. *The Plant Cell*, *26*(1), 296–309. https://doi.org/10.1105/tpc.113.118943

Zhao, J. (2015). Flavonoid transport mechanisms : how to go , and with whom. *Trends in Plant Science*, *20*(9), 576–585. https://doi.org/10.1016/j.tplants.2015.06.007

Zheng, Y., Li, J. H., Xin, H. P., Wang, N., Guan, L., Wu, B. H., & Li, S. H. (2013). Anthocyanin profile and gene expression in berry skin of two red Vitis vinifera grape cultivars that are sunlight dependent versus sunlight independent. *Australian Journal of Grape and Wine Research*, *19*(2), 238–248. https://doi.org/10.1111/ajgw.12023

CHAPTER IV

General discussion and further work

Part of the discussion below has been used in the conclusion of the book chapter by Kong et al, 2019 "Epigenetic regulation in fleshy fruit: perspective for grape berry development and ripening" in press in "The Grape Genome. 2019 Eds: Dario Cantu & M. Andrew Walker"; https://www.springer.com/gp/product-marketing-tool/flyer/9783030186005?downloadType=PRODUCTFLYER.

Several evidences illustrate the prominent roles of epigenetic regulations in plant development and adaptation to stresses (Ahmad et al., 2010; Chinnusamy et al., 2009). Of particular interest, recent works have demonstrated that both histone PTMs and DNA methylation have important functions in the control of fruit development (see introduction part 1.4.1 and 1.4.2, page 37-44; Bucher et al., 2018; Gallusci et al., 2016a). More particularly, DNA methylation was recently shown to be of critical importance in the control of fruit ripening, although the mechanisms involved vary between plant species. For example in tomato the DNA demethylase *SlDML2* mediates the active demethylation of tomato fruit genomic DNA, a process necessary to tomato fruit ripening (Liu et al., 2015; Lang et al., 2017), whereas in strawberry ripening specific DNA demethylation is controlled by inhibition of *de novo* methylation through the RdDM pathway (Cheng et al., 2018), and in some other cases such as sweet orange it is not DNA demethylation that is associated with fruit ripening, but an increase in genomic DNA methylation (Huang et al., 2019).

When this PhD work was initiated no information about the role of DNA methylation in grape berry was available. Grape berry is a non-climacteric fruit that presents specific developmental features, including a double sigmoid growth curve (Robinson et al, 1992; Conde et al., 2007) and a rather long ripening period that lasts 7 to 8 weeks. It is also characterized by tissues, the skin and the pulp, with distinct metabolite and transcriptomic profiles (Lijavetzky et al., 2012; chapter 2). In the frame of my PhD work, I have investigated (1) the potential role of DNA methylation in controlling grape berry ripening (chapter 2), and eventual differences between the peel and the pulp; (2) the function of DNA methylation in the control of anthocyanin accumulation in grape using a cell culture derived from cells initiated from the berry of Gamay Teinturier (chapter 3). Here below I will discuss the main conclusions of my PhD work and propose further development.

DNA methylation distribution in the grape genome presents typical features of other angiosperms

It has recently been suggested that epigenetic regulations may have much stronger impacts on plant phenotypes and gene expression in crops than in the model plant Arabidopsis (Mirouze & Vitte., 2014; Gallusci et al., 2016a). A diversity of reasons may contribute to this observation including the lower methylation level and transposon content of Arabidopsis as compared to most crops (Lee & Kim, 2014), and differences in genome organization, as for example the distance between genes and transposons (Niederhuth et al., 2016a).

In the present case, the grapevine genome is 450 Mb large, roughly 3.6 times larger than the Arabidopsis genome. It contains more transposons than Arabidopsis (Jaillon et al., 2007), the most striking difference

between the two species being the alternation in grapevines of regions with high and low gene density along chromosomes,and a higher density of transposons nearby genes and within inrtrons.

The Arabidopsis genome is characterized by a rather low methylation level, in average 5.8% (Lister et al., 2008). Recent studies have suggested a correlation between genome size and methylation level. Genome wide methylation levels were calculated to increase by about 1.1% every 100Mbs (Vidalis et al., 2016). Based on this hypothesis, we would expect the methylation level of the grape genome which is 325Mb larger than the Arabidopsis one, to be close to 10% (5.8% + (3.25x1.1)). In accordance with this calculation, we found that the grape fruit genome methylation level was close to 10% in both the peel and the pulp. This is however a bit higher than the 7 to 8% of methylation level previously described for grape leaves (Vidalis et al., 2016)(Niederhuth et al., 2016) and as expected much lower than tomato with 22% of methylation level in fruits and a 900MB large genome (Zhong et al., 2013a).

As expected, the methylation levels of the grape chromosomes are very high in centromeric and pericentromeric regions in all sequence contexts (Figure II-25, page 101, Figure II-26, page 102, Supplymentary data Figure II-34, page 123). These regions are enriched in transposable elements (TEs) and tandem repeats, and are classically the most heavily methylated (Cokus et al., 2008)(Lister et al., 2008)(Seymour et al., 2014), although some variations between plant species were observed (Niederhuth et al., 2016a). High methylation levels at transposons is consistent with 5mC being of primary importance in the control of their activity and is thought to inhibit their transcription (Cui & Cao, 2014). In contrast methylation levels are low in gene rich region (Figure II-25, page 101, Figure II-26, page 102, Supplymentary data Figure II-34, page 123).

In angiosperms, the CG methylation is responsible for the major part of the total genomic DNA methylation (Niederhuth et al., 2016b). We observed a similar situation with 52 to 57.7 % of methylation in the CG context whereas methylation in the CHG context ranged between 26.5% and 31.2% and in the CHH context between 3.9 and 5.4%. Interestingly these values are higher than previous data by Niederhuth et al (2016), who found 44%, 20% and 1.1% of methylation in the CG, CHG and CHH context respectively, and as mentioned above a lower global methylation level. Of note, in tomato the CHH methylation level was also higher in fruits (13.5-14.2%) than in leaves (8.6%). Whether the higher methylation we observed as compare to the work Niederhuth et al (2016) is also due to difference in the organ analyzed (fruits here, versus leaves) is unclear and will require further investigation. However, in contrast to tomato for which the converse was observed in the CHG and CG contexts (Zhong et al., 2013), this is not the case in grape as in all sequence context the methylation level is lower in leaves than in fruits Whereas this is due to different cultivars, growing conditions or reflect differences in the methods is so far unclear.

A classical methylation pattern is observed in transposons in all sequence contexts. It is characterized by an enrichment in methylation within the TE (Figure II-25, page 101, Supplymentary data Figure II-34, page 123). As far as genes are concerned, enrichment in CG methylation was found in gene bodies, a situation that has been described in many plant species now (Niederhuth et al., 2016a). Gene body methylation (GbM) refers to an enrichment in CG methylation associated to depletion in non CG methylation in the transcribed part of genes, and a depletion of all types of methylation at the TSS and

TTS. We have not yet analyzed the relationship between gene expression and CG GbM, but genes with CG methylation in their body are usually constitutively expressed (Zilberman et al., 2007). GbM has been associated with the CMT DNA methylase activity. The grape genome contains four *VvCMT* genes that named *VvCMT1* to *4*. Two of these genes, *VvCMT2* and *VvCMT4* are orthologous to *AtCMT2* and *VvCMT1* and *VvCMT3* are orthologous to *AtCMT1* and *AtCMT3*, respectively (Figure II-10, page 70). All of these genes are expressed in grape berries at low level though (Supplymentary data Figure II-33, page 122).

We also found that grape genes are methylated in the CHG context, with an average methylation of 20%, and the CHH context with a low methylation level, close to 3% (Table II-9, page 104). It remains to be determined whether the same genes contain both CG and non CG methylation within their bodies, or whether these are different gene populations. Indeed, early studies in Arabidopsis have indicated that non CG-GbM is associated with gene repression. However, it has now been described that in many angiosperms non CG methylation also occurs in the body of genes, and can be associated with the presence of TEs within genes. The link between non CG methylation, gene expression and the presence of TEs genes has not been analyzed yet in grape. The distribution of non CG- and CG-GbM will be compared between tissues and developmental stages to determine whether the same genes are concerned. Correlation with gene expression profile will also be performed to determine whether this type of methylation contributes to the tissue and developmental specificity in grape berries.

DNA methylation changes during grape berry ripening are limited and do not correlate with changes in gene expression

In addition to GbM-methylation, DNA methylation also occurs in regulatory regions where it is suspected to play important roles in the control of gene expression (Chan, Henderson, & Jacobsen, 2005). Of course an inverse correlation between DNA methylation in promoters and gene expression has been demonstrated more specifically considering genes with differentially methylated regions in the CHH context (An et al., 2017). In fruits low methylation levels during ripening at promoters of genes has been correlated with their ripening specific induction (Lang et al., 2017b; Liu et al., 2015; Zhong et al., 2013a), but for some of them to their repression as well (Lang et al., 2017b). Hence DNA methylation variations in regulatory regions is likely important for the control of gene expression probably by interfering with transcriptional activators or repressors binding to the DNA (O'Malley et al., 2016).

We have identified Differentially Methylated Regions (DMRs) that are associated with promoters both in pulp and peel during ripening. However their number remains limited as compared to other fruits such as tomato or strawberry. In addition, we could not identify any correlation between gene expression and either increase or decrease in methylation, suggesting that in the conditions tested in this study, and at the stages analyzed DNA methylation does not play a critical role in the control of gene expression. Indeed, correlation analyses were only performed with C-DMRs that do not discriminate between the sequence contexts. We cannot rule out that context specific DMRs, more specifically CHH-DMRs that are enriched in promoter regions as compared to C, CG and CHG DMRs (TableII-7, page 100), are important for the control of gene expression in grape fruits as well. Systematic correlative analysis between DMRs

and gene expression profile will now be performed to determine possible relationship between DMRs type and locations and gene expression. However given the rather limited number of DMRs identified during ripening as compared to other fruits that have been analyzed, it is unclear whether DNA methylation will have a similar role at this developmental transition as previously described in tomato (Lang et al., 2017b), strawberry (Cheng et al., 2018) or sweet orange (Huang et al., 2019). Indeed, *in vitro* experiments using 2 week old young fruits have showed that DNA methyltransferase inhibitors (zebularine, RG108) severely limit ripening, which is consistent with the idea that methylation, rather than demethylation is important for grape fruit ripening. However a similar treatment with older fruits had no such effects and in combination with ABA and DNA methyltransferase inhibitors treatments were shown to accelerate ripening when berries were treated prior to véraison, and had no effect after véraison induction (Chapter2, pages 58-59). These results suggest that DNA methylation has a more complex role in grape fruits than anticipated based on previous work on other fruit crops.

Hence the analyses that were performed in the present study might not have targeted the stages when DNA methylation is the most critical. Additional work is on-going to address more precisely this question. In the frame of a collaboration with the University of Verona (METGRAPE project), I have harvested fruits from Cabernet sauvignon and Pinot Noir during my PhD work, at 4 developmental stages F3, F7, V and V3 (Figure IV-1). This more complete developmental kinetic will be used to analyze variations of DNA methylation in relation with gene expression and changes in small RNA populations in order to better asses potential role of DNA methylation in the pulp during grape berry growth and ripening.

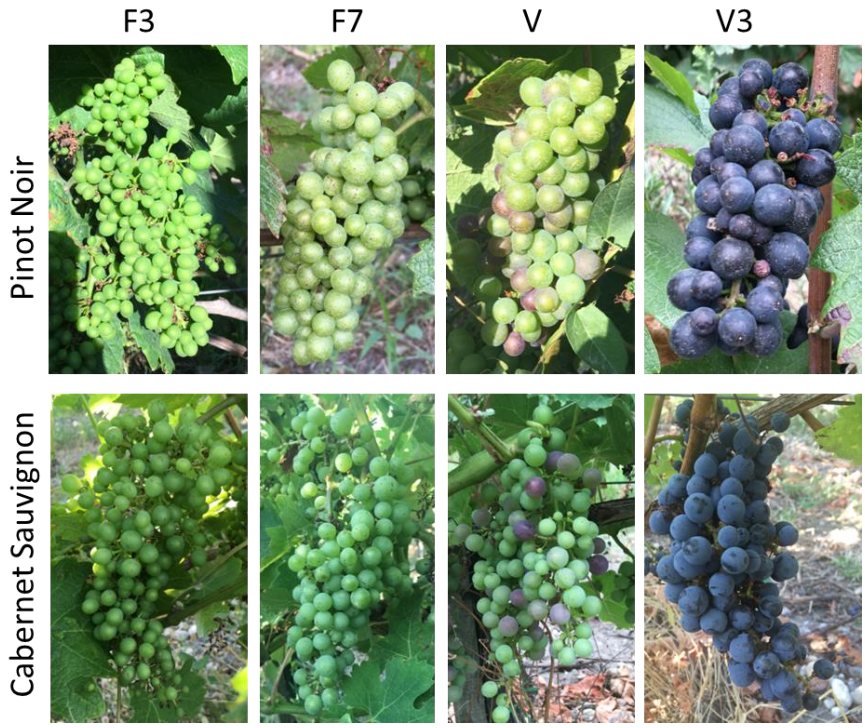

Figure IV-1: Grape berry sample of Pinot Noir and Cabernet Sauvignon at 4 developmental stages, F3, F7, V and V3. F, fruit set; F3, 3 weeks after fruit set; F7, 7 weeks after fruit set; V, Véraison; V3, 3 weeks after Véraison.

Alternatively, we cannot rule out that other epigenetic mechanisms other than DNA methylation are also involved in the control of grape fruit development as histone PTMs are also likely important at various phases of fleshy fruit development (reviewed in (Gallusci et al., 2016b)). So far, evidence of the role of both types of epigenetic marks in grape berries, (in many other fruit crops as well), awaits demonstration. It requires the combination of high throughput sequencing and chromatin immunoprecipitation to shed light on the dynamics of epigenetic marks in fruit. This was illustrated in the fruit ENCODE project (Lü et al., 2018), even though such approaches remain correlative in nature and will required to be completed by functional analysis of corresponding genes. In particular Lü et al have suggested that instead of DNA methylation, the histone mark H3K27me3 could be critical in many fruits, including grape berry. So far, *in silico* analyses conducted on grapevine have identified candidate genes involved in the control of epigenetic marks including 7 HAT, 13 HDAC, 33 HMT and 6 PRC2-like genes (M Berger, EGFV personal communication). Many of these genes are differentially expressed in grape berries(Aquea et al., 2010)(Aquea et al., 2011)(Almada et al., 2011), suggesting that histone PTMs – and more globally, chromatin remodeling – could play a key role in grape fruit development and ripening. Noteworthy, given the clear metabolic and transcriptomic differences observed between the skin and the pulp (see chapter 2), such studies should be performed in each tissue separately.

DNA methyltransferase inhibitors have multiple effects that may not be linked to change in DNA methylation patterns

Studies based on methylome, metabolic and transcriptomic analyses are essentially correlative. Therefore, the demonstration of the role of epigenetic marks in grape berries, as in other plant systems, requires studying the effects of mutations affecting genes that encode epigenetic regulators, including histones writers and erasers, and enzymes involved in DNA methylation control. In grapevine, generation of loss of function mutants is hampered by the difficulty to generate RNAi or Crisper-Cas9 mutation, due to the limited efficiency of plant regeneration processes in this species (Laimer et al., 2007). Indeed experiments to limit the expression of *MET* and *DML* genes have been initiated in the course of my PhD thesis (collaboration with Dr M Malnoy). Constructs specifically targeting either the two *MET* genes or the three DML genes in the grape genomes have been generated (see supplementary Figure IV-3, page 189 and Figure IV-4, page 190) and sent to Dr Malnoy to transform the microwine genotype. However, no plant could be obtained with the *DML* RNAi constructs, whereas only one of the few generated plants using the *MET* RNAi constructs could survive (see Figure IV-2). Further work is going to generate more lines with the microwine genotype and with other cultivars as well.

FigureIV-2: MET1 RNAi plants were generated in Italy (Foundation Edmund Mach, Italy), growing in vitro

However, in parallel we have developed a functional approach based on the use of DNA methylation inhibitors. This approach was tested both on fruits (chapter 2), but also on fruit cells cultured *in vitro* (chapter 3), with the aim to decipher the role of DNA methylation in the control of fruit ripening, and its possible function in regulating anthocyanin accumulation, respectively.

In both cases we could show that the use of zebularine (Zhou et al., 2002) and/or RG108 (Brueckner et al., 2005) impacted both the fruit ripening kinetic, and the phenotype of plant cells in culture. As discussed above (and chapter 2 discussion 2.4.1, page 113-114) zebularine and RG108 inhibit grape berry ripening when young fruits are treated, but these drugs have more complex effects at later developmental stages. Similarly, treatment of grape cells initiated from the pulp of Gamay Teinturier berry, a red cultivar that accumulates anthocyanins in all fruit tissues (Wu et al., 2012; Jeong et al., 2006), showed that zebularine impacts anthocyanin accumulation in these cells. In the light, which are conditions where GT cells normally synthesizes anthocyanins; their accumulation is significantly stimulated by the zebularine treatment. Even more remarkable, whereas GT cells do not produce anthocyanins in the absence of light, the addition of zebularine was sufficient to induce their synthesis. However, a comprehensive analysis of cell gene expression profiles as well as their metabolic characterization and a locus specific methylation analysis suggest that zebularine induced phenotypes in cells may not directly be due to change in methylation profiles. Data failed to demonstrate a change in methylation level either at genes or at the GRET 1 transposon. Results suggests that zebularine has a quite broad effects on the GT cells including primary metabolite modifications, and indicate an interaction between light and the drug treatment. Of particular importance, zebularine affects the expression of many genes involved in the responses to stresses, including oxidative stress and DNA damage responses, an observation that was previously done in Arabidopsis young plants (C. Liu et al., 2015). Thus, as far as GT cells are concerned, zebularine induced phenotypes may rather be due to a stress response than to changes of DNA methylation pattern.

Whether fruit phenotypes generated by zebularine treatment are also primarily due to stress response is however unlikely. First, although we have used two DNA methylation inhibitors with clearly different mechanisms of action (see chapter 2), they both limit the ripening of 2 week old berries in culture. Second, only RG108 had an effect on more advanced fruits, whereas zebularine had none. Genotoxic effects were only reported for zebularine, which is incorporated into DNA as a cytosine analogue, whereas RG108 directly interact with DNA methyltransferases and is not used by cells for DNA synthesis. Of course, the confirmation that fruit phenotypes generated by the DNA methylation inhibitors are due to change in methylation pattern now awaits the analysis of genes/ loci that were shown to be differentially methylated during berry ripening (chapter 2).

Chapter IV Supplymentary Material

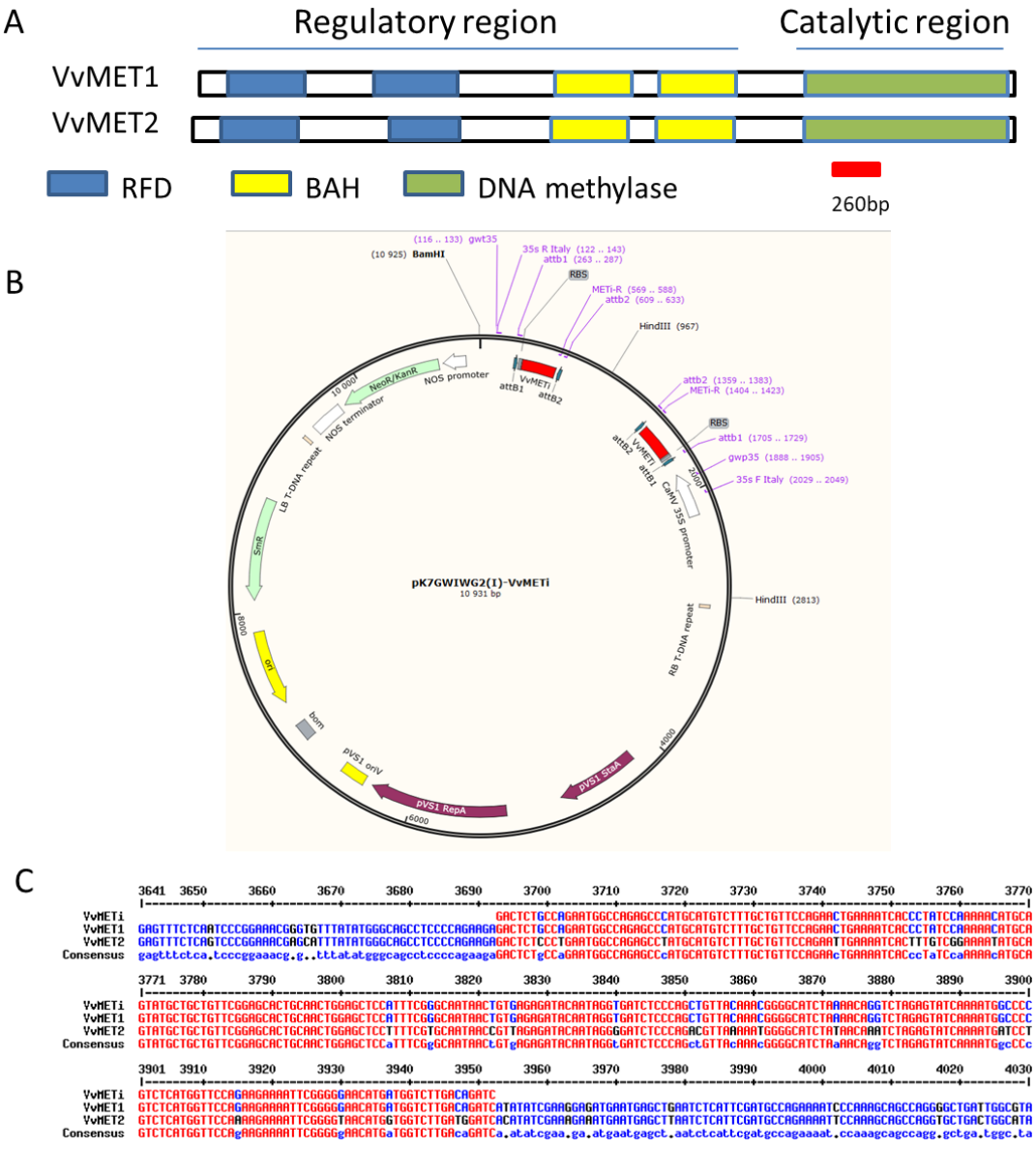

Figure IV-3: RNAi constructs of VvMETi. Two DNA methyltransferase (MET) encoding genes were identified in grape, namely VvMET1 and VvMET2. Structure and conserved domains in MET protein were shown in (A). A 260bp fragment encoding part of catalytic domain DNA methylase was used to generate an RNAi construct in the vector pK7GWIWG2 (I) (B). The construct was validated by sequencing(C).

A

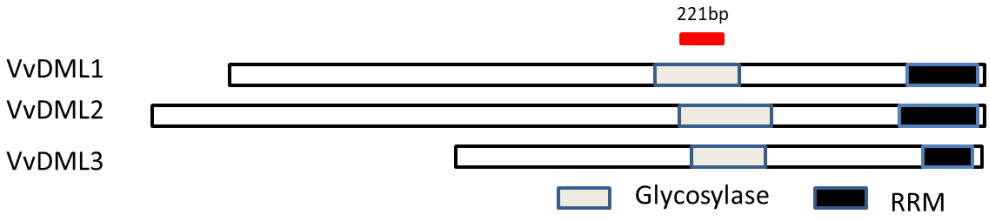

B

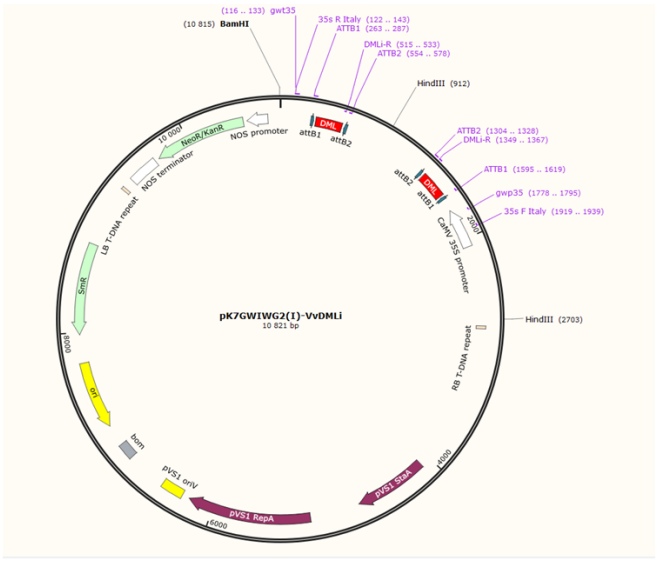

C

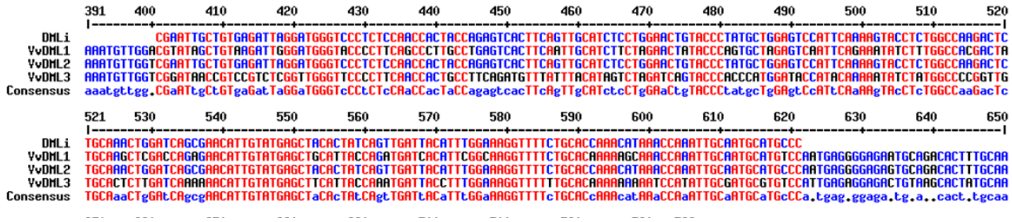

Figure IV-4: RNAi constructs of VvDMLi.

Three DNA demethylase were identified in grape, namely VvDML1, VvDML2 and VvDML3. Structure and conserved domains in MET protein were shown in (A). A 221bp fragment encoding part of catalytic domain Glycosylase was used to generate an RNAi construct in the vector pK7GWIWG2 (I) (B). The construct was validated by sequencing (C).

Chapter IV references

Ahmad, A., Zhang, Y., & Cao, X. F. (2010). Decoding the epigenetic language of plant development. *Molecular Plant*, *3*(4), 719–728. https://doi.org/10.1093/mp/ssq026

Almada, R., Cabrera, N., Casaretto, J. A., Peña-Cortés, H., Ruiz-Lara, S., & González Villanueva, E. (2011). Epigenetic repressor-like genes are differentially regulated during grapevine (Vitis vinifera L.) development. *Plant Cell Reports*, *30*(10), 1959–1968. https://doi.org/10.1007/s00299-011-1104-0

An, Y.-Q. C., Goettel, W., Han, Q., Bartels, A., Liu, Z., & Xiao, W. (2017). Dynamic Changes of Genome-Wide DNA Methylation during Soybean Seed Development. *Scientific Reports*, *7*(1), 12263. https://doi.org/10.1038/s41598-017-12510-4

Aquea, F., Timmermann, T., & Arce-Johnson, P. (2010). Analysis of histone acetyltransferase and deacetylase families of Vitis vinifera. *Plant Physiology and Biochemistry*, *48*(2–3), 194–199. https://doi.org/10.1016/j.plaphy.2009.12.009

Aquea, F., Vega, A., Timmermann, T., Poupin, M. J., & Arce-Johnson, P. (2011). Genome-wide analysis of the SET DOMAIN GROUP family in Grapevine. *Plant Cell Reports*, *30*(6), 1087–1097. https://doi.org/10.1007/s00299-011-1015-0

Brueckner, B., Boy, R. G., Siedlecki, P., Musch, T., Kliem, H. C., Zielenkiewicz, P., … Lyko, F. (2005). Epigenetic Reactivation of Tumor Suppressor Genes by a Novel Small-Molecule Inhibitor of Human DNA Methyltransferases, (14), 6305–6312.

Bucher, E., Kong, J., Teyssier, E., & Gallusci, P. (2018). Chapter Ten - Epigenetic Regulations of Fleshy Fruit Development and Ripening and Their Potential Applications to Breeding Strategies. In M. Mirouze, E. Bucher, & P. B. T.-A. in B. R. Gallusci (Eds.), *Plant Epigenetics Coming of Age for Breeding Applications* (Vol. 88, pp. 327–360). Academic Press. https://doi.org/https://doi.org/10.1016/bs.abr.2018.09.015

Chan, S. W. L., Henderson, I. R., & Jacobsen, S. E. (2005). Gardening the genome: DNA methylation in Arabidopsis thaliana. *Nature Reviews Genetics*, *6*(5), 351–360. https://doi.org/10.1038/nrg1601

Cheng, J., Niu, Q., Zhang, B., Chen, K., Yang, R., Zhu, J. K., … Lang, Z. (2018). Downregulation of RdDM during strawberry fruit ripening. *Genome Biology*, *19*(1), 1–14. https://doi.org/10.1186/s13059-018-1587-x

Chinnusamy, V., & Zhu, J. K. (2009). Epigenetic regulation of stress responses in plants. *Current Opinion in Plant Biology*, *12*(2), 133–139. https://doi.org/10.1016/j.pbi.2008.12.006

Cokus, S. J., Feng, S., Zhang, X., Chen, Z., Merriman, B., Haudenschild, C. D., … Jacobsen, S. E. (2008). Shotgun bisulphite sequencing of the Arabidopsis genome reveals DNA methylation patterning. *Nature*, *452*(7184), 215–219. https://doi.org/10.1038/nature06745

Conde, C., Paulo Silva, B., Natacha Fontes, B., Alberto P Dias, B. C., Rui Tavares, B. M., Maria Sousa, B. J., … Hernâni Gerós, B. (2007). Biochemical Changes throughout Grape Berry Development and Fruit and Wine Quality.

Cui, X., & Cao, X. (2014). Epigenetic regulation and functional exaptation of transposable elements in

higher plants. *Current Opinion in Plant Biology*, *21*, 83–88. https://doi.org/https://doi.org/10.1016/j.pbi.2014.07.001

Gallusci, P., Hodgman, C., Teyssier, E., & Seymour, G. B. (2016a). DNA Methylation and Chromatin Regulation during Fleshy Fruit Development and Ripening. *Frontiers in Plant Science*, *7*. https://doi.org/10.3389/fpls.2016.00807

Gallusci, P., Hodgman, C., Teyssier, E., & Seymour, G. B. (2016b). DNA Methylation and Chromatin Regulation during Fleshy Fruit Development and Ripening. *Frontiers in Plant Science*, *7*(June), 1–14. https://doi.org/10.3389/fpls.2016.00807

Grif, P. T., Niederhuth, C. E., & Schmitz, R. J. (2016). A Comparative Analysis of 5-Azacytidine- and Zebularine-Induced DNA Demethylation, *6*(September), 2773–2780. https://doi.org/10.1534/g3.116.030262

Huang, H., Liu, R., Niu, Q., Tang, K., Zhang, B., Zhang, H., … Lang, Z. (2019). Global increase in DNA methylation during orange fruit development and ripening. *Proceedings of the National Academy of Sciences*, *116*(4), 1430–1436. https://doi.org/10.1073/pnas.1815441116

Jaillon, O., Aury, J.-M., Noel, B., Policriti, A., Clepet, C., Casagrande, A., … French-Italian Public Consortium for Grapevine Genome Characterization. (2007). The grapevine genome sequence suggests ancestral hexaploidization in major angiosperm phyla. *Nature*, *449*(7161), 463–467. https://doi.org/10.1038/nature06148

Laimer, M. (2007). Transgenic Plant Journal ©2007 Global Science Books Transgenic Grapevines. Retrieved from

http://www.globalsciencebooks.info/Online/GSBOnline/images/0706/TPJ_1(1)/TPJ_1(1)219-227o.pdf

Lang, Z., Wang, Y., Tang, K., Tang, D., Datsenka, T., Cheng, J., … Zhu, J.-K. (2017a). Critical roles of DNA demethylation in the activation of ripening-induced genes and inhibition of ripening-repressed genes in tomato fruit. *Proceedings of the National Academy of Sciences*, *114*(22), E4511–E4519. https://doi.org/10.1073/pnas.1705233114

Lang, Z., Wang, Y., Tang, K., Tang, D., Datsenka, T., Cheng, J., … Zhu, J.-K. (2017b). Critical roles of DNA demethylation in the activation of ripening-induced genes and inhibition of ripening-repressed genes in tomato fruit. *Proceedings of the National Academy of Sciences of the United States of America*, *114*(22), E4511–E4519. https://doi.org/10.1073/pnas.1705233114

Lee, S.-I., & Kim, N.-S. (2014). Transposable elements and genome size variations in plants. *Genomics & Informatics*, *12*(3), 87–97. https://doi.org/10.5808/GI.2014.12.3.87

Lister, R., O'Malley, R. C., Tonti-Filippini, J., Gregory, B. D., Berry, C. C., Millar, A. H., & Ecker, J. R. (2008). Highly Integrated Single-Base Resolution Maps of the Epigenome in Arabidopsis. *Cell*, *133*(3), 523–536. https://doi.org/10.1016/j.cell.2008.03.029

Liu, C., Finke, A., Rozhon, W., Poppenberger, B., Baubec, T., & Pecinka, A. (2015). Repair of DNA Damage Induced by the Cytidine Analog Zebularine Requires ATR and ATM in Arabidopsis, *27*(June), 1788–1800. https://doi.org/10.1105/tpc.114.135467

Liu, R., How-Kit, A., Stammitti, L., Teyssier, E., Rolin, D., Mortain-Bertrand, A., … Gallusci, P. (2015). A

DEMETER-like DNA demethylase governs tomato fruit ripening. *Proceedings of the National Academy of Sciences*, *112*(34), 10804–10809. https://doi.org/10.1073/pnas.1503362112

Lü, P., Yu, S., Zhu, N., Chen, Y.-R., Zhou, B., Pan, Y., … Zhong, S. (2018). Genome encode analyses reveal the basis of convergent evolution of fleshy fruit ripening. *Nature Plants*, *4*(10), 784–791. https://doi.org/10.1038/s41477-018-0249-z

Mirouze, M., & Vitte, C. (2014). Transposable elements, a treasure trove to decipher epigenetic variation: insights from Arabidopsis and crop epigenomes. *Journal of Experimental Botany*, *65*(10), 2801–2812. https://doi.org/10.1093/jxb/eru120

Niederhuth, C. E., Bewick, A. J., Ji, L., Alabady, M. S., Kim, K. Do, Li, Q., … Schmitz, R. J. (2016a). Widespread natural variation of DNA methylation within angiosperms. *Genome Biology*, *17*(1), 194. https://doi.org/10.1186/s13059-016-1059-0

Niederhuth, C. E., Bewick, A. J., Ji, L., Alabady, M. S., Kim, K. Do, Li, Q., … Schmitz, R. J. (2016b). Widespread natural variation of DNA methylation within angiosperms. *Genome Biology*, *17*(1), 1–19. https://doi.org/10.1186/s13059-016-1059-0

O'Malley, R. C., Huang, S.-S. C., Song, L., Lewsey, M. G., Bartlett, A., Nery, J. R., … Ecker, J. R. (2016). Cistrome and Epicistrome Features Shape the Regulatory DNA Landscape. *Cell*, *165*(5), 1280–1292. https://doi.org/10.1016/j.cell.2016.04.038

Robinson, S. P., Davies, C., Industry, C. P., Box, P. O., & Osmond, G. (1992). Molecular biology of grape berry ripening, (Coombe).

Seymour, D. K., Koenig, D., Hagmann, J., Becker, C., & Weigel, D. (2014). Evolution of DNA Methylation Patterns in the Brassicaceae is Driven by Differences in Genome Organization. *PLoS Genetics*, *10*(11). https://doi.org/10.1371/journal.pgen.1004785

Vidalis, A., Živković, D., Wardenaar, R., Roquis, D., Tellier, A., & Johannes, F. (2016). Methylome evolution in plants. *Genome Biology*, *17*(1). https://doi.org/10.1186/s13059-016-1127-5

Wu, B. H., Guan, L., Li, J. H., Fan, P. G., Chen, S., Fang, J. B., & Li, S. H. (2012). Anthocyanin accumulation in various organs of a teinturier cultivar (vitis vinifera L.) during the growing season. *American Journal of Enology and Viticulture*, *63*(2), 177–184. https://doi.org/10.5344/ajev.2011.11063

Zhong, S., Fei, Z., Chen, Y. R., Zheng, Y., Huang, M., Vrebalov, J., … Giovannoni, J. J. (2013a). Single-base resolution methylomes of tomato fruit development reveal epigenome modifications associated with ripening. *Nature Biotechnology*, *31*(2), 154–159. https://doi.org/10.1038/nbt.2462

Zhou, L., Cheng, X., Connolly, B. A., Dickman, M. J., Hurd, P. J., & Hornby, D. P. (2002). Zebularine: a novel DNA methylation inhibitor that forms a covalent complex with DNA methyltransferases. *Journal of Molecular Biology*, *321*(4), 591–599. https://doi.org/10.1016/S0022-2836(02)00676-9

Zilberman, D., Gehring, M., Tran, R. K., Ballinger, T., & Henikoff, S. (2007). Genome-wide analysis of Arabidopsis thaliana DNA methylation uncovers an interdependence between methylation and transcription. *Nature Genetics*, *39*(1), 61–69. https://doi.org/10.1038/ng1929

Chapter I References

Achour, M., Jacq, X., Rondé, P., Alhosin, M., Charlot, C., Chataigneau, T., … Bronner, C. (2007). The interaction of the SRA domain of ICBP90 with a novel domain of DNMT1 is involved in the regulation of VEGF gene expression. *Oncogene*, *27*, 2187.

Agius, F., Kapoor, A., & Zhu, J.-K. (2006). Role of the Arabidopsis DNA glycosylase/lyase ROS1 in active DNA demethylation. *Proceedings of the National Academy of Sciences*, *103*(31), 11796–11801. https://doi.org/10.1073/pnas.0603563103

Aiese Cigliano, R., Sanseverino, W., Cremona, G., Ercolano, M. R., Conicella, C., & Consiglio, F. M. (2013). Genome-wide analysis of histone modifiers in tomato: gaining an insight into their developmental roles. *BMC Genomics*, *14*(1), 57. https://doi.org/10.1186/1471-2164-14-57

Almada, R., Cabrera, N., Casaretto, J. A., Peña-Cortés, H., Ruiz-Lara, S., & González Villanueva, E. (2011). Epigenetic repressor-like genes are differentially regulated during grapevine (Vitis vinifera L.) development. *Plant Cell Reports*, *30*(10), 1959–1968. https://doi.org/10.1007/s00299-011-1104-0

An, Y.-Q. C., Goettel, W., Han, Q., Bartels, A., Liu, Z., & Xiao, W. (2017). Dynamic Changes of Genome-Wide DNA Methylation during Soybean Seed Development. *Scientific Reports*, *7*(1), 12263. https://doi.org/10.1038/s41598-017-12510-4

Aquea, F., Timmermann, T., & Arce-Johnson, P. (2010). Analysis of histone acetyltransferase and deacetylase families of Vitis vinifera. *Plant Physiology and Biochemistry*, *48*(2–3), 194–199. https://doi.org/10.1016/j.plaphy.2009.12.009

Aquea, F., Vega, A., Timmermann, T., Poupin, M. J., & Arce-Johnson, P. (2011). Genome-wide analysis of the SET DOMAIN GROUP family in Grapevine. *Plant Cell Reports*, *30*(6), 1087–1097. https://doi.org/10.1007/s00299-011-1015-0

Baker, K., Dhillon, T., Colas, I., Cook, N., Milne, I., Milne, L., … Flavell, A. J. (2015). Chromatin state analysis of the barley epigenome reveals a higher-order structure defined by H3K27me1 and H3K27me3 abundance. *Plant Journal*, *84*(1), 111–124. https://doi.org/10.1111/tpj.12963

Baker, M. (2011). Making sense of chromatin states. *Nature Methods*, *8*(9), 717–722. https://doi.org/10.1038/nmeth.1673

Bannister, A. J., & Kouzarides, T. (2011). Regulation of chromatin by histone modifications. *Cell Research*, *21*(3), 381–395. https://doi.org/10.1038/cr.2011.22

Bapat, V. A., Trivedi, P. K., Ghosh, A., Sane, V. A., Ganapathi, T. R., & Nath, P. (2010). Ripening of fleshy fruit: Molecular insight and the role of ethylene. *Biotechnology Advances*, *28*(1), 94–107. https://doi.org/https://doi.org/10.1016/j.biotechadv.2009.10.002

Bartee, L., Malagnac, F., & Bender, J. (2001). Arabidopsis cmt3 chromomethylase mutations block non-CG methylation and silencing of an endogenous gene. *Genes and Development*, *15*(14), 1753–1758. https://doi.org/10.1101/gad.905701

Barth, T. K., & Imhof, A. (2010). Fast signals and slow marks: the dynamics of histone modifications. *Trends in Biochemical Sciences*, *35*(11), 618–626. https://doi.org/10.1016/j.tibs.2010.05.006

Battilana, J., Dunlevy, J. D., & Boss, P. K. (2017). Histone modifications at the grapevine VvOMT3 locus, which encodes an enzyme responsible for methoxypyrazine production in the berry. *Functional Plant Biology*, *44*(7), 655–664. https://doi.org/10.1071/FP16434

Bauer, M. J., & Fischer, R. L. (2011). Genome demethylation and imprinting in the endosperm. *Current Opinion in Plant Biology*, *14*(2), 162–167. https://doi.org/10.1016/j.pbi.2011.02.006

Beck, S., & Rakyan, V. K. (2008). The methylome: approaches for global DNA methylation profiling. *Trends in Genetics*, *24*(5), 231–237. https://doi.org/https://doi.org/10.1016/j.tig.2008.01.006

Becker, J. S., Nicetto, D., & Zaret, K. S. (2016). H3K9me3-Dependent Heterochromatin: Barrier to Cell Fate Changes. *Trends in Genetics*, *32*(1), 29–41. https://doi.org/10.1016/j.tig.2015.11.001

Benvenuto, G., Formiggini, F., Laflamme, P., Malakhov, M., & Bowler, C. (2002). The Photomorphogenesis Regulator DET1 Binds the Amino-Terminal Tail of Histone H2B in a Nucleosome Context. *Current Biology*, *12*(17), 1529–1534. https://doi.org/10.1016/S0960-9822(02)01105-3

Berger, S. L. (2007). The complex language of chromatin regulation during transcription. *Nature*, *447*(7143), 407–412. https://doi.org/10.1038/nature05915

Bernatavichute, Y. V., Zhang, X., Cokus, S., Pellegrini, M., & Jacobsen, S. E. (2008). Genome-wide association of histone H3 lysine nine methylation with CHG DNA methylation in Arabidopsis thaliana. *PLoS ONE*, *3*(9). https://doi.org/10.1371/journal.pone.0003156

Berry, S., & Dean, C. (2015). Environmental perception and epigenetic memory: Mechanistic insight through FLC. *Plant Journal*, *83*(1), 133–148. https://doi.org/10.1111/tpj.12869

Bewick, A. J., Niederhuth, C. E., Ji, L., Rohr, N. A., Griffin, P. T., Leebens-Mack, J., & Schmitz, R. J. (2017). The evolution of CHROMOMETHYLASES and gene body DNA methylation in plants. *Genome Biology*, *18*(1), 65. https://doi.org/10.1186/s13059-017-1195-1

Bewick, A. J., & Schmitz, R. J. (2017). Gene body DNA methylation in plants. *Current Opinion in Plant Biology*. https://doi.org/10.1016/j.pbi.2016.12.007

Birnbaum, K. D., & Roudier, F. (2017). Epigenetic memory and cell fate reprogramming in plants. *Regeneration*, *4*(1), 15–20. https://doi.org/10.1002/reg2.73

Boureau, L., How-Kit, A., Teyssier, E., Drevensek, S., Rainieri, M., Joubès, J., … Gallusci, P. (2016). A CURLY LEAF homologue controls both vegetative and reproductive development of tomato plants. *Plant Molecular Biology*, *90*(4–5), 485–501. https://doi.org/10.1007/s11103-016-0436-0

Bowers, J. E., & Meredith, C. P. (1997). • © 199 7, *16*(may), 14–17.

Bu, Z., Yu, Y., Li, Z., Liu, Y., Jiang, W., Huang, Y., & Dong, A. W. (2014). Regulation of Arabidopsis Flowering by the Histone Mark Readers MRG1/2 via Interaction with CONSTANS to Modulate FT Expression. *PLoS Genetics*, *10*(9), 1–11. https://doi.org/10.1371/journal.pgen.1004617

Bucher, E., Kong, J., Teyssier, E., & Gallusci, P. (2018). Chapter Ten - Epigenetic Regulations of Fleshy Fruit Development and Ripening and Their Potential Applications to Breeding Strategies. In M. Mirouze, E. Bucher, & P. B. T.-A. in B. R. Gallusci (Eds.), *Plant Epigenetics Coming of Age for Breeding Applications* (Vol. 88, pp. 327–360). Academic Press.

https://doi.org/https://doi.org/10.1016/bs.abr.2018.09.015

Canaguier, A., Grimplet, J., Di Gaspero, G., Scalabrin, S., Duchêne, E., Choisne, N., … Adam-Blondon, A.-F. (2017). A new version of the grapevine reference genome assembly (12X.v2) and of its annotation (VCost.v3). *Genomics Data*, *14*(September), 56–62. https://doi.org/10.1016/j.gdata.2017.09.002

Castellarin, S. D., Gambetta, G. A., Wada, H., Krasnow, M. N., Cramer, G. R., Peterlunger, E., … Matthews, M. A. (2016). Characterization of major ripening events during softening in grape: Turgor, sugar accumulation, abscisic acid metabolism, colour development, and their relationship with growth. *Journal of Experimental Botany*, *67*(3), 709–722. https://doi.org/10.1093/jxb/erv483

Castellarin, S. D., Gambetta, G. A., Wada, H., Shackel, K. A., & Matthews, M. A. (2011). Fruit ripening in Vitis vinifera: Spatiotemporal relationships among turgor, sugar accumulation, and anthocyanin biosynthesis. *Journal of Experimental Botany*, *62*(12), 4345–4354. https://doi.org/10.1093/jxb/err150

Chaïb, J., Torregrosa, L., MacKenzie, D., Corena, P., Bouquet, A., & Thomas, M. R. (2010). The grape microvine - A model system for rapid forward and reverse genetics of grapevines. *Plant Journal*, *62*(6), 1083–1092. https://doi.org/10.1111/j.1365-313X.2010.04219.x

Chanvivattana, Y., Bishopp, A., Schubert, D., Stock, C., Moon, Y.-H., Sung, Z. R., & Goodrich, J. (2004). Interaction of Polycomb-group proteins controlling flowering in Arabidopsis. *Development*, *131*(21), 5263–5276. https://doi.org/10.1242/dev.01400

Chaudhury, A. M., Ming, L., Miller, C., Craig, S., Dennis, E. S., & Peacock, W. J. (1997). Fertilization-independent seed development in Arabidopsis thaliana. *Proceedings of the National Academy of Sciences*, *94*(8), 4223–4228. https://doi.org/10.1073/pnas.94.8.4223

Chen, W., Kong, J., Qin, C., Yu, S., Tan, J., Chen, Y. R., … Hong, Y. (2015). Requirement of CHROMOMETHYLASE3 for somatic inheritance of the spontaneous tomato epimutation Colourless non-ripening. *Scientific Reports*, *5*, 1–7. https://doi.org/10.1038/srep09192

Chen, X., Hu, Y., & Zhou, D. X. (2011). Epigenetic gene regulation by plant Jumonji group of histone demethylase. *Biochimica et Biophysica Acta - Gene Regulatory Mechanisms*, *1809*(8), 421–426. https://doi.org/10.1016/j.bbagrm.2011.03.004

Cheng, J., Niu, Q., Zhang, B., Chen, K., Yang, R., Zhu, J.-K., … Lang, Z. (2018). Downregulation of RdDM during strawberry fruit ripening. *Genome Biology*, *19*(1), 212. https://doi.org/10.1186/s13059-018-1587-x

Cheng, S., Tan, F., Lu, Y., Liu, X., Li, T., Yuan, W., … Zhou, D. X. (2018). WOX11 recruits a histone H3K27me3 demethylase to promote gene expression during shoot development in rice. *Nucleic Acids Research*, *46*(5), 2356–2369. https://doi.org/10.1093/nar/gky017

Cheng, X., Zhang, S., Tao, W., Zhang, X., Liu, J., Sun, J., … Chen, T. (2018). INDETERMINATE SPIKELET 1 recruits histone deacetylase and a transcriptional repression complex to regulate rice salt tolerance. *Plant Physiology*, *178*(October), pp.00324.2018. https://doi.org/10.1104/pp.18.00324

Chinnusamy, V., & Zhu, J. K. (2009). Epigenetic regulation of stress responses in plants. *Current Opinion in Plant Biology*, *12*(2), 133–139. https://doi.org/10.1016/j.pbi.2008.12.006

Chodavarapu, R. K., Feng, S., Ding, B., Simon, S. A., Lopez, D., Jia, Y., … Pellegrini, M. (2012). Transcriptome and methylome interactions in rice hybrids. *Proceedings of the National Academy of Sciences of the United States of America*, *109*(30), 12040–12045. https://doi.org/10.1073/pnas.1209297109

Choi, Y., Gehring, M., Johnson, L., Hannon, M., Harada, J. J., Goldberg, R. B., … Fischer, R. L. (2002). DEMETER, a DNA glycosylase domain protein, is required for endosperm gene imprinting and seed viability in Arabidopsis. *Cell*, *110*(1), 33–42. https://doi.org/10.1016/S0092-8674(02)00807-3

Cokus, S. J., Feng, S., Zhang, X., Chen, Z., Merriman, B., Haudenschild, C. D., … Jacobsen, S. E. (2008). Shotgun bisulphite sequencing of the Arabidopsis genome reveals DNA methylation patterning. *Nature*, *452*(7184), 215–219. https://doi.org/10.1038/nature06745

Coleman-Derr, D., & Zilberman, D. (2012). Deposition of Histone Variant H2A.Z within Gene Bodies Regulates Responsive Genes. *PLoS Genetics*, *8*(10). https://doi.org/10.1371/journal.pgen.1002988

Collepardo-Guevara, R., Portella, G., Vendruscolo, M., Frenkel, D., Schlick, T., & Orozco, M. (2015). Chromatin unfolding by epigenetic modifications explained by dramatic impairment of internucleosome interactions: A multiscale computational study. *Journal of the American Chemical Society*, *137*(32), 10205–10215. https://doi.org/10.1021/jacs.5b04086

Conde, C., Paulo Silva, B., Natacha Fontes, B., Alberto P Dias, B. C., Rui Tavares, B. M., Maria Sousa, B. J., … Hernâni Gerós, B. (2007). Biochemical Changes throughout Grape Berry Development and Fruit and Wine Quality.

Coombe BG. (1995). Growth Stages of the Grapevine: Adoption of a system for identifying grapevine growth stages. *Australian Journal of Grape and Wine Research*, *1*(2), 104–110.

Corem, S., Doron-Faigenboim, A., jouffroy, O., Maumus, F., Arazi, T., & Bouché, N. (2018). Redistribution of CHH Methylation and Small Interfering RNAs across the Genome of Tomato ddm1 Mutants. *The Plant Cell*, *30*(July), tpc.00167.2018. https://doi.org/10.1105/tpc.18.00167

Crisp, P. A., Ganguly, D., Eichten, S. R., Borevitz, J. O., & Pogson, B. J. (2016). Reconsidering plant memory: Intersections between stress recovery, RNA turnover, and epigenetics. *Science Advances*, *2*(2), e1501340–e1501340. https://doi.org/10.1126/sciadv.1501340

Cui, Xia, Lu, F., Qiu, Q., Zhou, B., Gu, L., Zhang, S., … Cao, X. (2016). REF6 recognizes a specific DNA sequence to demethylate H3K27me3 and regulate organ boundary formation in Arabidopsis. *Nature Genetics*, *48*(6), 694–699. https://doi.org/10.1002/chem.201601686

Cui, Xiekui, & Cao, X. (2014). Epigenetic regulation and functional exaptation of transposable elements in higher plants. *Current Opinion in Plant Biology*, *21*, 83–88. https://doi.org/https://doi.org/10.1016/j.pbi.2014.07.001

Daccord, N., Celton, J. M., Linsmith, G., Becker, C., Choisne, N., Schijlen, E., … Bucher, E. (2017). High-quality de novo assembly of the apple genome and methylome dynamics of early fruit development. *Nature Genetics*, *49*(7), 1099–1106. https://doi.org/10.1038/ng.3886

Dai, Z. W., Ollat, N., Gomès, E., Decroocq, S., Tandonnet, J. P., Bordenave, L., … Delrot, S. (2011). Ecophysiological, genetic, and molecular causes of variation in grape berry weight and composition: A review. *American Journal of Enology and Viticulture*, *62*(4), 413–425.

https://doi.org/10.5344/ajev.2011.10116

Del Prete, S., Mikulski, P., Schubert, D., & Gaudin, V. (2015). One, two, three: Polycomb proteins hit all dimensions of gene regulation. *Genes*, *6*(3), 520–542. https://doi.org/10.3390/genes6030520

Deng, X., Qiu, Q., He, K., & Cao, X. (2018). The seekers: how epigenetic modifying enzymes find their hidden genomic targets in Arabidopsis. *Current Opinion in Plant Biology*, *45*, 75–81. https://doi.org/10.1016/j.pbi.2018.05.006

Derkacheva, M., & Hennig, L. (2014). Variations on a theme: Polycomb group proteins in plants. *Journal of Experimental Botany*, *65*(10), 2769–2784. https://doi.org/10.1093/jxb/ert410

Du, J., Johnson, L. M., Groth, M., Feng, S., Hale, C. J., Li, S., … Jacobsen, S. E. (2014). Mechanism of DNA methylation-directed histone methylation by KRYPTONITE. *Molecular Cell*, *55*(3), 495–504. https://doi.org/10.1016/j.molcel.2014.06.009

Du, J., Johnson, L. M., Jacobsen, S. E., & Patel, D. J. (2015). DNA methylation pathways and their crosstalk with histone methylation. *Nature Reviews Molecular Cell Biology*, *16*(9), 519–532. https://doi.org/10.1038/nrm4043

Du, J., Zhong, X., Bernatavichute, Y. V., Stroud, H., Feng, S., Caro, E., … Jacobsen, S. E. (2012). Dual binding of chromomethylase domains to H3K9me2-containing nucleosomes directs DNA methylation in plants. *Cell*, *151*(1), 167–180. https://doi.org/10.1016/j.cell.2012.07.034

Duan, C.-G., Wang, X., Xie, S., Pan, L., Miki, D., Tang, K., … Zhu, J.-K. (2017). A pair of transposon-derived proteins function in a histone acetyltransferase complex for active DNA demethylation. *Cell Research*, *27*(2), 226–240. https://doi.org/10.1038/cr.2016.147

Dubin, M. J., Zhang, P., Meng, D., Remigereau, M.-S., Osborne, E. J., Paolo Casale, F., … Nordborg, M. (2015). DNA methylation in Arabidopsis has a genetic basis and shows evidence of local adaptation. *ELife*, *4*, e05255–e05255. https://doi.org/10.7554/eLife.05255

Dussert, S., Verdeil, J. L., Jaligot, E., Beulé, T., & Rival, A. (2000). Somaclonal variation in oil palm (Elaeis guineensis Jacq.): the DNA methylation hypothesis. *Plant Cell Reports*, *19*(7), 684–690. https://doi.org/10.1007/s002999900177

Eichten, S. R., Briskine, R., Song, J., Li, Q., Swanson-Wagner, R., Hermanson, P. J., … Springer, N. M. (2013). Epigenetic and Genetic Influences on DNA Methylation Variation in Maize Populations. *The Plant Cell*, *25*(8), 2783–2797. https://doi.org/10.1105/tpc.113.114793

Eichten, Steven R, Schmitz, R. J., & Springer, N. M. (2014). Epigenetics: Beyond Chromatin Modifications and Complex Genetic Regulation. *Plant Physiology*, *165*(3), 933–947. https://doi.org/10.1104/pp.113.234211

El-Sharkawy, I., Liang, D., & Xu, K. (2015). Transcriptome analysis of an apple (Malus × domestica) yellow fruit somatic mutation identifies a gene network module highly associated with anthocyanin and epigenetic regulation. *Journal of Experimental Botany*, *66*(22), 7359–7376. https://doi.org/10.1093/jxb/erv433

Engelhorn, J., Blanvillain, R., & Carles, C. C. (2014). Gene activation and cell fate control in plants: A chromatin perspective. *Cellular and Molecular Life Sciences*, *71*(16), 3119–3137.

https://doi.org/10.1007/s00018-014-1609-0

Eriksson, E. M., Bovy, A., Manning, K., Harrison, L., Andrews, J., De Silva, J., … Seymour, G. B. (2004). Effect of the Colorless non-ripening mutation on cell wall biochemistry and gene expression during tomato fruit development and ripening. *Plant Physiology*, *136*(4), 4184–4197. https://doi.org/10.1104/pp.104.045765

Exner, V., & Hennig, L. (2008). Chromatin rearrangements in development. *Current Opinion in Plant Biology*, *11*(1), 64–69. https://doi.org/10.1016/j.pbi.2007.10.004

Fan, D., Wang, X., Tang, X., Ye, X., Ren, S., Wang, D., & Luo, K. (2018). Histone H3K9 demethylase JMJ25 epigenetically modulates anthocyanin biosynthesis in poplar. *Plant Journal*, 1–16. https://doi.org/10.1111/tpj.14092

Feng, S., Bostick, M., Sadler, K. C., Cokus, S. J., Strauss, S. H., Jain, J., … Chen, P.-Y. (2010). Conservation and divergence of methylation patterning in plants and animals. *Proceedings of the National Academy of Sciences*, *107*(19), 8689–8694. https://doi.org/10.1073/pnas.1002720107

Feng, Suhua, & Jacobsen, S. E. (2011). Epigenetic modifications in plants: an evolutionary perspective. *Current Opinion in Plant Biology*, *14*(02), 179–186.

FitzGerald, J., Luo, M., Chaudhury, A., & Berger, F. (2008). DNA methylation causes predominant maternal controls of plant embryo growth. *PloS One*, *3*(5), e2298–e2298. https://doi.org/10.1371/journal.pone.0002298

Fletcher, J. C. (2017). State of the Art: trxG Factor Regulation of Post-embryonic Plant Development. *Frontiers in Plant Science*, *8*(November), 1–8. https://doi.org/10.3389/fpls.2017.01925

Fontes, N., Gerós, H., & Delrot, S. (2011). Grape berry vacuole: A complex and heterogeneous membrane system specialized in the accumulation of solutes. *American Journal of Enology and Viticulture*, *62*(3), 270–278. https://doi.org/10.5344/ajev.2011.10125

Forestan, C., Farinati, S., Rouster, J., Lassagne, H., Lauria, M., Ferro, N. D., & Varotto, S. (2018). Control of Maize Vegetative and Reproductive. *Genetics*, *208*, 1443–1466. https://doi.org/10.1534/genetics.117.300625/-/DC1.1

Fortes, A. M., Teixeira, R. T., & Agudelo-Romero, P. (2015a). Complex interplay of hormonal signals during grape berry ripening. *Molecules*, *20*(5), 9326–9343. https://doi.org/10.3390/molecules20059326

Fortes, A. M., Teixeira, R. T., & Agudelo-Romero, P. (2015b). Complex Interplay of Hormonal Signals during Grape Berry Ripening. *Molecules (Basel, Switzerland)*, *20*(5), 9326–9343. https://doi.org/10.3390/molecules20059326

Fraige, K., Pereira-Filho, E. R., & Carrilho, E. (2014). Fingerprinting of anthocyanins from grapes produced in Brazil using HPLC-DAD-MS and exploratory analysis by principal component analysis. *Food Chemistry*, *145*, 395–403. https://doi.org/10.1016/j.foodchem.2013.08.066

Fu, C.-C., Han, Y.-C., Guo, Y.-F., Kuang, J.-F., Chen, J.-Y., Shan, W., & Lu, W.-J. (2018). Differential expression of histone deacetylases during banana ripening and identification of MaHDA6 in regulating ripening-associated genes. *Postharvest Biology and Technology*, *141*, 24–32.

https://doi.org/https://doi.org/10.1016/j.postharvbio.2018.03.010

Fu, F.-F., Dawe, R. K., & Gent, J. I. (2018). Loss of RNA-directed DNA Methylation in Maize Chromomethylase and DDM1-type Nucleosome Remodeler Mutants. *The Plant Cell*, *30*(July), tpc.00053.2018. https://doi.org/10.1105/tpc.18.00053

Fuchs, J., Demidov, D., Houben, A., & Schubert, I. (2006). Chromosomal histone modification patterns - from conservation to diversity. *Trends in Plant Science*, *11*(4), 199–208. https://doi.org/10.1016/j.tplants.2006.02.008

Gallusci, P., Hodgman, C., Teyssier, E., & Seymour, G. B. (2016). DNA Methylation and Chromatin Regulation during Fleshy Fruit Development and Ripening. *Frontiers in Plant Science*, *7*(June), 1–14. https://doi.org/10.3389/fpls.2016.00807

Gambetta, G. A., Matthews, M. A., Shaghasi, T. H., McElrone, A. J., & Castellarin, S. D. (2010). Sugar and abscisic acid signaling orthologs are activated at the onset of ripening in grape. *Planta*, *232*(1), 219–234. https://doi.org/10.1007/s00425-010-1165-2

Gapper, N. E., Giovannoni, J. J., & Watkins, C. B. (2014). Understanding development and ripening of fruit crops in an "omics" era. *Horticulture Research*, *1*, 14034. https://doi.org/10.1038/hortres.2014.34

Gillaspy, G. (1993). Fruits: A Developmental Perspective. *The Plant Cell Online*, *5*(10), 1439–1451. https://doi.org/10.1105/tpc.5.10.1439

Giovannoni, J., Nguyen, C., Ampofo, B., Zhong, S., & Fei, Z. (2017a). The Epigenome and Transcriptional Dynamics of Fruit Ripening. *Annual Review of Plant Biology*, *68*(1), 61–84. https://doi.org/10.1146/annurev-arplant-042916-040906

Giovannoni, J., Nguyen, C., Ampofo, B., Zhong, S., & Fei, Z. (2017b). The Epigenome and Transcriptional Dynamics of Fruit Ripening. *Annual Review of Plant Biology*, *68*(1), 61–84. https://doi.org/10.1146/annurev-arplant-042916-040906

Gong, Z., Morales-Ruiz, T., Ariza, R. R., Roldán-Arjona, T., David, L., & Zhu, J. K. (2002). ROS1, a repressor of transcriptional gene silencing in Arabidopsis, encodes a DNA glycosylase/lyase. *Cell*, *111*(6), 803–814. https://doi.org/10.1016/S0092-8674(02)01133-9

Goodrich, J., Puangsomlee, P., Martin, M., Long, D., Meyerowitz, E. M., & Coupland, G. (1997). A Polycomb-group gene regulates homeotic gene expression in Arabidopsis. *Nature*, *386*(6620), 44–51. https://doi.org/10.1038/386044a0

Gouil, Q., & Baulcombe, D. C. (2016). DNA Methylation Signatures of the Plant Chromomethyltransferases. *PLoS Genetics*, *12*(12), e1006526–e1006526. https://doi.org/10.1371/journal.pgen.1006526

Gouil, Q., & Baulcombe, D. C. (2018). Paramutation-like features of multiple natural epialleles in tomato. *BMC Genomics*, *19*(1), 203. https://doi.org/10.1186/s12864-018-4590-4

Gu, T., Han, Y., Huang, R., McAvoy, R. J., & Li, Y. (2016). Identification and characterization of histone lysine methylation modifiers in Fragaria vesca. *Scientific Reports*, *6*(December 2015), 1–13. https://doi.org/10.1038/srep23581

Guo, J.-E., Hu, Z., Yu, X., Li, A., Li, F., Wang, Y., … Chen, G. (2018). A histone deacetylase gene, SlHDA3,

acts as a negative regulator of fruit ripening and carotenoid accumulation. *Plant Cell Reports*, *37*(1), 125–135. https://doi.org/10.1007/s00299-017-2211-3

Guo, J.-E., Hu, Z., Zhu, M., Li, F., Zhu, Z., Lu, Y., & Chen, G. (2017). The tomato histone deacetylase SlHDA1 contributes to the repression of fruit ripening and carotenoid accumulation. *Scientific Reports*, *7*(1), 7930. https://doi.org/10.1038/s41598-017-08512-x

Guo, J. E., Hu, Z., Li, F., Zhang, L., Yu, X., Tang, B., & Chen, G. (2017). Silencing of histone deacetylase SlHDT3 delays fruit ripening and suppresses carotenoid accumulation in tomato. *Plant Science*, *265*(June), 29–38. https://doi.org/10.1016/j.plantsci.2017.09.013

Hadfield, K. A., Dandekar, A. M., & Romani, R. J. (1993). Demethylation of ripening specific genes in tomato fruit. *Plant Science*, *92*(1), 13–18. https://doi.org/https://doi.org/10.1016/0168-9452(93)90061-4

Han, Y., Kuang, J., Chen, J., Liu, X., Xiao, Y., Fu, C., … Lu, W. (2016). Banana Transcription Factor MaERF11 Recruits Histone Deacetylase MaHDA1 and Represses the Expression of MaACO1 and Expansins during Fruit Ripening. *Plant Physiology*, *171*(June), pp.00301.2016. https://doi.org/10.1104/pp.16.00301

He, X. J., Chen, T., & Zhu, J. K. (2011). Regulation and function of DNA methylation in plants and animals. *Cell Research*, *21*(3), 442–465. https://doi.org/10.1038/cr.2011.23

Heo, J. B., & Sung, S. (2011). Vernalization-mediated epigenetic silencing by a long intronic noncoding RNA. *Science*, *331*(6013), 76–79. https://doi.org/10.1126/science.1197349

Hepworth, J., & Dean, C. (2015). Flowering Locus C's Lessons: Conserved Chromatin Switches Underpinning Developmental Timing and Adaptation. *Plant Physiology*, *168*(4), 1237–1245. https://doi.org/10.1104/pp.15.00496

Hou, X., Zhou, J., Liu, C., Liu, L., Shen, L., & Yu, H. (2014). Nuclear factor Y-mediated H3K27me3 demethylation of the SOC1 locus orchestrates flowering responses of Arabidopsis. *Nature Communications*, *5*, 1–14. https://doi.org/10.1038/ncomms5601

How Kit, A., Boureau, L., Stammitti-Bert, L., Rolin, D., Teyssier, E., & Gallusci, P. (2010). Functional analysis of SlEZ1 a tomato Enhancer of zeste (E(z)) gene demonstrates a role in flower development. *Plant Molecular Biology*, *74*(3), 201–213. https://doi.org/10.1007/s11103-010-9657-9

Hsieh, T. F., Ibarra, C. A., Silva, P., Zemach, A., Eshed-Williams, L., Fischer, R. L., & Zilberman, D. (2009). Genome-wide demethylation of Arabidopsis endosperm. *Science*, *324*(5933), 1451–1454. https://doi.org/10.1126/science.1172417

Hu, J., McCall, C. M., Ohta, T., & Xiong, Y. (2004). Targeted ubiquitination of CDT1 by the DDB1–CUL4A–ROC1 ligase in response to DNA damage. *Nature Cell Biology*, *6*, 1003.

Hu, L., Li, N., Xu, C., Zhong, S., Lin, X., Yang, J., … Liu, B. (2014). Mutation of a major CG methylase in rice causes genome-wide hypomethylation, dysregulated genome expression, and seedling lethality. *Proceedings of the National Academy of Sciences*, *111*(29), 10642–10647. https://doi.org/10.1073/pnas.1410761111

Huang, H., Liu, R., Niu, Q., Tang, K., Zhang, B., Zhang, H., … Lang, Z. (2019). Global increase in DNA

methylation during orange fruit development and ripening. *Proceedings of the National Academy of Sciences*, *116*(4), 1430 LP – 1436. https://doi.org/10.1073/pnas.1815441116

Hung, F. Y., Chen, F. F., Li, C., Chen, C., Lai, Y. C., Chen, J. H., … Wu, K. (2018). The Arabidopsis LDL1/2-HDA6 histone modification complex is functionally associated with CCA1/LHY in regulation of circadian clock genes. *Nucleic Acids Research*, *46*(20), 10669–10681. https://doi.org/10.1093/nar/gky749

Inagaki, S., Miura-Kamio, A., Nakamura, Y., Lu, F., Cui, X., Cao, X., … Kakutani, T. (2010). Autocatalytic differentiation of epigenetic modifications within the Arabidopsis genome. *The EMBO Journal*, *29*(20), 3496–3506. https://doi.org/10.1038/emboj.2010.227

Jackson, J. P., Lindroth, A. M., Cao, X., & Jacobsen, S. E. (2002). Control of CpNpG DNA methylation by the KRYPTONITE histone H3 methyltransferase. *Nature*, *416*(6880), 556–560. https://doi.org/10.1038/nature731

Jacob, Y., Feng, S., LeBlanc, C. A., Bernatavichute, Y. V., Stroud, H., Cokus, S., … Michaels, S. D. (2009). ATXR5 and ATXR6 are H3K27 monomethyltransferases required for chromatin structure and gene silencing. *Nature Structural and Molecular Biology*, *16*(7), 763–768. https://doi.org/10.1038/nsmb.1611

Jaillon, O., Aury, J.-M., Noel, B., Policriti, A., Clepet, C., Casagrande, A., … French-Italian Public Consortium for Grapevine Genome Characterization. (2007). The grapevine genome sequence suggests ancestral hexaploidization in major angiosperm phyla. *Nature*, *449*(7161), 463–467. https://doi.org/10.1038/nature06148

Janssen, B. J., Thodey, K., Schaffer, R. J., Alba, R., Balakrishnan, L., Bishop, R., … Ward, S. (2008). Global gene expression analysis of apple fruit development from the floral bud to ripe fruit. *BMC Plant Biology*, *8*, 16. https://doi.org/10.1186/1471-2229-8-16

Jenuwein, T., & Allis, C. D. (2001). Translating the Histone Code. *Science*, *293*(August), 1074–1080. https://doi.org/10.1088/1751-8113/44/8/085201

Jeong, S. T., Goto-Yamamoto, N., Hashizume, K., & Esaka, M. (2006). Expression of the flavonoid 3′-hydroxylase and flavonoid 3′,5′-hydroxylase genes and flavonoid composition in grape (Vitis vinifera). *Plant Science*, *170*(1), 61–69. https://doi.org/10.1016/j.plantsci.2005.07.025

Jiang, D., & Berger, F. (2017). Histone variants in plant transcriptional regulation. *Biochimica et Biophysica Acta - Gene Regulatory Mechanisms*, *1860*(1), 123–130. https://doi.org/10.1016/j.bbagrm.2016.07.002

Jiang, L., Li, D., Jin, L., Ruan, Y., Shen, W. H., & Liu, C. (2018). Histone lysine methyltransferases BnaSDG8.A and BnaSDG8.C are involved in the floral transition in Brassica napus. *Plant Journal*, *95*(4), 672–685. https://doi.org/10.1111/tpj.13978

Jiang, P., Wang, S., Jiang, H., Cheng, B., Wu, K., & Ding, Y. (2018). The COMPASS-Like Complex Promotes Flowering and Panicle Branching in Rice. *Plant Physiology*, *176*(4), 2761–2771. https://doi.org/10.1104/pp.17.01749

Jiang, P., Wang, S., Zheng, H., Li, H., Zhang, F., Su, Y., … Ding, Y. (2018). SIP1 participates in regulation of flowering time in rice by recruiting OsTrx1 to Ehd1. *New Phytologist*, *219*(1), 422–435.

https://doi.org/10.1111/nph.15122

Joldersma, D., & Liu, Z. (2018). The making of virgin fruit: the molecular and genetic basis of parthenocarpy. *Journal of Experimental Botany*, *69*(5), 955–962. https://doi.org/10.1093/jxb/erx446

Jones, M. A., Covington, M. F., DiTacchio, L., Vollmers, C., Panda, S., & Harmer, S. L. (2010). Jumonji domain protein JMJD5 functions in both the plant and human circadian systems. *Proceedings of the National Academy of Sciences*, *107*(50), 21623–21628. https://doi.org/10.1073/pnas.1014204108

Kawakatsu, T., Nery, J. R., Castanon, R., & Ecker, J. R. (2017). Dynamic DNA methylation reconfiguration during seed development and germination. *Genome Biology*, *18*(1), 171. https://doi.org/10.1186/s13059-017-1251-x

Kawakatsu, T., Stuart, T., Valdes, M., Breakfield, N., Schmitz, R. J., Nery, J. R., … Ecker, J. R. (2016). Unique cell-type-specific patterns of DNA methylation in the root meristem. *Nature Plants*, *2*(5). https://doi.org/10.1038/NPLANTS.2016.58

Kim, D. H., & Sung, S. (2017). Vernalization-Triggered Intragenic Chromatin Loop Formation by Long Noncoding RNAs. *Developmental Cell*, *40*(3), 302-312.e4. https://doi.org/10.1016/j.devcel.2016.12.021

Kim, D. H., Xi, Y., & Sung, S. (2017). Modular function of long noncoding RNA, COLDAIR, in the vernalization response. *PLoS Genetics*, *13*(7), 1–18. https://doi.org/10.1371/journal.pgen.1006939

Kim, K. Do, El Baidouri, M., & Jackson, S. A. (2014). Accessing epigenetic variation in the plant methylome. *Briefings in Functional Genomics*, *13*(4), 318–327. https://doi.org/10.1093/bfgp/elu003

Kim, J., Kim, J. H., Richards, E. J., Chung, K. M., & Woo, H. R. (2014). Arabidopsis VIM proteins regulate epigenetic silencing by modulating DNA methylation and histone modification in cooperation with MET1. *Molecular Plant*, *7*(9), 1470–1485. https://doi.org/10.1093/mp/ssu079

Kim, Y. J., Wang, R., Gao, L., Li, D., Xu, C., Mang, H., … Chen, X. (2016). POWERDRESS and HDA9 interact and promote histone H3 deacetylation at specific genomic sites in *Arabidopsis*. *Proceedings of the National Academy of Sciences*, *113*(51), 14858–14863. https://doi.org/10.1073/pnas.1618618114

Kinoshita, T., Harada, J., Goldberg, R., & Fischer, R. (2001). Polycomb repression of flowering during early plant development. *Proceedings of the National Academy of Sciences of the United States of America*, *98*(24), 14156–14161. https://doi.org/10.1073/pnas.241507798

Kit, A. H., Boureau, L., Stammitti-Bert, L., Rolin, D., Teyssier, E., & Gallusci, P. (2010). Functional analysis of SlEZ1 a tomato Enhancer of zeste (E(Z)) gene demonstrates a role in flower development. *Plant Molecular Biology*, *74*(3), 201–213. https://doi.org/10.1007/s11103-010-9657-9

Klee, H. J., & Giovannoni, J. J. (2011). Genetics and Control of Tomato Fruit Ripening and Quality Attributes. *Annual Review of Genetics*, *45*(1), 41–59. https://doi.org/10.1146/annurev-genet-110410-132507

Kliewer, W. M. (1967). The glucose-fructose ratio of Vitis Vinifera grapes. *American Journal of Enology and Viticulture*, *18*(1), 33–41. Retrieved from http://www.ajevonline.org/cgi/content/abstract/18/1/33

Koyama, K., Ikeda, H., Poudel, P. R., & Goto-Yamamoto, N. (2012). Light quality affects flavonoid biosynthesis in young berries of Cabernet Sauvignon grape. *Phytochemistry*, *78*, 54–64. https://doi.org/10.1016/j.phytochem.2012.02.026

Kuang, J., Chen, J., Luo, M., Wu, K., Sun, W., Jiang, Y., & Lu, W. (2012). Histone deacetylase HD2 interacts with ERF1 and is involved in longan fruit senescence. *Journal of Experimental Botany*, *63*(1), 441–454. https://doi.org/10.1093/jxb/err290

Kumar, R., Khurana, A., & Sharma, A. K. (2014). Role of plant hormones and their interplay in development and ripening of fleshy fruits. *Journal of Experimental Botany*, *65*(16), 4561–4575. https://doi.org/10.1093/jxb/eru277

Kurth, E. G., Peremyslov, V. V., Prokhnevsky, A. I., Kasschau, K. D., Miller, M., Carrington, J. C., & Dolja, V. V. (2012). Virus-Derived Gene Expression and RNA Interference Vector for Grapevine. *Journal of Virology*, *86*(11), 6002–6009. https://doi.org/10.1128/JVI.00436-12

Kyriacou, M. C., Rouphael, Y., Colla, G., Zrenner, R., & Schwarz, D. (2017). Vegetable Grafting: The Implications of a Growing Agronomic Imperative for Vegetable Fruit Quality and Nutritive Value. *Frontiers in Plant Science*, *8*(May), 1–23. https://doi.org/10.3389/fpls.2017.00741

Lafos, M., Kroll, P., Hohenstatt, M. L., Thorpe, F. L., Clarenz, O., & Schubert, D. (2011). Dynamic regulation of H3K27 trimethylation during Arabidopsis differentiation. *PLoS Genetics*, *7*(4), e1002040–e1002040. https://doi.org/10.1371/journal.pgen.1002040

Lang, Z., Lei, M., Wang, X., Tang, K., Miki, D., Zhang, H., … Zhu, J.-K. (2015). The methyl-CpG-binding protein MBD7 facilitates active DNA demethylation to limit DNA hyper-methylation and transcriptional gene silencing. *Molecular Cell*, *57*(6), 971–983. https://doi.org/10.1016/j.molcel.2015.01.009

Lang, Z., Wang, Y., Tang, K., Tang, D., Datsenka, T., Cheng, J., … Zhu, J.-K. (2017). Critical roles of DNA demethylation in the activation of ripening-induced genes and inhibition of ripening-repressed genes in tomato fruit. *Proceedings of the National Academy of Sciences of the United States of America*, *114*(22), E4511–E4519. https://doi.org/10.1073/pnas.1705233114

Law, J. A., & Jacobsen, S. E. (2010a). Establishing, maintaining and modifying DNA methylation patterns in plants and animals. *Nature Reviews. Genetics*. https://doi.org/10.1038/nrg2719

Law, J. A., & Jacobsen, S. E. (2010b). Establishing, maintaining and modifying DNA methylation patterns in plants and animals. *Nature Reviews Genetics*, *11*(3), 204–220. https://doi.org/10.1038/nrg2719

Lee, J. M., Joung, J. G., McQuinn, R., Chung, M. Y., Fei, Z., Tieman, D., … Giovannoni, J. (2012). Combined transcriptome, genetic diversity and metabolite profiling in tomato fruit reveals that the ethylene response factor SlERF6 plays an important role in ripening and carotenoid accumulation. *Plant Journal*, *70*(2), 191–204. https://doi.org/10.1111/j.1365-313X.2011.04863.x

Lei, M., Zhang, H., Julian, R., Tang, K., Xie, S., & Zhu, J.-K. (2015). Regulatory link between DNA methylation and active demethylation in *Arabidopsis*. *Proceedings of the National Academy of Sciences*, *112*(11), 3553–3557. https://doi.org/10.1073/pnas.1502279112

Li, C., Gu, L., Gao, L., Chen, C., Wei, C. Q., Qiu, Q., … Cui, Y. (2016). Concerted genomic targeting of H3K27 demethylase REF6 and chromatin-remodeling ATPase BRM in Arabidopsis. *Nature Genetics*, *48*(6),

687–693. https://doi.org/10.1038/ng.3555

Li, S., Zhou, B., Peng, X., Kuang, Q., Huang, X., Yao, J., … Sun, M. X. (2014). OsFIE2 plays an essential role in the regulation of rice vegetative and reproductive development. *New Phytologist*, *201*(1), 66–79. https://doi.org/10.1111/nph.12472

Li, X., Wang, X., He, K., Ma, Y., Su, N., He, H., … Deng, X. W. (2008). High-Resolution Mapping of Epigenetic Modifications of the Rice Genome Uncovers Interplay between DNA Methylation, Histone Methylation, and Gene Expression. *The Plant Cell Online*, *20*(2), 259–276. https://doi.org/10.1105/tpc.107.056879

Li, Xin, Zhu, J., Hu, F., Ge, S., Ye, M., Xiang, H., … Wang, W. (2012). Single-base resolution maps of cultivated and wild rice methylomes and regulatory roles of DNA methylation in plant gene expression. *BMC Genomics*, *13*(1), 300. https://doi.org/10.1186/1471-2164-13-300

Li, Y., Kumar, S., & Qian, W. (2018). Active DNA demethylation: mechanism and role in plant development. *Plant Cell Reports*, *37*(1), 77–85. https://doi.org/10.1007/s00299-017-2215-z

Lieberman, M., Segev, O., Gilboa, N., Lalazar, A., & Levin, I. (2004). The tomato homolog of the gene encoding UV-damaged DNA binding protein 1 (DDB1) underlined as the gene that causes the high pigment-1 mutant phenotype. *Theoretical and Applied Genetics*, *108*(8), 1574–1581. https://doi.org/10.1007/s00122-004-1584-1

Lindroth, A. M., Cao, X., Jackson, J. P., Zilberman, D., McCallum, C. M., Henikoff, S., & Jacobsen, S. E. (2001). Requirement of CHROMOMETHYLASE3 for Maintenance of CpXpG Methylation. *Science*, *292*(5524), 2077 LP – 2080.

Lindroth, A., Shultis, D., Jasencakova, Z., Fuchs, J., Johnson, L., Schubert, D., … Jacobsen, S. E. (2004). Dual histone H3 methylation marks at lysines 9 and 27 required for interaction with CHROMOMETHYLASE3. *EMBO Journal*, *23*(21), 4286–4296.

Lister, R., O'Malley, R. C., Tonti-Filippini, J., Gregory, B. D., Berry, C. C., Millar, A. H., & Ecker, J. R. (2008). Highly Integrated Single-Base Resolution Maps of the Epigenome in Arabidopsis. *Cell*, *133*(3), 523–536. https://doi.org/10.1016/j.cell.2008.03.029

Liu, Chang, Wang, C., Wang, G., Becker, C., Zaidem, M., & Weigel, D. (2016). Genome-wide analysis of chromatin packing in Arabidopsis thaliana at single-gene resolution. *Genome Research*, *26*(8), 1057–1068. https://doi.org/10.1101/gr.204032.116

Liu, Chunyan, Lu, F., Cui, X., & Cao, X. (2010). Histone Methylation in Higher Plants. *Annual Review of Plant Biology*, *61*(1), 395–420. https://doi.org/10.1146/annurev.arplant.043008.091939

Liu, D.-D., Dong, Q.-L., Fang, M.-J., Chen, K.-Q., & Hao, Y.-J. (2012a). Ectopic expression of an apple apomixis-related gene MhFIE induces co-suppression and results in abnormal vegetative and reproductive development in tomato. *Journal of Plant Physiology*, *169*(18), 1866–1873. https://doi.org/10.1016/j.jplph.2012.07.018

Liu, D.-D., Dong, Q.-L., Fang, M.-J., Chen, K.-Q., & Hao, Y.-J. (2012b). Ectopic expression of an apple apomixis-related gene MhFIE induces co-suppression and results in abnormal vegetative and reproductive development in tomato. *Journal of Plant Physiology*, *169*(18), 1866–1873. https://doi.org/https://doi.org/10.1016/j.jplph.2012.07.018

Liu, D.-D., Zhou, L.-J., Fang, M.-J., Dong, Q.-L., An, X.-H., You, C.-X., & Hao, Y.-J. (2016). Polycomb-group protein SlMSI1 represses the expression of fruit-ripening genes to prolong shelf life in tomato. *Scientific Reports*, *6*, 31806. https://doi.org/10.1038/srep31806

Liu, J., Zhi, P., Wang, X., Fan, Q., & Chang, C. (2018). Wheat WD40-repeat protein TaHOS15 functions in a histone deacetylase complex to fine-tune defense responses to Blumeria graminis f.sp. tritici. *Journal of Experimental Botany*, (September), 1–14. https://doi.org/10.1093/jxb/ery330

Liu, K., Yu, Y., Dong, A., & Shen, W. H. (2017). SET DOMAIN GROUP701 encodes a H3K4-methytransferase and regulates multiple key processes of rice plant development. *New Phytologist*, *215*(2), 609–623. https://doi.org/10.1111/nph.14596

Liu, R., How-Kit, A., Stammitti, L., Teyssier, E., Rolin, D., Mortain-Bertrand, A., … Gallusci, P. (2015). A DEMETER-like DNA demethylase governs tomato fruit ripening. *Proceedings of the National Academy of Sciences*, *112*(34), 10804–10809. https://doi.org/10.1073/pnas.1503362112

Lü, P., Yu, S., Zhu, N., Chen, Y.-R., Zhou, B., Pan, Y., … Zhong, S. (2018). Genome encode analyses reveal the basis of convergent evolution of fleshy fruit ripening. *Nature Plants*, *4*(10), 784–791. https://doi.org/10.1038/s41477-018-0249-z

Lu, S. X., Knowles, S. M., Webb, C. J., Celaya, R. B., Cha, C., Siu, J. P., & Tobin, E. M. (2011). The Jumonji C Domain-Containing Protein JMJ30 Regulates Period Length in the Arabidopsis Circadian Clock. *Plant Physiology*, *155*(2), 906–915. https://doi.org/10.1104/pp.110.167015

Luo, C., Sidote, D. J., Zhang, Y., Kerstetter, R. A., Michael, T. P., & Lam, E. (2013). Integrative analysis of chromatin states in Arabidopsis identified potential regulatory mechanisms for natural antisense transcript production. *Plant Journal*, *73*(1), 77–90. https://doi.org/10.1111/tpj.12017

Luo, X., Gao, Z., Wang, Y., Chen, Z., Zhang, W., Huang, J., … He, Y. (2018). The NUCLEAR FACTOR-CONSTANS complex antagonizes Polycomb repression to de-repress FLOWERING LOCUS T expression in response to inductive long days in Arabidopsis. *Plant Journal*, *95*(1), 17–29. https://doi.org/10.1111/tpj.13926

Maeji, H., & Nishimura, T. (2018). Chapter Two - Epigenetic Mechanisms in Plants. In M. Mirouze, E. Bucher, & P. B. T.-A. in B. R. Gallusci (Eds.), *Plant Epigenetics Coming of Age for Breeding Applications* (Vol. 88, pp. 21–47). Academic Press. https://doi.org/https://doi.org/10.1016/bs.abr.2018.09.014

Malagnac, F., Bartee, L., & Bender, J. (2002). An Arabidopsis SET domain protein required for maintenance but not establishment of DNA methylation. *The EMBO Journal*, *21*(24), 6842–6852. https://doi.org/10.1093/emboj/cdf687

Manning, K., Tör, M., Poole, M., Hong, Y., Thompson, A. J., King, G. J., … Seymour, G. B. (2006). A naturally occurring epigenetic mutation in a gene encoding an SBP-box transcription factor inhibits tomato fruit ripening. *Nature Genetics*, *38*(8), 948–952. https://doi.org/10.1038/ng1841

Martı, J., Montealegre, R. R., Peces, R. R., & Chaco, J. L. (2006). Phenolic compounds in skins and seeds of ten grape Vitis vinifera varieties grown in a warm climate, *19*, 687–693. https://doi.org/10.1016/j.jfca.2005.05.003

Mathieu, O., Reinders, J., Čaikovski, M., Smathajitt, C., & Paszkowski, J. (2007). Transgenerational

Stability of the Arabidopsis Epigenome Is Coordinated by CG Methylation. *Cell*, *130*(5), 851–862. https://doi.org/10.1016/j.cell.2007.07.007

Matus, J. T., Loyola, R., Vega, A., Peña-Neira, A., Bordeu, E., Arce-Johnson, P., & Alcalde, J. A. (2009). Post-veraison sunlight exposure induces MYB-mediated transcriptional regulation of anthocyanin and flavonol synthesis in berry skins of Vitis vinifera. *Journal of Experimental Botany*, *60*(3), 853–867. https://doi.org/10.1093/jxb/ern336

Matzke, M. A., Kanno, T., & Matzke, A. J. M. (2015). RNA-Directed DNA Methylation: The Evolution of a Complex Epigenetic Pathway in Flowering Plants. *Annual Review of Plant Biology*, *66*(1), 243–267. https://doi.org/10.1146/annurev-arplant-043014-114633

Matzke, M. A., & Mosher, R. A. (2014). RNA-directed DNA methylation: An epigenetic pathway of increasing complexity. *Nature Reviews Genetics*, *15*(6), 394–408. https://doi.org/10.1038/nrg3683

McAtee, P., Karim, S., Schaffer, R., & David, K. (2013). A dynamic interplay between phytohormones is required for fruit development, maturation, and ripening. *Frontiers in Plant Science*, *4*, 79. https://doi.org/10.3389/fpls.2013.00079

Melnyk, C. W., Schuster, C., Leyser, O., & Meyerowitz, E. M. (2015). A developmental framework for graft formation and vascular reconnection in arabidopsis thaliana. *Current Biology*, *25*(10), 1306–1318. https://doi.org/10.1016/j.cub.2015.03.032

Miller, A. J., & Gross, B. L. (2011). From forest to field: Perennial fruit crop domestication. *American Journal of Botany*, *98*(9), 1389–1414. https://doi.org/10.3732/ajb.1000522

Mozgova, I., & Hennig, L. (2015). The Polycomb Group Protein Regulatory Network. *Annual Review of Plant Biology*, *66*(1), 269–296. https://doi.org/10.1146/annurev-arplant-043014-115627

Mudge, K., Janick, J., Scofield, S., & Goldschmidt, E. E. (2009). A History of Grafting. *Horticultural Reviews*, *35*, 437–493. https://doi.org/10.1002/9780470593776.ch9

Niederhuth, C. E., Bewick, A. J., Ji, L., Alabady, M. S., Kim, K. Do, Li, Q., … Schmitz, R. J. (2016). Widespread natural variation of DNA methylation within angiosperms. *Genome Biology*, *17*(1), 194. https://doi.org/10.1186/s13059-016-1059-0

Ning, Y. Q., Ma, Z. Y., Huang, H. W., Mo, H., Zhao, T. T., Li, L., … He, X. J. (2015). Two novel NAC transcription factors regulate gene expression and flowering time by associating with the histone demethylase JMJ14. *Nucleic Acids Research*, *43*(3), 1469–1484. https://doi.org/10.1093/nar/gku1382

OIV. (2018). OIV Statistical Report on World Vitiviniculture. *International Organisation of Vine and Wine*, 27. https://doi.org/64/19/6835 [pii]\n10.1158/0008-5472.CAN-04-1678

Ojolo, S. P., Cao, S., Priyadarshani, S. V. G. N., Li, W., Yan, M., Aslam, M., … Qin, Y. (2018). Regulation of Plant Growth and Development: A Review From a Chromatin Remodeling Perspective. *Frontiers in Plant Science*, *9*(August), 1–13. https://doi.org/10.3389/fpls.2018.01232

Ong-Abdullah, M., Ordway, J. M., Jiang, N., Ooi, S. E., Kok, S. Y., Sarpan, N., … Martienssen, R. A. (2015). Loss of Karma transposon methylation underlies the mantled somaclonal variant of oil palm. *Nature*, *525*(7570), 533–537. https://doi.org/10.1038/nature15365

Ortega-Galisteo, A. P., Morales-Ruiz, T., Ariza, R. R., & Roldán-Arjona, T. (2008). Arabidopsis DEMETER-LIKE proteins DML2 and DML3 are required for appropriate distribution of DNA methylation marks. *Plant Molecular Biology*, *67*(6), 671–681. https://doi.org/10.1007/s11103-008-9346-0

Papa, C. M., Springer, N. M., Muszynski, M. G., Meeley, R., & Kaeppler, S. M. (2007). Maize Chromomethylase Zea methyltransferase2 Is Required for CpNpG Methylation. *The Plant Cell*, *13*(8), 1919. https://doi.org/10.2307/3871328

Park, K., Kim, M. Y., Vickers, M., Park, J.-S., Hyun, Y., Okamoto, T., … Scholten, S. (2016). DNA demethylation is initiated in the central cells of Arabidopsis and rice. *Proceedings of the National Academy of Sciences*, *113*(52), 15138 LP – 15143. https://doi.org/10.1073/pnas.1619047114

Penterman, J., Zilberman, D., Huh, J. H., Ballinger, T., Henikoff, S., & Fischer, R. L. (2007). DNA demethylation in the Arabidopsis genome. *Proceedings of the National Academy of Sciences*, *104*(16), 6752–6757. https://doi.org/10.1073/pnas.0701861104

Pikaard, C. S., & Mittelsten Scheid, O. (2014). Epigenetic regulation in plants. *Cold Spring Harbor Perspectives in Biology*, *6*(12), a019315–a019315. https://doi.org/10.1101/cshperspect.a019315

Pilati, S., Bagagli, G., Sonego, P., Moretto, M., Brazzale, D., Castorina, G., … Moser, C. (2017). Abscisic Acid Is a Major Regulator of Grape Berry Ripening Onset: New Insights into ABA Signaling Network. *Frontiers in Plant Science*, *8*(June), 1–16. https://doi.org/10.3389/fpls.2017.01093

Qian, S., Lv, X., Scheid, R. N., Lu, L., Yang, Z., Chen, W., … Du, J. (2018). Dual recognition of H3K4me3 and H3K27me3 by a plant histone reader SHL. *Nature Communications*, *9*(1), 1–11. https://doi.org/10.1007/978-981-287-128-2_3

Qian, W., Miki, D., Zhang, H., Liu, Y., Zhang, X., Tang, K., … Zhu, J. (2012). in Arabidopsis, *336*(June), 1445–1448.

Quadrana, L., Almeida, J., Asís, R., Duffy, T., Dominguez, P. G., Bermúdez, L., … Carrari, F. (2014). Natural occurring epialleles determine vitamin E accumulation in tomato fruits. *Nature Communications*, *5*, 4027.

Questa, J. I., Song, J., Geraldo, N., & An, H. (2016). The sequence specific transcriptional repressor VAL1 triggers Polycomb silencing at FLC. *Science*, *1*(6298), 1–5.

Ristic, R., & Iland, P. G. (2005). Relationships between seed and berry development of Vitis Vinifera L. cv Shiraz: Developmental changes in seed morphology and phenolic composition. *Australian Journal of Grape and Wine Research*, *11*(1), 43–58. https://doi.org/10.1111/j.1755-0238.2005.tb00278.x

Rival, A., Tregear, J., Verdeil, J. L., Richaud, F., Beulé, T., Duval, Y., … Rode, A. (1998). MOLECULAR SEARCH FOR MRNA AND GENOMIC MARKERS OF THE OIL PALM “MANTLED” SOMACLONAL VARIATION. In *Acta Horticulturae* (pp. 165–172). International Society for Horticultural Science (ISHS), Leuven, Belgium. https://doi.org/10.17660/ActaHortic.1998.461.16

ROBY, G., & MATTHEWS, M. A. (2008). Relative proportions of seed, skin and flesh, in ripe berries from Cabernet Sauvignon grapevines grown in a vineyard either well irrigated or under water deficit. *Australian Journal of Grape and Wine Research*, *10*(1), 74–82. https://doi.org/10.1111/j.1755-0238.2004.tb00009.x

Rodriguez-Granados, N. Y., Ramirez-Prado, J. S., Veluchamy, A., Latrasse, D., Raynaud, C., Crespi, M., … Benhamed, M. (2016). Put your 3D glasses on: Plant chromatin is on show. *Journal of Experimental Botany*, *67*(11), 3205–3221. https://doi.org/10.1093/jxb/erw168

Rossi, V., Locatelli, S., Varotto, S., Donn, G., Pirona, R., Henderson, D. A., … Motto, M. (2007). Maize Histone Deacetylase hda101 Is Involved in Plant Development, Gene Transcription, and Sequence-Specific Modulation of Histone Modification of Genes and Repeats. *The Plant Cell Online*, *19*(4), 1145–1162. https://doi.org/10.1105/tpc.106.042549

Rothbart, S. B., & Strahl, B. D. (2014). Interpreting the language of histone and DNA modifications. *Biochimica et Biophysica Acta*, *1839*(8), 627–643. https://doi.org/10.1016/j.bbagrm.2014.03.001

Roudier, F., Ahmed, I., Bérard, C., Sarazin, A., Mary-Huard, T., Cortijo, S., … Colot, V. (2011). Integrative epigenomic mapping defines four main chromatin states in Arabidopsis. *EMBO Journal*, *30*(10), 1928–1938. https://doi.org/10.1038/emboj.2011.103

Roy, S., Gupta, P., Rajabhoj, M. P., Maruthachalam, R., & Nandi, A. K. (2018). The polycomb-group repressor MEDEA attenuates pathogen defense. *Plant Physiology*, *177*(August), pp.01579.2017. https://doi.org/10.1104/pp.17.01579

S.T., L., & J., B. (2006). The molecular basis for wine grape quality - a volatile subject. *Science*, *311*(February), 804–805.

Saleh, A., Al-Abdallat, A., Ndamukong, I., Alvarez-Venegas, R., & Avramova, Z. (2007). The Arabidopsis homologs of trithorax (ATX1) and enhancer of zeste (CLF) establish “bivalent chromatin marks” at the silent AGAMOUS locus. *Nucleic Acids Research*, *35*(18), 6290–6296. https://doi.org/10.1093/nar/gkm464

Santiago, J. L., González, I., Gago, P., Alonso-Villaverde, V., Boso, S., & Martínez, M. C. (2008). Identification of and relationships among a number of teinturier grapevines that expanded across Europe in the early 20th century. *Australian Journal of Grape and Wine Research*, *14*(3), 223–229. https://doi.org/10.1111/j.1755-0238.2008.00022.x

Satgé, C., Moreau, S., Sallet, E., Lefort, G., Auriac, M.-C., Remblière, C., … Gamas, P. (2016). Reprogramming of DNA methylation is critical for nodule development in Medicago truncatula. *Nature Plants*, *2*, 16166.

Saze, H., Shiraishi, A., Miura, A., & Kakutani, T. (2008). Control of genic DNA methylation by a jmjC domain-containing protein in Arabidopsis thaliana. *Science*, *319*(5862), 462–465. https://doi.org/10.1126/science.1150987

Schoft, V. K., Chumak, N., Choi, Y., Hannon, M., Garcia-Aguilar, M., Machlicova, A., … Tamaru, H. (2011). Function of the DEMETER DNA glycosylase in the Arabidopsis thaliana male gametophyte. *Proceedings of the National Academy of Sciences of the United States of America*, *108*(19), 8042–8047. https://doi.org/10.1073/pnas.1105117108

Schubert, D., Clarenz, O., & Goodrich, J. (2005). Epigenetic control of plant development by Polycomb-group proteins. *Current Opinion in Plant Biology*, *8*(5), 553–561. https://doi.org/10.1016/j.pbi.2005.07.005

Sequeira-Mendes, J., Araguez, I., Peiro, R., Mendez-Giraldez, R., Zhang, X., Jacobsen, S. E., … Gutierrez, C.

(2014). The Functional Topography of the Arabidopsis Genome Is Organized in a Reduced Number of Linear Motifs of Chromatin States. *The Plant Cell*, *26*(6), 2351–2366. https://doi.org/10.1105/tpc.114.124578

Serrano, A., Espinoza, C., Armijo, G., Inostroza-Blancheteau, C., Poblete, E., Meyer-Regueiro, C., … Arce-Johnson, P. (2017). Omics Approaches for Understanding Grapevine Berry Development: Regulatory Networks Associated with Endogenous Processes and Environmental Responses. *Frontiers in Plant Science*, *8*(September), 1–15. https://doi.org/10.3389/fpls.2017.01486

Seymour, D. K., Koenig, D., Hagmann, J., Becker, C., & Weigel, D. (2014). Evolution of DNA Methylation Patterns in the Brassicaceae is Driven by Differences in Genome Organization. *PLoS Genetics*, *10*(11). https://doi.org/10.1371/journal.pgen.1004785

Seymour, G. B., Østergaard, L., Chapman, N. H., Knapp, S., & Martin, C. (2013). Fruit Development and Ripening. https://doi.org/10.1146/annurev-arplant-050312-120057

Sharif, J., Muto, M., Takebayashi, S., Suetake, I., Iwamatsu, A., Endo, T. A., … Koseki, H. (2007). The SRA protein Np95 mediates epigenetic inheritance by recruiting Dnmt1 to methylated DNA. *Nature*, *450*, 908.

Shen, Y., Issakidis-Bourguet, E., & Zhou, D. X. (2016). Perspectives on the interactions between metabolism, redox, and epigenetics in plants. *Journal of Experimental Botany*, *67*(18), 5291–5300. https://doi.org/10.1093/jxb/erw310

Spillane, C., MacDougall, C., Stock, C., Köhler, C., Vielle-Calzada, J. P., Nunes, S. M., … Goodrich, J. (2000). Interaction of the Arabidopsis Polycomb group proteins FIE and MEA mediates their common phenotypes. *Current Biology*, *10*(23), 1535–1538. https://doi.org/10.1016/S0960-9822(00)00839-3

Stroud, H., Do, T., Du, J., Zhong, X., Feng, S., Johnson, L., … Jacobsen, S. E. (2014). Non-CG methylation patterns shape the epigenetic landscape in Arabidopsis. *Nature Structural and Molecular Biology*, *21*(1), 64–72. https://doi.org/10.1038/nsmb.2735

Stroud, H., Greenberg, M. V. C., Feng, S., Bernatavichute, Y. V., & Jacobsen, S. E. (2013). Comprehensive analysis of silencing mutants reveals complex regulation of the Arabidopsis methylome. *Cell*, *152*(1–2), 352–364. https://doi.org/10.1016/j.cell.2012.10.054

Sun, B., Looi, L. S., Guo, S., He, Z., Gan, E. S., Huang, J., … Ito, T. (2014). Timing mechanism dependent on cell division is invoked by Polycomb eviction in plant stem cells. *Science*, *343*(6170). https://doi.org/10.1126/science.1248559

Sweetman, C., Deluc, L. G., Cramer, G. R., Ford, C. M., & Soole, K. L. (2009). Regulation of malate metabolism in grape berry and other developing fruits. *Phytochemistry*, *70*(11–12), 1329–1344. https://doi.org/10.1016/j.phytochem.2009.08.006

Takuno, S., & Gaut, B. S. (2012). Body-methylated genes in arabidopsis thaliana are functionally important and evolve slowly. *Molecular Biology and Evolution*, *29*(1), 219–227. https://doi.org/10.1093/molbev/msr188

Talbert, P. B., & Henikoff, S. (2017). Histone variants on the move: Substrates for chromatin dynamics. *Nature Reviews Molecular Cell Biology*. https://doi.org/10.1038/nrm.2016.148

Tang, N., Ma, S., Zong, W., Yang, N., Lv, Y., Yan, C., … Xiong, L. (2016). MODD Mediates Deactivation and Degradation of OsbZIP46 to Negatively Regulate ABA Signaling and Drought Resistance in Rice. *The Plant Cell*, *28*(9), 2161–2177. https://doi.org/10.1105/tpc.16.00171

Tang, X., Miao, M., Niu, X., Zhang, D., Cao, X., Jin, X., … Liu, Y. (2016). Ubiquitin-conjugated degradation of golden 2-like transcription factor is mediated by CUL4-DDB1-based E3 ligase complex in tomato. *New Phytologist*, *209*(3), 1028–1039. https://doi.org/10.1111/nph.13635

Tang, Y., Liu, X., Liu, X., Li, Y., Wu, K., & Hou, X. (2017). Arabidopsis NF-YCs Mediate the Light-Controlled Hypocotyl Elongation via Modulating Histone Acetylation. *Molecular Plant*, *10*(2), 260–273. https://doi.org/10.1016/j.molp.2016.11.007

Telias, A., Lin-Wang, K., Stevenson, D. E., Cooney, J. M., Hellens, R. P., Allan, A. C., … Bradeen, J. M. (2011). Apple skin patterning is associated with differential expression of MYB10. *BMC Plant Biology*, *11*, 93. https://doi.org/10.1186/1471-2229-11-93

Teyssier, E., Bernacchia, G., Maury, S., How Kit, A., Stammitti-Bert, L., Rolin, D., & Gallusci, P. (2008). Tissue dependent variations of DNA methylation and endoreduplication levels during tomato fruit development and ripening. *Planta*, *228*(3), 391–399. https://doi.org/10.1007/s00425-008-0743-z

Thompson, A. J., Tor, M., Barry, C. S., Vrebalov, J., Orfila, C., Jarvis, M. C., … Seymour, G. B. (1999). Molecular and genetic characterization of a novel pleiotropic tomato-ripening mutant. *Plant Physiology*, *120*(2), 383–389. https://doi.org/10.1104/pp.120.2.383

Torres, I. O., & Fujimori, D. G. (2015). Functional coupling between writers, erasers and readers of histone and DNA methylation. *Current Opinion in Structural Biology*, *35*, 68–75. https://doi.org/10.1016/j.sbi.2015.09.007

Trindade, I., Schubert, D., & Gaudin, V. (2017). Epigenetic Regulation of Phase Transitions in Arabidopsis thaliana. In *Plant Epigenetics* (pp. 359–383). https://doi.org/10.1007/978-3-319-55520-1_18

Vachon, G., Engelhorn, J., & Carles, C. C. (2018). Interactions between transcription factors and chromatin regulators in the control of flower development. *Journal of Experimental Botany*, *69*(10), 2461–2471. https://doi.org/10.1093/jxb/ery079

Veluchamy, A., Jégu, T., Ariel, F., Latrasse, D., Mariappan, K. G., Kim, S. K., … Benhamed, M. (2016). LHP1 Regulates H3K27me3 Spreading and Shapes the Three-Dimensional Conformation of the Arabidopsis Genome. *PLoS ONE*, *11*(7), 1–25. https://doi.org/10.1371/journal.pone.0158936

Vergara, Z., & Gutierrez, C. (2017). Emerging roles of chromatin in the maintenance of genome organization and function in plants. *Genome Biology*, *18*(1), 1–12. https://doi.org/10.1186/s13059-017-1236-9

Vongs, A., Kakutani, T., Martienssen, R. A., & Richards, E. J. (1993). Arabidopsis thaliana DNA methylation mutants. *Science*, *260*(5116), 1926 LP – 1928. https://doi.org/10.1126/science.8316832

Waddington, C. H. (1942). The epigenotype. *Endeavour*, *1*(18–2).

Wang, C., Liu, C., Roqueiro, D., Grimm, D., Schwab, R., Becker, C., … Weigel, D. (2015). Genome-wide analysis of local chromatin packing in Arabidopsis thaliana. *Genome Research*, *25*, 246–256. https://doi.org/10.1101/gr.204032.116

Wang, G., & Köhler, C. (2017). Epigenetic processes in flowering plant reproduction. *Journal of Experimental Botany*. https://doi.org/10.1093/jxb/erw486

Wang, H., Zhai, L., Xu, J., Joo, H.-Y., Jackson, S., Erdjument-Bromage, H., … Zhang, Y. (2006). Histone H3 and H4 Ubiquitylation by the CUL4-DDB-ROC1 Ubiquitin Ligase Facilitates Cellular Response to DNA Damage. *Molecular Cell*, *22*(3), 383–394. https://doi.org/10.1016/J.MOLCEL.2006.03.035

Wang, Z., Meng, D., Wang, A., Li, T., Jiang, S., Cong, P., & Li, T. (2013). The methylation of the PcMYB10 promoter is associated with green-skinned sport in Max Red Bartlett pear. *Plant Physiology*, *162*(2), 885–896. https://doi.org/10.1104/pp.113.214700

Warschefsky, E. J., Klein, L. L., Frank, M. H., Chitwood, D. H., Londo, J. P., von Wettberg, E. J. B., & Miller, A. J. (2016). Rootstocks: Diversity, Domestication, and Impacts on Shoot Phenotypes. *Trends in Plant Science*. https://doi.org/10.1016/j.tplants.2015.11.008

Waterhouse AL. (2002). Determination of Total Phenolics. *CCurrent Protocol in Food Analytical Chemistry*, *11*(1), 130–143. https://doi.org/10.3923/ijcr.2009.130.143

Weinert, B. T., Narita, T., Satpathy, S., Srinivasan, B., Hansen, B. K., Schölz, C., … Choudhary, C. (2018). Time-resolved Analysis Reveals Rapid Dynamics and Broad Scope of the CBP/p300 Acetylome. *Cell*, *174*, 231–244. https://doi.org/10.1016/j.cell.2018.04.033

Wendte, J. M., & Pikaard, C. S. (2017). The RNAs of RNA-directed DNA methylation. *Biochimica et Biophysica Acta. Gene Regulatory Mechanisms*, *1860*(1), 140–148. https://doi.org/10.1016/j.bbagrm.2016.08.004

Whittaker, C., & Dean, C. (2017). The *FLC* Locus: A Platform for Discoveries in Epigenetics and Adaptation. *Annual Review of Cell and Developmental Biology*, *33*(1), 555–575. https://doi.org/10.1146/annurev-cellbio-100616-060546

Williams, B. P., Pignatta, D., Henikoff, S., & Gehring, M. (2015). Methylation-Sensitive Expression of a DNA Demethylase Gene Serves As an Epigenetic Rheostat. *PLoS Genetics*, *11*(3), 1–18. https://doi.org/10.1371/journal.pgen.1005142

Woo, H. R., Dittmer, T. A., & Richards, E. J. (2008). Three SRA-domain methylcytosine-binding proteins cooperate to maintain global CpG methylation and epigenetic silencing in arabidopsis. *PLoS Genetics*, *4*(8). https://doi.org/10.1371/journal.pgen.1000156

Woong, C., Roh, H., Vi, T., Do, Y., Fischer, R. L., Seob, J., … Choi, Y. D. Y. (2011). An E3 ligase complex regulates SET-domain polycomb group protein activity in Arabidopsis thaliana. *Pnas*, *108*(19), 8036–8041. https://doi.org/10.1073/pnas.1104232108/-/DCSupplemental.www.pnas.org/cgi/doi/10.1073/pnas.1104232108

Wu, B. H., Guan, L., Li, J. H., Fan, P. G., Chen, S., Fang, J. B., & Li, S. H. (2012). Anthocyanin accumulation in various organs of a teinturier cultivar (vitis vinifera L.) during the growing season. *American Journal of Enology and Viticulture*, *63*(2), 177–184. https://doi.org/10.5344/ajev.2011.11063

Wu, C. -t., & Morris, J. R. (2001). Genes, Genetics, and Epigenetics: A Correspondence. *Science*, *293*(5532), 1103 LP – 1105. https://doi.org/10.1126/science.293.5532.1103

Wu, H. W., Deng, S., Xu, H., Mao, H. Z., Liu, J., Niu, Q. W., … Chua, N. H. (2018). A noncoding RNA

transcribed from the AGAMOUS (AG) second intron binds to CURLY LEAF and represses AG expression in leaves. *New Phytologist*, *219*(4), 1480–1491. https://doi.org/10.1111/nph.15231

Xiao, J., Jin, R., Yu, X., Shen, M., Wagner, J. D., Pai, A., … Wagner, D. (2017). Cis and trans determinants of epigenetic silencing by Polycomb repressive complex 2 in Arabidopsis. *Nature Genetics*, *49*(10), 1546–1552. https://doi.org/10.1038/ng.3937

Xiao, J., Lee, U. S., & Wagner, D. (2016). Tug of war: adding and removing histone lysine methylation in Arabidopsis. *Current Opinion in Plant Biology*, *34*, 41–53. https://doi.org/10.1016/j.pbi.2016.08.002

Xing, L., Liu, Y., Xu, S., Xiao, J., Wang, B., Deng, H., … Chong, K. (2018). Arabidopsis O -GlcNAc transferase SEC activates histone methyltransferase ATX1 to regulate flowering. *The EMBO Journal*, *37*(19), e98115. https://doi.org/10.15252/embj.201798115

Xu, J., Xu, H., Liu, Y., Wang, X., Xu, Q., & Deng, X. (2015). Genome-wide identification of sweet orange (Citrus sinensis) histone modification gene families and their expression analysis during the fruit development and fruit-blue mold infection process. *Frontiers in Plant Science*, *6*(August), 1–16. https://doi.org/10.3389/fpls.2015.00607

Yadegari, R., Kinoshita, T., Lotan, O., Cohen, G., Katz, A., Choi, Y., … Ohad, N. (2000). Mutations in the FIE and MEA genes that encode interacting Polycomb proteins cause parent-of-origin effects on seed development by distinct mechanisms. *Plant Cell*, *12*(12), 2367–2382. https://doi.org/10.1105/tpc.12.12.2367

Yamamuro, C., Zhu, J. K., & Yang, Z. (2016). Epigenetic Modifications and Plant Hormone Action. *Molecular Plant*, *9*(1), 57–70. https://doi.org/10.1016/j.molp.2015.10.008

Yong, W.-S., Hsu, F.-M., & Chen, P.-Y. (2016). Profiling genome-wide DNA methylation. *Epigenetics & Chromatin*, *9*, 26. https://doi.org/10.1186/s13072-016-0075-3

Yu, C.-W., Tai, R., Wang, S.-C., Yang, P., Luo, M., Yang, S., … Wu, K. (2017). HISTONE DEACETYLASE6 Acts in Concert with Histone Methyltransferases SUVH4, SUVH5, and SUVH6 to Regulate Transposon Silencing. *The Plant Cell*, *29*(August), tpc.00570.2016. https://doi.org/10.1105/tpc.16.00570

Yuan, W., Luo, X., Li, Z., Yang, W., Wang, Y., Liu, R., … He, Y. (2016). A cis cold memory element and a trans epigenome reader mediate Polycomb silencing of FLC by vernalization in Arabidopsis. *Nature Genetics*, *48*(12), 1527–1534. https://doi.org/10.1038/ng.3712

Zemach, A., Kim, M. Y., Hsieh, P. H., Coleman-Derr, D., Eshed-Williams, L., Thao, K., … Zilberman, D. (2013). The arabidopsis nucleosome remodeler DDM1 allows DNA methyltransferases to access H1-containing heterochromatin. *Cell*, *153*(1), 193–205. https://doi.org/10.1016/j.cell.2013.02.033

Zemach, A., McDaniel, I. E., Silva, P., & Zilberman, D. (2010). Genome-wide evolutionary analysis of eukaryotic DNA methylation. *Science*, *328*(5980), 916–919.

Zhang, S., Zhou, B., Kang, Y., Cui, X., Liu, A., Deleris, A., … Cao, X. (2015). C-terminal domains of histone demethylase JMJ14 interact with a pair of NAC transcription factors to mediate specific chromatin association. *Cell Discovery*, *1*, 15003. https://doi.org/10.1038/celldisc.2015.3

Zhang, X., Yazaki, J., Sundaresan, A., Cokus, S., Chan, S. W.-L., Chen, H., … Ecker, J. R. (2006). Genome-wide High-Resolution Mapping and Functional Analysis of DNA Methylation in Arabidopsis. *Cell*,

126(6), 1189–1201. https://doi.org/10.1016/j.cell.2006.08.003

Zhao, H., Zhao, K., Wang, J., Chen, X., Chen, Z., Cai, R., & Xiang, Y. (2015). Comprehensive Analysis of Dicer-Like, Argonaute, and RNA-dependent RNA Polymerase Gene Families in Grapevine (Vitis Vinifera). *Journal of Plant Growth Regulation*, *34*(1), 108–121. https://doi.org/10.1007/s00344-014-9448-7

Zheng, M., Wang, Y., Wang, Y., Wang, C., Ren, Y., Lv, J., … Wan, J. (2015). DEFORMED FLORAL ORGAN1 (DFO1) regulates floral organ identity by epigenetically repressing the expression of OsMADS58 in rice (Oryza sativa). *New Phytologist*, *206*(4), 1476–1490. https://doi.org/10.1111/nph.13318

Zheng, X., Pontes, O., Zhu, J., Miki, D., Zhang, F., Li, W.-X., … Zhu, J.-K. (2008). ROS3 is an RNA-binding protein required for DNA demethylation in Arabidopsis. *Nature*, *455*(7217), 1259–1262. https://doi.org/10.1038/nature07305

Zheng, Yan, & Liu, X. (2019). Review: Chromatin organization in plant and animal stem cell maintenance. *Plant Science*, *281*, 173–179. https://doi.org/https://doi.org/10.1016/j.plantsci.2018.12.026

Zheng, Yupeng, Thomas, P. M., & Kelleher, N. L. (2013). Measurement of acetylation turnover at distinct lysines in human histones identifies long-lived acetylation sites. *Nature Communications*, *4*, 2203.

Zhong, S., Fei, Z., Chen, Y. R., Zheng, Y., Huang, M., Vrebalov, J., … Giovannoni, J. J. (2013). Single-base resolution methylomes of tomato fruit development reveal epigenome modifications associated with ripening. *Nature Biotechnology*, *31*(2), 154–159. https://doi.org/10.1038/nbt.2462

Zhou, Y., Wang, Y., Krause, K., Yang, T., Dongus, J. A., Zhang, Y., & Turck, F. (2018). Telobox motifs recruit CLF/SWN-PRC2 for H3K27me3 deposition via TRB factors in Arabidopsis. *Nature Genetics*, *50*(5), 638–644. https://doi.org/10.1038/s41588-018-0109-9

Zilberman, D., Gehring, M., Tran, R. K., Ballinger, T., & Henikoff, S. (2007). Genome-wide analysis of Arabidopsis thaliana DNA methylation uncovers an interdependence between methylation and transcription. *Nature Genetics*, *39*(1), 61–69. https://doi.org/10.1038/ng1929

Zuo, J., Wang, Y., Zhu, B., Luo, Y., Wang, Q., & Gao, L. (2018). Comparative analysis of DNA methylation reveals specific regulations on ethylene pathway in tomato fruit. *Genes*, *9*(5), 1–15. https://doi.org/10.3390/genes9050266